

The hydraulic limitation of tree height attainment

Alexander Callum Chambers-Ostler

Submitted in accordance with the requirements for the degree of

Doctor of Philosophy

The University of Leeds

School of Geography

February 2021

The candidate confirms that the work submitted is their own, except where work which has formed part of jointly authored publications has been included. The contribution of the candidate and the other authors to this work has been explicitly indicated below. The candidate confirms that appropriate credit has been given within the thesis where reference has been made to the work of others.

Chapter 3

In preparation. Abel Monteagudo-Mendoza, Adriana Prieto, Adriane Esquivel Muelbert, Alejandro Araujo-Murakami, Ângelo Gilberto Manzatto, Armando Torres-Lezama, Barbara Vicenti, Beatriz Marimon, Ben Hur Marimon Junior, Bente Klitgaard, Carlos Quesada, Carlos Reynel Rodriguez, David Galbraith, David Neill, Edmar Almeida de Oliveira, Emilio Vilanova Torre, Esteban Álvarez Dávila, Eurídice, Honorio Coronado, Fabrício Alvim Carvalho , Fernanda Coelho, Fernando Elias, Flávia Costa, Gerardo A. Aymard C., Gerardo Flores Llampazo, Hirma Ramírez-Angulo, Irina Mendoza Polo, Jean-Pierre Veillon, Jérôme Chave, Jhon del Aguila Pasquel, Joice Ferreira, Jon Lloyd, Jos Barlow, Jose Luis Marcelo Peña, Juliana Schietti, Julio Serrano, Karla Pedra de Abreu, Kyle Dexter, Lilian Blanc, Lourens Poorter, Luisa Fernanda Duque, Luzmila Arroyo, Marcelo Nascimento, Marcos Silveira, Mat Disney, Michelle Kalamandeen, Niro Higuchi, Omar Aurelio Melo Cruz, Paulo Morandi, Pieter Zuidema, Rafael Herrera Fernández, Rene Boot, Richarly da Costa Silva, Rodolfo Vasquez Martinez, Roel Brienem, Sabina Cerruto Ribeiro, Samuel Almeida, Sandra Patiño, Sonia Cesarina Palacios Ramos, Ted Feldpausch, Thaianie Rodrigues de Sousa, Timothy Baker, Timothy Killeen, Toby Pennington, Tomas Dario Gutierrez, Tony Di Fiore, Victor Chama Moscoso, William E. Magnusson, William Milliken, Wilmar Lopez Oviedo and Zorayda Restrepo Correa provided

field data. Alexander Chambers-Ostler, Roel Brienen, David Galbraith and Emanuel Gloor designed the study. Alexander Chambers-Ostler analysed the data and wrote the manuscript.

Chapter 4

Alexander Chambers-Ostler, Roel Brienen, David Galbraith, Peter Groenendijk, Emanuel Gloor. ***In review in Tree Physiology - Vessel tapering conserved along a precipitation gradient in tropical trees of the genus Cedrela.***

Alexander Chambers-Ostler, Roel Brienen, David Galbraith, Emanuel Gloor designed the study. Roel Brienen, Peter Groenendijk collected field samples. Alexander Chambers-Ostler analysed the data and wrote the manuscript.

Chapter 5

In preparation. Alexander Chambers-Ostler, Roel Brienen, David Galbraith, Emanuel Gloor designed the study. Alexander Chambers-Ostler collected field samples, analysed the data and wrote the manuscript.

This copy has been supplied on the understanding that it is copyright material and that no quotation from the thesis may be published without proper acknowledgement

The right of Alexander Chambers-Ostler to be identified as Author of this work has been asserted by him in accordance with the Copyright, Designs and Patents Act 1988.

Acknowledgements

This research has been carried out by a team which has included my supervisors: Emanuel Gloor, Roel Brienen and David Galbraith who helped in all matters. Additional help was given by Santiago Clerici, David Ashley and Rafael Schmidt in the laboratory in the School of Geography at the University of Leeds. Julia Tavares, Caroline Signori Müller, Martin Gilpin and Francisco Carvalho Diniz for training on how to perform field measurements in Chapter 5.

I thank the RAINFOR network and Aurora Levesley at FORESTPLOTS.net for contributing data.

For fieldwork conducted for Chapter 5 I thank Ezequiel Chavez for aiding logistics for fieldwork in Bolivia, Alex “Junior” Omar Ninantay for climbing trees like a whippet, and my brother William Chambers-Ostler for free labour provided and enduring long days from pre-dawn leaf water potential measurements to late nights scanning leaves. I also thank the tree identification skills of Manuel Jesus Marca Zevallos and Carlos Antonio Salas Yupayccana.

The Leeds-York NERC DTP funded the majority of this work (NE/L002574/1) in addition to supplemental funding from the Climate Research Bursary Fund from the University of Leeds **(95535048)**.

Lastly, I would like to thank my partner Arthur Sá Anunciação for constant emotional support regardless of how badly things were going, as well as practical support in the amelioration of police corruption related passport tampering in Bolivia.

Abstract

Tree height is an important determinant of tropical forest structure, biomass and diversity. Maximum tree height globally and in the tropics is linked to water availability. Different ecophysiological mechanisms behind this link have been hypothesised and explored, though with little focus on tropical forest trees. This thesis aims to contribute to understanding how tree height might be limited in tropical forests. We first study (Chapter 3) patterns of tropical forest height at the community and taxon level across neotropical forests. We found that neotropical forests and families are similarly limited by mean annual precipitation (MAP). Tree height increases until a peak at ~2400-2700mm MAP, above ~3000mm tree height decreases. We next study (Chapter 4) the patterns of basal xylem vessel widening with tree height the tropical tree genus *Cedrela* across a range of water availability. The widening of basal vessels is similar regardless of water availability, therefore in trees of a given height vessel diameter is similar within the study species across its range. This has implications for how trees cope with hydraulically stressful conditions and may suggest mechanisms behind declines in maximum tree height with water availability. We finally study (Chapter 5) the changes in a suite of ecophysiological properties and functional traits with tree height in three species along the shade-tolerance spectrum. We show that with height leaves become smaller and thicker, and the theoretical maximum stomatal conductance per leaf area and intrinsic water use efficiency increase. Additionally, xylem vessels taper at the rate consistent with tapering theory. We show that traits covary for these species with differences in shade-tolerance according to expectations from the literature. Specifically, the slow growing shade-tolerant species has narrower xylem, higher LMA and a relatively isohydric leaf water potential regulation relative to the fast-growing shade-intolerant species. Overall, this thesis

shows how neotropical trees are limited in their height attainment and explores what ecophysiological mechanisms may underpin this.

Contents

Acknowledgements.....	iv
Abstract.....	v
Contents.....	vii
List of Tables	xi
List of Figures	xii
Abbreviations.....	xiv
1 Chapter 1 Introduction	1
1.1 Background.....	1
1.2 Climate change in neotropics, drought, current trends in biomass change and mortality.....	1
1.2.1 The climate of the neotropics and forest biomes	1
1.2.2 Future climate	4
1.2.3 Expected trends in biomass and mortality with climatic change	4
1.2.4 Height patterns of neotropical forests	5
1.3 Hydraulic theory of water movement and physiological consequences for tree height	7
1.3.1 Moving water vertically	7
1.3.2 The role of stomatal regulation for water flow	16
1.3.3 Embolism avoidance	17
1.3.4 Water use efficiency and carbon balance.....	20
1.3.5 The consequences of height for tall trees	21
1.4 Limitation of tree height hypotheses.....	22
1.4.1 Hydraulic limitation of tree height.....	23
1.4.2 Evidence for the hydraulic limitation of tree height	24
1.4.3 Nutrient limitation of maximum tree height	26
1.4.4 Metabolic allometry limits to tree height.....	27
1.4.5 Other limiting factors.....	28
1.4.6 Co-limitation among limiting factors	30

1.4.7	The study of tree height limitation in the tropics.....	30
1.5	Thesis aims and objectives	31
1.5.1	Describe the role of water availability in determining the height of neotropical forest trees and differences at the taxon specific and community scale	32
1.5.2	Examine the impact of climate on the xylem vessel tapering within a tropical tree species.....	33
1.5.3	Investigate how functional traits and ecophysiological properties vary with height through the canopy and match the life-history strategies of three tropical tree species	33
1.5.4	Research questions	34
2	Chapter 2 Overview of Methods	35
2.1	Introduction.....	35
2.2	Species and site selection	36
2.3	Environmental data for our sites	37
2.4	Height measurement	39
2.5	Wood samples and xylem vessel anatomy measurement.....	39
2.6	Functional traits and ecophysiological properties	41
2.7	Determining relationships with height	43
3	Chapter 3 Environmental and taxonomic variation in maximum tree height across the neotropics	45
3.1	Introduction.....	46
3.1.1	Hypotheses	51
3.2	Methods	52
3.2.1	Sites and plot data	52
3.2.2	Calculating Maximum height	53
3.2.3	Analysis	54
3.3	Results	56
3.3.1	Environmental predictors of maximum tree height.....	56
3.3.2	Taxa	59
3.4	Discussion.....	63
3.4.1	Explaining variation in forest height	63
3.4.2	Taxon specific maximum height relationships	67
3.4.3	Conclusions	72
4	Chapter 4 Vessel tapering conserved along a precipitation gradient in tropical trees of the genus <i>Cedrela</i>	74

4.1	Introduction.....	75
4.1.1	Hypotheses	81
4.2	Methods	81
4.2.1	Species	81
4.2.2	Sites and Sampling procedure	82
4.2.3	Analysis	89
4.3	Results	90
4.3.1	Effects of climate on basal xylem vessel diameter and density	90
4.4	Discussion.....	94
4.4.1	The universal scaling of vessel diameter	98
4.4.2	Conclusions	101
5	Chapter 5 Effects of tree height on ecophysiological traits for three neotropical tree species differing in life-history strategy.....	102
5.1	Introduction.....	103
5.1.1	Hydraulic strategies of tropical trees.....	103
5.1.2	Height and hydraulic stress.....	104
5.1.3	Tree trait and functional changes transitioning from below to above canopy life stage.....	105
5.1.4	Aims and objectives	107
5.1.5	Expectations of ecophysiological properties and functional trait variation with changing height and position relative to the canopy.....	108
5.1.6	Hypotheses	109
5.2	Methods	110
5.2.1	Study sites	110
5.2.2	Study species.....	110
5.2.3	Sample strategy	111
5.2.4	Measurements and sampling techniques.....	113
5.2.5	Analysis	121
5.3	Results	123
5.3.1	Leaf traits	123
5.3.2	Xylem vessel anatomy	125
5.3.3	Leaf water potential.....	126
5.3.4	Vulnerability curves	129
5.3.5	Between-trait relationships	133

5.4	Discussion.....	134
5.4.1	Changes in functional traits with tree height	135
5.4.2	Leaf water potential and embolism vulnerability.....	141
5.4.3	Alignment of traits with life-history strategy	144
5.4.4	A trade-off between safety and productivity?	149
5.4.5	Conclusions	150
6	Chapter 6 Conclusions and synthesis	151
6.1	Research conclusions	151
6.1.1	Chapter 3 Mean annual precipitation consistently predicts neotropical maximum tree height, both at the community and individual taxa level.....	152
6.1.2	Chapter 4 A large water availability gradient does not affect the xylem vessel tapering of <i>Cedrela odorata</i>	153
6.1.3	Chapter 5 ecophysiological and functional traits change with tree height, and differences between species likely reflect life-history strategy.....	154
6.2	Synthesis and research implications	155
6.2.1	Evidence for the hydraulic limitation of maximum tree height in neotropical trees. 155	
6.2.2	Drivers and mechanisms of observed tree height- precipitation relationships. 157	
6.2.3	The role of trait and biological diversity in determining maximum height attainment.....	160
6.3	Future research	162
	References	165
	Appendix for Chapter 3.....	190
	Appendix for Chapter 4.....	208
	Appendix for Chapter 5.....	214

List of Tables

Table 3.1 Generalised additive model results for individual independent variables	59
Table 4.1 Site information	83
Table 4.2 Results of linear mixed effects models	92
Table 5.1 List of measurements and their ecophysiological significance.....	107
Table 5.2 Results of the vulnerability curve analysis for the three species.....	130
Table 5.3 Linear relationships between sample height and different ecophysiological and functional traits.....	132
Table 5.4 20 species traits from this study and based on the literature (lower rows).....	148
SI Table 3.1. Species mean maximum height with position of mean maximum height along a mean annual precipitation (MAP) gradient.....	190
SI Table 3.2. List of explanatory variables used to relate to maximum height	191
SI Table 3.3. Multivariate GAM results	193
SI Table 3.4 Table of GAM results per taxon.....	194
SI Table 3.5. Plot properties for plots used in analyses	198
SI Table 4.1 Linear mixed effects model results for the relationship between tree height and vessel density.....	211
SI Table 4.2. Intercept comparisons between sites	212
SI Table 4.3. The mean height for the 2.5-7.5m tree height bin	213
SI Table 5.4 Species specific relationship fit values between traits	216
SI Table 5.5 Coefficient values for between traits relationships	217

List of Figures

Figure 1.1 Climate of the neotropics	3
Figure 1.2 Map of LiDAR derived forest canopy height across tropical South America.....	6
Figure 1.3 Diagram of leaf mesophyll and air space.....	9
Figure 1.4 An example of the effects of vessel tapering on path length resistance	13
Figure 1.5 Representation of a tree and the movement of water	15
Figure 3.1 Conceptual diagram of hypothetical individual taxon relationships between tree height and water availability	50
Figure 3.2 Distribution of forest plots included in this study	53
Figure 3.3 Relationships between maximum height and environmental variables.....	58
Figure 3.4 Relationship between mean annual precipitation and maximum tree height	61
Figure 3.5 The maximum height of each species.....	62
Figure 3.6 Relationship between the location in mean annual precipitation (MAP) of maximum height per species	63
Figure 4.1. Conceptual illustration of three possible hydraulic strategies of trees in response to water availability	79
Figure 4.2 Location of sampling sites, diameter-height allometries at the sampling sites, and site climate.....	85
Figure 4.3 Schematic of two sampling approaches to assess the effect of tree height on vessel anatomy.	88
Figure 4.4 Relationships between mean basal vessel diameter and basal vessel density, and tree height.....	91
Figure 4.5 Mean vessel diameter and vessel density for 5m tall trees and the 5 tallest trees per site	94
Figure 5.1 Scheme of sampling within a tree	113
Figure 5.2 Scheme of pneumatic apparatus for measuring gas discharge.....	115
Figure 5.3 Images of different sampling and measuring techniques	120
Figure 5.4 Relationships between sample height and leaf traits	124

Figure 5.5 Relationships between distance to apex of mean vessel diameter and vessel density.....	125
Figure 5.6 Species specific apical mean xylem vessel area – sample height relationships ...	126
Figure 5.7 Daily curves of leaf water potential	128
Figure 5.8 Linear relationships between sample height and leaf water potential.....	129
Figure 5.9 Vulnerability curves measured for <i>A. ruizii</i> , <i>P. laevis</i> , and <i>C. microchaete</i>	131
Figure 5.10 Relationships between traits for three species	134
Figure 5.11 Scheme of two constant tapering strategies describing the effects of increasing apical vessel width with path length	141
Figure 6.1 Predictions of changes in the maximum height of the forest community with changes in mean annual precipitation.....	153
Figure 6.2 Plots demonstrating how to test ecophysiological traits and properties for their role in maximum height limitation	164
SI Figure 4.1. Comparison of two sampling methods	208
SI Figure 4.2. Histograms of the number of vessels measured in each sample	210
SI Figure 5.1 Trees sampled per species per height class	214
SI Figure 5.2 Relationship between height and light index	215

Abbreviations

a	-	Cross sectional area
A	-	Rate of assimilation of CO ₂ in photosynthesis
\bar{a}	-	Tapering coefficient
AD	-	Air discharge
AIC	-	Akaike information criterion
A _L	-	Leaf area
C _a	-	CO ₂ concentration in air
C _i	-	CO ₂ concentration in the leaf
d	-	Diameter
D	-	Vapour pressure deficit
DBH	-	Diameter at breast height
DNI	-	Direct normal irradiance
dpi	-	Dots per inch
dw	-	Diffusivity of water vapour
E	-	Transpiration rate
G	-	Acceleration due to gravity
g	-	Conductance
GAM	-	Generalised additive model
GCV	-	Minimised generalised cross-validation
g _{max}	-	Theoretical maximum stomatal conductance
g _s	-	Stomatal conductance
H	-	Height
HSM	-	Hydraulic safety margin
iWUE	-	Intrinsic water use efficiency
l	-	Vessel length
L	-	Path Length
LMM	-	Linear mixed effects model
M	-	Whole tree biomass
MAP	-	Mean annual precipitation
n	-	Branching ratio between levels
P	-	Pressure
P50	-	Water potential that gives a loss of conductance equal to 50% of maximum conductance
pa _{max}	-	Maximum stomatal pore area
pd	-	Pore depth
PLC	-	Percentage loss of conductance
P-PET	-	Precipitation minus potential evapotranspiration
Q	-	Sap flow
R	-	Resistance to water flow

r	-	Radius
R_{gc}	-	Universal gas constant
RH	-	Relative humidity
r_{pore}	-	Radius of mesophyll pores
$R_{standard}$	-	ratio of ^{13}C relative to ^{12}C in cellulose in a standard
R_{sample}	-	ratio of ^{13}C relative to ^{12}C in cellulose in a sample
SD	-	Stomatal density
SST	-	Sea surface temperature
T	-	Temperature
v	-	Molar volume of air
VD	-	Vessel density
v_{liquid}	-	Molar volume of the water
Y	-	Metabolic rate of respiration
γ	-	Surface tension
ΔP	-	Pressure gradient
η	-	Viscosity of water
θ	-	Angle of concavity
ρ	-	Density of water
Ψ	-	Water potential

Chapter 1 Introduction

1.1 Background

The Amazon forest is the largest continuous tropical forest, ~23 times the area of the UK. The neotropics hold 37% of global plant diversity (Antonelli and Sanmartin 2011), and 108PgC in above ground biomass of live trees which is 26% of total terrestrial biomass (Feldpausch et al. 2012; Spawn et al. 2020). The need for trees to pump water from soil to canopy where it is lost to the atmosphere influences the climate of South America recycling 35% of water via evapotranspiration (Eltahir and Bras 1994; Trenberth 1999), and cooling surface temperatures (Baker and Spracklen 2019; Winckler et al. 2019). Rising temperatures and changes to precipitation regimes associated with climate change and deforestation across the neotropics are likely to affect tree growth and mortality (Brienen et al. 2015; McDowell et al. 2018). Consequently, the biodiversity, biomass and climate modulation they currently provide are in jeopardy.

1.2 Climate change in neotropics, drought, current trends in biomass change and mortality.

1.2.1 The climate of the neotropics and forest biomes

The neotropics are largely warm and wet, lacking large deserts. The majority of the lowland area experiences >1500mm per year of precipitation (Figure 1.1A). In lowland regions temperatures are higher and precipitation is less seasonal toward the equator (Figure 1.1). The climate of the neotropics supports a variety of forest types, from wet montane forests of the Andes, to lowland terra firme forest of the Amazon basin, to seasonal dry forest at the

Amazon-savanna transition zone and semi-arid and scrub forest of the Chaco and Caatinga biomes (Dexter et al. 2018; Killeen et al. 2006). The last glacial maximum was drier than today for much of the Amazon basin (Haggi et al. 2017). As the climate has warmed and become wetter tropical rainforest dominates in tropical South America, largely in the Amazon basin. The majority of the Amazon basin has a mean annual precipitation of between 1800 – 3000mm, and is generally warm as the majority of the basin is at low elevation (Figure 1.1). Lowland forests tend to be wetter closer to the Andes and forests tend to be drier and more seasonal further from the equator. Forests close to the equator tend to be aseasonal with consistent rainfall throughout the year, whilst forests close to the edge of the Amazon rainforest have several months long dry seasons. Further into dry forest and semi-arid regions the dry season is longer than the wet season (Villar et al. 2009).

Rainfall across the north and east of the Amazon basin is driven by input from the tropical north Atlantic Ocean (Gloor et al. 2015; Gloor et al. 2013). The Amazon basin retains much of its water through evapotranspiration and subsequent convective rainfall. This accounts for ~35% of total precipitation across the Amazon basin (Eltahir and Bras 1994; Trenberth 1999). Evapotranspiration also contributes to the rainfall of nearby regions of South America, e.g. the *Rio de la Plata* basin.

Extremes of precipitation occur across the Amazon basin periodically. Notable recent droughts include 2005 and 2010, recent flooding events include 2009 and 2014 (Marengo and Espinoza 2016). Extreme events are often associated with sea surface temperature (SST) anomalies in the tropical north Atlantic, where warmer SST has been associated with both drought and flood events (Marengo and Espinoza 2016). Additionally, drought years may also be associated with El Niño conditions, and flood years may be associated with La Niña.

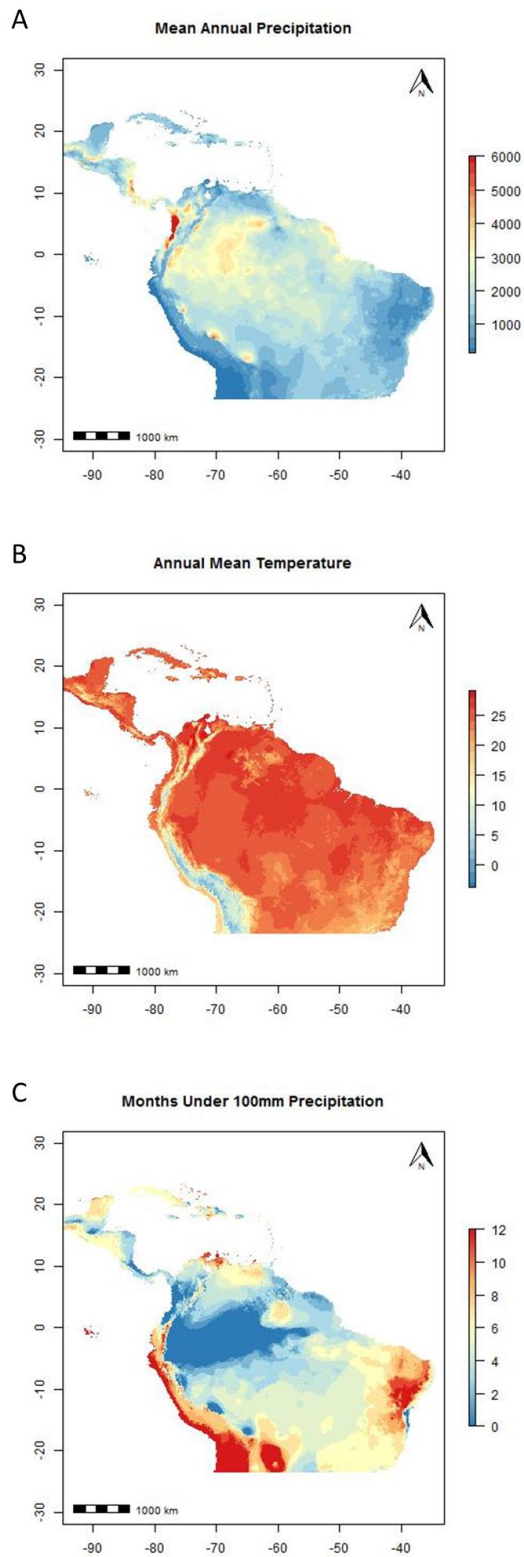


Figure 1.1 Climate of the neotropics. A) mean annual precipitation (mm), B) annual mean temperature (°C), C) number of months with less than 100mm of precipitation indicating dry season length. Climate data from Worldclim (Fick and Hijmans 2017).

1.2.2 Future climate

The future climate for the Amazon region is uncertain (Marengo et al. 2018; Satyamurty et al. 2010). However trends in historical precipitation show that northern Amazonia is generally becoming wetter while there is evidence that southern Amazonia is becoming drier (Espinoza et al. 2019; Gloor et al. 2013; Shiogama et al. 2011). Additionally, there is an expectation that severe events such as sporadic droughts and heavy rainfall will increase in frequency, in part due to increasing ENSO event frequency due to warming sea surface temperatures in the equatorial Pacific ocean and atmospheric teleconnection to the Amazon basin (Fasullo et al. 2018; Yeh et al. 2018).

In addition to global climate change, Amazonian forests are likely to suffer from local microclimate changes as a result of deforestation. Since interception of rainfall and subsequent evapotranspiration by trees recycles much of the water of the region, it is likely that as forest continues to be converted to pasture, increased runoff to rivers will reduce further water recycling (D'Almeida et al. 2007; Moore et al. 2007). Furthermore, temperature has increased by 0.6-0.7°C over the last 40 years, and will continue to increase as a result of rising CO₂ concentrations in the atmosphere, up to 4-6°C by 2100 under a high emission scenario, increasing the vapour pressure deficit acting on tree's leaves (Marengo et al. 2018). These predicted changes in climate are anticipated to have a large impact on the forests of the neotropics (Alvarez-Davila et al. 2017; Brienen et al. 2015; Esquivel-Muelbert et al. 2019; Fajardo et al. 2019; McDowell et al. 2018; Vilanova et al. 2018; Yang et al. 2018a).

1.2.3 Expected trends in biomass and mortality with climatic change

Over past decades Amazonian forests have absorbed around 0.38 Pg of Carbon every year, however this capacity of the Amazon to fix carbon is decreasing (Brienen et al. 2015). This is

because of increasing mortality and reduction in the increase of growth rates of trees. There are several possible drivers behind this trend; one is the increasing climatic variability, such as pronounced droughts, which leads to higher mortality of trees and reduces growth rates in the drier regions of the Amazon. Another is CO₂ fertilisation leading to increasing growth rates and consequent declines in tree longevity (Brienen et al. 2020; Bugmann and Bigler 2011). Furthermore, increasing temperatures are likely to increase the respiration demand of trees as well as possibly inhibiting photosynthesis at very high temperatures (Gloor et al. 2018; Lloyd and Farquhar 2008; Sullivan et al. 2020). Mortality is a strong driver of biomass change across the Amazon and understanding the mechanisms behind tree mortality is thus of great importance to determine the future of tropical forests in a changing climate (Allen et al. 2010; McDowell et al. 2018).

1.2.4 Height patterns of neotropical forests

In the lowland tropics where forests are continuous several climatic and edaphic factors affect forest height, but satellite observations from LiDAR data show that the primary climatic variable associated with changes in forest height is water availability (Klein et al. 2015; Tao et al. 2016). The tallest tropical forests are those in the wet tropics, in particular in south east Asia grow the tallest tropical trees, where trees with 100.8m height have been found (Shenkin et al. 2019). In South America the tallest tropical trees are found in the Guyana shield region (Feldpausch et al. 2012; Sawada et al. 2015; Simard et al. 2011). This has been exemplified by the recent discovery of an 88.5m tall tree in the Amapá region of Brazil (Gorgens et al. 2019). Whilst particularly short-statured forests are found where soils have a high percentage of sand, where nutrient concentrations are low and do not retain water well (Adeney et al. 2016). Most of the Amazon region's forest ends abruptly to form savanna, however the forest

at the southern edge of the Amazonian forest biome transitions continuously to semi-deciduous forest (1500-1300mm yr⁻¹), deciduous forest (1300-1000mm yr⁻¹) and then semi-arid scrub (<1000mm yr⁻¹) where forest height is relatively low (specifically southern Bolivia Figure 1.2) (Seiler et al. 2014). The variability in forest height across the Amazon is not well understood. However, global evidence including from South America suggests that forest height is at least partially water limited except in the very wet equatorial regions (Gorgens et al. 2020; Klein et al. 2015; Ryan and Yoder 1997; Tao et al. 2016).

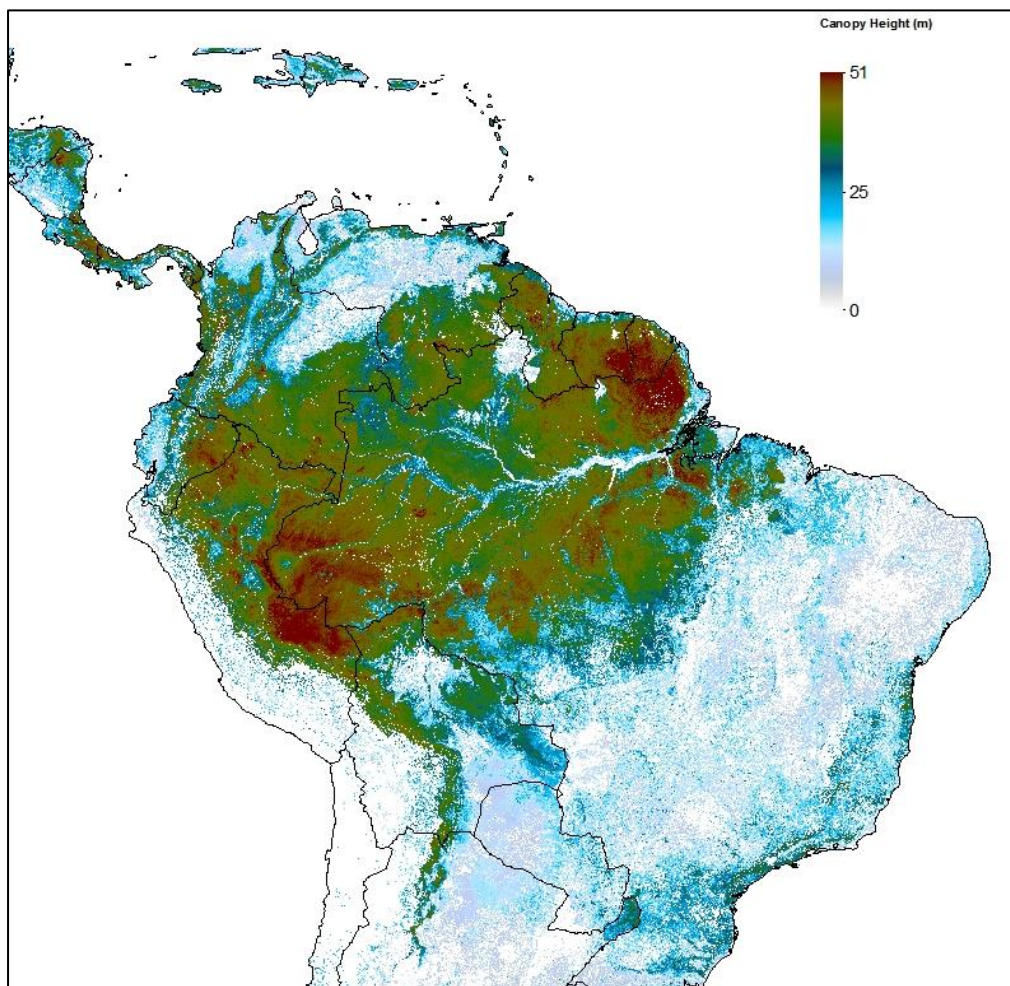


Figure 1.2 Map of LiDAR derived forest canopy height across tropical South America. Canopy height is provided at 1km resolution (Simard et al. 2011).

1.3 Hydraulic theory of water movement and physiological consequences for tree height

1.3.1 Moving water vertically

Plants require light for energy and growth, so for these static organisms competition between individuals for light drove them to grow tall (Falster and Westoby 2003; Kenrick and Crane 1997). Plants like all living things require water to live. When plants were short statured water was easy to transport to above ground tissues through capillary action alone, provided the environment was sufficiently moist, however, upon growing tall the problem of pulling water against gravity arose (Pittermann 2010). This need to grow tall and transport water vertically beyond the capacity of capillary action led to the evolution of the first vascular plants by 430 million years ago, and the first forests with tree like forms by 385 million years ago (Gerrienne et al. 2011; Meyer-Berthaud et al. 1999; Stein et al. 2007). The difficulty in pulling water over distances over 1m is that capillary action in typically sized xylem will not overcome the gravitational pull. Instead, plants use a pressure differential between water within the plant and water in the atmosphere, where water in the atmosphere is typically at a much lower pressure (Lautrup 2005; Lautrup 2011; Lee et al. 2017; Shi et al. 2020; Stroock et al. 2014; Venturas et al. 2017). The cohesion-tension theory of water transport is the best accepted model describing how water movement from roots to canopy is driven by evaporation at the leaf mesophyll cells generating a pressure differential for water to flow up (Figure 1.3) (Angeles et al. 2004; Dixon and Joly 1895). The cohesion part of the theory states that water molecules are linked by intermolecular forces and so water can form a continuous column. The tension is generated as water evaporates into leaf air spaces via the network of small pores (of radius r_{pore} , nm) of the leaf mesophyll. The surface tension, γ (N m^{-1}), at the point of

evaporation between cells causes the formation of a concave meniscus. This generates negative pressure on the water below the meniscus P_{leaf} (Pa), where a greater angle of concavity, θ , or smaller radius of pores exerts greater pressure (Levitt 1956). The effective pressure acting upon the liquid below the meniscus also depends on the humidity of the leaf space into which the water from the pores of the mesophyll evaporates (Lautrup 2011):

$$P_{leaf} = -\ln\left(\frac{P_{vapour}}{P_{saturation}}\right) = -\frac{2\gamma v_{liquid} \cos\theta}{r_{pore} R_{gc} T} \quad 1.1$$

where T is temperature ($^{\circ}\text{C}$), R_{gc} is the universal gas constant ($\text{m}^3 \text{Pa K}^{-1} \text{mol}^{-1}$) and v_{liquid} is the molar volume of the water in the meniscus (Pa s). Equation 1.1 shows that at high humidity, i.e. $P_{vapour}/P_{saturation}$ approaching 1, pressures acting on the water below the meniscus are low (Figure 1.3A) (Lautrup 2011; Venturas et al. 2017). At lower humidity and higher temperature, the rate of evaporation increases and the concavity of the meniscus consequently increases, thus contributing to increase the tension on the water column (Figure 1.3B). If the vapour pressure is much greater than the surface tension the water level retreats, and the tissues of the plant dehydrate and die (Figure 1.3C). Reducing r_{pore} enables the water column to better withstand low humidity as a greater angle of concavity can be maintained (Figure 1.3D-E). Note that P_{leaf} must be more negative than that of the equivalent root-soil interface in order for water to travel up the plant. So, negative pressure (i.e. a stress) at the air-water interface in the leaf pulls cohesive columns of water molecules up the xylem from root to leaf (Shi et al. 2020).

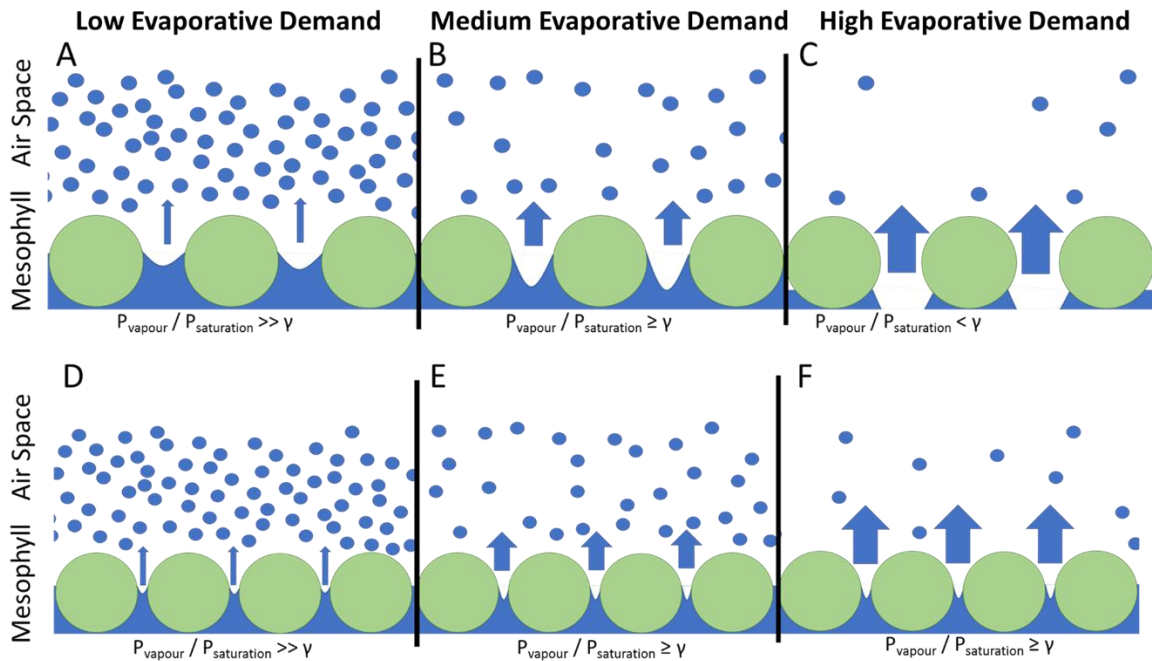


Figure 1.3 Diagram of leaf mesophyll and air space demonstrating the action of water evaporating from a liquid state to a vapour. Less humid air produces greater evaporation, leading to greater pressure difference between the water vapour and the water at saturation, in turn generating greater negative pressure in the liquid water. Water evaporates generating a concave meniscus (A-B) until the negative pressure is greater than the energy of the surface tension of the water at which point the leaf dehydrates (C). D-F show a similar process as A-B, but in F the surface tension is not broken by the evaporative demand at low humidity because of narrower pores between mesophyll cells, thus preventing dehydration of the leaf. Note that specific sites of evaporation and mechanisms of water movement within the leaf are not well known (Sack and Holbrook 2006) but the mechanism shown here can be artificially recreated to drive evaporation powered water pumps (Lee et al. 2017) and is broadly accepted (Stroock et al. 2014).

The rate of water flow from root to leaf is defined in part by the difference in water potential along a gradient between lower and upper parts of the plant. Water potential is measured in units of energy which can be converted to pressure units. Pure water has a water potential of 0MPa at 25°C and atmospheric pressure.

Water potential is directly related to water flow using the Ohm's law analogue for water movement, where Q is water flux ($\text{m}^3 \text{s}^{-1}$), ΔP is the pressure gradient between two points (MPa), and R is the resistance to water flow along that gradient (MPa s m^{-3}) (Gardner 1965):

$$Q = \frac{\Delta P}{R} \quad 1.2$$

So, the more negative the water potential at the apex of the tree relative to the water potential at the base the faster water flows. The water potential of a tissue can be defined by the sum of its component potentials (Ψ_t). These are substrate potential (Ψ_s), gravitational potential (Ψ_g), frictional potential (Ψ_f), osmotic potential (Ψ_o) and pressure potential (Ψ_p). Those that most affect a plants water status are the osmotic, gravitational and pressure potentials (Wallace et al. 1983).

$$\Psi_t = \Psi_s + \Psi_g + \Psi_f + \Psi_o + \Psi_p \quad 1.3$$

For the considerations of this study only negative water potentials are expected due to the direction of flow to the highly negative atmosphere (air humidity at 20°C <10%= -300MPa, 50% = -93.5MPa, 90% = - 14.2MPa, 100% = 0MPa, see inset graph of Figure 1.5). The water potential of the xylem is generally greater than -10MPa, and therefore under most air humidity water can be moved within a plant by the negative pressure of the atmosphere (Choat et al. 2012).

Equation 1.2 permits a basic understanding of flow through a pipe, to which the plant flow path up the water conducting xylem tissue is fundamentally analogous. The importance of gravitational potential is not implicitly included in the measurement of water potential and thus must be included in the equation, where the pressure differential between the root and leaf is given by $\Psi_r - \Psi_l$, and ρGH gives, respectively, the water density (g m^{-3}), acceleration due to gravity (m s^{-2}) and height of the tissue (m) in question (Woodruff et al. 2004).

$$Q = \frac{\Psi_r - \Psi_l - \rho GH}{R} \quad 1.4$$

So, at fixed ρ and G we can see that attempting to pull water higher reduces flow rates for fixed resistance of the flow path. This gravitational component of water potential acts on leaves whether the xylem is open to the atmosphere or not.

The xylem vessel network of angiosperms is equivalent to a network of vertically interconnected and branching pipes, as per Figure 1.5 (Shinozaki et al. 1964; Tyree and Ewers 1991). The resistance, R , of an individual section of xylem vessel, k , is defined by the length, l (m) and cross sectional xylem lumen radius, r (m), considering a constant viscosity of sap within the plant's xylem tissue, η (Pa s).

$$R_k = (8\eta l_k) / (\pi r_k^4) \quad 1.5$$

This equation shows that resistance increases with the length of the conduit but decreases in wider conduits (Tyree and Ewers 1991). This is because a greater volume of water is not in contact with the frictional forces associated with the wall of the xylem vessel, and since area increases greatly for a given increase in diameter small changes in xylem conduit diameter yield large decreases in resistance (Jeje and Zimmermann 1979).

Should xylem vessel diameter remain the same up a plant, then the resistance should increase linearly with the length of the stem, and therefore flow rates would decrease without adjusting the water potential gradient. Plants have therefore evolved tapering of xylem vessels from the apex of the plant to the base which permits resistance to increase more

slowly with increasing tree height or path length, where increasing xylem vessel lumen area from apex to base reduces the additive effects of path length, as per Figure 1.4 and Figure 1.5 (Ewers and Zimmermann 1984; West et al. 1999).

The equation below shows how total resistance of a vertical system of interconnected xylem vessels that branch repeatedly from the base of the plant to the tip of the plant can be maintained despite increases in path length (West et al. 1999). This simple model of xylem structure assumes a similar branch rate (n) along the flow path and also similar vessel length (l) along the flow path with a total length L . The model includes $N-1$ bifurcation levels. If the vessels are numbered from the base upwards and resistances (R_1, \dots, R_N) then the total flow path resistance (R_{tot}) is

$$R_{tot} = \sum_{k=0}^N R_k = \left[1 - \frac{[(n^{-\frac{1}{3}} - 1)L/l]^{(1-6\bar{a})}}{1 - n^{\frac{1}{3} - 2\bar{a}}} \right] R_N \quad 1.6$$

Total resistance is calculated as the sum of resistance R_k of conduits of each level k from the smallest vessel at the apex (level N) to the base where vessels are widest (level $k=0$). The rate of change in vessel diameter along the flow path is described by \bar{a} , known as the tapering coefficient (West et al. 1999). This value defines how large vessels become at each subsequent level. The tapering coefficient (\bar{a}) is calculated as the ratio of vessel radii at subsequent levels (r_{k+1}/r_k) divided by the rate of branching between subsequent levels (n_{k+1}/n_k) (see Figure 1.5 for a representation of vessel tapering).

$$\bar{a} = - \frac{(\log(r_{k+1}/r_k)/\log(n_{k+1}/n_k))}{2} \quad 1.7$$

This shows that a greater branch rate for a given change in vessel diameter increases resistance, because there are more smaller vessels leading to a greater surface area to provide resistance.

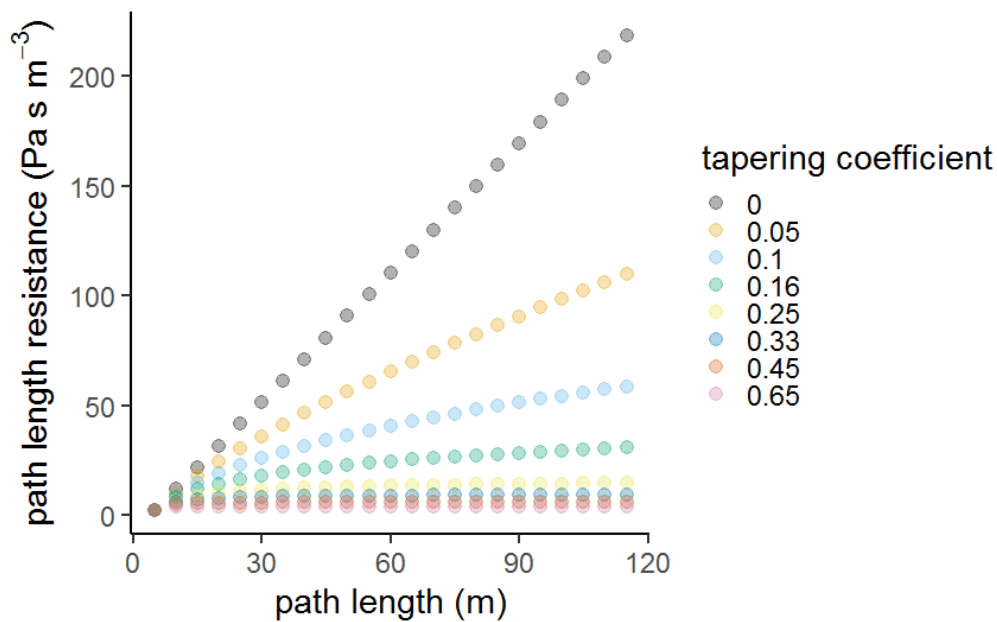


Figure 1.4 An example of the effects of vessel tapering on path length resistance. In this example different tapering coefficients are applied to equation 1.6, where the tapering coefficient was calculated using equation 1.7, in which branch rate, n , was kept constant across the different individuals represented here by colours.

Different values of \bar{a} give different values of total resistance with path length. A \bar{a} with a value higher than 0.2 indicates that path length after a certain point ceases to contribute to path length resistance. For values much greater than 0.2 there is diminishing benefit in resistance reduction (Figure 1.4). Bifurcating vessels ($n_{k+1}/n_k=2$) would need to increase in diameter by a factor of 1.6 between subsequent vessel sections in order to achieve $\bar{a} = 0.2$ (Anfodillo et al. 2006; West et al. 1999).

So, at high enough rates of tapering the additive effects of path length resistance can be almost completely compensated for. However, it is important to note that these resistance values ignore other vessel anatomical characteristics that play an important role, such as the end wall and inter-vessel pits that increase the surface in contact with water molecules and thus increase resistance to water flow (Lancashire and Ennos 2002; Lazzarin et al. 2016a; Medeiros et al. 2019). These anatomical features may also become less resistive as trees grow taller in order to provide similar effects to vessel diameter tapering (Lazzarin et al. 2016a).

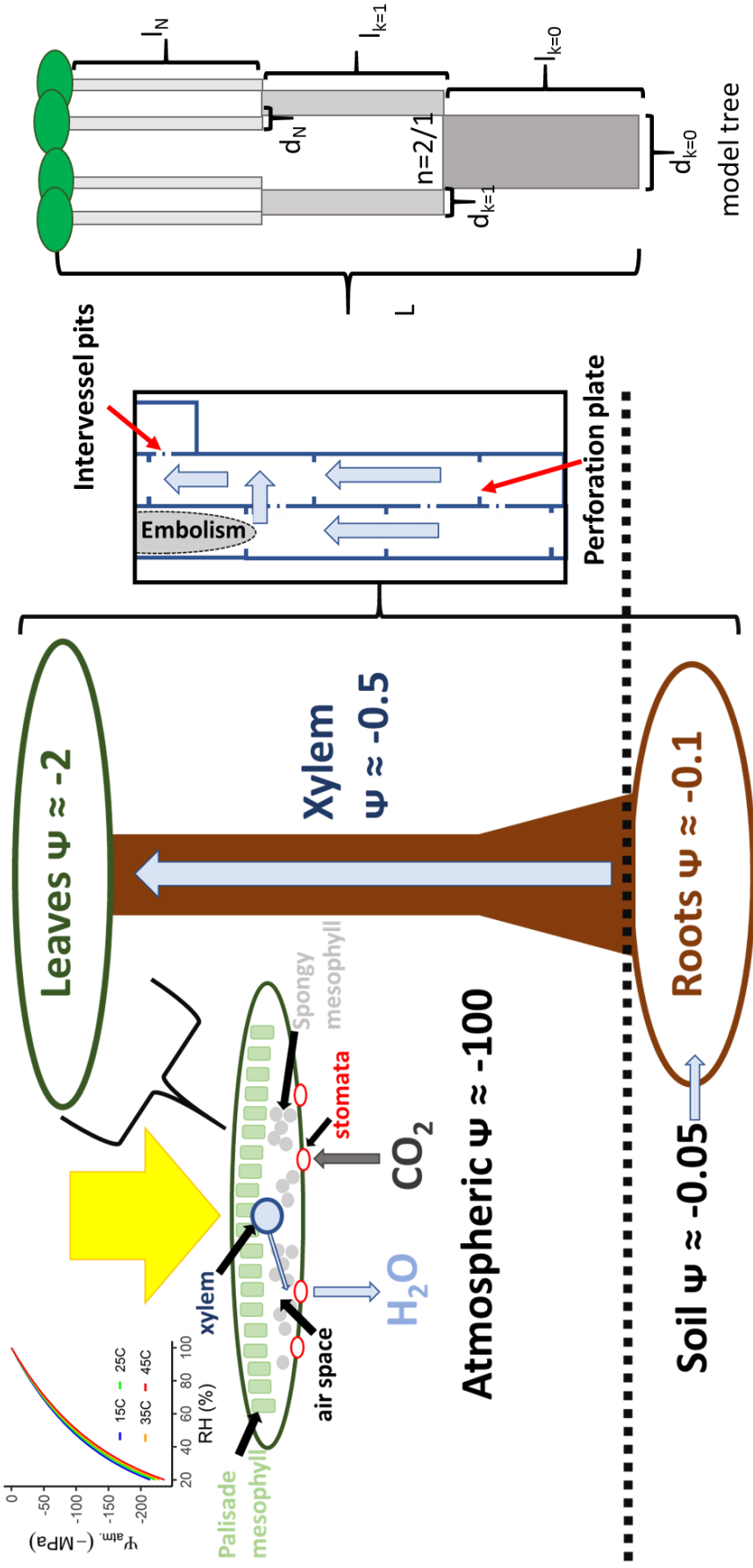


Figure 1.5 Representation of a tree and the movement of water from the soil where water potentials are high, to the atmosphere where water potentials are low. Water along a gradient in water potential from the base of the tree to the leaf, where water evaporates at the spongy mesophyll in the leaf and exits to the highly negative atmosphere through the stomata. Xylem vessels decrease in size from the trunk to the leaves and simultaneously divide to supply water to the many leaves. This reduces the resistance increases due to growing tall since the lower vessels are wide and few. When water potential becomes low, e.g. due to increasing temperature and reduced humidity (see inset graph) embolisms may form. Water travelling up the xylem can circumvent blocked vessels by lateral flow through inter-vessel pits.

1.3.2 The role of stomatal regulation for water flow

We have described how trees can pull water vertically and need to have a pressure gradient and specific xylem structure to do so. By increasing the pressure gradient and decreasing the resistance along the flow path the rate of water flow can be maximised. Xylem structure cannot change in the short term. Within a growing season or even across many years the xylem vessels are fixed. Climatic conditions and evaporative demand however do change within days therefore modulation of sap flow depends upon changing the pressure gradient by closing the air spaces within leaves (Hogg and Hurdle 1997). This thereby controls the rate of evaporation (i.e. water loss) from the leaf and therefore the pressure gradient between root and leaf.

Under steady state sap flow conditions, transpiration at an area of leaf, E_L ($\text{m}^3 \text{s}^{-1}$), and leaf area specific sap flow, Q_L , are equal due to conservation of mass of water. Transpiration can be calculated as the conductance of water for an area of leaf (g_L , $\text{m}^3 \text{s}^{-1} \text{m}^{-2}$), multiplied by the total leaf area (A_L , $\mu\text{mol m}^{-2} \text{s}^{-1}$) (Martinez-Vilalta et al. 2014). This is increased by the tendency of water to evaporate to the atmosphere at increased rate at higher temperature and lower humidity (see inset graph of Figure 1.5) i.e. higher vapour pressure deficit (D , kPa):

$$Q_L = E_L = g_L A_L D \quad 1.8$$

From this we can see how altering the conductance of the leaf by closing the stomata can control water loss.

Stomata close in response to abscisic acid signalling and directly via low water potential in the leaf (Brodribb and McAdam 2013; Kang et al. 2010). Stomatal responses vary from isohydric where stomata maintain the water potential of the leaf at a similar level in response to water

stress, and anisohydric where plants permit water potential to fall (Brodribb and McAdam 2013; Klein 2014). So stomatal control of water potential in-turn controls water flow (Yi et al. 2017). This alleviates one of the main negative consequences of the cohesion tension mechanism of water transport; the maintenance of water at negative pressure which puts water in a metastable state in which gas bubbles are more likely to form (Hacke and Sauter 1995; Sperry and Tyree 1988; Tyree and Sperry 1989a).

1.3.3 Embolism avoidance

The origin of gas bubbles within xylem vessels is not certain, but evidence shows two origins for gas bubbles within xylem conduits:

- negative xylem pressures to draw air in to the xylem from outside the xylem, known as air-seeding, e.g. via cracks to the atmosphere (Choat et al. 2016; Choat et al. 2015; Ponomarenko et al. 2014).
- for water to spontaneously evaporate, or dissolved air to come out of solution, under negative pressure (Duan et al. 2012; Ponomarenko et al. 2014; Schenk et al. 2016).

Whatever the origin of the gas within xylem tissue, negative pressures appear to encourage the spread of these gas bubbles to neighbouring vessels (Choat et al. 2016).

Narrow vessels have been shown to prevent embolism formation and spread (Levionnois et al. 2021; Lobo et al. 2018; Olson et al. 2018; Prendin et al. 2018; Scoffoni et al. 2017; Sperry et al. 2006). This may be linked directly to smaller vessels directly resisting embolism spread, or indirectly because of a smaller area of inter-vessel connections in smaller vessels known as inter-vessel pits (Christman et al. 2009; Hacke et al. 2006; Wheeler et al. 2005). Inter-vessel pits are thought to limit bubble spread between individual conduits (Kaack et al. 2019), and

may enable water to circumvent blockages (see Figure 1.5 for an example of lateral flow via inter-vessel pits) (Taneda and Tateno 2007). Although in many angiosperms that grow in xeric habitats, xylem vessels tend to be isolated from one-another, presumably to prevent lateral spread of embolism across vessels (Brodersen et al. 2013; Schenk et al. 2008). Small pores lead to high surface tension through which gas bubbles cannot pass, but as water pressure becomes more negative the force of surface tension, γ , may be overcome and the bubble spread (Domec 2011). The smaller the pore the more negative the pressure difference, P , that can be sustained between connected vessels. So, the maximum pore radius, r , that can hold gas bubbles for a given pressure can be calculated:

$$r = -\frac{2\gamma}{P} \quad 1.9$$

The relationship between conductance loss due to embolism and water potential decrease under drying conditions is called a vulnerability curve. It is typically sigmoidal in shape and often is fitted to the following equation (Pammenter & Willigen 1998):

$$PLC = \frac{100}{1 + \exp(a(\Psi - b))} \quad 1.10$$

The greater the percentage loss of conductance (PLC) for a given water potential the less tolerant is a tree to dry conditions. Plant vulnerabilities to embolism are typically described by the water potential that gives a loss of conductance equal to 50% of maximum conductance, b , known as the P50 value.

These values must be placed in their ecophysiological context in order to give a meaningful view of the impacts that low water potentials will likely have on plant health. This can be done for example by calculating the hydraulic safety margin (HSM):

$$\text{HSM} = \Psi_{\min} - \Psi_{\text{P50}} \quad 1.11$$

The HSM is an ecologically interesting value since it compares the minimum water potential experienced at a site with the innate likelihood of a damaging level of embolism, the water potential that causes 50% loss of conductance (Delzon and Cochard 2014). The difference between the two values shows how close a tree is at a particular site to experience dangerous embolism. A global analysis by Choat *et al.* (2012) suggests that plants maintain minimum water potentials close to their P50 value regardless of biome type (<1MPa).

Propensity for vessels to embolise at a given water potential is strongly associated with xylem vessel diameter, where wider vessels lose conductance more rapidly under drought stress (Hacke *et al.* 2006; Holtta *et al.* 2011). Tropical trees, via selection and evolution, must select how to grow and survive, either by reducing vessel size and/or maintaining larger HSMs, but simultaneously reducing gas exchange with the atmosphere and thus productivity, or have wide vessels and/or permit low water potentials, improving productivity at the risk of embolism formation (Hacke *et al.* 2006; Markesteijn *et al.* 2011; van der Sande *et al.* 2019).

1.3.4 Water use efficiency and carbon balance

Intrinsic water use efficiency (iWUE, $\mu\text{mol m}^{-3}$) is a measure of how much photosynthesis (A) is done per amount of water that evaporates from the leaf via the stomata in exchange for CO_2 (Farquhar et al. 1989).

$$\text{iWUE} = A/g_s \quad 1.12$$

Photosynthesis depends upon the stomatal conductance and tendency for CO_2 to move from the air (C_a , $\mu\text{mol mol}^{-1}$) to the evaporation site in the leaf (C_i , $\mu\text{mol mol}^{-1}$) where water and CO_2 are exchanged (g_s is the stomatal conductance for CO_2) (Farquhar et al. 1989; Kusumi et al. 2012; Wong et al. 1979).

$$A = g_s (C_a - C_i) \quad 1.13$$

Isotope fractionation is used to assess iWUE in plants as ^{12}C is preferentially used in photosynthesis, therefore under stomatal closure when ^{12}C diminishes in air within the leaf a higher proportion of ^{13}C is used during photosynthesis (Farquhar et al. 1989). Because CO_2 concentrations in the atmosphere are increasing the iWUE of trees should also increase, potentially making them less vulnerable to drought events (Guerrieri et al. 2019; Swann et al. 2016). Stomatal closure may play a key role in the hydraulic strategies of trees, in particular the trade-off between carbon starvation during drought or hydraulic failure (Chen et al. 2019b; McDowell et al. 2008; Mencuccini et al. 2015).

As trees grow larger their respiration increases. In small trees this increase is relatively isometric as there is little tissue that is not metabolically active (Mori et al. 2010). In large trees the proportion of non-metabolically active tissue increases, thus the relationship between whole plant respiration and plant size may be expressed as a power law (Mori et al. 2010; Savage et al. 2008):

$$Y = FM^f \quad 1.14$$

Here Y is the metabolic rate of respiration ($\mu\text{mol s}^{-1}$), F is a constant ($\mu\text{mol s}^{-1} \text{kg}^{-f}$), M is the whole tree biomass (kg) and f is the exponent which dictates the shape of the relationship, which for herbaceous plants is close to 1, and in large woody plants is much less than 1 (Mori et al. 2010; Savage et al. 2008; West et al. 1997). However, Mori et al. (2010) show that f changes as tree size increases and thus a mixed-power function can be used to capture the transition from small tree power law to large, due to the differences in relative respiration per body mass. So, with each increment in growth of larger trees the relative cost increase in terms of respiration decreases.

1.3.5 The consequences of height for tall trees

As explained above Ψ_l declines with gravity at a rate of -0.1MPa for every 10m (Woodruff et al. 2004) and the resistance of the xylem, although may be maintained due to xylem tapering, likely makes xylem more vulnerable to embolism formation with increasing tree height (Olson et al. 2018). If resistance were not completely compensated by tapering, for example due to an increased number of inter-vessel pit connections (Kaack et al. 2019), then leaves would require even more negative water potentials to pull water to greater heights at a similar rate

of flow as per the original hydraulic limitation hypothesis that did not account for complete mitigation of resistance with height caused by vessel tapering (Ryan and Yoder 1997). As the HSM would become smaller, this would further increase embolism likelihood.

Taller trees are therefore at greater hydraulic risk due to lower water potentials and larger vessels (Prendin et al. 2018). As trees grow taller they may opt to reduce hydraulic risk e.g. by increasing stomatal control of water potential (Ambrose et al. 2010) or limiting the increase in vessel size, and thus embolism vulnerability for a given water potential with tree height, though this appears not to occur, and rather the opposite, apical vessels increase with tree height in order maintain constant hydraulic resistance with increasing path length (Echeverria et al. 2019; Olson et al. 2014). In particular CO₂ concentration within the leaf declines upon stomatal closure, and therefore photosynthesis rates and productivity decline. This problem may be exacerbated by the higher respiration costs of larger trees (Mori et al. 2010).

As trees grow taller they have broadly two options: to maintain productivity or hydraulic function. Either option has costs and may explain; why tree height is limited across precipitation gradients (Klein et al. 2015; Tao et al. 2016), tree mortality and growth during droughts (Bennett et al. 2015), and how trees and forests are likely to experience future changes in water availability associated with a changing climate (Fajardo et al. 2019).

1.4 Limitation of tree height hypotheses

What limits the height that trees can attain is not certain. Trees can grow very tall (Gorgens et al. 2019; Shenkin et al. 2019; Tng et al. 2012), but rarely do (Gorgens et al. 2020; Tao et al. 2016). Whatever causes limitation must be mediated by height growth rates (trees grow less in height as they get taller) and/or mortality rate (trees die before they can grow taller). There

are many complex processes that may affect the height growth and mortality of trees, but at the broad scale several hypotheses are more likely. Known ecophysiological disadvantages of pulling water to great height suggest water limitation of tree height attainment (Ryan and Yoder 1997). Nutrient limitation of plant growth is a well-established concept in plant biology and too may affect how tall trees may grow since larger bodies require more nutrients over their life and thereby deplete surrounding soil, necessitating greater fine root investment (Gower et al. 1996). Larger bodies also require more energy from photosynthesis, so unless photosynthetic capacity also increases height may be limited by respiration demand relative to photosynthesis (Gower et al. 1996; Koch et al. 2004). Additionally, being tall puts trees under greater mechanical strain and at risk of breaking or falling in strong winds (Niklas 2007). Thus, several mechanisms may influence tree height limits.

1.4.1 Hydraulic limitation of tree height

The hydraulic limitation hypothesis states that as trees grow taller their ability to pull water to great height diminishes (Ryan and Yoder 1997). Part of the reasoning behind this is the work (energy) needed to move water against gravity and increasing resistance of the xylem network increases with tree height. The tapering of xylem conduits represents a way to negate resistance increases with increasing tree height, while the effects of gravity are unavoidable. So taller trees have wider basal vessels to overcome resistance increases and have more negative water potentials due to the gravitational component of water potential at the apex of the tree. This makes them more vulnerable to embolism, and therefore more at risk of dehydration related mortality during droughts (Levionnois et al. ; Liu et al. 2019; Liu et al. 2018; Prendin et al. 2018). Trees may adapt to this increase in risk by changing their hydraulic behaviour. For example, trees that are isohydric are likely to maintain their leaf

water potential at a less negative value in order to reduce embolism risk (Martin-StPaul et al. 2017). The consequences of this however are that photosynthesis rates are reduced under stomatal closure (Flexas and Medrano 2002). Alternatively taller trees may shed leaves in order to maintain moderate water potentials within the xylem and avoid dehydration and death either as a process or due to death from dehydration of leaves with smaller hydraulic safety margins (Liu et al. 2015; Wolfe 2017).

Thus, we might expect tall trees to experience more hydraulic stress under a given water availability than shorter trees. So, when a drought occurs tall trees might be expected to be highly impacted relative to shorter trees, either by reduced growth rates, partial crown mortality or whole tree mortality.

1.4.2 Evidence for the hydraulic limitation of tree height

Early studies demonstrated the hydraulic limitation of tree height by showing vertical trends in physiological properties with tree height. A seminal study in giant 112m *Sequoia sempervirens* showed reduced water potential with increased tree height in addition to increased leaf mass per area (LMA), decreasing maximum photosynthesis rate and increased water use efficiency. Based on these observations the authors estimated a hydraulic limit to tree height of 123-130m based on (Koch et al. 2004). Negative water potentials in the stem have been shown to reduce shoot expansion in very tall conifers resulting in leaf structural modification such as increased LMA (Ambrose et al. 2016; Chin and Sillett 2016; Chin and Sillett 2017; Koch et al. 2004; Mullin et al. 2009; Nonami and Boyer 1990; Woodruff et al. 2004). This may explain a maximum theoretical limit to trees height under ideal conditions (Burgess and Dawson 2007).

Tree height distribution along water availability gradients provides evidence for the HLH. Across the Amazon trees grow taller in regions with high water availability, namely high clay percentage soils, high number of cloudy days indicating low seasonality and moderate to high precipitation between 1500 and 2500 mm per year (Gorgens et al. 2020). Other remote sensing based studies have shown a strong relationship between forest height and water availability, using potential evapotranspiration and precipitation minus evapotranspiration that estimate the amount of water available to the plant (Klein et al. 2015; Tao et al. 2016). These studies show that below a certain value of water availability forest height increases linearly with water availability, as expected under the HLH. Above this value of water availability forest height ceases to increase, likely as other factors limit height attainment.

The drought responses of tall trees may reflect limitation of tree height, namely whether trees stop growing due to hydraulic stress reducing photosynthesis or die from either hydraulic failure due to embolism formation, or Carbon starvation (McDowell et al. 2008). Droughts provide a way to test whether tall trees are suffering from more hydraulic stress relative to short trees as any negative change in environmental water availability should induce greater physiological stress in tall trees. A global metanalysis of the studies analysing tree responses to drought showed both that large diameter trees experience lower growth rates and higher mortality rates during drought relative to smaller diameter trees (Bennett et al. 2015). A recent study of an 8 year drought event in California showed that taller trees were more likely to die (Stovall et al. 2019). Evidence from long term drought experiments in the Amazon show that after only 60% of rainfall was permitted to reach the soil tall trees die at a much higher rate than medium and short trees (Nepstad et al. 2007). A similar Amazonian throughfall study showed rapid death and lack of decline in growth rates of tall trees to indicate hydraulic failure as the mechanism behind drought mortality of tall trees (Rowland et al. 2015). Satellite

derived forest height measurements taken before and after the 2005 Amazonian drought showed forest height decreased by ~1m in the worst drought affected regions within 2 years, likely due to defoliation and mortality associated with hydraulic stress (Yang et al. 2018b).

1.4.3 Nutrient limitation of maximum tree height

As trees grow taller they use the nutrients which they need to acquire in the soil in their immediate vicinity. The nutrients that are being locked within a large living tree are not available, so the soil around the tree is likely to be depleted in soil nutrients and limits further growth (Gower et al. 1996). This point of limiting low nutrient availability should occur at lower height in soils that have an initial low soil nutrient concentration.

Many studies show some degree of nutrient limitation of the growth of tropical trees, typically by showing changes in growth rate upon nutrient addition relative to controls, as well as along naturally occurring gradients, but few show limitation of the maximum height attainable by trees and none in the tropics (Turner et al. 2018; Wright 2019). Some of the few studies that examines the effects of nutrient addition in relation to tree size finds no impact of nutrient addition to tree diameter growth in the largest examined size classes of tropical and subtropical trees (Fisher et al. 2013; Li et al. 2018). A recent study located in lowland Guiana shield forest, which produce some of the tallest neotropical trees, showed that nutrient availability did not impact forest biomass (Soong et al. 2020a). Evidence also suggests the largest trees continue to increase in biomass, i.e. increasing diameter (Stephenson et al. 2014), suggesting nutrient availability may not directly set limits to tree stature.

1.4.4 Metabolic allometry limits to tree height

Taller trees have larger bodies. The height-diameter allometries of most trees show that trunk diameter increases at a greater rate relative to height as trees grow taller (Feldpausch et al. 2012). These larger bodies use more energy in order to respire (Mori et al. 2010; West et al. 1997). Allocation of resources to other non-photosynthesising organs also increases with tree size, e.g. reproduction often starts in tall mature trees (Wright et al. 2005). Allocation to root biomass relative to shoot biomass (implying a measure of productivity) however decreases with tree height across biomes (Qi et al. 2019). Total leaf area tends to increase more slowly with body size in larger trees, and photosynthetic capacity per leaf mass tends to decrease with tree size, suggesting limits to photosynthetic productivity (Koch et al. 2004; Tu 2019; Xu et al. 2014). The leaf area relative to conducting wood also decreases with tree height, suggesting further reductions in productivity relative to respiration with increasing body size (McDowell et al. 2002). So, trees with limited photosynthetic capacity use a larger percentage of the maximum photosynthate. At some point the tree will either stop growing or starve. Trees in drier conditions tend to have larger trunk diameter and increased allocation of biomass to the roots for a given height and thus may explain partly why trees in drier regions should be shorter (Banin et al. 2012; Feldpausch et al. 2012; Givnish et al. 2014). However, if trees follow the power law of metabolic demand and body size (equation 1.14), and metabolically active sapwood relative to inactive heartwood decreases with tree size (Lehnebach et al. 2017), the increasingly small incremental increase in energy demand with increasing tree size may not limit height.

Considering that as trees grow taller leaf size tends to decrease, and leaf mass per area increases, it might be expected that productivity should decrease with body size, regardless

of increased metabolic demand of the woody portion of the tree. However, some studies have shown photosynthetic capacity of tropical trees increases with tree height (Kenzo et al. 2006; Rijkers et al. 2000). In line with this several studies including very large tree sizes show that growth rates increase with tree size (Sillett et al. 2010; Stephenson et al. 2014), though there is a paucity of evidence of this type showing changes in growth within individual trees (Sheil et al. 2017), and several studies demonstrate slowing of diameter growth with tree size (Lehnebach et al. 2017; Mencuccini et al. 2005). This might suggest that this mode of height limitation does not occur widely (Banin et al. 2014). Unfortunately, total respiration is difficult to measure in large trees in nature, so understanding the contribution of size related changes to tree Carbon budgets and thus height limitation are unclear, and though theoretically possible are inconsistently supported by evidence (Ryan et al. 2006; West 2020).

1.4.5 Other limiting factors

Being tall is associated with other risks that might limit achievable height. For example, tall trees experience higher wind stress (Mayer 1987). Therefore regions with high wind speeds, such as Caribbean islands and Australian rainforest that are exposed to hurricanes and cyclones have lower maximum tree height compared to nearby tropical forests outside of the path of such storms (Ibanez et al. 2019). A study of remotely sensed forest height showed that across the Brazilian Amazon tall trees are strongly associated with regions with low wind speed (Gorgens et al. 2020). Also, anecdotally the tallest tropical tree found in Borneo was located on the sheltered side of a ridge. Trees on the exposed side of the ridge were ~30m shorter (Shenkin et al. 2019). Lightning strike is an additional source of mortality that affects taller trees in lowland tropical forests more than shorter trees (Yanoviak et al. 2020). Since storm intensity may increase with climate warming tropical forest maximum height may be

negatively affected (Pinto and lee 2013; Walsh et al. 2019). The frequency and intensity of other disturbance events that increase mortality rates such as floods, fire may also play a role in limiting forest height (Balch et al. 2015; Resende et al. 2020).

Tree height may be limited due to lack of need to grow taller. For example, understory rainforest tree species do not grow tall, they maintain their height below the canopy in less productive but hydraulically safe conditions with few competitors (Guo et al. 2017; Nepstad et al. 2007). Canopy level trees tend to grow to a similar height in the canopy, with outstanding emergent trees being rare, likely due to a balance between the losses of productivity in shade and the hydraulic stress and carbon costs for growing tall (Kuppers et al. 1996; Niklas 2007; Olson et al. 2018; Rijkers et al. 2000; Rodriguez-Calcerrada et al. 2019). Canopy trees have been shown to reduce their height growth increment upon reaching the age at which flowering occurs and likely represents a decrease in resource allocation to height growth due to increasing demand of reproduction (Suzuki et al. 2019). Competition for light should drive most canopy trees in a forest to their maximum productive height however (Schuster et al. 2008). Once trees reach a canopy and wind action increases they contact other trees, and experience wind strain, this causes mechanical stress thus inhibiting growth in branches and induces diameter growth in the mechanically stressed portion of the bole to increase strength (Anten et al. 2009; Coutand and Moulia 2000; Jaouen et al. 2010; Putz et al. 1984). This process of growth responses to mechanical stress is known as thigmomorphogenesis may therefore limit the ability of trees to grow further once they have reached the crown as they must invest more in reaction to mechanical stress.

1.4.6 Co-limitation among limiting factors

Limitation in a complex natural environment is often not caused by single factors but by a complex of factors. For example, low nutrient availability may limit a tree's ability to construct root systems and invest in hydraulically safe xylem networks or osmotic adjustment of water potential (Santiago 2015). Across a range of water availability *Eucalyptus* spp. tree height was found to be constrained by both water availability and the carbon resources required to produce new growth (Givnish et al. 2014). Another example of a complex of height limiting factors has been shown by the preference for some insect species to attack larger more hydraulically stressed trees during drought (Stephenson et al. 2019). Height limitation has also been shown to be caused by a trade-off between hydraulic limitation and nutrient limitation independently and when both hydraulic and nutrient resources are high the tallest trees are produced (Cramer 2012). Amazonian examples of complex factors affecting tree height limitation can be shown by white-sand ecosystems, where disturbance, water availability, nutrient poor soils, fire and waterlogging likely impact forest stature in localised pockets with highly sandy soils (Adeney et al. 2016). Modelled forest height that included a number of predictor variables found that multiple limiting factors enabled better predictions of maximum tree height, including allometric limitation, hydraulic limitation and radiation (Kempes et al. 2011).

1.4.7 The study of tree height limitation in the tropics

Tropical trees may differ from trees at higher latitudes in the mechanisms of height limitation. This is most obviously true when examining the limitation of height along the arctic tree line (Mao et al. 2019). Tropical forests do not freeze, excluding one of the main problems for trees growing in regions where tree sap freezes, namely freezing induced embolism formation

(Lemoine et al. 1999). Such differences may well confer differences in the limitations to the heights tropical trees may attain.

However, a high proportion of studies assessing the limitation of maximum tree height focus on temperate regions, specifically, those trees that attain particularly great heights e.g. *Sequoia* spp. and *Eucalyptus* spp. (Ryan et al. 2006). So, there is a lack of studies of tropical trees which can also reach great heights. Many of the previous studies assessing how hydraulics may limit tree height do so at single sites. Multi-site studies are particularly interesting in order to investigate the limits that trees can attain as these more clearly show limitation (Givnish et al. 2014). Current tropical studies of height limitation are restricted to remotely sensed data (Gorgens et al. 2020; Klein et al. 2015; Tao et al. 2016). Whilst extremely useful, this type of data is limited by relatively low resolution at large scale and lack of individual tree information such as taxon and many ecophysiological properties and functional traits.

The ecotonal regions of forest biomes are perhaps most interesting as these are most likely to experience dramatic shifts in tree communities. Such ecotones are where the limitation of tree height is expected to be most strongly experienced at the community level, as per the shape of the relationship between remotely sensed tropical forest height and water availability (Klein et al. 2015; Tao et al. 2016). Studies should focus on these regions in particular in order to assess how vulnerable tall trees are to changes in water availability.

1.5 Thesis aims and objectives

The overall aims of this thesis are to examine how tree height might be limited in tropical forests. Tree height is an important determinant of forest biomass and thus is important to

understand future impacts of climate change. Despite the importance of tropical forests relatively few studies focus on these highly biodiverse regions. Relatively recent discoveries of giant trees in tropical forests perhaps highlights the need to better understand height limit before tall trees are eliminated from these threatened regions (Gorgens et al. 2019; Shenkin et al. 2019).

1.5.1 Describe the role of water availability in determining the height of neotropical forest trees and differences at the taxon specific and community scale

Previous work has shown that tropical forest height is strongly determined by water availability (Gorgens et al. 2020; Klein et al. 2015; Tao et al. 2016). This matches the expectation that tree height is limited in many tropical forest communities by increased stress due to the need to pull water to greater heights (Ryan and Yoder 1997). Thus, in drier regions it becomes more difficult for trees to pull water to a certain height relative to wet regions. These studies have broadly been at the forest community level, either due to the broad scale nature of the data, such as LiDAR (Gorgens et al. 2020; Klein et al. 2015; Tao et al. 2016), or was not the aim of the study to delve beyond the level of the community (Feldpausch et al. 2012). What these broader studies do not show are taxonomic scale relationships between water availability and tree height attainment and how might the overall community canopy maximum height be composed of families, genera, and species. The first aim of this thesis which concerns tree height in neotropical forests specifically is to establish whether, using a large number of forest plot height data, neotropical forests are indeed limited by water availability and what metric of water availability best describes this. Then, are changes in the community maximum height reflected in changes in maximum height of individual taxa.

1.5.2 Examine the impact of climate on the xylem vessel tapering within a tropical tree species

Trees are likely to be able to avoid one of the main negative consequences of growing tall, namely frictional resistance to water flow up the tree, by increasing vessel diameter in vessels basal to the apex as height increases, thus each additional vessel added contributes increasingly little to overall resistance, provided that the increase in vessel diameter is high enough in relation to height increases (Anfodillo et al. 2006; Olson et al. 2014; West et al. 1999). This increase in basal vessel diameter with height is known as tapering. There are however negative consequences with having large diameter vessels, particularly in relation to embolism resistance, where numerous studies have shown larger vessels to increase the likelihood of embolism formation (which block water flow) at a given water potential (Levionnois et al. 2021; Lobo et al. 2018; Olson et al. 2018; Prendin et al. 2018; Scoffoni et al. 2017; Sperry et al. 2006). In drier regions water potentials tend to be more negative, thus a tree of a given height in a dry and wet habitat might be expected to differ in vessel diameter in order for the drier site tree to compensate for the increased embolism risk. We ask whether, in a broadly distributed tropical forest tree species, vessel diameter does indeed decrease for trees of a given height in dry relative to wet sites.

1.5.3 Investigate how functional traits and ecophysiological properties vary with height through the canopy and match the life-history strategies of three tropical tree species

Considering that different tropical forest species have different growth strategies, it has been shown that their ecophysiological properties in relation to growth and survival match, i.e. hydraulic properties and functional traits associated with high growth rate align with fast growing trees and properties associated with hydraulic caution align with slower growth

(Markesteijn et al. 2011; Poorter et al. 2010). Most studies in this regard in tropical forests focus on seedlings and ignore the potential impacts of height to adult stature and changing conditions through the canopy. We ask whether ecophysiological properties and functional traits change with height and whether clear differences between species are apparent and whether these align with their life-history strategies.

1.5.4 Research questions

In relation to the aims of this thesis we ask the following research questions:

- Using a large dataset of ground measured tree height across the neotropics, which environmental variables limit maximum forest height across the neotropics?
- Do individual neotropical taxa follow the same relationship as the overall forest tree height relationship?
- What degree is forest maximum tree height reduced due to shifts in composition or due to decrease in tree stature of the same taxa with water availability?
- Do tropical *Cedrela odorata* trees maintain a xylem network that minimises resistance according to the predicted scaling law?
- Do tropical *Cedrela odorata* trees favour hydraulic efficiency or safety when growing in dry versus wet conditions?
- How do ecophysiological properties and traits change up a height gradient in three neotropical species differing in life-history strategy?
- Do these different species' physiological properties and traits represent different life-history strategies?

Chapter 2 Overview of Methods

2.1 Introduction

We investigate a range of scales to assess the question what determines height in neotropical trees. From within tree measurements at a single site, across-sites measurements of individual trees and across the whole neotropical forest community. Such an approach requires a variety of research techniques and data acquisition methods. Integrating data from different scales on tree height attainment and ecophysiological relationships with height will help to capture some of the complexity of the height limitation of tropical trees that may be less well appreciated by looking at a single scale.

Specifically, our approach asks how water availability limits the maximum sizes of trees at the community and taxon level. This is answered using plot data, small inventoried areas of forest that have the trees identified to species level within them and measured their height. Previous studies in the tropics have used remote-sensing data to determine the relationships of forest maximum height with water availability, which though very useful lack the detail that in-situ data can bring (Gorgens et al. 2020; Klein et al. 2015; Tao et al. 2016). We also ask how across sites differing in water availability tree xylem vessel anatomy differs. We answer this question using a small number of sites covering the range of water availabilities of a single species and one congeneric species. Very little work has investigated how xylem vessels taper with height in the tropical trees. The only existing similar study has looked at this question for low statured temperate trees (Fajardo et al. 2020). We then ask how tree height determines a suite of functional traits and ecophysiological properties within and across individual trees at a single site, and across species differing in life-history strategy. To answer this, we select

three species on a spectrum of shade-tolerance at a single site that experiences a pronounced dry season and attempt to determine the hydraulic stress trees at different height experience as well as other functional trait changes as trees grow taller. Previous studies in these same species focused only in juvenile trees (Markesteijn and Poorter 2009; Poorter and Bongers 2006), we however use a range of tree sizes from juvenile to the maximum heights available at the site.

2.2 Species and site selection

Our research focuses on neotropical forests, a region that contains the highest angiosperm plant diversity (Antonelli and Sanmartin 2011; Antonelli et al. 2015). We do not use any montane forest sites, as altitude related temperature and atmospheric pressure (CO_2 partial pressure) may complicate interpretation of results (Körner 1998; Malizia et al. 2020; Wittich et al. 2012). We also do not use any sites that have trees but are not forest, e.g. savanna, nor sites that are frequently inundated, e.g. mangrove or swamp forest. This avoids a number of complicating factors, e.g. large-scale fire disturbance (dry forest sites we investigate do burn, but evidently not severely enough to reduce forest cover) (Gould et al. 2002), and a presumed relative independence from climate induced water availability due to high water tables (Sousa et al. 2020).

This research concerns only arborescent species, in the lowland neotropics this is almost entirely angiosperm species (Ghazoul and Sheil 2010b). The neotropical angiosperm tree species we study can be divided between palms (Arecaceae, monocots) and non-palms (eudicots, the majority of neotropical tree species, and magnoliids, most within Lauraceae) (Byng et al. 2016).

We study the tropical forest community as a whole in Chapter 3, utilising the majority of tree species, genera and families that fit the abundance criteria we lay out in that chapter. We study some selected species more closely in Chapters 4 and 5. Chapter 4 attempts to show how xylem vessel anatomy changes over large gradients of water availability within a species. There are few tropical species that range from very low water availability (for a tropical forest) to very high water availability (Esquivel-Muelbert et al. 2017a). We selected a species that occurs from seasonally dry forest to aseasonal wet tropical forest, *Cedrela odorata* (L. Meliaceae), and a congeneric, *C. salvadorensis* (Standl.). For Chapter 5 we focus on three tropical tree species, *Ampelocera ruizii*, *Pseudolmedia laevis*, and *Centrolobium microchaete* which co-occur in a semi-evergreen forest at the ecotone between wet Amazonian type forest and seasonally-dry Chiquitano forest. These species have been shown in juvenile trees to be classified along a gradient of shade-tolerance and with different functional traits (Markestijn and Poorter 2009; Poorter and Bongers 2006). *P. laevis* is a slower growing shade-tolerant tree, *C. microchaete* being a faster growing shade-intolerant species, and *A. ruizii* being an intermediate with fast growth and shade-tolerance traits.

2.3 Environmental data for our sites

Data characterising the environment of the study sites used in the research Chapters in this thesis were collected from different sources. The environmental data of Chapter 3, soil texture, insolation, and climate were taken from global datasets in order to cover the wide range of forest locations in this study across tropical South America. Precipitation and temperature variables were downloaded from Worldclim at 2.5 minute spatial resolution (Fick and Hijmans 2017). Direct normal irradiation (kWh m^{-2}), the radiation that arrives perpendicular to any unit area of the earth's surface, was obtained from Global Solar Atlas

2.0 (Solargis). We also used global maps of soil texture characteristics (bulk density kg m^{-3} , clay %, sand % and silt % at 15cm) which were downloaded from SoilGrids at 1km resolution (Hengl et al. 2014). See SI Table 3.2 for full details.

In Chapter 4 four sites were used to compare the xylem anatomy of trees across a water availability gradient. Using the Global Historical Climatology Network-Monthly (GHCN-M) dataset (Peterson and Vose 1997) we collected weather station data from the two nearest weather stations for most sites, but for one site there was only one weather station near to the study site (Selva Negra, Bolivia). These weather stations had data covering different time-periods and differed in completeness (i.e. years and months with missing data). We averaged the monthly mean temperature and precipitation across the available years for each site to estimate monthly precipitation and temperature, and annual precipitation total. See Table 4.1 for full details.

For Chapter 5 we focus research at a single site. Here we directly measure the environmental conditions of the site at the time of measurement to assess the progress of the dry season using a Hobo climate sensor (UX120 series, Onset Computer Corporation, Bourne, USA). Whilst the background monthly climate data and soil characteristics of the site were previously measured using a temporary weather station (Araujo-Murakami et al. 2014). Specifically, the site has a MAP of 1352mm year^{-1} , with a 6-month dry season with less than 100mm month^{-1} . It has sandy loam type soil (76% sand, 16% clay) and relatively high phosphorous concentration.

2.4 Height measurement

The methods of height measurement differed amongst the three research Chapters. Chapter 3 uses tree height measured over many plots by different teams. The different methods include estimation by eye, clinometer where the angle to the top of the canopy and the distance to the base of the tree are manually measured to calculate tree height, with laser range finder, where the angle and distance are automatically measured and height calculated, as well as direct measurement (e.g. climbing or using a tower). Chapter 4 uses only the estimated height of trees. Teams who collected the height data calibrated their estimates of height with some trees of known height that were felled. Chapter 5 used only laser range finder measurements to determine the height of trees and sample points, except in the case of very small trees where a tape measure was more practical.

2.5 Wood samples and xylem vessel anatomy measurement

We use wood samples to measure the xylem vessel width and density (number of vessels within an area) in Chapter 4 and 5. In Chapter 4 wood samples were collected only from the bases of trees at a measured trunk diameter and height above ground. Wood samples were usually collected using an increment borer of either 5mm or 10mm increment borers where wood cores were withdrawn (generally to the centre of the tree). Wood cores were then fixed to wood panels using glue. In the cases of very small trees the entire base of the tree was available to use as the wood sample. Wood cores were stored for several years after the sample collection from the field before being used for this thesis.

The wood samples of Chapter 5 were collected in a similar manner to Chapter 4. Wood samples were collected from the trunk of the sampled trees, however not only at the tree

base. We also collected one sample at the point of the lowest branch of the crown and one sample between that point and the base. Due to difficulty in extracting cores using an increment borer whilst suspended on a rope to collect the upper two trunk samples it was often only possible to collect shallow cores of several centimetres depth. Branch wood samples were also collected, which consisted of 4 disks sawed off of a large cut branch. One disk was cut at the apex (5cm below tip), one at the base of the branch and two equidistant in the middle between the apex and base of the branch (see the methods section of Chapter 5 for diagram of wood sampling strategy).

Photographs were taken of the exposed wood surface of the wood cores for Chapter 4, different from the methods typical used for wood anatomy studies, which generally use thin sections cut using a microtome and placed in glass slides for visualisation. We proceeded in this way in Chapter 4 because we had fixed the wood cores with glue to a wooded frame and because some wood cores had been damaged by wood worm and fungus at the wood surface. Early attempts to liberate cores from their wood frames resulted in disastrous breakage of the wood cores. Photographs consisted of two sample types (see methods section of Chapter 4 for specific details). Type 1 (inter-tree): outer sapwood photographs of many individual trees (with the height of the tree known). Type 2 (intra-tree): photographs taken along the whole length of a wood core from outermost sapwood to the inner core at the centre of the tree. The centre was determined by the concentric nature of rings and often a central pith and height of any sample point estimated by site-specific diameter height allometry. Wood photographs covered areas of 2cm in the outer wood but the measured area became smaller in the very central wood where vessels were very densely packed and growth rings much thinner. For Chapter 5 thin sections were taken of the wood samples using a microtome, typically cut to 20 μ m thickness depending upon the structural qualities of the wood of each

species and position of the sample (branch sections were cut using a saw first if too large to fit within the microtome) (Gartner and Nievergelt 2010). Thin sections were then placed within slides for photography under a microscope.

Images were taken at different magnification depending upon the size of the vessels within the sample i.e. higher magnification at the apex and in small trees (see Chapter specific methods). Vessels within the images of the wood surface and thin sections were measured manually using image-J (Fiji, version 1.52p). The area of wood in which vessel area was measured was used to calculate the density of vessels per wood surface area. Generally, ~100 vessels were measured per sample (Scholz et al. 2013). When vessels were very densely packed (e.g. in small trees or at the apex of a branch) the measured area was reduced to reduce the workload.

2.6 Functional traits and ecophysiological properties

In Chapter 5 we present and analyse a number of ecophysiological properties and functional traits in addition to xylem vessel anatomy (as outlined in the previous section) that reflect hydraulic safety and productivity. Specifically, we measure the leaf area and leaf mass to obtain the mean and maximum leaf area and leaf mass per area (LMA) of each sample.

We also measure the length and density of stomata guard cells in a subsection of the same leaves used for leaf area and LMA. We impressed dental putty onto the underside of the leaves to generate a negative of a small area of the underside of a leaf. This putty was then painted with nail varnish which once dried produces a copy of the stomatal anatomy of the underside of the leaf. The transparent nail varnish was then transferred to a glass slide and photographed using a GXCAM microscope mounted digital camera (GXCAM-U3PRO-6.3, GT

Vision Ltd.) with a 6.3 megapixel lens mounted to an Olympus CX43 microscope at 40X magnification. ImageJ was then used to measure stomatal length using the software's measuring tools and count the number of stomata in area of 0.33mm^2 to determine the density.

Additionally, we use the same leaves for the extraction of α -cellulose following the protocol of Wieloch et al. (2011) in order to measure the proportion of ^{13}C to ^{12}C . In this process leaves were cut into small pieces and placed in 5% NaOH solution twice for two hours. Samples were washed with boiling water to remove remaining NaOH solution. Samples were then placed in 7.5% NaClO_2 solution for 8 hours. Samples were again washed with boiling water to remove remaining NaClO_2 solution. After this samples were freeze dried overnight and kept dry in airtight centrifuge tubes. 0.3mg of each cellulose sample were transferred to tin capsules for mass spectrometry analysis. The mass spectrometry analysis was performed at the University of Leicester using an isotope ratio mass spectrometer (20-20 continuous flow isotope ratio mass spectrometer, Sercon Ltd.). The Carbon isotope ratio of the samples was compared to the isotope ratio of an α -cellulose standard.

We measured the leaf water potential of leaves collected in the field using a pressure chamber (PMS 1505D, USA) which uses nitrogen gas to generate pressure within a chamber. Leaves were cut from a tree and immediately placed in a plastic bag made humid by blowing into them. This maintains the hydraulic status of the leaf as little water will evaporate from the leaf. Within ~ 15 minutes of being cut leaves were then placed within the pressure chamber with a freshly cut petiole exposed to the atmosphere where it can be easily viewed. As nitrogen enters the chamber it increases the pressure. As the positive pressure within the chamber cancels the negative pressure within the leaf, water is squeezed out of the petiole.

The pressure within the chamber at the point that water first appears out of the petiole is the leaf water potential. This was measured at several points throughout the day, at two points as the dry season progressed. Drier conditions lead to more negative leaf water potential. The water potential of the leaf gives a snapshot of the plants water status at the time of measurement.

We also measured vulnerability curves for the assessment of embolism risk for a given water potential. The method used in Chapter 5 is the pneumatic method, which measures the volume of gas expelled during drying. This measures embolism indirectly since the air discharged represents the embolism present within the branch (Pereira et al. 2016). This method produces similar results to the hydraulic method of producing the vulnerability curve which measures the change in conductance to water flow of xylem vessels (Pereira et al. 2016).

2.7 Determining relationships with height

For Chapter 3 we determined the relationships between environment and tree height across a large area and at different scales from community to species. We did not assume any functional form of these relationships a priori. We used generalised additive models to constrain these functional relationships. These models were limited to predict smooth relationships in tree height per unit change in any environmental variable. This avoids overfitting and we did not expect large erratic changes in tree height for small changes in any environmental variable (Zuur et al. 2009). We used the R^2 value, and AIC (Akaike information criterion) and GCV (minimised generalised cross-validation) scores to compare between models to find which environmental variables best predicted maximum tree height, and both

the R^2 and the effective degrees of freedom (a measure of underfitting) in order to determine if any relationship was present at the taxon level.

Relationships between wood xylem vessel diameter and density and height we observed non-linear relationships, as expected, therefore to linearise and to compare with the literature we log-transformed our dependant variables (height and xylem vessel diameter and density). All traits and physiological properties in Chapters 4 and 5 were related to height by linear regression analysis. All analyses were made using R version 3.5.1 (R Core Team 2018).

Chapter 3 Environmental and taxonomic variation in maximum tree height across the neotropics

Abstract

Tree height is an important determinant of tropical forest structure, biomass and diversity. Canopy height is known to decrease with water availability, but it is poorly known to which degree this variation in tree height is the result of changes in species composition, or rather due to universal within-species changes in height with water availability. Few studies have investigated how maximum tree height varies and its climatic controls across taxa since remote sensing data do not permit analysis at the taxonomic level. We address the question whether forest height changes with environmental variables are the result of changes in taxa across environmental gradients, or due to height-environmental relationships within taxa. Answering this question contributes to predicting how tropical forest height, and thus biomass, may shift in response to changing precipitation and temperature under climate change. We investigate this question here for the neo-tropics, using data from 202 plots, including height data from 45,000 trees and 2500 species. We find that maximum forest height of all forest plot data is strongly positively related to mean annual precipitation (MAP) up to ~2700mm, with a decline in maximum height at higher MAP. Across families a remarkably similar relationship to the overall forest dataset is found, with maximum height attainment peaking on average at 2450mm MAP, though reaching different maximum

heights. Similar results are found for those genera with sufficient data. Species with small ranges or abundances tend to attain maximum height closer to the maximum height of the community rather than their own centre of abundance, implying within-species changes in maximum height with MAP. Similar responses of families to MAP in terms of maximum height attainment suggest that under climate shifts trees of these families will behave similarly to the overall forest community, so composition of forest upper canopies at specific locations at the family level may be similar regardless of changes in water availability.

3.1 Introduction

Tropical forests hold 62% of global forest biomass (Chen et al. 2019a). Neotropical forests have particularly high biomass density, 1.7 times greater than temperate forests and 3.3 times greater than boreal forests (Chen et al. 2019a). However, Amazonia is gradually losing its capacity to act as a carbon sink due to increasing tree mortality and stagnating growth rates (Brienen et al. 2015). The height that trees attain is a major determinant of forest biomass (Feldpausch et al. 2012). The largest trees in Amazonian forests are responsible for a disproportionately large fraction of overall Amazonian biomass (Fauset et al. 2015). Understanding what limits how tall Amazonian trees grow, and therefore their capacity to store carbon, is important for predicting forest responses to climate change.

Current distributions of neotropical forest heights as determined by remote sensing show a strong positive relationship with water availability (Klein et al. 2015). This relationship with water availability breaks down at high water availabilities, as forest height ceases to increase, or even decreases with further increases in water availability (Gorgens et al. 2020; Tao et al. 2016). The positive change in forest height with water availability is likely due to the hydraulic limitation of forest height at lower water availability (Koch et al. 2004; Ryan and Yoder 1997).

Whilst the negative change in forest height with water availability at very high water availability may be due to stressful soil saturation causing anoxic conditions that may inhibit root growth and thus make trees vulnerable to windfall (Aubry-Kientz et al. 2015; Ferry et al. 2010; Herault and Piconiot 2018). Cloud cover inhibiting photosynthesis may also play a role (Graham et al. 2003; Guan et al. 2015). At locations with very high precipitation nutrient limitation may become increasingly limiting, possibly enhanced by high precipitation leaching soil nutrients (Cramer 2012; Fisher et al. 2013; Fujii et al. 2018; Givnish et al. 2014; Posada and Schuur 2011). Thus, water availability is likely one of the main factors determining why tropical forests grow to the heights they currently achieve.

Climate change is likely to increase the frequency of droughts, such as during ENSO events (Jimenez et al. 2018; Jimenez-Munoz et al. 2016), and, as a consequence of deforestation on the hydrological cycle, precipitation for parts of the Amazon will be reduced (D'Almeida et al. 2007). These changes in water availability are likely to disproportionately affect tall trees, as shown by drought experiments in the Amazon (da Costa et al. 2010; Nepstad et al. 2007; Rowland et al. 2015), leading to reductions in forest height and loss of carbon (Yang et al. 2018b). Tall trees are likely to be most at risk since they must conduct water to great heights, requiring larger vessels to overcome hydraulic resistance (Olson et al. 2014; Olson et al. 2018; Savage et al. 2010; West et al. 1999). Larger vessels incur dangerous embolism more readily (Adams et al. 2017; Brodribb and Cochard 2009; Hammond et al. 2019; Olson et al. 2018; Scoffoni et al. 2017; Sperry et al. 2006). Trees must also pull water against gravity and this effect increases with tree height (Koch et al. 2004; Ryan and Yoder 1997), requiring greater tension upon the water column for taller trees (Sperry 1986; Sperry and Love 2015; Sperry and Tyree 1988). Dry soil makes it harder to pull water to the leaves, incurring even greater stress (Vilagrosa 2012). Thus, tall trees are likely to experience greater hydraulic stress under

drought conditions (da Costa et al. 2010; Nepstad et al. 2007; Rowland et al. 2015). Further, increasing vapour pressure deficit from increasing temperature would also likely induce lower leaf water potentials, and thereby hydraulic stress (McDowell and Allen 2015). It may therefore be expected that forests under increased hydraulic stress will decrease in height (Anderegg et al. 2019; Fajardo et al. 2019; Shenkin et al. 2018; Stovall et al. 2019). On the other hand, as atmospheric CO₂ increases in conjunction with climate change, increasing water use efficiency could mitigate some of the hydraulic stress associated with increasing temperature and reduced water availability by permitting more isohydric behaviour (Yi et al. 2019). However, evidence suggests increasing WUE from CO₂ fertilisation does not induce higher growth rates in trees (Ahlstrom et al. 2017; Penuelas et al. 2011; van der Sleen et al. 2015).

Tropical tree species may grow large by using different strategies: rapid growth but high mortality, or slow growth and low mortality (Ruger et al. 2020). Tree species that have high reproductive rates tend to be shorter, prioritising fecundity over stature (Kohyama et al. 2003; Ruger et al. 2020). Likely as an effect of life-history strategy, different species respond differently to hydraulic stress and are adapted to particular growing conditions (Barros et al. 2019; Choat et al. 2012). Aleixo et al. (2019) showed, based on data from long term monitoring of forest mortality, that certain functional groups are more likely to die during drought in the Amazon, namely pioneers with high growth rates and low wood density. This may be because of a strategy of high growth conferring low hydraulic safety, resulting in greater risk of death from embolism during periods of low soil moisture (Rowland et al. 2015). Because of the different abilities of species to cope with hydraulic stress, change in species composition is expected as forests become drier (Esquivel-Muelbert et al. 2019). Predicting any future changes requires descriptions of the current distributions of tree height across a

large water availability gradient, including how taxa may contribute to changes in forest height with climate change.

Thus, we ask here first which environmental variables limit forest height across the neotropics? We then ask, for individual taxa, how does maximum tree height change over environmental gradients and how does this make up the forest community at large?

Different scenarios can be envisaged of taxon specific responses of maximum tree height attained along a gradient of water availability relative to that of the overall forest maximum height (Figure 3.1, stippled line shape with a decrease in maximum tree height at high water availability as per Tao et al. (2016) and Gorgens et al. (2020)):

- 1) **No change in tree height within taxa and thus increasing tree height due to shift in species composition leading to increases in maximum forest height.** Species differ in their drought tolerance and hydraulic strategies (Bittencourt et al. 2020), and are differently distributed along gradients of water availability (Engelbrecht et al. 2007; Esquivel-Muelbert et al. 2017b), but height does not change across the water availability gradient, thus individual taxa are not limited in height by water availability. This is represented in Figure 3.1A.
- 2) **Change in tree height within individual taxa leads to change in forest maximum height.** Relationships may be similar to that of the overall forest (but offset in the value of maximum height attained). Specifically, most studies show water availability to be linearly related to maximum tree height at lower water availability, thus it is conceivable that individual taxa may increase in maximum height linearly with water availability (Figure 3.1A B). Alternatively, taxa may

follow the maximum height of the community more closely, i.e. increasing linearly at lower water availability and decreasing at high water availability (Figure 3.1A C).

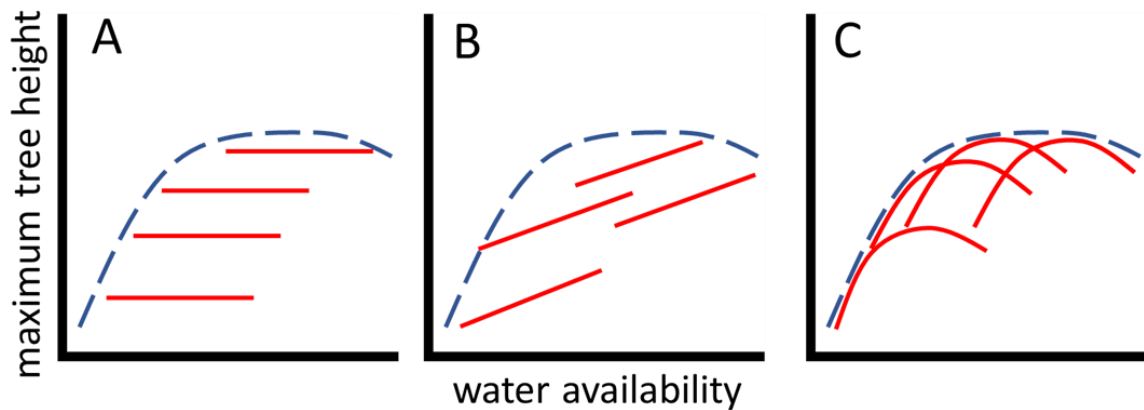


Figure 3.1 Conceptual diagram of hypothetical individual taxon relationships between tree height and water availability (solid red lines) with reference to the overall forest community relationship (stippled line). Different scenarios are posed that are possible based on the literature. Individual taxa show no relationship with tree height (A), taxa increase in height with water availability independent of the overall forest relationship (B), taxa show similar relationships to the overall forest relationship and thereby compose the overall forest relationship (C). A-B show how species may compose the overall forest relationship via turnover in taxa, i.e. taxa represent community maximum height for short distances in water availability, whilst in C taxon specific relationships are similar to that of the overall community maximum height and thus compose the community maximum height.

The first scenario of maximum tree height per taxon being similar across gradients of precipitation would require taxa to be below their maximum stress along most of the range, or adaptability within the taxon to be able to cope with changing environmental conditions, e.g. greater hydraulic stress in drier sites. Scenario A also is likely where taxa have short

ranges, so that tall taxa only compose the maximum forest height at narrow environmental windows (Esquivel-Muelbert et al. 2017a). In either way the increasing tree height with increasing water availability of the forest may be due to shifts in taxa. Alternatively, we show scenarios where forest maximum height is composed of taxa which also change in maximum tree height. In scenario B tree taxa change in their maximum height along a gradient of water availability dissimilarly to the forest community, whilst in C the taxa change in a similar manner. There is little evidence for any scenario in the literature as this topic has been little studied at the taxonomic level. A study by Givnish et al. (2014) of southern Australian *Eucalyptus* showed a similar change in the maximum height of the genus with water availability to scenario B in Figure 3.1. Considering the forests there are dominated by *Eucalyptus* it is likely that the within taxon relationship also represented the forest community.

3.1.1 Hypotheses

In this chapter we test which of a suite of environmental variables predict neotropical forest maximum height, specifically whether maximum height of trees in this novel dataset is limited by water availability in a similar way to previously reported (Klein, Randin and Korner 2015, Tao et al. 2016, Gorgens et al. 2020). Additionally, we will assess whether individual taxon maximum height shows a similar response as the overall forest community maximum height. This then enables the further questioning of whether changes in the maximum forest height of the neotropics is driven by shifts in taxonomic composition or changes in stature within taxa. This has not been previously reported and has interesting implications for tropical forest responses to climate change.

3.2 Methods

3.2.1 Sites and plot data

In order to describe the relationships between forest height and water availability across taxa this study uses tree height and diameter at breast height (DBH) data from 202 permanent monitoring plots (Figure 3.2) accessed from ForestPlots.net (see SI Table 3.5 for plot information) (Lopez-Gonzalez et al. 2011; Lopez-Gonzalez et al. 2009). Data from these plots includes 45,804 individual trees with height measurement, 2500 species, 585 genera and 111 families, encompassing trees from three clades: magnoliids (e.g. Lauraceae), monocots (only Arecaceae) and the eudicots (most trees in this study). Tree height across these plots was measured by independent research teams and using different methodologies, specifically laser range finder (46%), by-eye estimated height (7%), clinometers (21%) and directly (9%), whilst 15% had mixed methods.

Mean annual precipitation (MAP), and other precipitation and temperature variables were downloaded from Worldclim (Fick and Hijmans 2017) at 2.5 minute spatial resolution. Direct normal irradiance (DNI kWh m⁻²), the amount of solar radiation arriving perpendicular to a given area of the earth's surface, was obtained from Global Solar Atlas 2.0 (Solargis). Soil maps of texture (bulk density kg m⁻³, clay %, sand % and silt % at 15cm) were downloaded from SoilGrids at 1km resolution (Hengl et al. 2014).

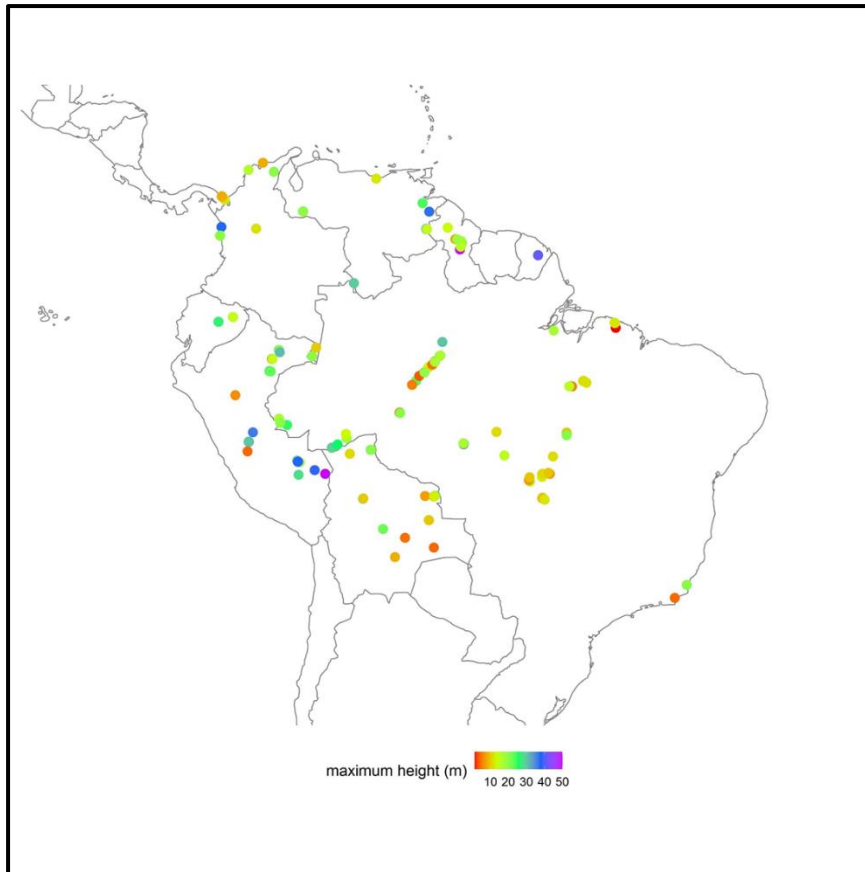


Figure 3.2 Distribution of forest plots included in this study that have height data available, plots including non-forest, flooded forest and high-altitude forest have been excluded. The mean of the 100th, 99th, 98th, 97th, 96th, 95th percentiles of tree height per plot are shown as point colour. See SI Table 3.5 for plot information.

3.2.2 Calculating Maximum height

In early data exploration of this large dataset it became clear through data inspection (i.e. site-specific histograms of tree height, diameter-height allometry (Feldpausch et al. 2012)) that the absolute maximum height was highly susceptible to measurement error and results were highly influenced by single data points. We excluded trees that lay far from the expected diameter-height allometry (Feldpausch et al. 2012), assuming the height measurements to be erroneous. Thus, we decided to calculate a maximum height that integrated several of the tallest trees per taxon/plot/climate bin (see below for elaboration).

We assess the relationships between maximum tree height and MAP at different taxonomic levels. For family, genus relationships we filtered those taxa to include those that occurred in ranges over 1000mm in MAP, and that had >20 individuals per 200mm climate bin (filtered to 30 families, 28 genera). Because of a lack of species that fit the criteria for family and genus level (10 species), species were filtered to those that occurred over 800mm ranges in MAP, and that had >10 individuals per 200mm climate bin. This increases the number of species for analysis (26 species) but reduces the robustness as the minimum number of trees to calculate maximum height was 10 individuals per MAP bin. In order to calculate the maximum height we averaged the 6 tallest percentile heights (100th, 99th, 98th, 97th, 96th, 95th) per 200mm MAP bin per family, genus and species. These percentiles are hereon referred to as 'maximum height'.

Due to the lack of species with high range and abundance we additionally filter species to those with >50 individuals across 800mm of MAP. We then examine at which point the maximum height (calculated as the mean of the top 6 percentiles across the MAP range) occurs along the MAP range of each species relative to their average occurrence within the dataset in order to show a relation to the community maximum height. Each taxon has a maximum height (mean of the percentiles) in meters and a MAP at which this maximum height occurs in millimetres (mean of occurrence in MAP range).

3.2.3 Analysis

We estimated parameters of individual generalised additive models (GAMs) for each environmental variable to assess which variable best captures water availability limitation of tree height. Individual variable GAMs relate the maximum height per 1/20th environmental variable bin with the binned environmental variable. This binning method shows the

maximum height trees are able to grow to under a specific environmental condition. Model suitability was assessed by the R^2 , estimated degrees of freedom relative to the degrees of freedom (measure of model underfit), and the p-value of the smooth term (Zuur et al. 2009).

We fitted multivariate GAMs selecting models based upon R^2 , and AIC (Akaike information criterion) and GCV (minimised generalised cross-validation) scores. Initial variable selection was based on the single predictor variable model results where the best fitting of two similar variables which were highly correlated was selected, e.g. mean temperature of the wettest quarter and mean temperature of the wettest month. The highly correlated nature of most climate variables strongly limited the possible combinations of variables. Maximum height calculated per bin could not be used since bins are climate variable specific, and thus we calculated maximum height per plot as the 6 highest percentiles of tree height per plot.

We also used GAMs in order to assess relationships between maximum height and MAP for the whole dataset segregated by family, genus and species taxonomic levels. Relationships are only plotted where the $R^2 > 0.1$ and the effective degrees of freedom is lower than the degrees of freedom (a measure of underfitting).

The single predictor GAMs that predict maximum tree height, $\max H$, from a particular environmental variable, x , use a penalised cubic polynomial regression spline that produces smooth curves, for the smoothing function, f , for the number of knots, i , which are evenly spaced across the range of the predictor variable

$$\max H_i = f(x_i) + \epsilon_i$$

3.1

Between each knot a penalisation function reduces the effect of the smoothing function that interpolates subsequent knots (x_i, x_{i+1}) , which may be reduced to a linear relationship across all knots if the relationship between the environmental variable and maximum tree height is linear.

For multiple environmental predictor variables (x_1, x_2, \dots) the GAMs follow the same logic but adding several predictor variables.

$$\text{maxH}_i = f_1(x_{1i}) + f_2(x_{2i}) \dots + \epsilon_i \quad 3.2$$

The number of knots was limited to 4 in order to avoid over fitting. We assumed similar degrees of smoothness as previous studies have found (Klein et al. 2015; Perperoglou et al. 2019; Tao et al. 2016).

3.3 Results

3.3.1 Environmental predictors of maximum tree height

We assess which of a suite of climate and soil variables are best predictors of maximum height. Avoidance of collinearity reduced the model to only three variables, MAP, maximum temperature of warmest month and % sand. MAP alone explains as much variation in tree height as the model that also included T and % sand (see SI Table 3.3 for multiple variable GAM results).

In the models using only one predictor variable the best individual climatic predictor was MAP ($R^2 = 0.41$), whilst % sand explains a similar proportion of the variation in maximum height than MAP ($R^2 = 0.43$) (Table 3.1). Combined explanatory variable of MAP/log % sand ($R^2 = 0.42$) does not greatly improve the model relative to MAP alone, and does not improve relative to sand % alone. The best individual explanatory variables relate strongly to water availability and show similar patterns of increasing maximum tree height from low water availability, e.g. high sand %, low MAP or low P-PET until a certain point, after which maximum height decreases at very high water availability across these variables (Figure 3.3, Table 3.1). We select here MAP as the variable to test taxon specific relationships with maximum tree height because MAP explains similar amounts of variation in maximum tree height as % sand and is a measure of water availability that enables predictions of the effects of changes in climate on forest stature.

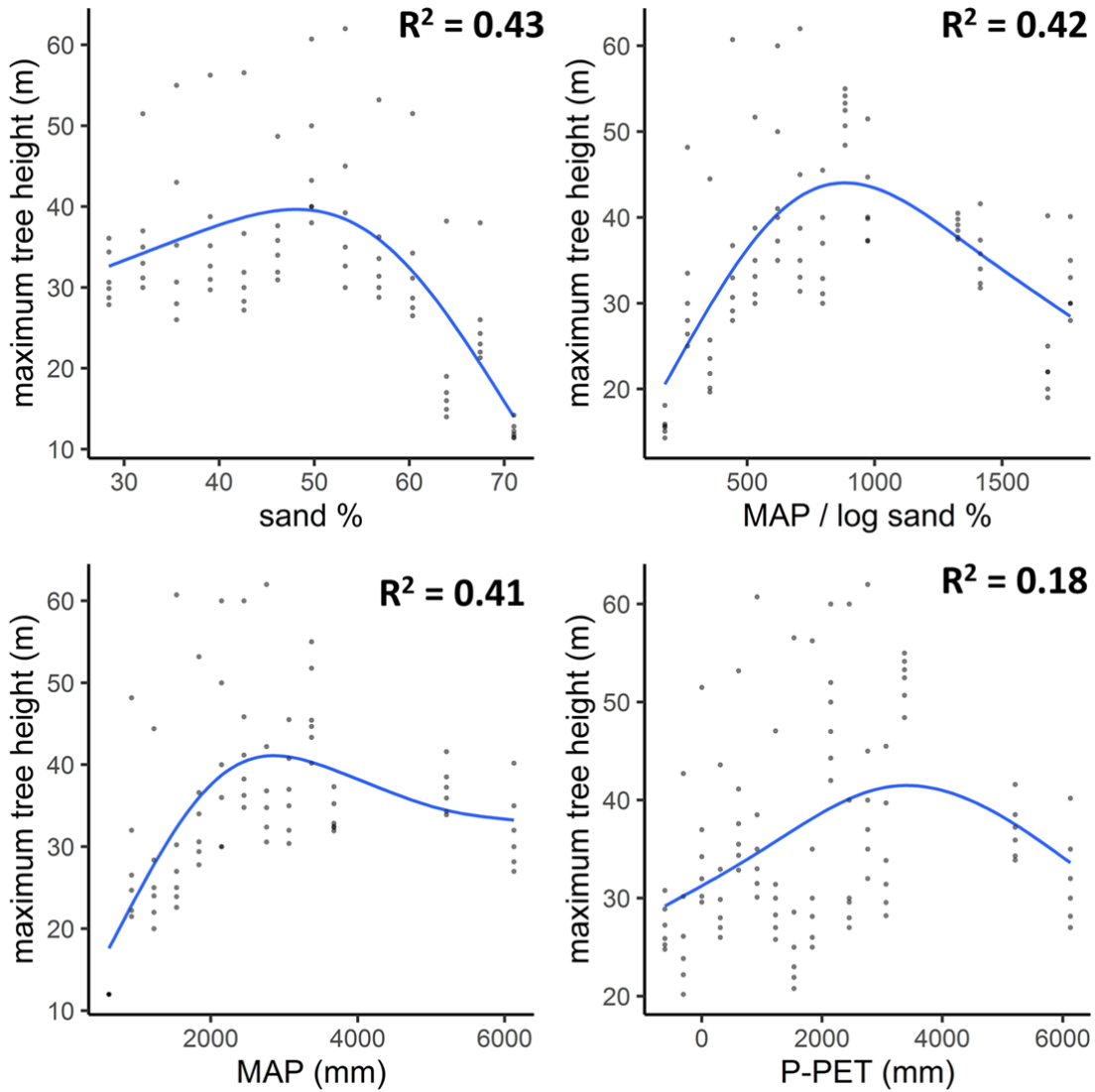


Figure 3.3 Relationships between maximum height and environmental variables. Maximum height is calculated per y axis bin (1/20 range of environmental variable), each point is a percentile of the height of trees in each bin (95th, 96th, 97th, 98th, 99th 100th percentiles). The blue line represents the GAM fit for each relationship and the R^2 is shown inset into each panel, as in Table 3.1. MAP = mean annual precipitation, P-PET = precipitation minus potential evapotranspiration.

Table 3.1 Generalised additive model results for individual independent variables relationships with maximum tree height calculated as the top 6 percentiles per independent variable bin (bin width = 1/20 maximum independent variable range). The 12 independent variables with highest R² are shown here.

Independent variable	R²	dev.expl	edf	Ref.df	F	p.value
Sand%	0.43	0.46	2.80	3.31	17.99	<0.0001
MAP/ log Sand%	0.42	0.45	2.86	3.36	17.38	<0.0001
MAP	0.41	0.43	2.99	3.43	15.42	<0.0001
P-PET	0.18	0.21	3.64	3.91	5.52	0.0005
Irradiance	0.28	0.30	2.36	2.86	10.83	<0.0001
Precipitation of Wettest Quarter	0.26	0.28	2.32	2.76	10.38	<0.0001
Mean Diurnal T Range	0.24	0.26	2.34	2.83	7.52	0.0005
Precipitation of Coldest Quarter	0.23	0.27	3.87	3.99	8.41	<0.0001
potential evapotranspiration	0.21	0.23	2.64	3.15	8.84	<0.0001
Silt%	0.21	0.23	3.35	3.77	7.50	<0.0001
Temperature Annual Range	0.20	0.23	2.84	3.35	5.92	0.0007
Precipitation of Wettest Month	0.20	0.22	2.26	2.72	8.00	0.0001

3.3.2 Taxa

Different families and genera follow relationships with MAP that are similar to the overall forest maximum height-precipitation relationship (Figure 3.4A, SI Table 3.4). Most of the families shown have a maximum height at a similar point to that of the overall forest with all

families combined (mean among families of 2450mm). At family level certain families are found to grow tall across the precipitation gradient, such as Fabaceae (maximum height = 47.9m), Lauraceae (peak height = 47.8m), Lecythidaceae (maximum height = 45.7m) and Apocynaceae (maximum height = 42.9m). Others, such as Arecaceae (maximum height = 28.1m) and Nyctaginaceae (maximum height = 26.1m), are found to have low maximum height relative to the canopy throughout their range. For these two families there is a linear relationship between maximum tree height and MAP, whilst for other low maximum height families such as Violaceae (maximum height = 26.5m) we find instead a curved relationship with precipitation similar to the overall forest. Relatively few genera show a strong relationship with MAP (Figure 3.4B, SI Table 3.4). However certain genera exhibit a similar relationship with precipitation as the forest in general, growing tall across the gradient, notably *Aspidosperma* (maximum height = 47.6m) and *Brosimum* (maximum height = 40.3m). Other genera, such as *Neea* (maximum height = 25.5m) and the palm *Oenocarpus* (maximum height = 24.9m) remain small throughout their range.

There are very few species with sufficiently high abundance across a large MAP gradient to produce statistically robust relationships (Figure 3.4B, SI Table 3.4). For species that are abundant across a large gradient we show some species to be tall across their range, such as *Apuleia leiocarpa* (maximum height = 42.7m), thus making up the overall forest maximum height across a range of precipitation levels, whilst others such as *Protium heptaphyllum* (maximum height = 23.8m) and particularly palms tend to be short across their range. Figure 3.5 shows the maximum heights achieved for species that do not form relationships with MAP. The species shown tend to achieve their maximum height close to the overall forest peak. However, is this simply because these species occur at this peak? The relationship between the mean occurrence of a species along the MAP gradient and MAP at maximum

height shows that maximum height tends not to occur at the mean of the occurrence, but rather the maximum height occurs closer to the community maximum height (Figure 3.6).

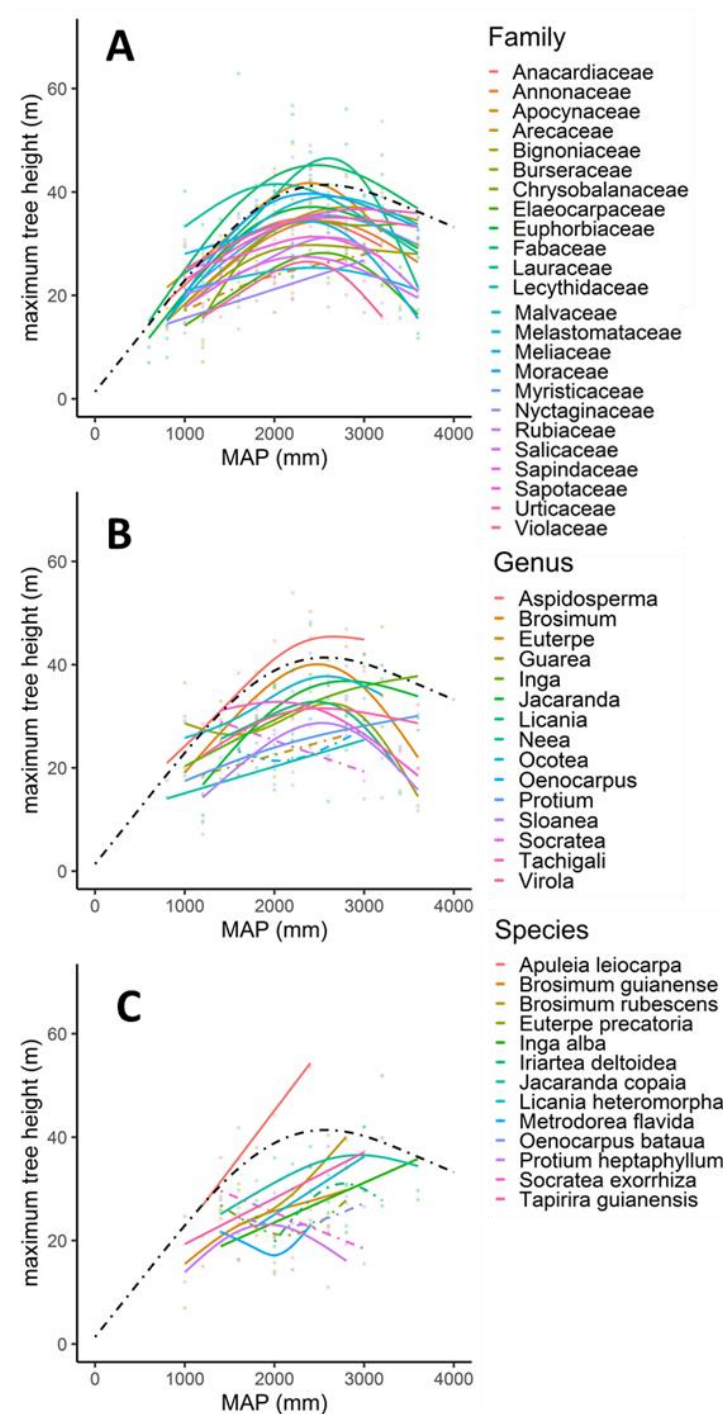


Figure 3.4 Relationships between mean annual precipitation (MAP) and maximum tree height at different taxonomic levels. A-C show the relationships for individual families, genera and species respectively. The individual taxa shown in A and B are those with ranges over 1000mm, with greater than 20 individuals per MAP bin, at species level individual taxa shown are those with ranges over 800mm with greater than 10 individuals per MAP bin. Maximum height is calculated as the top 6

percentiles in tree height per 200mm MAP bin. Coloured points represent these 6 percentiles per bin per taxon. Palm taxa are denoted by coloured stippled lines. The community maximum height relationship with MAP (Figure 3.3) is shown as the black stippled line.

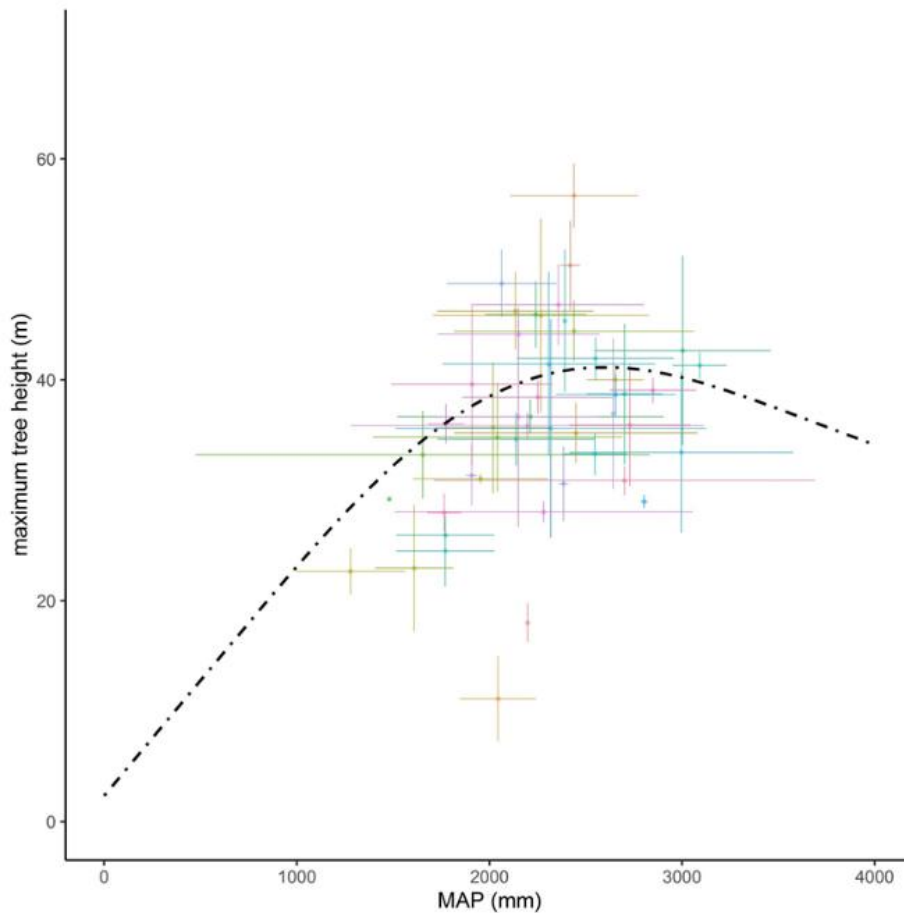


Figure 3.5 The maximum height of each species(47 see SI Table 3.1) with >50 individuals across 800mm of MAP and at what value of MAP this maximum occurs. The maximum height is calculated as the mean of top 5 percentiles of height. Error bars around points show the standard error of MAP and maximum height for each species mean of the top 5 percentiles in height. The community maximum height relationship with MAP (Figure 3.3) is shown as the black stippled line. Colours represent different species.

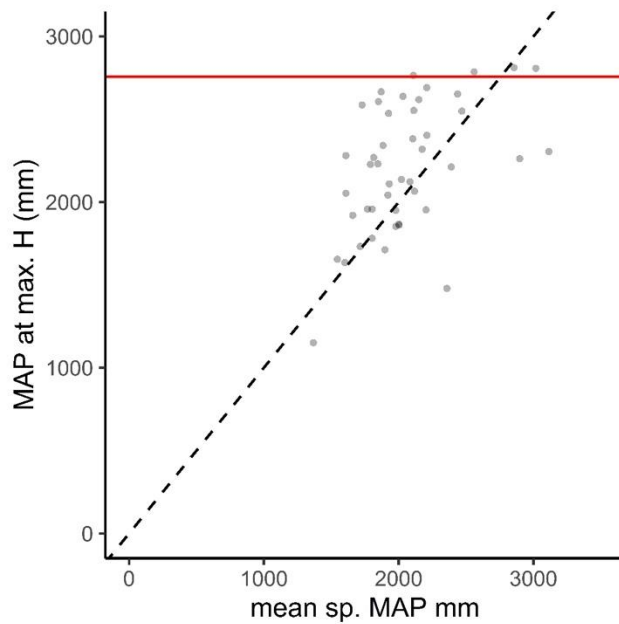


Figure 3.6 Relationship between the location in mean annual precipitation (MAP) of maximum height per species (as per Figure 3.5) and the mean of occurrences of each species in MAP, taking the abundance of the species at each MAP bin into account. The 1:1 black dashed line shows the expected distribution of points if the point of maximum height were associated exactly with the mean of the occurrence of the species. The red line shows the peak of the relationship between maximum tree height and MAP for the whole forest (2750mm).

3.4 Discussion

3.4.1 Explaining variation in forest height

We aimed to test which environmental variables best predict maximum tree height across neotropical forests. We found sand% to be the best environmental predictor variable for maximum tree height at the forest community level. Soil sandiness is likely to be an important variable for determining forest height due to a combination of effects upon tree growth and mortality in addition to effects stemming from water availability (Adeney et al. 2016; Hodnett and Tomasella 2002; Soong et al. 2020b). One of the main effects of high soil sandiness on tree growth and mortality are lower water availability due to large particle size which reduces the ability to retain water. Jimenez et al. (2020) found that during drought periods in the north western Amazon forests growing on sandy soils experienced higher mortality whereas forests

growing on more clay based soils did not experience any increase in mortality during the droughts. Highly sandy soils have also been shown to reduce nutrient cycling, thereby limiting the growth of trees (Soong et al. 2020; Vitousek and Sanford 1986).

Despite a theoretically likely combined effect of both rainfall and soil sandiness, e.g. low nutrient availability and exacerbation of water stress, the integration of sand% and MAP did not improve the model relative to sand% alone as we expected based on results of Quesada et al. (2012). They showed that the interaction of soil physical properties and climate predicted forest biomass variations across the Amazon basin, partly due to the correlation between particle size and Phosphorous content (Quesada et al. 2010). Why we find no improvement in explaining forest maximum height using both sand% and MAP is not certain. The two variables are not correlated with each other (data not shown), but each individually explains a high proportion of variability in the maximum height of tropical forest trees. We expected high sand% to exacerbate low MAP (less water available in the soil) and low sand (high clay) to exacerbate high MAP (more easily waterlogged soil). This suggests that these variables do not act together to affect forest height. Future research could further investigate the role of soil conditions, specifically using plot level soil texture, and nutrient information rather than relatively coarse soil maps that we use here.

The overall forest relationships using ground data here are very similar to those relationships reported between space-born LiDAR derived maximum forest-water availability relationships (Klein et al. 2015; Tao et al. 2016). In particular this present study corroborates findings of previous studies based on LiDAR data of a strong increase in tree height with water availability followed by a plateau or slight decrease in forest height at high water availabilities. Our results show a peak in maximum height using P-PET as the dependant variable occurring at

~3500mm whilst previous global studies using the same dependant variable show the maximum height peak to occur at 467mm (Klein et al. 2015) to 680mm (Tao et al. 2016). This is likely because different regions show similar shaped relationships but shifted along the P-PET gradient, for example Tao et al. (2016) showed the maximum height of Chinese forests to peak at ~0mm P-PET, whilst the maximum height of forests in the United States peaked at ~1500mm, and for South America at ~750-1000mm. However, these authors did not attempt to explain these differences. Klein et al. (2015) suggest that differences in peaks of maximum forest height with P-PET amongst regions may occur due to either groundwater or runoff fed forests, so that water availability from direct precipitation contributes relatively little to local hydraulic conditions. A recent study by Gorgens et al. (2020) using airborne LiDAR data showed that MAP strongly predicted maximum forest height in the Brazilian Amazon, with an increase in maximum height until 2300mm, at values higher than this maximum forest height declines. We find a peak in maximum height along a MAP gradient to be at a higher value of 2700mm. Why this should be is not certain, however we use a dataset including other regions of the neotropics, not only the Brazilian Amazon.

We find the best climate variable to explain forest maximum height across tropical South America is MAP, whereas other studies found stronger relationships with P-PET. Combining precipitation and evapotranspiration may better predict water availability since it incorporates water gained through precipitation relative to water lost through evaporation. Why for our dataset MAP predicts maximum tree height better than other variables that take temperature, vapour pressure, or seasonality into account is not certain. We expected that models for maximum height with variables that integrate temperature and precipitation would increase the fit to the data.

The shape of the relationship between forest maximum height and MAP, as well as other variables conveying water availability, show that as water availability increases from a low value, maximum tree height increases strongly. However, this increase reduces toward a peak in maximum height and even reverses, so that high water availability appears to negatively affect height attainment. This has been shown by Tao et al. (2016) using space-borne LiDAR data and corroborated by inventory data across the USA, and tropical to temperate China. Our present study shows this relationship for the first time for neotropical forests. The reason for this result is likely a combination of factors, such as reduced light availability and thus reduced photosynthetic rates of plants due to cloud cover (Graham et al. 2003; Guan et al. 2015; Wagner et al. 2016; Wagner et al. 2017), and possibly also due to leaves that become covered in water and cannot exchange gasses with the atmosphere at an effective rate (Aparecido et al. 2016).

Additionally, plants can become water stressed and become more vulnerable to windfall due to less well developed roots when soils become saturated (and anoxic) if they don't have specific adaptations to waterlogged soil (Aubry-Kientz et al. 2015; Herault and Piconiot 2018; Pires et al. 2018). An example of how forests may be limited by waterlogging of soil can be seen by a recent study of forests with water tables close to the surface soil that experienced a major reduction in rainfall due to El Nino (Sousa et al. 2020). They found that rather than the drought causing mortality or inhibiting growth, biomass growth increased markedly, suggesting a release from a previous limitation, likely due to reduced anoxic conditions of the soil. Furthermore, a study by Ferry et al. (2010) found in an Amazonian forest that trees growing in valleys with waterlogged soils suffered from higher windfall rates than trees growing on well drained ridges, suggesting shallower and less well developed root systems in the waterlogged soils.

If forest productivity is indeed limited by excess soil water above 3000mm in MAP then some forests may possibly actually profit from increasingly dry or drought stressed climate (Duffy et al. 2015; Joetzjer et al. 2013; Marengo and Espinoza 2016; Marengo et al. 2018). Though some wetter regions of the western and northern Amazon may experience an increase in rainfall in contrast to the drier eastern and southern Amazon which are likely to experience reduced rainfall (Duffy et al. 2015; Espinoza et al. 2019; Gloor et al. 2013; Shiogama et al. 2011), and thus the majority of forests in the Amazon are expected to move towards climates that are limiting height attainment.

3.4.2 Taxon specific maximum height relationships

One of the aims of this study is to show how tree height is limited for individual taxa. As far as the authors are aware no study has examined taxon-specific tree height relationships for tropical regions across broad environmental gradients. We show that at the family level, tree height is limited in a very similar way to that of the overall forest: individual families tend to increase in maximum tree height until ~2500mm after which maximum tree height decreases (Figure 3.4A). Between families this relationship appears remarkably conserved, with family specific relationships which occupy the same relative position in the forest along the MAP gradient but at different heights. Thus, different families have different peak heights. This is similar to the hypothesised scenario C of Figure 3.1. This finding is significant due to implications for the impact of shifts in climate on forest composition and structure. These relationships suggest that for a given shift in MAP below 2700mm the forest community will experience a decrease in maximum tree height, but at the family level the community representing the tallest trees will likely be preserved.

This is also true to an extent at the genus level, but less so at the species level where we can draw few conclusions from species specific relationships between maximum height and MAP. This is because few species have wide enough ranges (along the MAP gradient) with sufficient data points within the database of tree height we use in this study. However, some species show similar patterns as the forest community level e.g. *Jacaranda copaia* (Figure 3.4C). We also show that for species with broad ranges (>800mm MAP in the dataset we use) species maximum height tends to occur toward the community maximum height rather than the centre of species occurrence (Figure 3.5, Figure 3.6), this is suggestive of scenario C of Figure 3.1. What we can conclude is that the observed changes in neotropical forest maximum height along a MAP gradient can be explained to a very large degree by changes in max height within families.

There are very few other studies assessing within taxon tree maximum height relationships with water availability, especially for the tropics. Givnish et al. (2014) showed in the highly diverse genus *Eucalyptus* in southern Australia, that maximum tree height increases with precipitation/pan evaporation in a similar non-linear way as this study, but do not show a decrease in maximum height at very high water availability. Another study of several temperate tree species in France found only linear relationships between precipitation and tree height (Fortin et al. 2018).

Forest canopy trees tend to grow toward a common height (Nagashima and Hikosaka 2011). Growing taller for no increase in light availability is generally not advantageous due to the mechanical (Niklas 2007), construction and respiration (Rodriguez-Calcerrada et al. 2019), and hydraulic costs of being tall (Olson et al. 2018; Scoffoni et al. 2017; Sperry et al. 2006). While low tree heights (relative to the canopy level) reduces light availability and potential

productivity in a competitive forest environment (Kuppers et al. 1996; Rijkers et al. 2000). Trees can grow large either by growing slowly but living a long time or by growing fast and living less long (de Souza et al. 2016; Ruger et al. 2020). This can be exemplified using the height data from this study: *Cedrelinga cateniformis* is a fast growing (DBH growth of 0.72 cm yr⁻¹) low wood density (0.50g cm⁻³) species that attains heights >55m in the Amazon, whilst *Chlorocardium rodiei* is a similarly large statured tree with a growth rate one quarter of *Cedrelinga cateniformis* (0.18 cm yr⁻¹) and has a high wood density (0.85g cm⁻³) (growth rate and wood density information from de Souza et al. (2016)). The question arises whether trees are able to utilise both fast growth and high mortality and slow growth and low mortality strategies to grow tall similarly at all points along the MAP gradient? In particular; can trees in dry regions use a fast growth strategy to grow tall when hydraulic stress forces seasonality in growth and higher mortality from droughts? And likewise, can trees in wet regions use a slow growing strategy when competition is likely to be more intense (Alvarez-Davila et al. 2017)? It has been shown that species with traits of slow growth and low mortality survive periodic droughts better, whilst in wet years species with fast growth and higher mortality outcompete the slower growers (Powell et al. 2018). Future research could pair similar height data as in this study with a suite of functional, ecophysiological, and life-history traits.

The tallest families in this present study are the Lecythidaceae, Lauraceae and Fabaceae (Figure 3.4, SI Table 3.1). These families have maximum heights >45m and are tall across the full MAP gradient. Lecythidaceae includes genera dominated by large, emergent trees, such as *Bertholetia*, *Cariniana*, and one of the most widespread Amazonian tree genera *Eschweilera* (Esquivel-Muelbert et al. 2017a). The Lauraceae family within the Magnoliid clade contains some of the tallest trees found this study, including *Chlorocardium* and *Licaria* trees

which reached heights > 60 m tall in Guyana. Tall genera in the Fabaceae family, include *Dicymbe* and *Dicorynia* in Guyana, and *Cedrelinga* and *Apuleia* elsewhere.

The ability of particular families to grow tall across a wide range of MAP, for example within the Lecythidaceae, may be due to plasticity of drought stress tolerance. A recent study showed that plasticity within families and genera permits growth across habitats of different water stress. For example, within the genus *Licania*, one species grows in dry habitats and is drought tolerant, whilst a different species grows in wet habitat and is not drought tolerant. Additionally a generalist species found in both dry and wet habitats has intermediate drought tolerance (Oliveira et al. 2019). Despite specific examples there is currently little information regarding the hydraulic properties of Amazonian trees to generalise about the hydraulic traits of higher order taxa. Despite potential plasticity in hydraulic stress tolerance over water availability gradients within higher order taxa and to a lesser extent at species level (Anderegg 2015), individual trees don't show plasticity in their drought stress tolerance under experimentally induced long-term water availability reductions (Bittencourt et al. 2020). Thus, under climate change individual trees close to their maximum height are likely to suffer mortality should conditions exceed their hydraulic stress tolerance. Previous studies have shown that the tallest trees are most at risk under drought and forests are likely to reduce maximum height under reductions in water availability (Anderegg et al. 2019; Fajardo et al. 2019; Shenkin et al. 2018; Stovall et al. 2019), we corroborate this with the relationships at the forest and higher taxon levels.

Our results furthermore show that some families composed of understory species also follow the overall forest relationship. It was hypothesised that understory trees may be able to grow tall independently of water availability (Scenario A of Figure 3.1) since they occupy a less

hydraulically stressful microclimate beneath the forest canopy that buffer against dry conditions (Nepstad et al. 2007), and because of reduced competition in the understory that typically drives trees to grow tall (Guo et al. 2017). For example, understory trees do not tend to lose leaves during the dry season unlike canopy trees. Rather they increase leaf area in response to the loss of canopy tree leaves and subsequent increase in light availability (Tang and Dubayah 2017). Why some tropical forest understory taxa may increase maximum height with MAP is uncertain, and as far as the authors are aware is unreported elsewhere. Perhaps understory trees increase in height with MAP to access a particular canopy layer and satisfy minimum light requirements. Above this minimum high irradiance may cause photoinhibition (Lovelock et al. 1994), higher vapour pressure deficit associated hydraulic stress (Christoffersen et al. 2016), and increased wind speed which causes mechanical stress further inhibiting height growth (Anten et al. 2009). In drier forests the height of this critical wind level may be closer to the ground due to relatively open canopies, whilst in wet forests a similar light and wind level is relatively high above ground due to a denser canopy and more complex forest structure (Brenes-Arguedas et al. 2011; Moon et al. 2019). Some understory families, like Melastomataceae, show the expected flat maximum tree height distribution (as in Figure 3.4A), growing similarly tall across the range of MAP. Why then do some understory taxa not grow taller? Tropical rainforest understory species tend to have deep and wide crowns, large diameter trunks for a given tree height relative to canopy tree species, as well as high reproductive rates (Iida et al. 2014; Kohyama et al. 2003; Poorter et al. 2006). This likely enables understory trees to survive under low light conditions but provides a disadvantage when competing for light with species that have characteristics that promote vertical growth and productivity and faster growth in high light, namely canopy species, thus depressing their maximum height whilst maximising survival and reproduction (Iida et al.

2014; Kohyama et al. 2003). This permits the coexistence of different taxa occupying different layers of the forest canopy that we show in the concentric maximum height relationships of Figure 3.4A, thereby adding to the biodiversity of tropical forests (Kohyama 1993).

Distinct among the tree taxa presented here are palms, being monocotyledonous plants. They tend to occupy the forest mid-story and lower canopy in lowland neotropical forests, though *Ceroxylon* palms can grow to 60m tall in montane neotropical forests (Bernal et al. 2018; Kahn et al. 1988). We show here that the palm family Arecaceae has a relatively short maximum height (28.1m) with a relatively weak linear increase in height from 17.5m to 28.1m along the MAP gradient (Figure 3.4A). Taller palm taxa like including *Iriatea deltoidea* and *Socratea exorrhiza* make up the taller palms at different points along the MAP gradient. *Socratea exorrhiza* is taller in drier forests whilst *Iriatea deltoidea* is taller in wetter forests (Figure 3.4C). *Socratea exorrhiza* has a dry affiliated distribution relative to *Iriatea deltoidea* (Esquivel-Muelbert et al. 2017a). There is some evidence that *Socratea* palms are somewhat drought tolerant (Esquivel-Muelbert et al. 2017b). These relatively dissimilar relationships to the overall forest relationship suggest that with climate change the palm communities that make up the forest canopy are likely to shift in composition.

3.4.3 Conclusions

We used forest inventory data with taxonomic information from different forest ecosystems across tropical South America to assess the relationships between water availability and maximum tree height. We find a relationship between maximum forest in height and MAP. Maximum forest height increases with MAP until ~2700mm, after which it declines. This is similar to LiDAR derived data presented in previous studies. We also show for the first-time relationships for individual taxa at different taxonomic levels. At the family level the

relationships are remarkably similar. We suggest mechanisms for the increase and subsequent decrease in maximum height of the forest community and individual taxa with increasing MAP. These results suggest a similar response among neotropical tree families of maximum height to changes in MAP associated with climate change and deforestation, and therefore a maintenance of the community of trees that grow tallest at the family level. At lower taxonomic levels we can be less certain. But as the maximum height of species tends to occur toward the peak of the community maximum height (along a MAP gradient) rather than the mean of occurrence of each species, it suggest species may also be similarly affected as higher order taxa.

Chapter 4 Vessel tapering

conserved along a precipitation

gradient in tropical trees of the genus

Cedrela

Abstract

Maximum tree height in the tropics decreases strongly with decreasing precipitation. It is unclear to what degree these changes in tree height result from changes in hydraulic architecture with decreasing water availability. The change in diameter of conducting vessels with tree height from base to tip are important determinants of hydraulic conductivity and safety. Previous research has shown that vessel diameter scales with tree height at a similar rate across biomes and taxa. However, knowledge of how the relationship between vessel diameter and tree height varies across precipitation gradients within one species is incomplete, especially for the tropics. Here we report for the first time, how vessel density and diameter, measured at the tree base, differ across four sites varying in precipitation (1014 to 2585 mm year⁻¹) for two tropical tree species of the genus *Cedrela*. We find that maximum tree height decreases with precipitation across sites from 42m to 13m. Despite the strong differences between sites in maximum tree height and water availability, the rate at which basal vessel diameter scales with tree height (i.e., tapering) is remarkably conserved and similar to published results based on multispecies analyses. Thus, basal vessel diameter is nearly constant for a given height, but maximum basal vessel size is two times smaller at the drier site (with the shortest trees) compared to the wettest site (with the tallest trees). One

possible explanation for these results is that maximum height of *Cedrela* trees is limited by constraints on maximum basal vessel diameter that can be sustained given increasing embolism risk with increasing dryness. While it remains unclear if this mechanism indeed is the ultimate control on maximum tree height, our results show no hydraulic adaptation across this wetness gradient and reveal a clear relationship between maximum tree height and maximum basal vessel size.

4.1 Introduction

Trees need light and thus strive to reach the canopy to optimise light capture in forests. At the same time, trees need to keep their leaves well-watered, and need to transport water to the canopy. This process requires work against gravity and friction. It has therefore been hypothesised that tree height might be limited by frictional losses and gravity (Ryan and Yoder 1997). Evidence for this hypothesis comes in part from patterns of increasing maximum tree height with water availability, suggesting a strong role for water availability in the limitation of maximum height (Tao et al. 2016).

Water flow from the roots to the treetop is driven by pull (negative pressure) from the leaf exerted on the water column. The xylem water transport network can be considered as a series of interconnected tubes that branch from the base of the tree trunk to provide water to the leaves (Tyree and Ewers 1991). One of the main impediments to water flow is the resistance, R , which decreases with the fourth power of the vessel diameter, according to Hagen-Poiseuille's law, i.e.,

$$R = \frac{8\eta L}{d^4}$$

4.1

According to this equation, the increase in resistance with greater path length, L (i.e. increase in tree height), for a fluid with viscosity η can be counteracted by increasing vessel diameter, d . Thus, a strategy for trees to reduce the frictional constraint on tree height is to steadily widen vessel diameter from the top of the tree towards its base. To permit constant volume flow and supply a branching canopy, vessels will have to divide accordingly from base to tip. Based on these principles it has been shown that total frictional resistance can be regulated to be independent of path length through coordinated changes in vessel division and vessel diameter with tree height (Savage et al. 2010; West et al. 1999). This rate of narrowing and dividing of xylem vessels from tree base to apex, is also known as tapering.

Water under the highly negative pressures in the xylem is in a metastable state that makes spontaneous cavitation and heterogenous air bubble nucleation possible (Knipfer et al. 2015; Tyree and Sperry 1989b). More negative water potentials are associated with greater risk of gas bubble formation and spread (Sperry 1986; Sperry and Love 2015; Sperry and Tyree 1988; Tyree and Sperry 1989b). If these air bubbles, known as embolisms, become large enough they may reduce or block water flow to the leaves, or even result in a complete loss of conductivity, culminating in dehydration and death (Adams et al. 2017; Brodribb and Cochard 2009; Hammond et al. 2019). This is likely to be the major mechanism of tree death during droughts (Adams et al. 2017), since lower soil water potential requires more negative pressures to induce water flow (Vilagrosa 2012). Taller trees that make wider vessels to counterbalance resistance are likely to be more vulnerable to embolism (Olson et al. 2018; Scoffoni et al. 2017; Sperry et al. 2006), and trees thus face a trade-off between producing

wider vessels to increase conductance and greater vulnerability to embolism (Levionnois et al. 2021; Lobo et al. 2018; Olson et al. 2018; Scoffoni et al. 2017; Sperry et al. 2006). Observations suggest that tall trees indeed suffer higher mortality during droughts (Bennett et al. 2015; Johnson et al. 2018b; Stovall et al. 2019), possibly due to greater occurrences of embolism. As a result of climate change associated droughts forest height may thus decrease in the future (Anderegg et al. 2019; Fajardo et al. 2019; Shenkin et al. 2018; Stovall et al. 2019).

Tapering is well documented in trees, with evidence that trees tend to optimize water conductance by offsetting of frictional losses through vessel widening (Anfodillo et al. 2006; Olson et al. 2014; Petit et al. 2010). Building on the work of West et al. (1999), Enquist (2002; 2003) suggested that biomechanical constraints and the need to reduce path flow resistance should lead to universal tapering, or in other words, the rate of vessel diameter decrease per unit height increase from the tree base to apex should be the same across trees and taxa. Hydraulic optimality models predict that xylem vessel diameter, d , tapers up trees with distance, L , from the apex following a power law $d=L^{\bar{a}}$ with scaling exponent $\bar{a}=0.2$ (i.e. a relationship between $\log d$ and $\log L$ with slope 0.2) (Anfodillo et al. 2006; Enquist 2003; Savage et al. 2010; West et al. 1999). Vessel widening at a rate lower than the scaling exponent of 0.2 results in large hydraulic resistance increases with path length, while tapering above this optimal value results in relatively small gains in resistance reduction, with larger risks to embolism and reduced mechanical strength due to larger basal vessel diameters (Christensen-Dalsgaard et al. 2007; Fan et al. 2017; Savage et al. 2010). Multi-taxa studies show that a fundamental, universal scaling relationship exists between vessel diameter and tree height across ecosystems and climates (Olson et al. 2014). This suggests that this trait is fixed or invariant with respect to climate, but few studies have investigated how vessel diameter changes with tree height within species and across large water availability gradients.

It is still largely unknown to what degree the relationship between vessel diameter and tree height is an evolutionary adaptation, and whether this relationship is conserved within a species growing under very different water availabilities. This has implications for how trees cope with changes in water availability and hydraulic stress associated with climate change, namely the abilities of trees to grow taller and the effects of tree height on mortality risks (Anderegg et al. 2012; Rosell et al. 2017). To our knowledge, this study provides the first assessment within one widespread tropical tree species how trees adjust hydraulic architecture in response to variation in water availability. We conceptualise three strategies (A – C below and Figure 4.1) as to how trees may adjust xylem diameter across differences in water availability:

A) ***Equal tapering across sites, but different basal vessel size for a given tree height.***

For a given tree height, trees at drier sites have vessels that are less conductive compared to those at wetter sites. Smaller basal vessels at the drier sites result in reduction in embolisms risk for trees, thus securing consistent water supply to the canopy, but lowering maximum flow rates.

B) ***Equal taper rate and basal vessel size for a given tree height irrespective of water availability.***

Hydraulic architecture remains largely unchanged across sites, and for a given height embolism risk and hydraulic efficiency are thus the same. As a result, trees growing at drier sites will experience greater hydraulic stress and embolism risk when compared to trees of the same height at wetter sites.

C) ***Reduced taper rate to reduce basal vessel size.***

For a given tree height, trees at drier sites have identical apical vessel diameter, but smaller basal vessels and thus reduced embolism risk but higher resistance and thus lower conductivity.

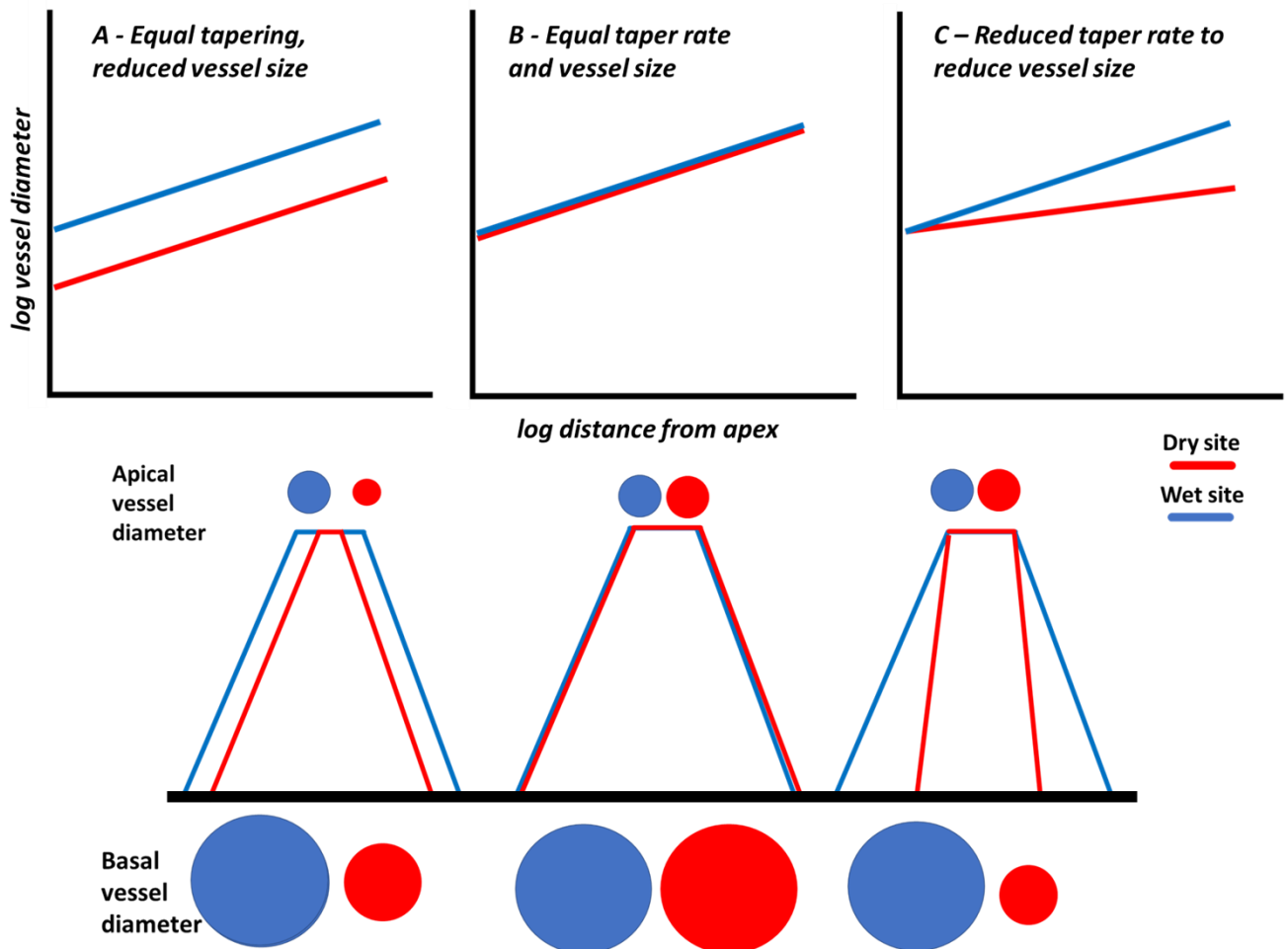


Figure 4.1. Conceptual illustration of three possible hydraulic strategies of trees in response to water availability. Upper panels show the expected log-log relationships between vessel diameter and tree height at wet (blue) and dry (red) sites. Lower panels show a schematic diagram of the vessel tapering along the tree stem and hypothetical difference in basal and apical vessel diameters between dry and wet sites. See main text for description of the two strategies. This present study analyses the relationship between basal vessel diameter and tree height. The log-log relationships in the upper panel between vessel diameter and distance from apex can represent similarly the basal vessel diameter, measured here, and the change in vessel diameters vertically from tip to base, not directly measured here (Fajardo et al. 2020; Olson et al. 2014).

The first strategy, *equal tapering across sites but different basal vessel size for a given tree height*, has previously been suggested as a mechanism of trees to cope with increasingly hydraulically stressful growing conditions (Enquist 2002; Rosell et al. 2017). As competition for light decreases, trees could prioritize traits designed to deal with water stress (i.e., make narrower and safer vessels) above traits that allow faster growth (i.e., wider vessels with greater hydraulic conductivity) (Brenes-Arguedas et al. 2011; Markesteijn et al. 2011). Evidence for this strategy has been observed in the widespread Australian genus *Eucalyptus*, where species growing in drier environments tend to have reduced basal vessel diameter for a given tree height relative to congeneric species in wetter sites, likely driven by genetic variation between species (Pfautsch et al. 2016). Support for the second strategy, *equal taper rate and vessel size (B)*, comes from recent studies assessing the role of climate on vessel anatomy within species. These show that tapering amongst wet and dry sites is similar and that for a given height average vessel diameter is the same (Fajardo et al. 2020; Garcia-Cervigon et al. 2018; Lechthaler et al. 2019; Pfautsch et al. 2016; Warwick et al. 2017). One recent study has provided evidence for both scenarios A and B in two species across a precipitation gradient in temperate southern Chile, dependent upon species (Garcia-Cervigon et al. 2018). Strategy C requires different members of the same species to have different vessel scaling with tree height. To our knowledge there is little evidence for differing tapering rate across climates, either within or between species. Similar vessel scaling with tree height appears to be a universal property of trees (Olson et al. 2014), however it is a possibility that certain species may deviate from the general rule.

For the first time we test which strategy is in use for two congeneric species in the tropical genus of *Cedrela* along a water availability gradient across four sites. Vessel anatomy-tree height relationships across broad climate gradients within taxa should provide insights to

what degree trees can adapt vessel anatomy to different growing conditions, and could help explaining variation in maximum tree heights along gradients of water availability (Fajardo et al. 2019; Moles et al. 2009; Rosell et al. 2017; Scheffer et al. 2018; Tao et al. 2016).

4.1.1 Hypotheses

The hypotheses being tested in this chapter are that, for *Cedrela* trees, basal xylem vessels increase in diameter and decrease in density with tree height at the predicted rate from the literature (West, Brown and Enquist 1999, Olson et al. 2014, Savage et al. 2010). Additionally, we test whether the rate of change of basal vessel diameter and density with tree height is similar across sites differing in water availability, and whether the basal vessel diameter and basal vessel density of trees of a given height are similar across sites differing in water availability. There have been very few studies showing how, within a taxon, xylem vessels taper with tree height across sites, and none for the tropics. This information may have interesting implications for the ability of trees to cope with drought across strong gradients in water availability and imply how tropical trees may cope with changing precipitation regimes.

4.2 Methods

4.2.1 Species

Cedrela is a widespread neotropical tree genus in the Meliaceae family. In this study two species have been sampled: *C. odorata* (L.), found throughout the neotropics, and *C. salvadorensis* (Standl.), restricted to Central America. *C. odorata* grows predominantly on well drained soils at altitudes below 1300m (Cintron 1990). Genetic studies of the biogeography

of *Cedrela* have suggested that *C. odorata* may be polyphyletic, with a distinction between Central American *C. odorata* and South American *C. odorata* populations (Finch et al. 2019; Muellner et al. 2009; Muellner et al. 2010). *Cedrela* trees are deciduous regardless of water availability and restrict growth to the wetter portion of the year, thus producing rings which are semi-ring porous (Baker et al. 2017). *C. odorata* is a fast growing species (Brienen et al. 2010; Worbes 1999) with a relatively low wood density ($0.32\text{-}0.35\text{ gcm}^{-3}$) which grows across a very broad precipitation range from aseasonal wet tropical forest to highly seasonal dry forest (Baker et al. 2017; Gutierrez-Vazquez et al. 2012). It is able to attain heights of over 40m, and grows rapidly, increasing in height by more than 1m per year in a wet tropical climate (Lamb 1968), but responds to low water availability by reducing radial growth (Worbes 1999). *C. odorata* is shallow rooted under most conditions and strongly relies on water from the upper 30cm of soil (Cintron 1990; Schwendenmann et al. 2015).

4.2.2 Sites and Sampling procedure

Cedrela trees were sampled at four sites (Figure 4.2A), Oaxaca (Mexico), Yucatan (Mexico), Selva Negra (Bolivia), and Yasuni (Ecuador). These sites span a broad precipitation gradient ranging from 1014 to 2585mm year⁻¹, and dry season lengths vary from 8 to 0 months with less than 100mm precipitation (Figure 4.2 C-F). Precipitation data are from the two (one for Selva Negra) weather stations closest to each site (Peterson and Vose 1997): for Oaxaca the stations are Santiago Chivela (16.7N, 95E) and Ixtepec (16.6N, 95.1E), for Yucatan Xcupil (19.7N, -89.9E) and Champoton (19.4N, -90.7E), for Selva Negra, an unnamed station (9.72N, 66.5E), and for Yasuni, Tiputini (-0.8N, -75.4E) and Nuevo Rocafuerte (-0.92N, -75.4E). Sites differ in soil type with well drained karstic soils at the two driest sites (Table 4.1) and clay-based soils at the wetter two sites. Forest at the two driest sites in Mexico can be classified

as seasonally dry forest (Perez-Garcia et al. 2010; White and Hood 2004), with trees growing in Oaxaca having the lowest water availability among all four sites. While mean annual precipitation is relatively similar to Yucatan, the trees grow on steep karstic slopes,

Table 4.1 Site information including number of samples per sample type (intra-tree and inter-tree as per Figure 4.3) and total number of samples, and mean annual precipitation (MAP). Soil type per site was derived from the literature, the available soil information for the Yucatan site only mentioned that it was highly Karstic (Brienen et al. 2010; Corona-Nunez et al. 2018; Valencia et al. 2004). Maximum longevity data at Yasuni could not be measured due to hollow trunks, but was estimated (Yasuni from Unpublished data, R. Brienen; Oaxaca from Unpublished data, P. Groenendijk; Yucatan and Selva Negra from Brienen et al. 2010)

site	latitude (N)	longitude (E)	intra- tree samples	inter- tree samples	total samples	MAP	max			soil	forest type	species
							height (min Height)	max DBH	max longevity			
Yasuni	-0.679	-76.394	29	22	51	2585	42.5 (3.5)	128	est. >250	Clay Ultisols	Tropical evergreen	<i>C. odorata</i>
Selva Negra	-10.161	-66.340	23	19	42	1846	35 (0.3)	66	308	Clay Xanthic Ferrosols	Tropical semi- evergreen	<i>C. odorata</i>
Yucatan	19.086	-90.007	19	18	37	1150	22 (2.5)	67	141	Karstic	Tropical dry	<i>C. odorata</i>
Oaxaca	16.666	-95.001	20	15	35	1014	13 (3.4)	58	117	Karstic Regosol	Tropical dry	<i>C. salvadorensis</i>

precipitation is concentrated over fewer months (Figure 4.2) and occurs in few high intensity events associated with hurricane activity (Brienen et al. 2013). This results in a xerophytic, low stature vegetation (Perez-Garcia et al. 2010). At Yucatan, Selva Negra and Yasuni the species sampled is *C. odorata*, whilst at Oaxaca it is *Cedrela salvadorensis*.

For each site we measured tree diameter and estimated tree height by eye. To decrease estimate errors, these height estimates were always based on two independent estimates from experienced forest scientists. Note that the measurement error is likely larger for tall trees (~5m) than for short trees (~1m). The maximum tree height decreased from 42.5m in Yasuni, the wettest site, to 13 m at the driest site in Oaxaca (Table 4.1). Forests at all four sites are relatively undisturbed. To our knowledge, sites in northern Bolivia and Yucatan have experienced some low intensity, selective logging focussed on high-value species (e.g., mahogany), while at the other two sites low intensity logging for local use cannot be excluded. At all sites, old and tall trees were still present and were included in this study.

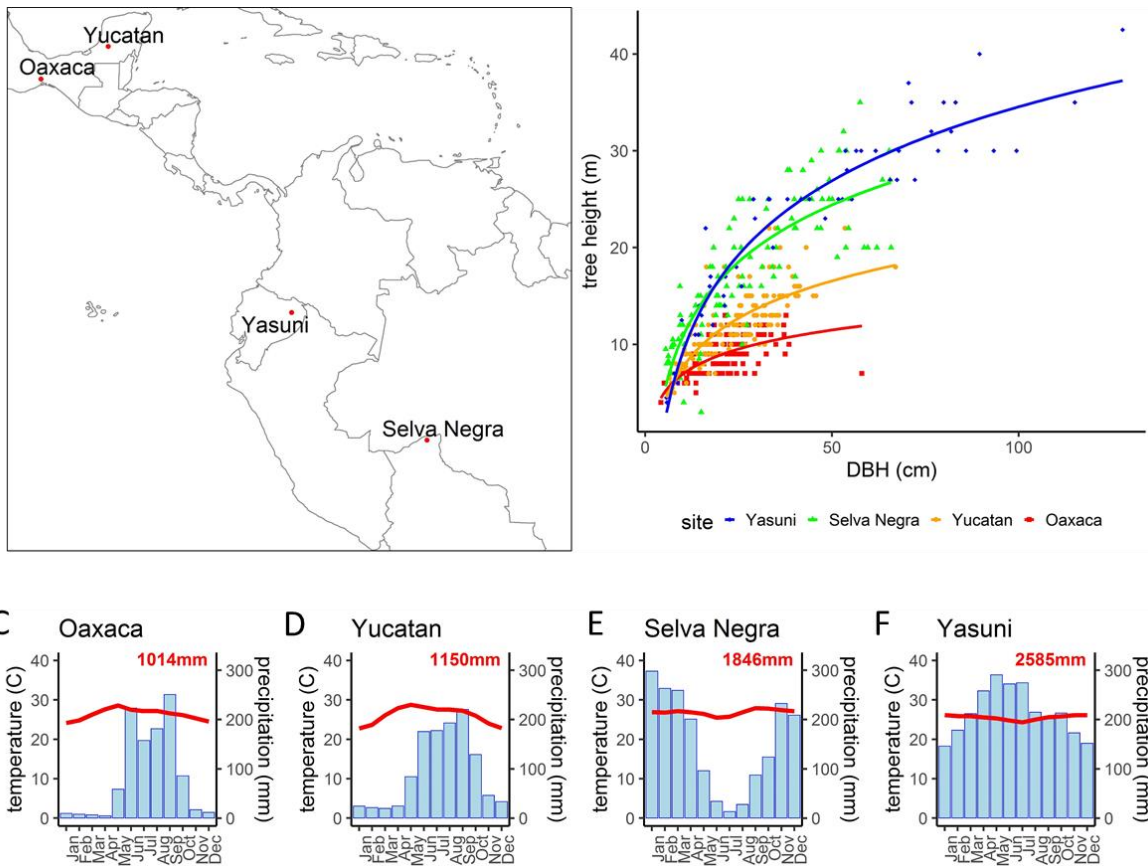


Figure 4.2 Location of sampling sites (A), diameter-height allometries at the sampling sites (B), and site monthly precipitation (C-F) with mean annual precipitation in red text (mm) and mean monthly temperature as the red line (°C). Climate data was taken from an average of the two closest climate recording stations to each site, except for Selva Negra, which had only one close climate recording station (Peterson and Vose 1997).

In order to measure how xylem vessel diameter and density varies across sites and with tree height we used tree cores taken from the base of trees *in vivo*, or stem discs taken from the bases of felled trees, and from small saplings (Brienen et al. 2010). We used a 5.15mm borer at the Oaxaca site and 10 mm increment borers at the wetter three sites. At each site, trees covering the full range of heights were sampled (see Table 4.1). Samples were generally taken

close to breast height (1.3 m). From here on 'tree height' refers to the height of the tree minus the height above ground at which the sample was taken.

For estimating how basal vessel diameter and density changes with tree height we adopted two approaches (see Figure 4.3). In the first method, the inter-tree sampling approach, we measured vessel diameter and density only in the outer wood at the base of different trees of known heights. In the second, the intra-tree approach, we sampled 2cm long radial increments at least 2cm apart from each other along a radius of a stem cross section (disk) or core. The number of samples analysed for each core or disc depended upon tree diameter: trees with large diameters were sampled at less regular distance with spacing of up to 8cm between sampled radial sections compared to smaller trees. This is justified as DBH-height allometry is not linear and large trees change less in tree height compared to smaller trees for a given diameter change (see DBH-height allometry plot in Figure 4.3). For these samples from the intra-tree approach the corresponding tree height for each sampling point was estimated using the site-specific diameter at breast height (DBH)-tree height allometry (Figure 4.3 shows how DBH allometry gives estimated height for a radial position). This intra-tree approach assumes that vessel diameter for a given height does not vary over time due to, for example, climate change or increases in CO₂. Fajardo et al. (2020) show that scaling relationships are similar across individuals and within individuals. We tested whether vessel diameter measurements differ between the intra-tree and inter-tree methods and found that they do not differ (see SI Figure 4.1). Therefore, for our main analysis we merged the two datasets. Sample sizes for both methods are shown in Table 4.1.

Wood cores were glued on wooden frames and either sanded or cut with a microtome blade to aid vessel visualisation. Photographs were taken of each wood section under a microscope

using a Canon EOS1100D camera with 2x magnification power lens using a Leica S6E microscope at 2x magnification power (4x for small trees). The digital images used for analysis had resolutions of 72 dpi, equivalent to 1.17 μm per pixel at 2x magnification. A stage micrometer was included in the images to provide a length scale. Photographs were analysed using ImageJ (Fiji, version 1.52p), and xylem vessels were identified manually. Vessel number per image varied, however in most cases over 100 vessels per image were measured (see SI Figure 4.2). A minimum of 50 vessels was recommended for sufficient statistical power considering vessel diameter variability in ring-porous species (Scholz et al. 2013).

For each wood section, the mean vessel area and number of vessels per unit area (vessel density) was later calculated using the total measured area of the image (the measured area was smaller where vessels were small and tightly packed, i.e. small trees). Vessel diameter was calculated from vessel area assuming vessels were circular, which was largely the case.

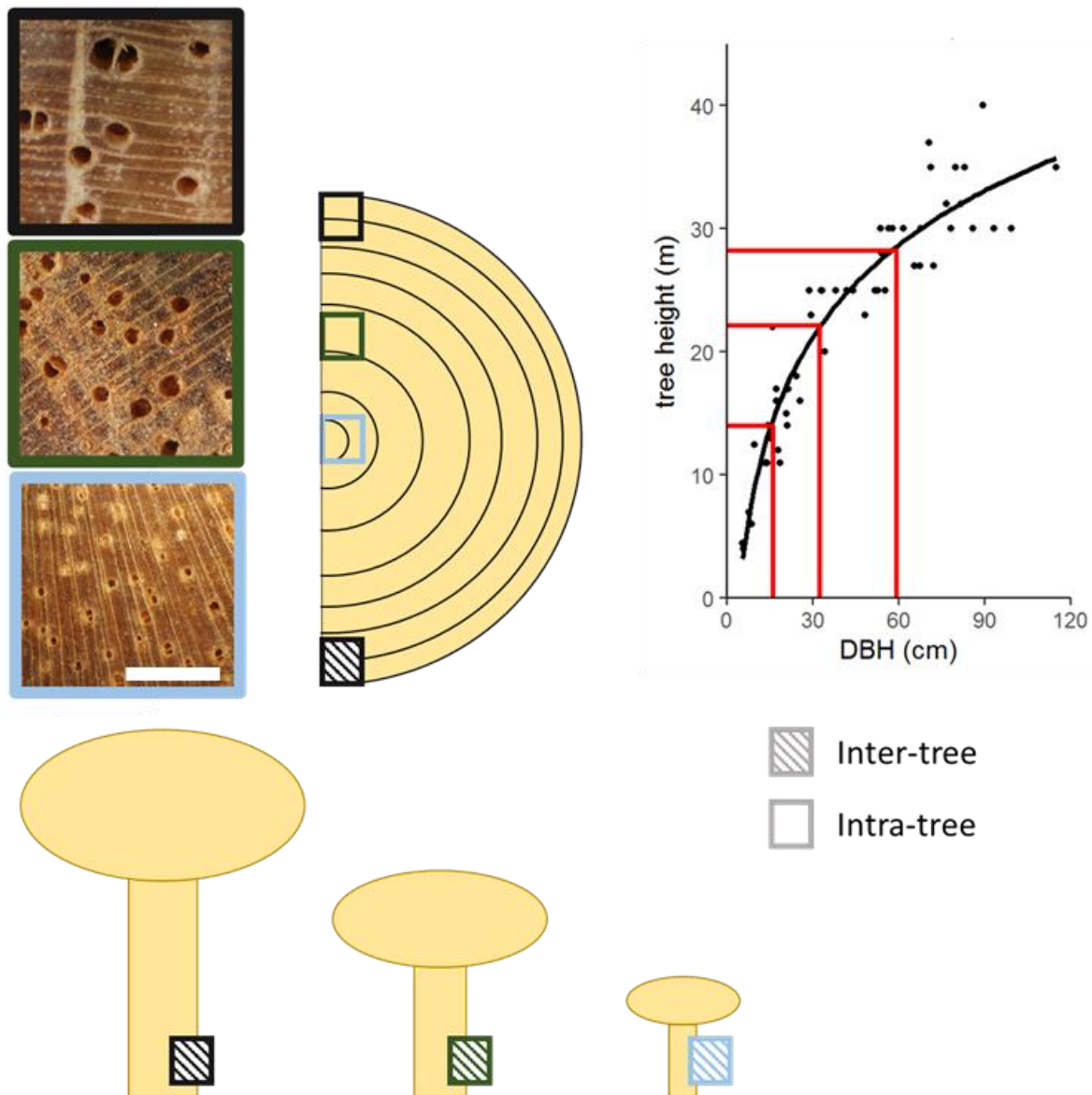


Figure 4.3 Schematic of two sampling approaches to assess the effect of tree height on vessel anatomy. In the inter-tree approach, we measured vessel diameter and density only in the outer wood at the base of different trees of known heights (hatched boxes). In the intra-tree approach, we sampled sections along the stem cross section at the base of trees at increasing distances from the tree pith within individual trees (open boxes). This results in within-tree ontogenetic patterns of changes in vessel anatomy with height, where we derived height at various sections using site specific allometric relationships between tree diameter and height (see Figure 4.2B, allometry for all sites). Left hand photographs show the surface of Cedrela tree cores that were used for image analysis, the scale bar is 1mm.

4.2.3 Analysis

In agreement with existing studies we find that the relationships between the dependent variables, vessel diameter d and density VD , with the independent variable, tree height H , follow a power law $d \propto H^\alpha$. α is the power law exponent and is equal to the slope of the relationships between $\log d$, $\log VD$ and $\log H$, respectively. To examine further how the basal vessel diameter and density tree height relationships depend on site we used linear mixed effects models (LMMs) of the form

$$\log(D) \sim \beta_0 + \beta_1 \log(H) + \beta_2 \text{site} + \beta_3 (\text{site} * \log(H)) + \mu_{0i} + \varepsilon_i \quad 4.2$$

Here μ_{0i} is the random intercept for each individual tree i and ε_i is the residual error for each individual tree. We incorporated a random intercept for individual trees since 74 individual trees were sampled more than once (i.e., along the stem disc or tree core, intra-tree approach, see Figure 4.3). Inclusion of these random intercepts improved the model fit according to AIC values, while inclusion of random slopes (for each tree) did not improve the fit. Note that slopes were similar between both sampling approaches, inter and intra-tree sampling (SI Figure 4.1), thus justifying the joint analysis of the two datasets in one statistical model. We log-transformed vessel diameter and vessel density to satisfy the assumption of linearity, as well as to permit comparison with other studies (Olson et al. 2014). We used the lme4 R package to produce the LMMs (Bates et al. 2015). Pseudo R^2 values were estimated for LMMs to assess the variance explained by the model, with and without the random effects as per (Nakagawa and Schielzeth 2013) using the MuMIn R package (Barton 2019). If the interaction effect of site with height is non-significant then slopes between sites can be considered similar. Bonferroni corrected t-tests were then carried out to determine if the

intercepts differed between sites, using the R package emmeans (Lenth 2018). All linear models were assessed for homogeneity of slopes using the anova R function, normality of the residuals (Shapiro-Wilk from the R package rstatix (Kassambara 2019) and Q-Q plots) and homogeneity of variance (Bartlett test from the R package stats (R Core Team 2018)).

We also compared sites for the magnitude difference between sites in vessel diameter and vessel density for the 5 tallest trees per site to examine the effect of being tall on basal vessel diameter and density between sites. In addition, we performed the same analysis on trees that are 2.5-7.5m tall (mean height per site was between 3.14m and 5.43m) to further assess the differences between sites with regards to vessel diameter and density for a given height (for mean height and standard deviation see SI Table 4.3). Non-parametric tests (Kruskal-Wallis, and Wilcoxon signed rank tests) were used since these subsets of the data were not normally distributed. P-values were adjusted for multiple comparisons using Bonferroni correction. All analyses were performed in R studio using R version 3.5.1 (R Core Team 2018).

4.3 Results

4.3.1 Effects of climate on basal xylem vessel diameter and density

Mean basal vessel diameter increased with tree height at similar rates at the different sites (0.393 to 0.474 log mm per log m), with non-significant interaction terms in the LMM (Figure 4.4 A and B, Table 4.2). The model explained a high proportion of the variance in vessel diameter across samples. The pseudo R^2 values suggest that fixed effects alone accounted for 86% of total variation whilst including random effects accounted for 95%. Across sites mean basal vessel diameter was similar for a given height between most site pairs as shown by non-

significantly different intercepts (Table 4.2). However, we found a significant ($p=0.006$) difference in the intercept between Selva Negra and Yucatan, with basal vessels in Yucatan being 1.763 times larger than those in Selva Negra (Table 4.2). Despite this difference, there was no evidence that trees in drier sites have consistently larger or smaller vessels for a given height than trees in wet sites.

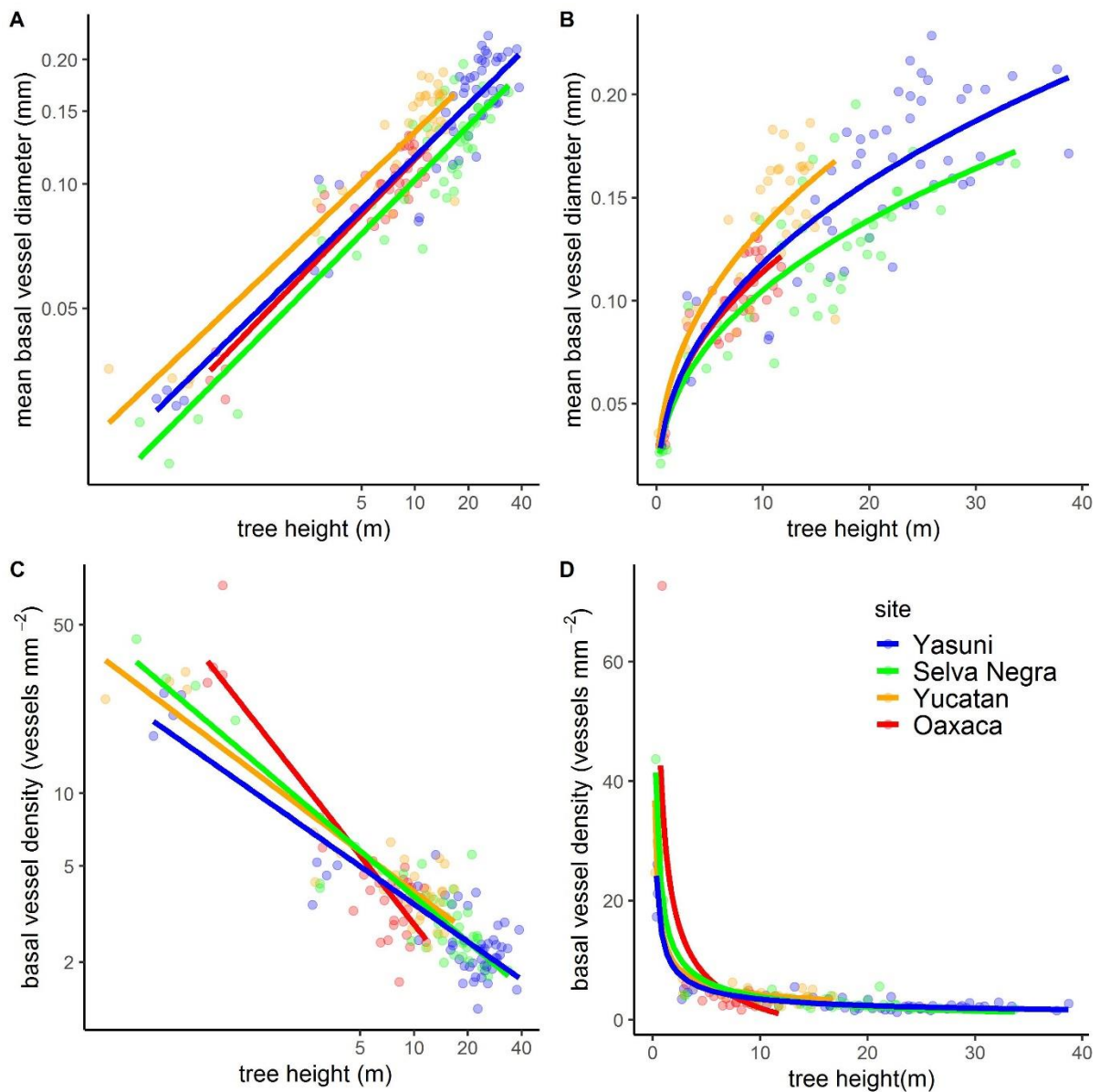


Figure 4.4 Relationships between mean basal vessel diameter (A,B) and basal vessel density, and tree height (C,D). A and C show log transformed data with linear regression lines for each site (for coefficients and comparisons of intercepts see Table 4.2). B and D show non-transformed data, with regression equations of the form resulting in $y = \text{const} * x^\alpha$ taken from the logged linear relationship coefficients of A and C.

Table 4.2 Results of linear mixed effects models predicting log mean vessel diameter and log vessel density from log tree height (leftmost column). Site is included as an interacting fixed effects factor with tree height representing the homogeneity of slopes between sites (n.s. = $p>0.05$, ** = $p<0.001$, *** = $p<0.0001$). Intercept and slope of the site-specific models are shown with upper and lower confidence intervals (CIs). Intercept and slope comparisons between sites for the linear mixed effects model for vessel diameter and vessel density are shown (multiple comparisons corrected t-tests), significant differences are represented by different letters after the site-specific intercepts and slopes (small letters for slopes, and capitals to intercepts). For vessel density, Oaxaca was excluded from intercept comparisons since the slope differed significantly from the other three sites (for further details of site slope and intercept comparisons see SI Table 4.2 and SI Table 4.3).

Independent variable and effects	Site	Terms (CIs)	df	
Basal vessel diameter ~	Yasuni	slope	0.406 (0.359 : 0.453) ^a	121.3
		intercept	-3.090 (-3.221 : -2.959) ^{AB}	109.2
Height (F= 882.102 ^{***}) +	Selva Negra	slope	0.474 (0.417 : 0.53) ^a	104.9
		intercept	-3.237 (-3.364 : -3.11) ^A	106.8
Site (F= 6.393 ^{***}) +	Yucatan	slope	0.393 (0.343 : 0.443) ^a	153.5
		intercept	-2.864 (-2.981 : -2.746) ^B	124.1
Site : Height (F= 1.845 ^{n.s.})	Oaxaca	slope	0.448 (0.372 : 0.523) ^a	144.7
		intercept	-3.108 (-3.239 : -2.975) ^{AB}	150.2
Basal vessel density ~	Yasuni	slope	-0.533 (-0.608 : -0.457) ^a	106.1
		intercept	2.471 (2.264 ; 2.678) ^A	99.6
Height (F= 748.897 ^{***}) +	Selva Negra	slope	-0.642 (-0.73 ; -0.552) ^a	98.1
		intercept	2.656 (2.454 : 2.858) ^A	113.5
Site (F= 6.036 ^{**}) +	Yucatan	slope	-0.551 (-0.636 : -0.466) ^a	145.2
		intercept	2.579 (2.389 : 2.769) ^A	119.7
Site : Height (F= 7.863 ^{***})	Oaxaca	slope	-0.876 (-1.00 : -0.75) ^b	136.7
		intercept	3.068 (2.846 : 3.29)	145.5

Basal vessel density decreased with tree height at a different rate for the different sites (Table 4.2). For trees at the driest site, Oaxaca, vessel density declined more rapidly with tree height (-0.876 log mm per log m) compared to the other three sites (-0.53 to -0.64 log mm per m) (Figure 4.4C and D, Table 4.2). The wetter three sites, all with *C. odorata*, share similar declines in vessel density with height (Table 4.2) and have similar intercepts with no indication for drier sites to have lower or higher vessel density (Table 4.2). The LMM accounted for a high proportion of the variance in vessel density across samples, the fixed effects alone accounted for 84% of total variation whilst including random effects accounted for 91%.

Basal vessel diameter of the tallest trees in each site increased with site wetness, nearly doubling between Oaxaca and Yasuni (Figure 4.5B). However, basal vessel density of the tallest trees was lower in wet sites relative to drier sites ($P < 0.05$) (Figure 4.5A).

species synthesis studies. Here we assessed how tree hydraulic architecture varies across a water availability gradient within the widespread and important tropical genus *Cedrela*.

We find that maximum observed tree height (from 13 m to 42.5 m) and longevity (117 to 308 years, Unpublished data, R. Brien; Unpublished data, P. Groenendijk; Brien et al. 2010) increase strongly with water availability across our sites, which is in line with other studies in the tropics (for effects on tree height see Klein et al. (2015); Tao et al. (2016); Gorgens et al. 2020, and for tree longevity, see Locosselli et al. (2020)). For *Cedrela*, amongst the three possible proposed scenarios of stem hydraulic property variation across climates outlined in Figure 4.1, we find that strategy B is realised. Thus, for this species there is no adaptation of examined hydraulic properties in response to water availability or climate, and basal vessel size for a given tree height is the same across sites irrespective of water availability as is the taper rate. Interestingly a very recently published study examining temperate-climate trees found similar results (Fajardo et al. 2020).

Our results raise interesting questions about causal relationships. The large difference in longevity means that environmentally caused mortality risk is much higher at drier sites which suggests that a drought stress-related mortality mechanism could be the reason. Such a mechanism is indeed plausible given the climate-independent nature of the hydraulic properties we examined. Given the self-similar nature of hydraulic properties, hydraulic efficiency (conductivity) will tend to be maintained with increasing height (Anfodillo et al. 2006; Gleason et al. 2012; Jacobsen et al. 2018; Lazzarin et al. 2016b; Losso et al. 2018; Olson et al. 2014; Petit et al. 2010; Prendin et al. 2018; Savage et al. 2010; Sperry et al. 2006; West et al. 1999), but hydraulic failure risk via embolism may increase as vessel diameter increases (Levionnois et al. 2021; Lobo et al. 2018; Olson et al. 2018; Prendin et al. 2018; Scoffoni et al.

2017; Sperry et al. 2006). However, there is debate regarding the extent to which vessel diameter affects embolism vulnerability (Gleason et al. 2016; Liu et al. 2020). Our finding of invariance of the basal vessel size-tree height relation across a water availability gradient is consistent with the general finding across a wide range of tree species and tree sizes that there is a strong correlation between basal vessel size and tree height (Olson et al. 2014). Furthermore, measurements of embolism risk of planted saplings with height up to 4 m for three species by the same authors reveal a strong decrease of the water potential at 50% stem conductivity loss with tree height (Olson et al. 2014). This latter finding is consistent with the interpretation of our results, that basal vessel diameter depends on tree height but not climate, and thus that increased mortality risk at drier sites is probably related to tree hydraulics. This interpretation is also consistent with the results of a study by Shenkin et al. (2018) who investigated the effect of the 2004/5 El Niño drought event on tree mortality in natural forests in Bolivia. These authors found strongest increases of mortality risk with increasing drought stress in tall trees and attribute the result to tree hydraulics. Increased risk of tall trees under drought stress has also been found in global meta-analyses (Bennett et al. 2015; Johnson et al. 2018b), and a long-term Amazon drought experiment (Rowland et al. 2015).

What these studies cannot discern, however, is to what extent increased mortality is indeed related to embolism risk in the stem or rather the roots, or yet to different drought related deleterious effects (Brodribb and Cochard 2009; Brunner et al. 2015; McDowell et al. 2008). We can of course also not rule out hydraulic adaptations that may offset the decreases in water availability across sites and mitigate drought stress. For example, trees may vary their inter-vessel pit architecture which has been shown to vary across species (Lens et al. 2016), and could result in decreases in embolism risk (Medeiros et al. 2019; Pittermann et al. 2010).

In addition, trees may increase investment in root tissue and rooting depth (Brum et al. 2019; Dawson and Pate 1996), or trees may reduce the effect of hydraulic stress through strict control of stomatal conductance (isohydry) (Jones 1998; Tardieu and Simonneau 1998), or by shedding leaves to avoid excessive water loss (Manzoni et al. 2015; Vico et al. 2017). *Cedrela* trees are indeed likely to be at least to some extent isohydric given their relatively large vessels and high water potential at which 50% loss of conductance occurs (>-1 MPa stem P50) (Hoeber et al. 2014; Villagra et al. 2013a; Villagra et al. 2013b). *Cedrela* is also a deciduous tree species, thereby limiting exposure to dangerously low water potentials during the dry season. Nonetheless, trees at the drier site are likely to experience greater hydraulic stress more frequently than trees of equivalent height at the wet site, due to lower wet season rainfall levels (see Figure 4.2 and Table 4.2), the steep slopes at which trees were growing, and fast draining karstic soils leading to very low soil water potentials.

We also show that for *Cedrela* trees vessel density decreases as vessel diameter increases with tree height. This is expected from tapering theory as vessels divide and become smaller, so wood increases in vessel density (Savage et al. 2010; West et al. 1999). Vessel density increases may be able to offset losses in conductance due to decreases in vessel diameter, thus providing a potential strategy to avoid embolism risk, whilst maintaining high conductance (Echeverria et al. 2019). Therefore, we may have expected that trees in drier sites would have higher vessel density and smaller vessels. This does not appear to be the case in *Cedrela* across the broad climate gradient covered in this study. *C. salvadorensis* trees from Oaxaca decrease in vessel density at a higher rate than the wetter three sites. This may, however, be due to inter-species variation, rather than any climatic influence on vessel density per se.

4.4.1 The universal scaling of vessel diameter

Using global multispecies data, Olson et al. (2014) found a slope of the relationship between log basal vessel diameter and log tree height of 0.46 (95% confidence interval of 0.41–0.51), compared with 0.39 to 0.47 we found here (Table 4.2). Thus, the taper rate of *Cedrela* trees is similar, but slightly lower relative to the global data. The slopes of the relationship between log basal vessel density and log tree height found here (-0.53 to -0.88) are largely within the range of those found in that same study, i.e., a slope of -0.73 (95% confidence interval of 0.86-0.61) (Table 4.2). Because of the global nature of their study they suggested that regardless of growing conditions trees should achieve similar rates of increase in vessel diameter with tree height. This present study and the recent study of Fajardo et al. (2020) show this also to be the case within species across a gradient of very different water availabilities. Together, these results suggest that the underlying mechanism behind the process of vessel production at different heights is likely highly conserved in evolution.

How trees should increase basal vessel diameter with height at such a fixed rate is unclear. Several possible mechanisms have been presented to explain constant scaling of vessel diameter with height (Fajardo et al. 2020). One hypothesis discussed by Fajardo et al. (2020) and proposed by Woodruff and Meinzer (2011) is that vessel diameter is controlled by the turgor pressure at the site and time of the formation of the vessel. The turgor pressure is in turn controlled by height, with the xylem water potential being more negative at greater heights, which also likely limits embolism risk further down the tree where vessels are wider. Our and Fajardo et al.'s (2020) data show that basal vessel diameters for trees of a given height are similar across climates while different xylem pressures are likely to differ given

difference in soil water availability. It is therefore unlikely that this could explain constant scaling of vessel diameter with tree height.

Instead the observed increase of vessel size towards the base may be the result of a hormonal control. Anfodillo et al. (2012) found that xylem conduit width increase with distance from apex in a conifer is caused by longer cell expansion, which was hypothesised to result from a gradient from apex to base of the growth hormone Auxin. In support of this Hacke et al. (2017) find that variation in vessel diameter for a given height is likely mediated by endogenous, hormonal stimulation of cell growth, and Johnson et al. (2018a) found that treatment of *Populus* trees with an Auxin transport inhibitor caused the formation of comparably narrower diameter and shorter vessels. However, Auxin transport is also affected by drought (Korver et al. 2018), which would lead to differences in tapering across a climate gradient, and is thus not consistent with our results.

While the ultimate mechanistic process behind tapering remains unresolved is it likely that the universal scaling of vessel diameter with tree height is the result of natural selection due to a cost-benefit trade-off between small vessels with low flow rates for a given body size impeding photosynthesis and thus productivity, and large vessels that have innate vulnerability to embolism (Knipfer et al. 2015; Olson et al. 2018; Scoffoni et al. 2017; Sperry et al. 2006) and may reduce mechanical strength (Christensen-Dalsgaard et al. 2007; Fan et al. 2017).

The rate of vessel tapering is highly conserved across taxa, but vessel diameter for a given height varies between related species (Lechthaler et al. 2019; Lens et al. 2004; Pfautsch et al. 2016). Plasticity in the diameter of vessels has been demonstrated in the short term in response to climate, similar to the effect of drought on tree ring width (Zweifel et al. 2006).

Using tree-ring data in two tropical species, Locosselli et al. (2013) showed that vessel area is positively correlated with precipitation and negatively with temperature. Similar results were also obtained by using tree-ring chronologies of *Tectona grandis* (Pumijumng and Park 1999).

Thus, it is conceivable that trees can alter their rate of tapering via endogenous stimulation in the short term, but the costs of doing so over long periods of time outweigh the benefits. Regardless of potential short term plasticity not assessed here, this study and previous studies show that the diameter and density of vessels for a given height appear highly conserved within species (Fajardo et al. 2020; Lechthaler et al. 2019; Pfautsch et al. 2016; Warwick et al. 2017), thus suggesting that many tree species cannot support long-term changes in vessel diameter and density for a given height due to the embolism, mechanical or carbon-balance costs of doing so. But, over evolutionary time, other adjustments in tree physiology that offset these costs may enable differences in vessel diameter for a given height across related taxa higher than species (Lechthaler et al. 2019; Lens et al. 2004; Pfautsch et al. 2016).

The invariant nature of basal vessel widening in relation to rainfall, has consequences for the ability of trees to adapt to future changes in rainfall in the tropics. Our results indicate that water availability puts a limit on maximum basal vessel size, which in turn seems to play a role in controlling maximum tree height, as well as tree longevity. Thus, rather than adjusting their principal hydraulic architecture tropical trees growing in areas with decreasing rainfall are likely to see a reduction in their longevity and overall change towards shorter maximum tree height, consistent with observations of decreases in tree height (Gorgens et al. 2020; Klein et al. 2015; Tao et al. 2016) and tree longevity (Locosselli et al. 2020) with increasing dryness in the tropics.

4.4.2 Conclusions

We show that maximum tree height of *Cedrela* increases almost threefold between dry and wet sites. Furthermore, we find that vessel diameter and density are remarkably similar at a given height across sites, and thus the rate at which basal vessel diameter scales with tree height (i.e. tapering) is remarkably conserved. Thus, variability in mean basal vessel diameter is likely not used to mediate hydraulic stress across sites in *Cedrela* in trees of a given height. At their maximum height, trees at the wettest site have almost two times larger basal vessels compared to trees at the driest site. These results suggest that maximum tree height is at least to some extent constrained by a fixed species-specific underlying hydraulic architecture and may indicate greater hydraulic vulnerability of similar sized trees at the drier sites. This could provide a mechanism for explaining decreases in tree height and longevity with decreasing water availability as generally observed in the tropics.

Chapter 5 Effects of tree height on ecophysiological traits for three neotropical tree species differing in life-history strategy

Abstract

Trees experience strong changes in light environment and water transport path length when growing through a tropical forest canopy. This will result in variation in leaf ecophysiological functioning and leaf and xylem morphology with tree height including changes in stomatal regulation of water potentials and change in leaf size and mass and intrinsic water use efficiency. The linkage between these aspects has not been studied in detail for tropical trees. Determining how hydraulic function changes as trees grow taller may help to reveal possible mechanisms enabling different tropical tree species to utilise different life-history strategies to grow and survive. This research aims to better understand the complexity of tropical forest species' eco-physiological adaptations to changes in tree height and light availability. We study three species varying along the growth and shade-tolerance spectrum from a fast-growing, shade-intolerant species, *Centropogon microchaete*, to intermediate *Ampelocera ruizii*, and shade-tolerant species, *Pseudolmedia laevis*. We find that leaf mass per area (LMA) and intrinsic water use efficiency (derived from $\delta^{13}\text{C}$) increases with tree height, while maximum leaf area decreases. Vessel tapering is relatively similar between the species and at the apex we do not find any relationship with tree height in vessel size or density. Temporal variation in leaf water potential shows greater hydraulic stress in the dry season compared to

end of the wet season, although for *P. laevis* leaf water potentials are maintained at relatively constant, high values ($>-1\text{MPa}$) throughout. Variation in leaf water potential with tree height shows greater hydraulic stress for taller trees in the dry season in *A. ruizii* only, for *P. laevis* leaf water potentials are maintained at relatively constant, high values ($>-1\text{MPa}$) regardless of tree height. Differences between species in ecophysiological properties align with life-history strategy. For example, we find that faster-growing, shade-intolerant *C. microchaete* has lower LMA, lower leaf water potentials, and larger vessel diameters compared to the slower-growing, shade-tolerant *P. laevis*. These differences agree with previous studies on functional traits of seedlings and saplings of these species.

5.1 Introduction

5.1.1 Hydraulic strategies of tropical trees

The trade-off between hydraulic safety and efficiency traits suggests that different strategies of growth and survival are possible for a given water availability, and this is confirmed by the observed diversity of hydraulic strategies in tropical forests (Anderegg et al. 2018; van der Sande et al. 2019). The life-history strategy used by a tree species is likely to be reflected in hydraulic strategy. Namely a strategy of long life and slow growth likely favours hydraulic safety to survive multiple droughts over the life of the tree, whereas short lived and fast growing species likely favour greater hydraulic efficiency to outcompete other trees in the race to the canopy at the expense of safety causing greater vulnerability to droughts (Aleixo et al. 2019; Markesteijn et al. 2011; Poorter et al. 2010).

Hydraulic efficiency and productivity are influenced by different anatomical and ecophysiological properties. Within the wood, increased xylem vessel diameter reduces resistance to water flow from root to leaf and thus increases the water flow rate up the xylem

for a given water potential gradient, thereby enhancing gas exchange and photosynthetic capacity (Fichot et al. 2009; Holtta and Nikinmaa 2013). Conversely smaller vessels tend to be less vulnerable to embolism at a given water potential, as indicated by a more negative P50 value, the water potential at which 50% of xylem conductance is lost (Knipfer et al. 2015; Olson et al. 2018; Scoffoni et al. 2017; Sperry et al. 2006; Wheeler et al. 2005).

A greater difference between apical and soil water potential increases vertical water flow (Brum et al. 2018; O'Brien et al. 2004), which is regulated over short timescales by stomatal conductance (Fisher et al. 2006; Huzulak and Matejka 1982; Myers et al. 1987). Higher productivity is associated with more negative water potential at which stomata close, greater stomatal area per leaf, and larger leaf area with a greater proportion of photosynthesising tissue per leaf area (Bertolino et al. 2019; Coble and Cavaleri 2017; Niinemets 1999; Wright et al. 2004). Having higher stomatal conductance for a given water potential however exposes the tree to lower water potentials and thus increased risk of embolism by being closer to the P50 value, also known as the hydraulic safety margin (Choat et al. 2012; Meinzer et al. 2009; Mencuccini 2003). Thus, we expect a trade-off between productivity and safety based on these functional traits and ecophysiological properties. Species with different strategies of growth and longevity should represent this trade-off in their measured functional traits which we measure across trees of different height from sapling size to tallest adults, whereas previous tropical studies often utilise juvenile trees (Markestijn and Poorter 2009; Poorter and Bongers 2006).

5.1.2 Height and hydraulic stress

Growing tall can generate hydraulic stress, requiring trees to pull water further against gravity and possibly against increasing resistance (Koch et al. 2004; Niklas 2007; Ryan and Yoder

1997). Because of this, taller trees require more negative pressures to be generated at the tree apex in order to maintain a similar water flow to a given area of leaf relative to that of a shorter tree, as per the hydraulic analogue of Ohm's law (Ryan and Yoder 1997). However, trees avoid resistance increases with increasing height by increasing xylem vessel diameter, as shown in Chapter 4 (Anfodillo et al. 2006; Olson et al. 2014; Savage et al. 2010; West et al. 1999). This however may subject trees to increased vulnerability to embolism as wider xylem vessels more readily form gas bubbles that may expand and block water flow throughout the xylem network (Knipfer et al. 2015; Olson et al. 2018; Scoffoni et al. 2017; Sperry et al. 2006; Wheeler et al. 2005). Thus, as trees grow taller the gradient of water potential must increase or path length resistance must be maintained by xylem anatomical adjustment, or else flow rates will reduce and so will productivity. Fundamentally, drought and tree height produce similar effects on the hydraulic functioning of trees, and decreasing water availability with climate change is likely to negatively affect forest height as taller trees become hydraulically stressed beyond physiological limits (Anderegg et al. 2019; Fajardo et al. 2019; Shenkin et al. 2018; Stovall et al. 2019).

5.1.3 Tree trait and functional changes transitioning from below to above canopy life stage

Trees experience increasing hydraulic stress with increasing height, and when growing in a tropical forest environment, growing tall means growing across a strong environmental gradient, from a dark and humid environment close to the forest floor to a sunny and dry environment in or above the canopy (Tymen et al. 2017). Trees higher in a canopy also experience greater evaporative demand which, if unregulated by stomatal control, reduces the water potential at the leaf level and in turn in the water column. These vertical changes are expected to require adjustment to hydraulic anatomy and physiological properties in

order to maximise productivity (Coble and Cavaleri 2017; Poorter 2009; Rijkers et al. 2000). Studies show that as trees grow taller leaves become smaller and thicker, i.e. a higher leaf mass per area (LMA) and smaller maximum leaf area (Cavaleri et al. 2010). Different studies have shown that the hydrostatic gradient with height affects the ability of leaves to expand and thus their area decreases and thickness increases (Koch et al. 2004; Oldham et al. 2010). A tighter packing of photosynthetic tissue in smaller leaves with a thicker palisade mesophyll enables leaves to maximise light absorption in a high light environment (Coble and Cavaleri 2017). A higher LMA may also result from a reduced proportion of leaf air space, the gaps between mesophyll cells into which water evaporates from the xylem and CO₂ from the atmosphere travels to photosynthesising cells, reducing water loss (Flexas et al. 2008; Hanba et al. 1999; Oldham et al. 2010). Thus, as tropical forest trees grow through the canopy, both changes in light and height may require leaves with a higher proportion of dry mass per leaf area (Cavaleri et al. 2010).

Leaves also control hydraulic status and photosynthesis rates by modulating stomatal conductance to control leaf level gas exchange (Brodribb and McAdam 2013; Klein 2014; Lawlor and Cornic 2002). The anatomy of stomata is important for determining gas exchange, since smaller stomata (at a given density) exchange less water for CO₂ with the atmosphere, and are more able to respond to changing conditions (Lawson and Blatt 2014). The stomatal control of gas exchange affects the intrinsic water use efficiency (iWUE), the amount of carbon assimilation per unit of water lost. As trees grow taller their iWUE is known to increase due to a combination of greater light intensity increasing assimilation rates, and lower water potential at greater evaporative demand inducing stomatal closure and thus reducing stomatal conductance (McDowell et al. 2011; Woodruff et al. 2009). Thus, we expect trade-offs as trees grow taller through a canopy gradient between traits that enable the

maximisation of light utilisation in photosynthesis and enduring an increasingly hydraulically stressful environment.

5.1.4 Aims and objectives

This study will investigate how hydraulic and ecophysiological traits change with tree height for three species with different life-history strategies. Traits include xylem vessel architecture and embolism vulnerability, stomatal anatomy, leaf size and mass, as well as carbon isotope ratios that indicate iWUE. We also measure leaf water potential and its response to environment. We chose three species with different life-history strategies; *Pseudolmedia laevis* (Ruiz & Pav., Moraceae), *Centrolobium microchaete* (Mart. Fabaceae) and *Ampelocera ruizii* (Klotzsch, Ulmaceae). *P. laevis* is a slow growing shade-tolerant evergreen species, *C. microchaete* is a fast-growing light-demanding deciduous pioneer species, and *A. ruizii* is an evergreen shade-tolerant tree with a high growth rate (Markesteyn and Poorter 2009).

Specifically, we measure several leaf properties; LMA, maximum leaf size and mean leaf size, stomatal size, density and theoretical maximum conductance, as well as leaf $\delta^{13}\text{C}$. We also measure wood traits, namely xylem vessel width and density at the apex of branches and incrementally down the tree to the base of the tree. Additionally, in order to assess hydraulic safety, we measure leaf water potential at several points in the day and assess the embolism resistance of branches (the water potential that induces 50% air discharge, which is equivalent to 50% loss of conductance). See Table 5.1 for list of measurements and the significance of each measurement for tree ecophysiology.

Table 5.1 List of measurements made in this study and their ecophysiological significance.

Measured trait/property	Ecological significance
Leaf mass per area (LMA)	Change in photosynthesising organ

Maximum leaf area	Change in photosynthesising organ
Stomatal pore length	Change in potential stomatal conductance
Stomatal pore density	Change in potential stomatal conductance
$\delta^{13}\text{C}$	Change in intrinsic water use efficiency (A/gs)
Xylem vessel diameter	Conductance to water
Xylem vessel density	Conductance to water
Daily profile of leaf water potential	Regulation of water potential and thus control of hydraulic stress
Hydraulic vulnerability curve	Impact of water potential on hydraulic function

5.1.5 Expectations of ecophysiological properties and functional trait variation with changing height and position relative to the canopy

We expected leaves to become smaller and thicker (reduced maximum leaf area and increased LMA) in response to changing hydraulic and light conditions at greater height (Cavaleri et al. 2010; Kenzo et al. 2006), and for theoretical maximum stomatal conductance to increase (Van Wittenberghe et al. 2012) and $\delta^{13}\text{C}$ to increase with height (McDowell et al. 2011). We also expected xylem vessel diameter to scale with distance to the apex at a predictable rate (slope of 0.2, log-log scale) (Anfodillo et al. 2006; Olson et al. 2014). With increasing height up through the canopy we expected leaf water potential to decline during pre-dawn by at least -0.01MPa m^{-1} due to gravity alone (Kenzo et al. 2006; Scholander et al. 1965), and during the day to decline with height by some greater value because of increasing evaporative demand through the canopy and increased need to exchange water for CO_2 with increasing light availability through the canopy (Kenzo et al. 2006). We also expected terminal twig xylem vessels to increase in diameter with height as suggested by previous studies (Olson et al. 2014), which in turn would suggest embolism vulnerability (P50 value) should increase with height (Olson et al. 2018).

Regarding differences between species we expect that the faster growing species will have lower LMA, higher maximum theoretical stomatal conductance, and wider and less densely packed xylem vessels in order to increase hydraulic conductance and photosynthesis rates relative to the slower growing species (Markesteijn et al. 2011; Poorter and Bongers 2006). We also expected differences between species in the leaf water potential changes throughout the day with greater declines in leaf water potential during the day for faster growing species due to maintenance of high stomatal conductance to sustain high rates of photosynthesis throughout the day (Poorter and Bongers 2006). Furthermore, we expected faster growing species to have greater xylem vessel diameter and higher P50 values, since these properties enable greater hydraulic conductance, and permit greater photosynthesis rates (Poorter et al. 2010).

5.1.6 Hypotheses

The hypotheses being tested in this chapter are that ecophysiological and anatomical traits and properties change with height in reflection of increasing hydraulic stress and light availability. There are some specific a priori expectations for several of the properties measured in this chapter as discussed above, e.g. water potential declining with height at a rate of 0.01MPa m^{-1} due to gravity, and xylem vessel diameter tapering at the rate predicted in the literature (West, Brown and Enquist 1999, Olson et al. 2014, Savage et al. 2010). We also test whether different species respond to increasing height differently based upon the study species' respective life-history strategies. This is novel since very little research has been conducted to understand how ecophysiological properties change with height in tropical trees. This has implications for how trees cope with increasing hydraulic stress associated with a changing climate.

5.2 Methods

5.2.1 Study sites

The study site, *Hacienda Kenia*, in Santa Cruz Department, Bolivia (16.0158°S, 62.7301°W) is located at the transition between wet Amazonian forest and dry Chiquitano forest (Araujo-Murakami et al. 2014). Amazonian forests tend to be taller (our observations), and have a higher proportion of evergreen species relative to Chiquitano forests (Araujo-Murakami et al. 2014). Typical Amazonian and Chiquitano species co-occur at this site, where the prevalence of species of each forest type depend upon edaphic conditions. At the study site Chiquitano species are prevalent on shallow soils (<1m) whilst Amazonian species are prevalent on deeper soils (>2m) (Araujo-Murakami et al. 2014). This study measured trees only in the tall Amazonian type forest. The climate of the study site is seasonal with a pronounced dry season of 6 months with less than 100mm rain month⁻¹, and an annual precipitation of 1352mm year⁻¹. The site is occasionally affected by fire (Araujo-Murakami et al. 2014).

5.2.2 Study species

We study three canopy tree species, *Ampelocera ruizii*, *Pseudolmedia laevis*, and *Centrolobium microchaete*. These species occupy distinct ranges in water availability that overlap at this study site due to its location at the ecotone between wet Amazonian and dry Chiquitano forest types (Esquivel-Muelbert et al. 2017a; GBIF 2019a; GBIF 2019b; GBIF 2019c). *A. ruizii* is distributed from Amazonian to Chiquitano dry forest ecosystems, *P. laevis* occurs only in Amazonian wet forests, and *C. microchaete* in Bolivia occurs largely in the Chiquitano dry forests. *A. ruizii* is classed as an evergreen, shade-tolerant with mid-high wood density of 0.55-0.648 g cm⁻³ (de Souza et al. 2016; Markesteijn et al. 2011). *P. laevis* is an

evergreen shade-tolerant species that grows slowly with mid-high wood density (de Souza et al. 2016; Rozendaal et al. 2010). *C. microchaete* is a fast-growing semi-deciduous shade-intolerant pioneer (Markesteyn et al. 2011). *C. microchaete* has compound leaves and all measurements were made using single leaflets unless otherwise stated.

5.2.3 Sample strategy

Samples of branches were collected from the crowns of trees which were accessed by rope in the case of tall trees or using telescopic cutters to cut branches of smaller trees. The sample strategy was to measure traits and collect samples from a range of heights for each species. An initial assessment of tree heights in the area of the study site was performed using a Nikon Forestry Pro laser range finder (Nikon Vision, Tokyo, Japan) from which three height classes were derived, namely, tall (>18m), medium (10-18m) and short statured trees (<10m) (see SI Figure 5.1). In each height class we sampled three individual trees. For the medium and tall height classes one upper crown branch and the lowest branch of the crown were sampled. This meant that we collected two branches per tree so we had to only climb one tree for two sample points. We sampled only one branch at the top of the crown from the smallest height class as the top and bottom of the crown were close together. Each point was also assessed using the 5 point Dawkins light index with subdivision of class 2 and 3, giving 8 total classes, which correspond well with openness to sky (Clark and Clark 1992; Keeling and Phillips 2007). Here, 1= very little direct light from any direction, 2= some light, only lateral direction, 3= high intensity lateral light only, 4= less than 50% of crown experiencing overhead direct light, 5= over 50% of crown experiencing overhead direct light, 6= over 90% of the crown receiving overhead direct light, 7= full direct light in all directions, please note that the lowest crown illumination class was not included because no sampled branches experienced no direct

lateral or overhead light, so in practice only 7 classes were used. Height and light indices were highly positively correlated for the three species (R^2 of 0.64, 0.70 and 0.32 for *A. ruizii*, *P. laevis*, and *C. microchaete* respectively (SI Figure 5.2)).

Leaf water potentials were measured before dawn, as an estimate of the water potential at equilibrium with soil water potential (Fisher et al. 2006). Samples were then collected at midday (12:00 – 13:30) and when possible during the late afternoon (15:30 – 17:00). For *A. ruizii* and *P. laevis* samples were collected during two distinct periods, one at the end of the wet season in June when heavy rainfall was recorded for several days at the beginning of the period, and another at the peak of the dry season when conditions were warmer with no rain in July. Climate was measured using a Hobo climate sensor (UX120 series, Onset Computer Corporation, Bourne, USA). Mean daily temperature was 19.3°C during the wet period and increased to 23.2°C in the dry period (separated by a 14 day period), mean daily relative humidity was similar between wet and dry periods, 80.4 and 81.6 respectively.

To analyse wood anatomy, we collected wood samples vertically up the trunk of each tree using an increment borer (either 5 or 10mm diameter cores depending upon wood hardness), and from the branch by cutting sections with a saw. The trunk of the tree was typically sampled in three places, one at the base of the tree, one at the point below crown insertion, and one in between (Figure 5.1).

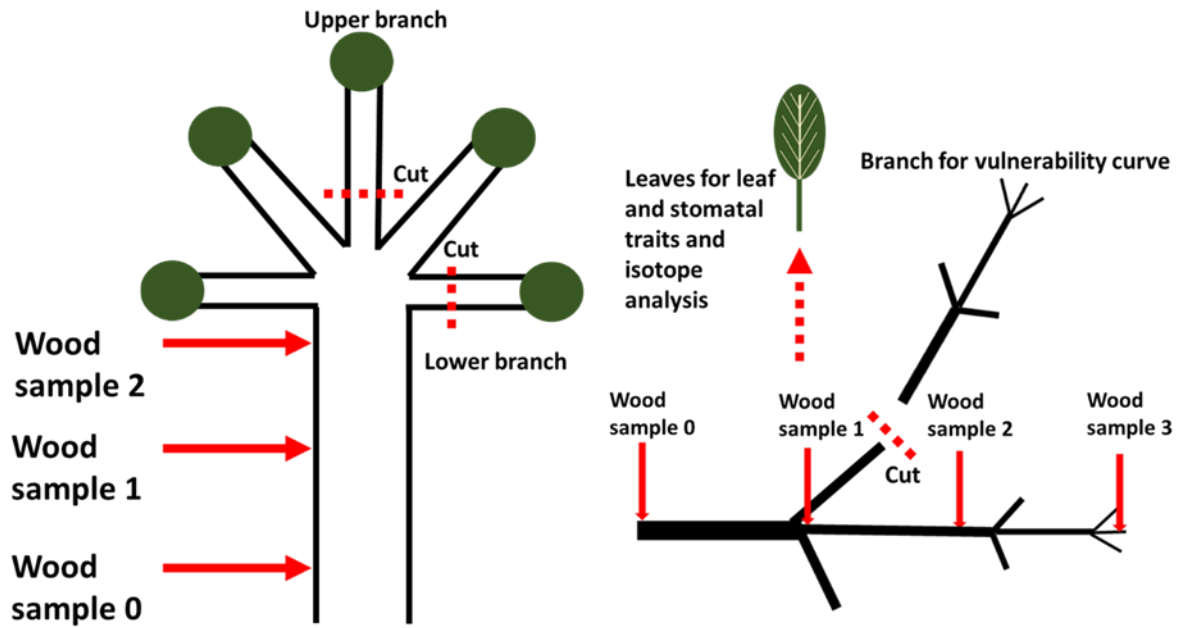


Figure 5.1 Scheme of sampling within a tree. Wood samples were taken vertically along the trunk and along cut branches from the upper crown and lower crown. The typically large upper and lower branches were also used for leaf sampling and for vulnerability curve measurements. In the case of small trees only one branch was cut and typically only basal cores were collected from the trunk.

5.2.4 Measurements and sampling techniques

We measured a suite of functional traits and ecophysiological properties which cover different aspects of hydraulic safety and productivity (Table 5.1). Leaf water potential was measured using a pressure chamber (PMS 1505D, USA). Mature and undamaged leaves were collected at different times of day by cutting small branches with telescopic pruners. Immediately after cutting and after falling to the ground small subsections of branches were placed into sealable plastic bags which had been humidified beforehand by breathing into them. These small branch subsections were kept in the dark until they could be measured. The maximum time between being cut from the tree and the leaf water potential measurement was 15 minutes. Leaves were then cut from the small branches with a razorblade at the petiole and measured for leaf water potential. Leaf water potential was

determined as the pressure at the instance when water first appears at the petiole cut. Note that for *C. microchaete* it was difficult to discern between a mucous like liquid produced by the leaf and water. The only way to distinguish between water and a mucous-like liquid under increasing pressure was via the difference of the viscosity of the liquids, recognizable by the way the liquid bubbled out of the leaf petiole (see example in Figure 5.3). Additionally, *P. laevis* when cut at the petiole produced a thick mucous that obscured observation of water production under pressure (see example in Figure 5.3). This was solved by frequently wiping the cut petiole surface with tissue.

Vulnerability curves were measured following the pneumatic method and protocol of Pereira et al. (2016). Large branches (generally ~ 2m) were cut before dawn and sealed in thick black plastic bags and kept under shade to keep cool until the first measurements could be taken. Smaller, ~30cm long, undamaged branches were cut from the main branch and was attached to the vacuum apparatus and exposed to the vacuum to measure air discharge for 150 seconds. After this, 2 leaves were measured for leaf water potential as above and an average taken. Where leaves were cut from the branch PVA glue was used to seal the wound. Branches were dried and similarly measured at frequent intervals in a series until air discharge plateaued whilst simultaneously leaf water potential declined. The time interval between measurements was determined by the weather. Branches dehydrated more quickly when the weather was warmer and less humid, and therefore more frequent measurements were required to sample many water potentials and air discharge values. Between branch dehydration and air discharge measurement, branches were placed in dark plastic bags to equilibrate the water potentials between the stem and the leaf so that measuring the water potential of the leaf will also give the water potential of the branch. For details of the apparatus and usage see Figure 5.2. Pereira et al. (2016) found the P50 value using this

pneumatic method to be similar to the P50 found when directly measuring hydraulic conductance to express conductance lost due to embolism.

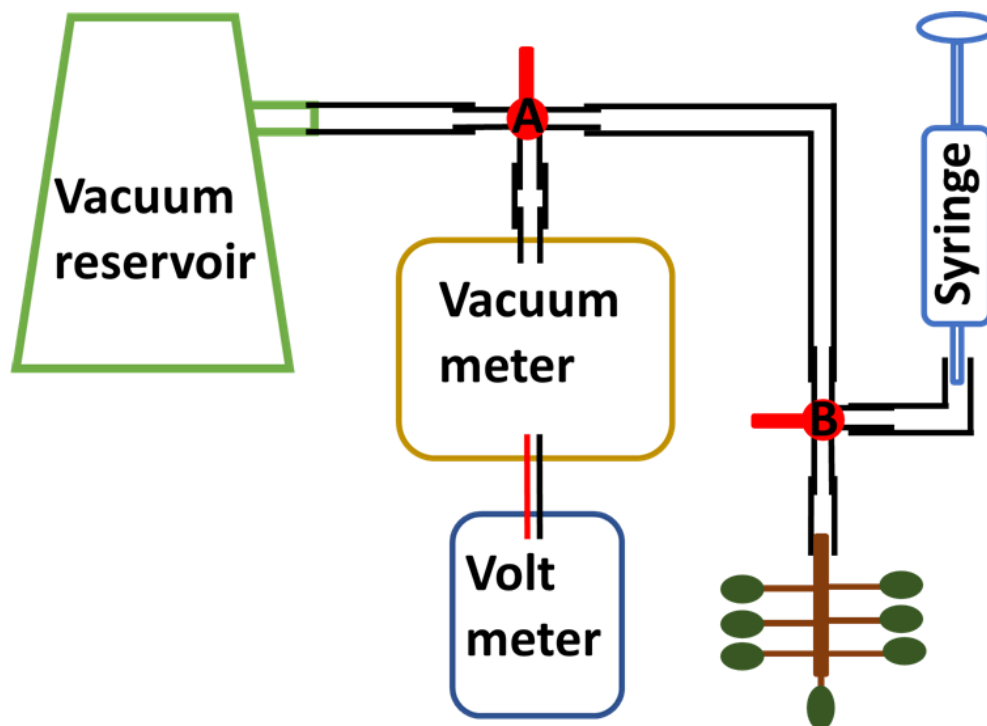


Figure 5.2 Scheme of pneumatic apparatus for measuring gas discharge from a desiccating branch as a proxy for loss of conductance. A vacuum is generated with the 50cl syringe and stored in a 2l Buchner flask vacuum reservoir. As the branch dries air within the branch that blocks water flow is drawn out and reduces the vacuum in the reservoir and surrounding tubes. This is recorded using a voltmeter attached to a vacuum sensor (Omega Engineering, USA, model PX141-015V5V). The three-way stopcocks (EW-30600-04, Cole Parmer, USA) labelled A, B enable control of exposure of the branch to vacuum or atmospheric pressures. In the present position all elements of the apparatus are under equal pressure. Closing stopcock B to the atmosphere (branch not yet attached and stored in a dark humid bag until used) enables the syringe to draw air out of the system, measuring the vacuum using the vacuum meter attached to the voltmeter sensitive to 0.001 volts, or ~ 0.07 kPa and maintaining a vacuum of 4.2 to 4.3 volts or ~ 32 kPa. Once the vacuum is achieved, the branch was exposed to the vacuum for 2.5 minutes with stopcock B between the syringe and the rest of the pneumatic apparatus closed. All components of the pneumatic apparatus are linked by rigid tubing (EW-30600-62, Cole Parmer, USA) and with screw connectors for airtight connection between sections of tubing and apparatus. This retained the volume of the system which is important for standardising measurements between sampling points in the drying series and producing stable vacuum measurements that did not vary due to, for example, vibrations in the workbench. The connection between branch and apparatus was made using parafilm and elastic tubing, further secured using adjustable hose clips to reduce any air gaps between bark and elastic tubing.

Leaves were taken from the larger branches cut for vulnerability curve analysis. Ten mature and largely in-tact leaves, with sizes ranging from largest to smallest, were selected for measuring leaf mass and leaf area. In the case of *C. microchaete* which has compound leaves 10 leaflets were used (sampling from 10 separate compound leaves and using only the middle leaflets). Leaves were stored in humid bags until used for measurements of leaf fresh mass and area. They were then weighed and scanned in the field. Then they were dried in an oven for a minimum of 5 days. Once dry leaves were then re-weighed. Dry leaves were retained for measuring stomatal traits. Leaf area was measured for each individual leaf using the images of scanned fresh leaves using ImageJ (Fiji, version 1.52p). For each leaf the dry mass of the leaf was divided by the fresh leaf area to produce leaf mass per area (LMA). The area of the largest leaf was used to estimate maximum leaf area for that height level and species.

For stomatal length and density, dry leaves were impressed with silicone based impression putty (President Light Body, Alstätten, Switzerland) to obtain a negative of a limited area of the underside of a leaf. The putty copy was then painted with nail varnish to obtain a positive and transparent copy of the leaf underside area. Once dried the varnish layer was peeled from the putty copy and was placed on a microscope slide. A GXCAM microscope mounted digital camera (GXCAM-U3PRO-6.3, GT Vision Ltd.) with a 6.3 megapixel lens mounted to an Olympus CX43 microscope at 40X magnification was used to photograph the stomata on the abaxial surface of the leaves. ImageJ was then used to measure stomatal length using the software's measuring tools and count the number of stomata in area of 0.33mm² to determine the density. This was performed for three leaves per branch sampled.

We calculated the theoretical maximum stomatal conductance to water per leaf area (g_{\max} mol m⁻² s⁻¹) following McElwain et al. (2016)

$$g_{max} = \frac{\left(\frac{dw}{v}\right) \cdot SD \cdot pa_{max}}{pd + \left(\frac{\pi}{2}\right) \sqrt{\left(\frac{pa_{max}}{\pi}\right)}} \quad 5.1$$

where dw is the diffusivity of water vapour ($0.0000249 \text{ m}^2 \text{ s}^{-1}$ at 25°C) and v is the molar volume of air ($0.0224 \text{ m}^3 \text{ mol}^{-1}$). SD is stomatal density (stomata m^{-2}), pa_{max} is the maximum stomatal pore area calculated from the long axis measurement only. The area was calculated as an ellipse with a width half the length. The stomatal pore depth, pd , was assumed to be the same as width (m) (Franks and Beerling 2009a; Franks and Beerling 2009b; McElwain et al. 2016).

The same dry leaves that were measured for LMA (leaf mass per area) were also used to measure the carbon isotope ratio, $\delta^{13}\text{C}$. The mixing ratio of ^{12}C is much higher than ^{13}C in the atmosphere. The ratio of ^{12}C to ^{13}C is higher still in plant cellulose since fractionation processes select against ^{13}C in the diffusion of CO_2 within the leaf and during the carboxylation during carbon fixation by the enzyme RuBisCO (McNevin et al. 2007; O'Leary 1988). The intrinsic water use efficiency of a plant (carbon assimilation rate/stomatal conductance) can be assessed by measuring the ratio of ^{13}C relative to ^{12}C in cellulose in a sample (R_{sample}) relative to a standard (R_{standard}) with a known carbon isotope ratio ($\delta^{13}\text{C} \text{ ‰}$) (Farquhar et al. 1989; Farquhar et al. 1982)

$$\delta^{13}\text{C} = \left(\frac{R_{\text{sample}}}{R_{\text{standard}}} - 1 \right) 1000 \quad 5.2$$

The intrinsic water use efficiency increases as the carbon assimilation rate increases relative to stomatal conductance or decreases as stomatal conductance increases relative to carbon assimilation rate. The $\delta^{13}\text{C}$ value increases (becomes less negative) with a greater proportion of ^{13}C relative to ^{12}C in air within the leaf, which happens when the concentration of CO_2 within the leaf declines relative to the atmosphere. We measure the $\delta^{13}\text{C}$ in 3 to 5 leaves per branch which were pooled to yield enough cellulose material for the analysis without destroying whole leaves (target weight 0.3mg cellulose). Cellulose was then extracted following Wieloch et al. (2011). $\delta^{13}\text{C}$ in cellulose was measured at the Leicester Environmental Stable Isotope Laboratory.

Wood samples were collected using 5 or 10mm increment borers at 3 positions from the stem base to the point of crown insertion, and at 4 positions in upper and lower crown branches using a saw or clippers (Figure 5.1). Although 10mm diameter wood cores were preferable (more sample material and more robust wood cores) the 5mm borers were used in denser wood, e.g. *A. ruizii*, whilst 10mm borers were used in less dense wood, e.g. *C. microchaete*. Wood samples were kept dry and were generally free from mould. Wood samples were cut using a microtome to 15-30um thickness depending upon the ease of cutting. The thin sections were placed on slides and photographed using a GXCAM microscope mounted digital camera (GXCAM-U3PRO-6.3, GT Vision Ltd.) with a 6.3 megapixel lens mounted to an Olympus CX43 microscope at 10X magnification for small vessels at the branch apex and in

small trees, and at 4X magnification for large vessels in the trunk of large trees. Images were then measured for vessel size and density using ImageJ (Fiji, version 1.52p).



Figure 5.3 Images of different sampling and measuring techniques for each of three species. The first row shows leaf water potential measurement, where *A. ruizii* produces only sap, *P. laevis* produces latex in addition to sap, and *C. microchaete* produces mucus in addition to sap. The second row shows stomatal impression from leaves of each species, where the scale bar shows 0.1mm. The third row shows leaf area with the ruler in cm increments for scale. The fourth row shows xylem anatomy in a twig 5cm below the apex with a scale bar 0.5mm long. These xylem photos show that the conductive wood containing xylem vessels (white circles) grew around a large diameter pith (removed in the process of producing the microtomed thin sections) in the twig. Thus xylem wood tissue occupied a only a narrow ring, hence the roughly semi-circular shape of the wood sections.

5.2.5 Analysis

To investigate the effects of sample height on different physiological and anatomical traits linear regressions of the form $y = a + bx$ were used, where y is the dependent variable (plant trait), x is the independent variable (sample specific height), and a and b are the intercept and slope respectively. Light availability classes were treated as continuous increments since the crown exposure index used in this study correlates well with measured proportions of openness to sky (Keeling and Phillips 2007). We show in SI Figure 5.2 that light index correlates well with height, as expected, and thus we cannot distinguish between the effects of height versus light availability. This is different for *C. microchaete*, where some small trees were growing across a range of light environments, including high light. Relationships between traits were also assessed using linear regressions. All linear models were assessed for homogeneity of slopes using the `anova` R function, normality of the residuals (Shapiro-Wilk from the R package `rstatix` (Kassambara 2019) and Q-Q plots) and homogeneity of variance (Bartlett test from the R package `stats` (R Core Team 2018)).

We compare mean trait values between species in order to assess possible alignment with life-history strategy. Between species comparisons of the mean value of the measured traits and physiological properties were made by Tukey's multiple comparisons test. We also compare the slopes of the relationships between tree height and each measured trait using the R package `emmeans` (Lenth 2018).

P50 curves were created by non-linear regression using the method of Pereira et al. (Pereira et al. 2016). Percentage air discharge (PAD) was calculated as the percentage of measured air

discharge AD (cm^3) relative to the difference between maximum and minimum measured air discharge, AD_{\max} and AD_{\min} respectively:

$$PAD(\%) = 100 \cdot \frac{AD - AD_{\min}}{AD_{\max} - AD_{\min}} \quad 5.3$$

The model describing the relationship between PAD and leaf water potential ψ during the drying series (described above) was of the form

$$PAD(\%) = \frac{100}{1 + \exp\left(\left(\frac{a}{25}\right) * (\psi - b)\right)} \quad 5.4$$

where a is the slope of the curve at point of 50% air discharge and b is the leaf water potential at which 50% air discharge is achieved. This model is the same as used in previous studies exemplifying the use of the pneumatic method to estimate a plants vulnerability to embolism (Pereira et al. 2016). 1000 starting values were generated to fit the model using the nls function (R Core Team 2018), retaining all models that fit according to the relative offset convergence criteria that the nls function uses to compare the imprecision of the parameter estimates and the residual sum of squares. All analyses were performed in R studio using R version 3.5.1 (R Core Team 2018).

5.3 Results

5.3.1 Leaf traits

Leaf mass per area (LMA) increases with tree height across species (Figure 5.4A). The slope of this increase is similar among species (Table 5.3). *A. ruizii* and *P. laevis* have similar mean LMA but the LMA of *P. laevis* is ~50% higher than the LMA of *C. microchaete*. Maximum leaf area, i.e. the area of the largest leaf, decreases with sample height similarly across the three species (Figure 5.4B). The mean maximum leaf area of *P. laevis* is nearly double that of *A. ruizii* and more than double that of *C. microchaete* (Table 5.3).

There is no evidence for stomatal size or density to change with sample height for *A. ruizii* nor *P. laevis*, though for *C. microchaete* stomatal density increases with sample height (Figure 5.4 C and D, Table 5.3). *P. laevis* and *C. microchaete* have similar mean guard cell length and density while *A. ruizii* has higher mean guard cell length and lower stomatal density. For both *A. ruizii* and *C. microchaete* theoretical maximum stomatal conductance per leaf area increases with height (Figure 5.4E, Table 5.3). *P. laevis* has the highest mean theoretical maximum stomatal conductance, 30% higher than *C. microchaete* and nearly 100% higher than that of *A. ruizii*.

The value of $\delta^{13}\text{C}$ increases with height across the three species. The rate of increase in $\delta^{13}\text{C}$ of *C. microchaete* with sample height compared to the other two species is significantly higher (Figure 5.4F, Table 5.3).

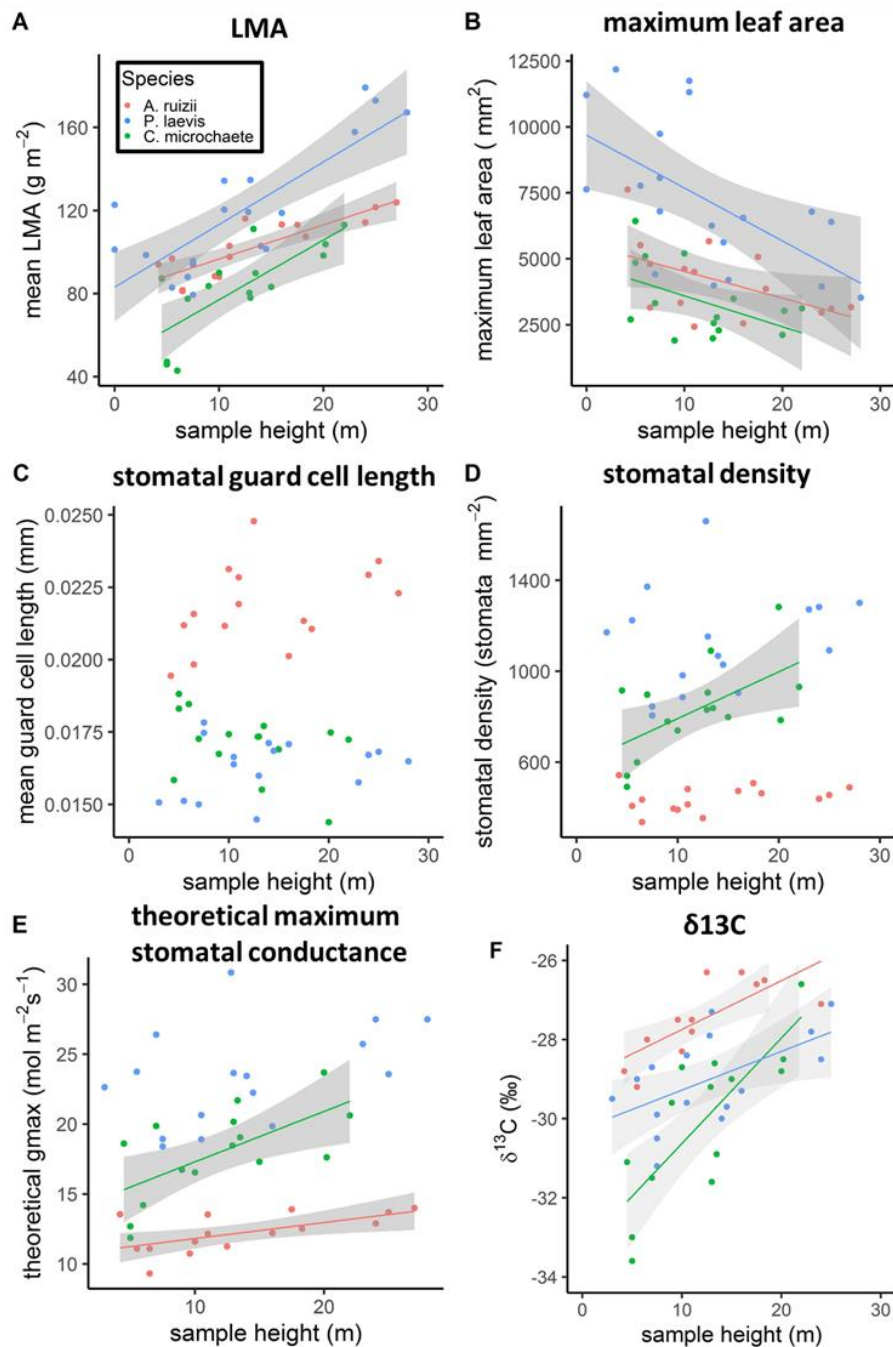


Figure 5.4 Relationships between sample height and leaf traits for the three species, *Ampelocera ruizii* (red), *Pseudolmedia laevis* (blue), and *Centrolobium microchaete* (green). Mean leaf mass per area (LMA) is shown in A, maximum leaf area in B, mean guard cell length in C, stomatal density in D, the theoretical maximum stomatal conductance (gmax) in E, and the $\delta^{13}\text{C}$ (‰) in F. Significant linear relationships are represented by a solid line with shading representing the confidence interval. See Table 5.3 for model details and comparisons between species.

5.3.2 Xylem vessel anatomy

The relationships between vessel size and density, and the distance to the tree apex within trees followed the expected patterns according to tapering theory (see Chapters 1 and 4 for more detail). We find similar increasing vessel diameter toward the bases of trees, and increasing vessel density toward the apex of the trees between species (Figure 5.5). The slopes of the log-transformed relationships between height and vessel diameter (with log transformed units) were 0.22 (s.e. 0.02), 0.24 (s.e. 0.016), 0.17 (s.e. 0.022), for *A. ruizii*, *P. laevis* and *C. microchaete* respectively (Table 5.3). *C. microchaete* has significantly larger mean vessel diameter relative to *A. ruizii* and *P. laevis* (Table 5.3).

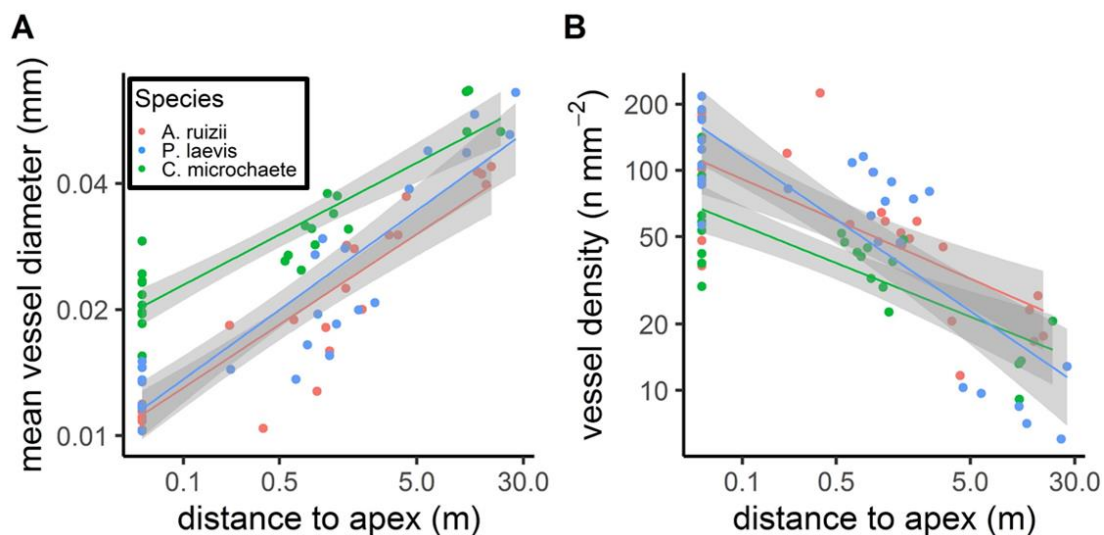


Figure 5.5 Relationships between distance to apex of mean vessel diameter and vessel density for three species, *Ampelocera ruizii* (red), *Pseudolmedia laevis* (blue), and *Centrolobium microchaete* (green). All axes are presented on a log scale. Significant linear relationships are represented by a solid line with shading representing the confidence interval. See Table 5.3 for model details and comparisons between species.

Vessel size and density is relatively constant at the apex regardless of the height of the branch sample (

Figure 5.6). We only found a significant relationship between vessel density and sample height in *C. microchaete* (

Figure 5.6 F). The mean apical vessel area and density was similar in *A. ruizii* and *P. laevis*, but vessels were significantly larger (~300% relative to *A. ruizii* and *P. laevis*) and packed less densely in *C. microchaete* (~50% relative to *P. laevis*).

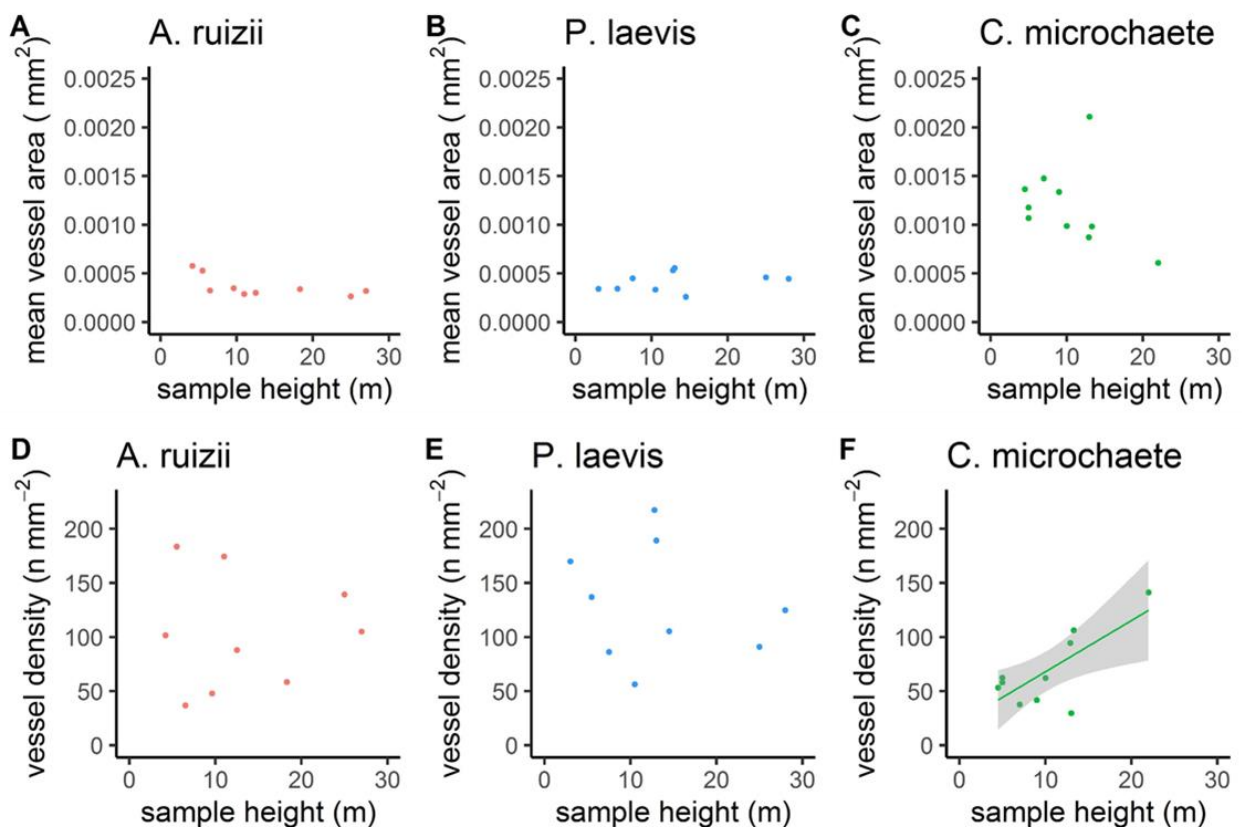


Figure 5.6 Species specific apical mean xylem vessel area – sample height relationships (A-C), and xylem vessel density – sample height relationships (D-F). Colours red, blue and green respectively represent *Ampelocera ruizii*, *Pseudolmedia laevis*, *Centrolobium microchaete*. Significant linear relationships are represented by a solid line with shading representing the confidence interval.

5.3.3 Leaf water potential

During a day leaf water potential decreases from pre-dawn to midday, after which it increases again (Figure 5.7). *A. ruizii* shows greater differences between pre-dawn and midday leaf water potential than *P. laevis* 2.38MPa (+0.34), and *C. microchaete* 0.7MPa (+- 0.17) respectively during the dry period). Furthermore, for *A. ruizii* during the dry period the pre-dawn leaf water potential is more negative compared to the wet period by 0.53MPa, and at midday by 0.43MPa (Table 5.3). In *P. laevis* there are only small changes between wet and dry periods during pre-dawn (0.07MPa), but midday leaf water potentials decrease between wet and dry periods from 0.31MPa (+0.08) to 0.64MPa (+0.08) respectively (Table 5.3). *C. microchaete* shows the largest mean difference between pre-dawn and midday leaf water potential 2.66 MPa (+0.33).

There are few apparent relationships between leaf water potential and sample height, either between pre-dawn leaf water potential and height or midday leaf water potential and height either in the wet period or the dry period (Figure 5.8). Pre-dawn leaf water potential increases with height for *C. microchaete* (0.029MPa m⁻¹). Leaf water potential decreases with height only for *A. ruizii* during midday in the dry period (0.046 MPa m⁻¹ Figure 5.8F), whilst pre-dawn leaf water potential does not change, thus resulting in an increase in the difference between pre-dawn and the minimum leaf water potential during the dry period (Figure 5.8F). Between species both pre-dawn and midday leaf water potential values are more negative for *C. microchaete* and *A. ruizii* relative to *P. laevis* during both wet and dry periods (~200-300% more negative, Table 5.3).

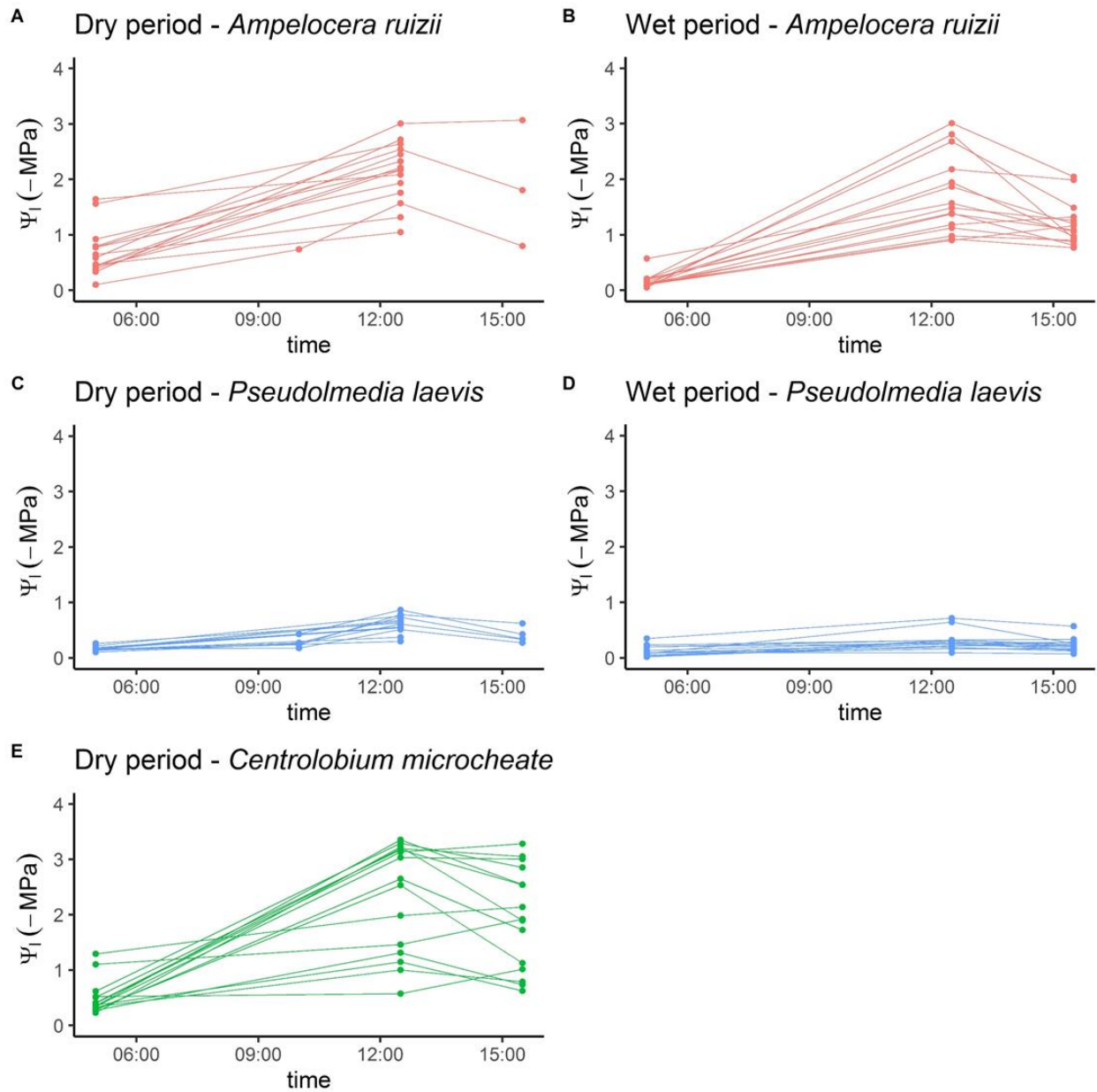


Figure 5.7 Daily curves of leaf water potential (ψ_1) for *Ampelocera ruizii* (A,B) and *Pseudolmedia laevis* (C,D), *Centrolobium microchaete* (E). Measurements of ψ_1 were taken during two distinct periods, one wet (B,D) and one dry (A,C). *C. microchaete* was only measured once, early in the dry period.

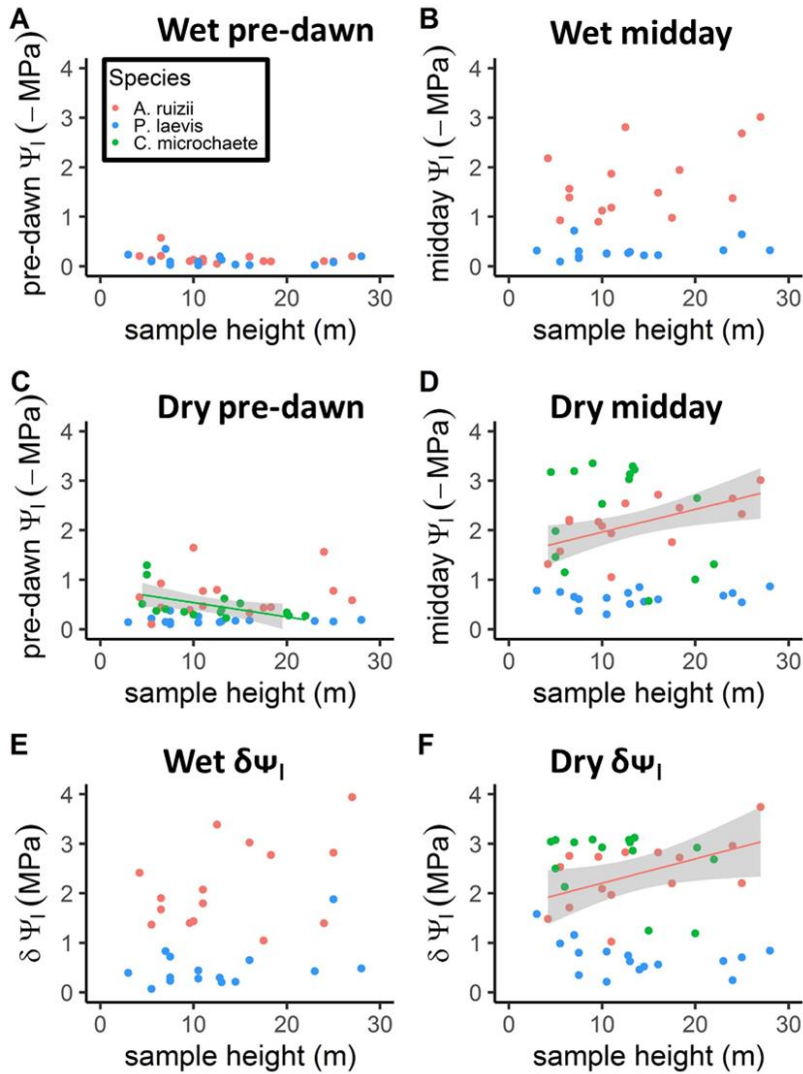


Figure 5.8 Linear relationships between sample height and leaf water potential for three species, *Ampelocera ruizii* (red), *Pseudolmedia laevis* (blue), and *Centrolobium microchaete* (green). Shown here are the leaf water potential measured before dawn (A,C), at midday (B,D), and the difference between the pre-dawn leaf water potential and the minimum leaf water potential (E,F). Each point represents the mean of 2-5 leaf water potential measurements. Measurements were taken during a wet period (A,B) and dry period (C,D). Significant linear relationships are represented by a solid line with shading representing the confidence interval. See Table 5.3 for the results of the linear relationships and differences between species mean values.

5.3.4 Vulnerability curves

P50 values were inferred from the vulnerability curves, measured as the water potential at which 50% of maximum air discharge occurs. For *A. ruizii* and *P. laevis* this is between -4.4 to -5.3MPa, and -2.3 to -4.5MPa respectively (Figure 5.9 A-C, and D-F respectively, Table 5.2).

This means that hydraulic conductance declines to half of maximum at these water potentials. For *C. microchaete* vulnerability curves had standard errors ~50% of the slope at the P50 value of the vulnerability curve, and as such are less statistically robust compared to the curves determined for the other two species (Figure 5.9 G-I, Table 5.2). According to these data there are no changes of the P50 value with increasing tree height for *A. ruizii* and *C. microchaete*, i.e. they are independent of height. For *P. laevis* there is a trend for higher P50 value with sample height.

Table 5.2 Results of the vulnerability curve analysis for the three species, *Ampelocera ruizii*, *Pseudolmedia laevis*, and *Centrolobium microchaete* at 3 height classes. See Figure 5.9 for the vulnerability curves used to calculate the P50 value. In brackets are the standard errors of the slope (% MPa⁻¹) and P50 (MPa) values, the water potential that induces 50% air discharge.

slopes (s.e.)	height class		
	<10m	10-18m	>18m
<i>A. ruizii</i>	12.32 (2.6)	23.51 (4.58)	31.31 (7.49)
<i>P. laevis</i>	11.69 (2.3)	19.56 (4.67)	35.9 (12.56)
<i>C. microchaete</i>	64.18 (32.92)	20.68 (8.83)	11.13 (4.82)
P50 (s.e.)			
<i>A. ruizii</i>	-5.07 (0.41)	-4.43 (0.19)	-5.31 (0.21)
<i>P. laevis</i>	-4.49 (0.5)	-2.73 (0.34)	-2.26 (0.29)
<i>C. microchaete</i>	-4.61 (0.19)	-4.75 (0.43)	-5.47 (1.06)

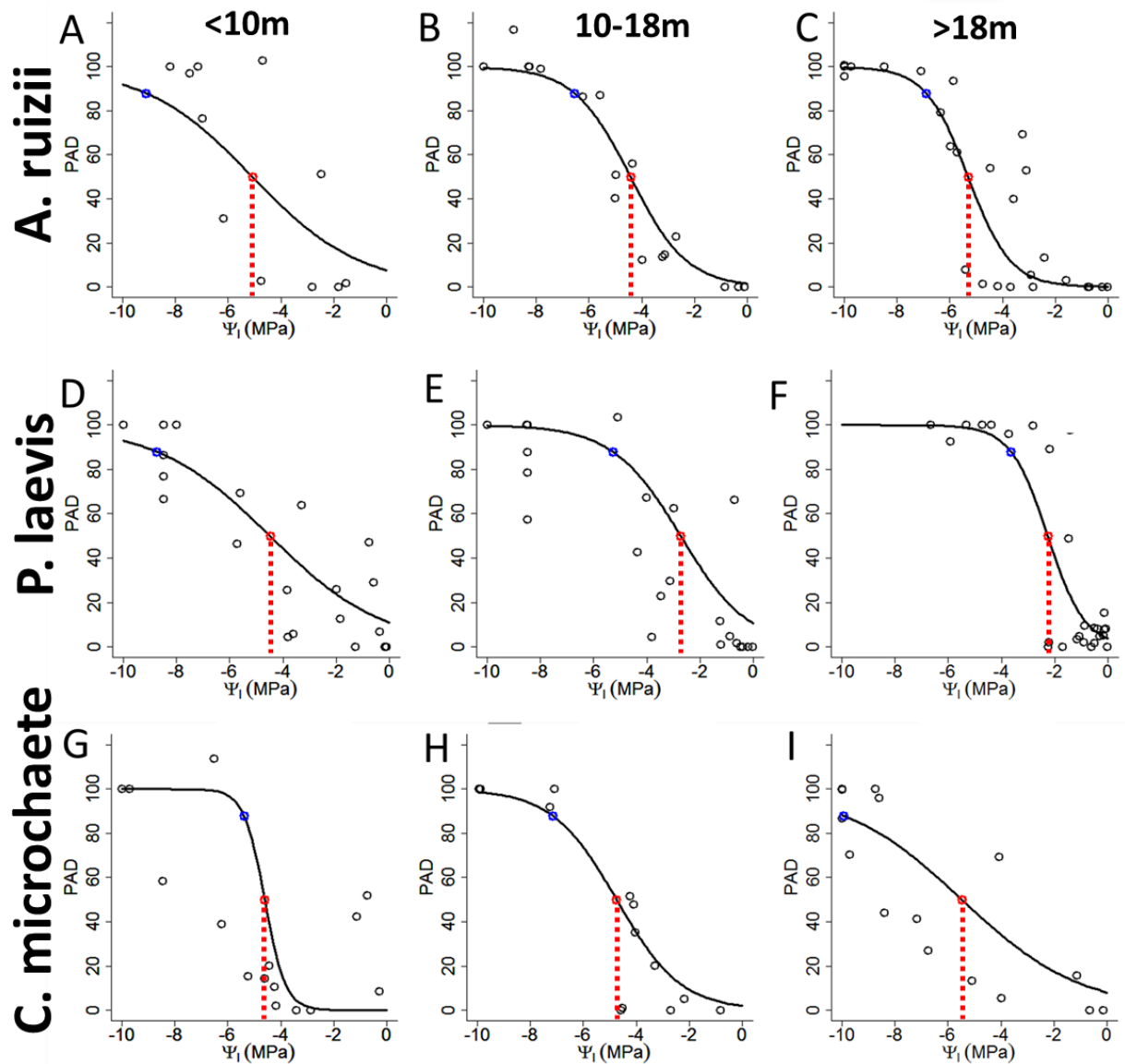


Figure 5.9 Vulnerability curves measured for *A. ruizii* (A-C), *P. laevis* (D-F), *C. microchaete*. The data here are collations of samples from different height classes: <10m (A,D,G), 10m - 18m (B,E,H), >18m (C,F,I). The red points and hatched line indicate the water potential that induces 50% of maximum air discharge from the branch, the blue points indicate the water potential that induces 88% of maximum air discharge from the branch. For a table of slope and P50 values with standard error see Table 5.2.

Table 5.3 Linear relationships between sample height and different ecophysiological and functional traits. The mean value of each trait is presented (with 95% confidence interval) and significant differences (as tested by t-tests) between species in the mean value are represented by different lower-case letters. The R^2 represents the fit of the linear relationships and the level of significance of the linear relationship is represented by: NS = $p > 0.1$, ns = > 0.05 , * = $p < 0.05$, ** = $p < 0.001$, *** = $p < 0.0001$. The slope of the linear relationship is given with the confidence interval, comparison between slopes as assessed by t-tests and significant differences are represented by different upper-case letters. For the relationship between sample height and log vessel diameter and log vessel density the units presented are log transformed. For all other variables the units are as per their associated linear regression plots. Please note *C. microchaete* does not have wet period values for water potential measurements and are thus left blank.

trait	<i>Ampelocera ruizii</i>		<i>Pseudolmedia laevis</i>		<i>Centrolobium microchaete</i>	
	mean trait value	effect of height (CI); R^2	mean trait value	effect of height (CI); R^2	mean trait value	effect of height (CI); R^2
LMA	102.67 (+- 7.19) ab	1.64 (+- 0.56); 0.73 *** A	119.53 (+- 13.89) b	3.014 (+- 1.09); 0.64 *** A	82.11 (+- 11.15) a	2.88 (+- 1.37); 0.58 ** A
Max. leaf area	4159.26 (+- 723.46) a	-101.23 (+- 91.88); 0.27 * A	7270.74 (+- 1262.81) b	-200.41 (+- 133.96); 0.34 * A	3392.17 (+- 694.06) a	-116.95 (+- 113.61); 0.25 ns
mean leaf area	2388.98 (+- 389.7) a	-39.26 (+- 53.76); 0.14 NS	4000.89 (+- 919.63) b	-113.58 (+- 107.21); 0.21 *	2374.81 (+- 524.14) a	-82.37 (+- 87.6); 0.21 ns
stomal length	0.0218 (+- 0.0007) b	0.000081(+ - 0.0001); 0.17 NS	0.016 (+- 0.0005) a	0.00003 (+- 0.000067); 0.05 NS	0.0171 (+- 0.0006) a	-0.00008 (+- 0.0001); 0.16 NS
stomatal density	439.07 (+- 28.86) a	2.3 (+- 4.1); 0.09 NS	1127.51 (+- 110.1) c	7.014 (+- 15.45); 0.06 NS	828.18 (+- 101.76) b	20.57 (+- 15.42); 0.35 *
Max. theoretical stomatal conductance	12.24 (+- 0.7) a	0.11 (+- 0.082); 0.37 * A	23.37 (+- 1.75) c	0.2 (+- 0.23); 0.19 ns	17.94 (+- 1.64) b	0.36 (+- 0.24); 0.42 * A
$\delta^{13}C$	-27.3 (+- 0.54) c	0.12 (+- 0.043); 0.71 *** A	-28.89 (+- 0.59) b	0.1 (+- 0.06); 0.42 * A	-30.33 (+- 1.1) a	0.3 (+- 0.13); 0.64 *** B
log mean vessel diameter	-3.95 (+- 0.19) a	0.22 (+- 0.039); 0.83 *** A	-3.86 (+- 0.22) ab	0.24 (+- 0.045); 0.82 *** A	-3.53 (+- 0.16) b	0.17 (+- 0.033); 0.83 *** A
log vessel density	4.03 (+- 0.3) a	-0.27 (+- 0.1); 0.53 *** A	4 (+- 0.42) a	-0.42 (+- 0.11); 0.69 *** A	3.67 (+- 0.26) a	-0.24 (+- 0.081); 0.63 *** A
apex vessel area	0.00036 (+- 0.000068) a	-0.0000078 (+- 0.0000074); 0.39 ns	0.00041 (+- 0.000064) a	0.0000035 (+- 0.0000084); 0.09 NS	0.0012 (+- 0.00026) b	-0.000027 (+- 0.000051); 0.12 NS
apex vessel density	103.97 (+- 34.68) ab	0.21 (+- 4.8); 0.0011 NS	130.83 (+- 34.46) b	-1.12 (+- 4.68); 0.0316 NS	68.76 (+- 21.66) a	4.74 (+- 3.12); 0.5353 *
pre-dawn ψ wet	0.16 (+- 0.06) a	-0.0052 (+- 0.0088); 0.1 NS	0.11 (+- 0.05) a	-0.0023 (+- 0.0071); 0.03 NS	-	-
midday ψ wet	1.7 (+- 0.35) b	0.044 (+- 0.047); 0.21 ns	0.31 (+- 0.08) a	0.0062 (+- 0.012); 0.08 NS	-	-
pre-dawn ψ dry	0.69 (+- 0.22) b	0.012 (+- 0.032); 0.04 NS	0.18 (+- 0.03) a	-0.00079 (+- 0.0049); 0.01 NS	0.49 (+- 0.16) b	-0.029 (+- 0.025); 0.3 *
midday ψ dry	2.13 (+- 0.27) b	0.046 (+- 0.031); 0.4 *	0.64 (+- 0.08) a	0.0044 (+- 0.011); 0.05 NS	2.34 (+- 0.5) b	-0.038 (+- 0.092); 0.05 NS
$\Delta\psi$ wet	2.16 (+- 0.43) b	0.051 (+- 0.058); 0.19 NS	0.49 (+- 0.22) a	0.026 (+- 0.029); 0.19 NS	-	-
$\Delta\psi$ dry	2.38 (+- 0.34) b	0.049 (+- 0.043); 0.29 *	0.7 (+- 0.17) a	-0.018 (+- 0.022); 0.16 NS	2.66 (+- 0.33) b	-0.036 (+- 0.058); 0.11 NS

5.3.5 Between-trait relationships

We find that some ecophysiological traits are strongly related to one another. Vessel diameter and vessel density, and stomatal length and stomatal density are both negatively related to one another (Figure 5.10 A,B). Note that the relationship between stomatal length and density for *A. ruizii* is only moderately significant ($R^2=0.24$, $p=0.067$). We also show that $\delta^{13}\text{C}$ is positively related to LMA across the three species (Figure 5.10 C). Maximum theoretical conductance per leaf area is positively related to LMA, but only for the species *A. ruizii* and *C. microchaete*, and though non-significant for *P. laevis* the same positive trend appears (Figure 5.10 D). There is also a positive relationship between maximum theoretical conductance per leaf area and $\delta^{13}\text{C}$ for *P. laevis* and *C. microchaete*, but not for *A. ruizii*, though the trend is also positive (Figure 5.10 E). For tables of relationship fits and coefficient values see SI Table 5.4 and SI Table 5.5 respectively.

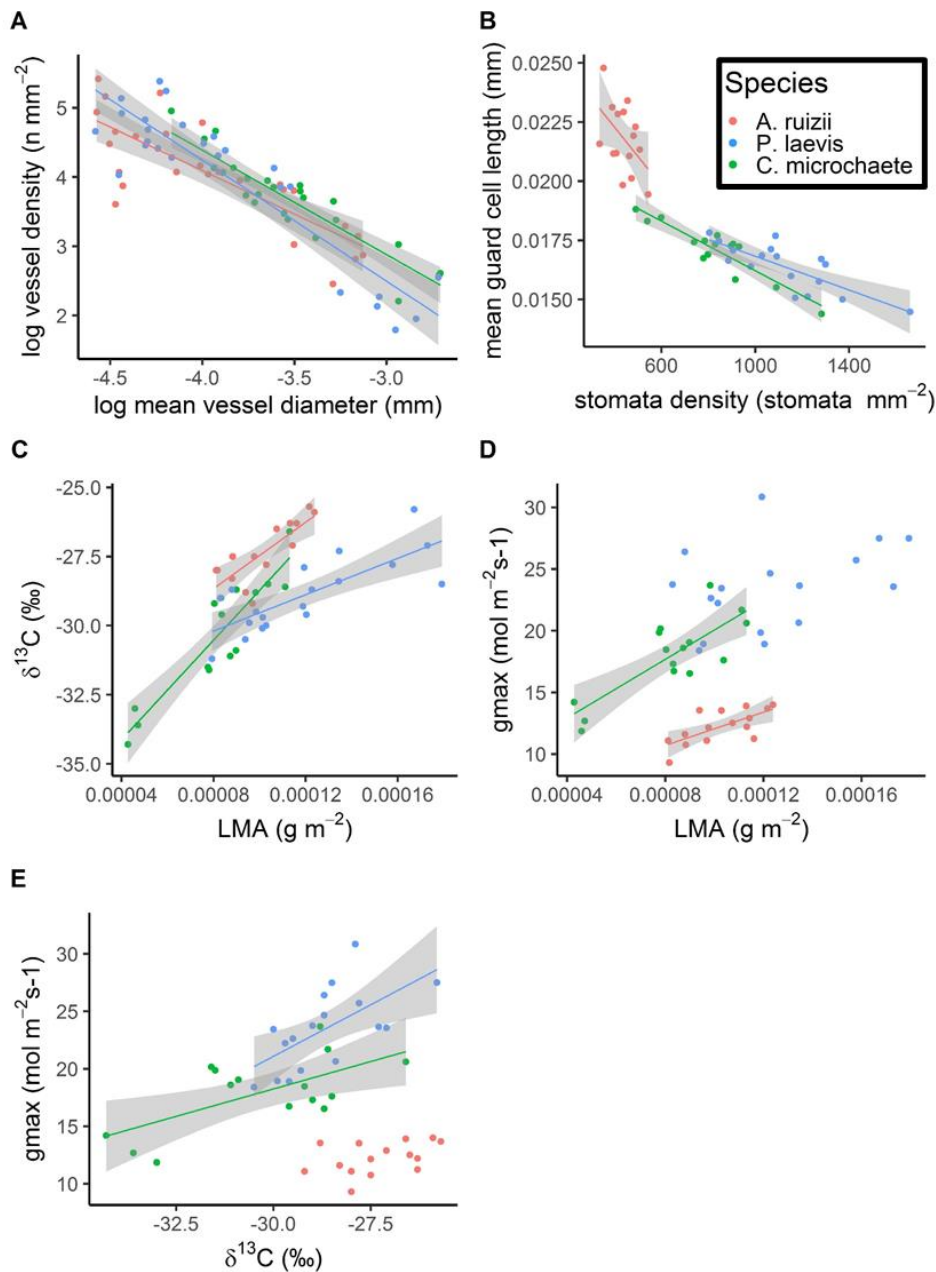


Figure 5.10 Relationships between traits for three species, *Ampelocera ruizii* (red), *Pseudolmedia laevis* (blue), and *Centrolobium microchaete* (green). A) Relationship between mean vessel diameter and density for vessels sampled along the entire range of sample heights, B) relationship between mean guard cell length and stomatal density per sample. C) relationship between $\delta^{13}\text{C}$ and mean leaf mass per area (LMA) per sample. D) relationship between mean LMA and the theoretical maximum stomatal conductance. E) relationship between $\delta^{13}\text{C}$ and theoretical maximum stomatal conductance. For tables of relationship fits and coefficient values see SI Table 5.4, SI Table 5.5.

5.4 Discussion

We investigated how different functional traits and ecophysiological properties of three species differing in life-history strategy vary with height in an ecotonal forest in Bolivia. We

found strong differences between species that likely relate to their life-history strategies as well as some striking relationships between functional traits and tree height, perhaps indicating trade-offs between productivity and hydraulic safety. We discuss these results in the context of the literature on tropical forest ecophysiology.

5.4.1 Changes in functional traits with tree height

We measured different functional traits and ecophysiological properties at different levels within a forest canopy, from the dark understory, to the canopy where trees experience full sun. In this study light availability and sample height are strongly linked (SI Figure 5.2), and thus any changes in the values of the different traits we measure may be linked to changes in height, i.e. resistance to water flow with path length, mechanical stress and gravitational effects on water potential (Ryan and Yoder 1997), as well the effects of light, temperature and humidity through the canopy (Ghazoul and Sheil 2010a).

5.4.1.1 Leaf traits

We find that with increasing tree height leaves become smaller and have a higher leaf mass per area (Figure 5.4). We also find that these trends are similar for the three species studied, though with differing mean values of LMA (Figure 5.4, Table 5.3). This is a well observed pattern in various tropical species (Cavaleri et al. 2010; Kafuti et al. 2020; Kenzo et al. 2006; Rijkers et al. 2000). It has been suggested to be due to a combination of hydraulic changes as well as light availability. The effects of light intensity have been shown under experimental conditions in saplings by Coste et al. (2010), who found that under experimental light conditions, higher light availability induced higher LMA, associated with increased leaf thickness. LMA may increase due to increasing light availability since in higher light a thicker palisade mesophyll, the tissue in which most photosynthesis occurs, and which holds more

nitrogen per leaf area, thus enabling higher photosynthesis per area (Coble and Cavaleri 2017; Coste et al. 2010; Niinemets 1999; Niinemets 2007; Niklas 1999; Poorter et al. 2019; Poorter et al. 2009). Leaves higher in the canopy may be subjected to more wind stress (Baldocchi et al. 2002) and require more structural carbohydrates to cope with mechanical wind stress and avoid breaking (He et al. 2019). Furthermore leaves higher in the canopy may be subject to wilting under low water potential (Scoffoni et al. 2014), as well as requiring increased hydraulic efficiency to cope with greater path length as tree grow taller so leaf vein thickness may increase to accommodate broader diameter vessels with height as suggested by Rosell et al. (2017) and shown in increasing leaf vein diameter with tree height by Coble and Cavaleri (2017). However, as we do not find any change in apical (branch) vessel size with height (Figure 5.6), we do not necessarily expect leaf vessel size to change with an increase in tree height.

Leaves higher in a canopy experience increased vapour pressure deficit and temperature which causes stress that may favour smaller surface area leaves which have been shown to be more effective for leaf cooling (England and Attiwill 2006; Sastry et al. 2018). Smaller leaves may also result directly from reduced turgor pressure due to lower water potentials in the crown, limiting cell expansion (Koch et al. 2004; Woodruff and Meinzer 2011). We show a strong decrease in the maximum leaf area of each species and increase in LMA with height but we show only a decline in leaf water potential with height in *A. ruizii* (Figure 5.8). It is therefore not likely that leaf size decreases and LMA increases are due to decreased cell expansion because of lower water potentials with height for *P. laevis* or *C. microchaete* which maintain similar water potentials with height (Figure 5.8). Therefore, universal LMA increases with height are likely a response to optimise photosynthetic capacity under increased light availability, as a response to more negative leaf water potentials (in *A. ruizii*), whilst aiding

control of leaf temperature and withstanding increased mechanical stress (Aranda et al. 2007; Baird et al. 2017).

For *C. microchaete* there is an increase in stomatal density with height, but not stomatal length (Figure 5.4 C, D). The theoretical maximum possible conductance is highest in leaves with smaller stomata because they may be packed at higher density (Bertolino et al. 2019; Henry et al. 2019). In *C. microchaete* we do find a strong increase in theoretical maximum stomatal conductance with height, likely driven by the increase in stomatal density (Figure 5.4D, E). This may be because it is a fast-growing pioneer that might be expected to maximise conductance for CO₂ as it has greater access to light (Poorter and Bongers 2006). The two other species, *A. ruizii* and *P. laevis*, showed no significant changes in guard cell length or density with tree height. Despite this *A. ruizii* shows a small (relative to *C. microchaete*) increase in theoretical maximum stomatal conductance, perhaps driven by a non-statistically significant increase in stomatal length but maintaining stomatal density. For *P. laevis* there is no change in any stomatal properties with tree height, therefore as leaves decrease in size with height, leaf specific conductance may decrease, whereas the other two species may be able to better maintain leaf specific conductance.

P. laevis has smaller stomata which probably permits greater control of water loss and thus leaf water potential (as shown in Figure 5.7 and Figure 5.8), which may be a mechanism for this species to avoid embolism (Drake et al. 2013). Such a potentially greater dynamic control of stomatal conductance may explain a lack of change in maximum theoretical stomatal conductance with height (Figure 5.4).

In contrast, the other two species appear to mitigate potential loss of leaf conductance (and thereby productivity) as leaves become smaller with height by increasing the leaf area specific

conductance, possibly risking hydraulic failure as greater conductance permits water potentials to decline as shown in Figure 5.7 and Figure 5.8 (Chen et al. 2019b; McDowell et al. 2008; Mencuccini et al. 2015). This trade-off is more apparent in *C. microchaete* as the theoretical maximum conductance on an area specific basis increases more rapidly with height than *A. ruizii*. Thus, the three species show distinct strategies with regard to stomatal properties changes with tree height, likely conferring trade-offs between productivity and hydraulic safety (Bartlett et al. 2016; Henry et al. 2019).

We find a strong increase in $\delta^{13}\text{C}$ with height across the three species (Figure 5.4F). Similar results have been found across biomes including tropical forests (Brienen et al. 2017; McDowell et al. 2011). As trees grow in height through a forest canopy their assimilation rate increases due to increased light intensity (Rijkers et al. 2000), as well as their stomatal conductance in order to improve gas exchange rates (Figure 5.4E) (Roberts et al. 1990). The increase in $\delta^{13}\text{C}$ of trees with height indicates that leaf internal CO_2 concentration decreases, and suggests that assimilation rates increase at a greater rate, relative to stomatal conductance (Aranda et al. 2007). Lower internal concentrations of CO_2 can be due to increasing light (resulting in increased assimilation of carbon) or decreasing conductance of the stomata to CO_2 . *P. laevis* appears to tightly control stomatal conductance with height (Figure 5.8). In contrast, for both *C. microchaete* and *A. ruizii* maximum theoretical conductance increases with height, and for *A. ruizii* leaf water potential declines with height (Figure 5.8D). This suggests that these species maintain high stomatal conductance which should increase the internal concentration of CO_2 . If this is the case any increase in $\delta^{13}\text{C}$ is likely due more to increasing assimilation rate with height and less to any decrease in stomatal conductance with height, relative to *P. laevis* (McDowell et al. 2011; Woodruff et al. 2009). For *C. microchaete* $\delta^{13}\text{C}$ increases more rapidly with height compared to the other two

species. This might suggest that at low heights leaves are less photosynthetically limited by stomatal conductance (i.e. for a given assimilation rate leaves have high stomatal conductance), but that as they grow taller they are increasingly limited (internal CO₂ concentration decreases more rapidly than the other two species). This would make sense considering that *C. microchaete*, as a pioneer species, needs to grow very fast whilst young in order to make use of short-lived canopy gaps.

5.4.1.2 Vessel characteristics

Vessel diameter increases with distance to the apex whilst vessel density decreases (Figure 5.5). We showed that the slopes of the vertical profile of vessel diameter were between 0.17 and 0.24 (log mm log m⁻¹), similar to the predicted minimum value of 0.2 required to overcome path length resistance increases with increasing path length as suggested in the literature (Anfodillo et al. 2006; Enquist 2003; Olson et al. 2014; Savage et al. 2010; West et al. 1999). A value much greater than 0.2 has been suggested to convey little benefit to the minimisation of hydraulic resistance whilst exacerbating problems such as embolism vulnerability and mechanical instability as vessel diameters increase (Christensen-Dalsgaard et al. 2007; Fan et al. 2017; Savage et al. 2010).

Between species the rate of increase in vessel diameter and decrease in vessel density is similar. *C. microchaete* has larger vessels for a given distance to the apex than *P. laevis* and *A. ruizii* which have a similar vessel sizes at a given distance to the apex. The greater vessel size of *C. microchaete* likely allows more efficient water conductivity required to sustain the greater rates of productivity of this species which, as a shade-intolerant pioneer species, are required to better utilise the brief canopy gaps (Hietz et al. 2017; Poorter et al. 2010). The other two species, *A. ruizii* and *P. laevis* are shade-tolerant species (Markesteyn and Poorter 2009) and seem to prioritise greater hydraulic safety to survive long periods in the understory

(Kupers et al. 2019), assuming narrower vessels convey greater hydraulic safety (Levionnois et al. 2021; Lobo et al. 2018; Olson et al. 2018; Prendin et al. 2018; Scoffoni et al. 2017; Sperry et al. 2006).

Previous studies that focus on the relationship between vessel diameter and tree height have often assumed a fixed apical vessel diameter regardless of tree height (Savage et al. 2010; West et al. 1999), although there is little evidence as far as the authors are aware to suggest this. Other studies have provided evidence that, for xylem vessels in near terminal twigs, vessel diameter increases with tree height, presumably to increase water conductance per leaf area in higher leaves (Echeverria et al. 2019; Olson et al. 2014). These findings are inconsistent with the assumption of fixed apical vessel diameter, if the terminal vessel is assumed to occur in the twig (and not in the leaf). We show that there is no apparent effect of sample height on the apical vessel diameter (

Figure 5.6). Thus our findings are consistent with the assumption made by West et al. (1999) and others (Savage et al. 2010), who suggest that the diameters of apical vessels are similar regardless of the path length below the apex. This therefore means that the resistance of the flow path cannot be exactly maintained along the flow path, but each meter in height adds a small amount of resistance as vessels increase in diameter (for an example of the effects of apical vessel widening see Figure 5.11).

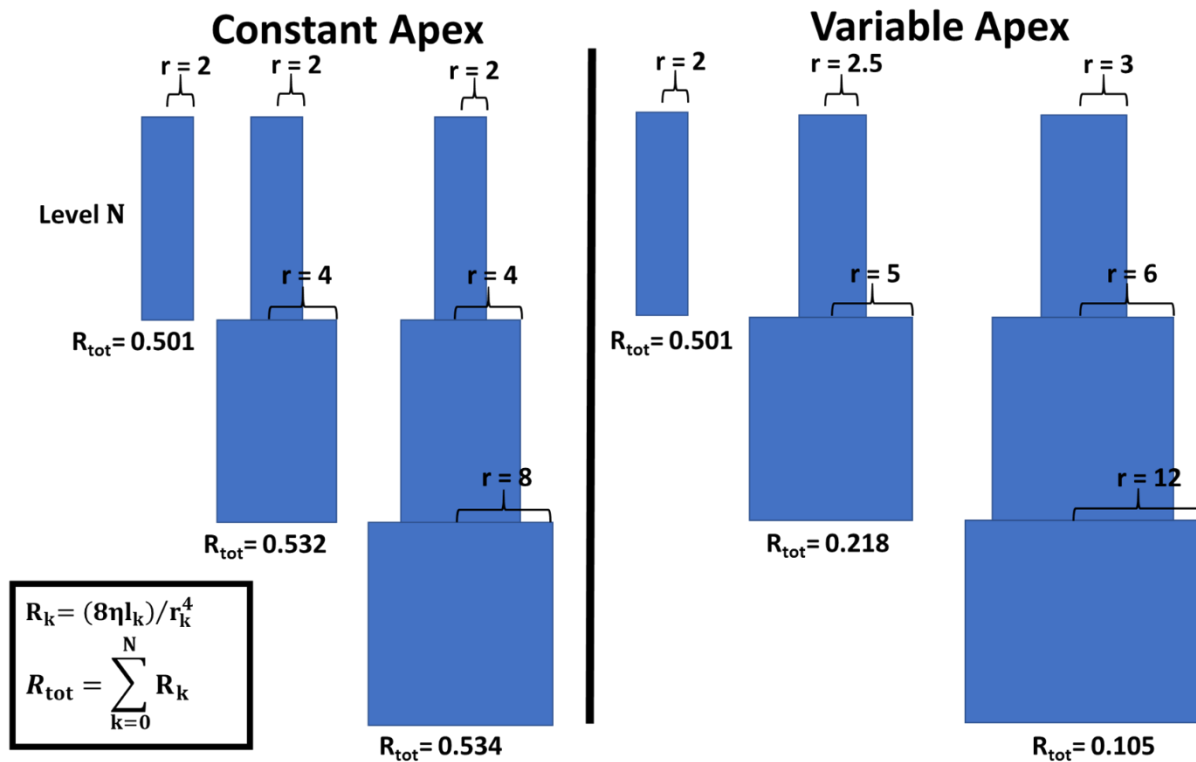


Figure 5.11 Scheme of two constant tapering strategies describing the effects of increasing apical vessel width with path length (different from the constant apical diameter assumption of Chapter 1 Figure 1.4). The left panel shows how, with constant apical diameter and constant taper rate (the ratio between levels, here 0.5 for simplicity), total resistance R_{tot} increases with path length (shown as the number of sections which have constant length). The right panel shows how (using the same taper rate as the left-hand panel) by increasing the width of the apical vessel the total resistance can be reduced. Previous studies have found that with increasing tree height the apical twig vessels increase in diameter (Echeverria et al. 2019; Olson et al. 2014), suggesting the variable apical diameter scenario, whilst in this study we find the constant apical diameter scenario (Figure 5.6), corroborating the assumptions of the West, Brown, Enquist model assumptions (West et al. 1999). Please note that the case above is not intended to be realistic, rather an exaggerated example using simple values of how vessel architecture may be modified to incur no resistance increases with path length. Calculation of the resistance R (MPa s m^{-3}) of any single vessel k was done using the Poiseuille formula shown inset in the figure, where η is the viscosity of water at 20°C (MPa s), l (m) is the length of the vessel and r is the radius (m). The sum of resistances in series from apex N to base gives the total resistance (R_{tot}). The West, Brown, Enquist model, and later related models of vessel tapering assume common apical vessel diameters with path length (Savage et al. 2010; West et al. 1999), whilst other studies have found the apical vessels to increase in diameter with path length (Olson et al. 2014; Olson et al. 2018). Although not indicated here the nature of volume preservation suggests that apical vessel number should decrease with increasing height inversely proportionally to diameter increases (Echeverria et al. 2019).

5.4.2 Leaf water potential and embolism vulnerability

The leaf water potentials of the three species show clear daily patterns as expected based on existing studies. Water potentials decrease during the day from pre-dawn when the plant

tissues and soil are in equilibrium, to midday when the tree experiences higher evaporative demand (Figure 5.7). In the afternoon the water potential raises again indicative of stomatal closure (Fisher et al. 2006; Huzulak and Matejka 1982; Myers et al. 1987). Based on the leaf water potential daily patterns and differences between wet and dry periods we can characterise the three species along the isohydry-anisohydry spectrum, a description of to what degree plants regulate their water potentials. Isohydric plants tend to maintain a similar minimum water potential regardless of water stress. Anisohydric plants permit water potentials to drop with water stress (Tardieu and Simonneau 1998). *P. laevis* appears to be relatively isohydric compared with *A. ruizii* and *C. microchaete* which are both relatively anisohydric. This suggests that, as expected, the fast-growing shade-intolerant species (*C. microchaete*) experiences lower water potentials and thus higher embolism risks in order to maintain water flow and productivity. Also, as it is deciduous it must make the most of the period in which it can photosynthesise. In contrast the slow growing shade-tolerant *P. laevis* shows a high degree of isohydry suggesting a need to maintain hydraulic safety at the cost of productivity (Eller et al. 2018; Markesteijn et al. 2011).

We expected to find relationships between leaf water potential and height through the canopy since up both height and light gradients the leaf water potential should decrease (Kenzo et al. 2006; Scholander et al. 1965). However we found only some evidence that leaf water potential decreases at increasing height for *A. ruizii* (Figure 5.8). The lack of decrease in leaf water potential for *P. laevis* is consistent with its isohydric character but for the relatively anisohydric species of *C. microchaete* we would expect leaf water potential to decrease with height. Measurement error due to latex production in *P. laevis* and mucus production in *C. microchaete* may have led to a lack of discernible relationships between height and leaf water potential (see upper panels in Figure 5.3). We noted that leaves were

often wet, caused by condensation in the morning, so it may have been possible for leaves to hydrate via the leaf cuticle thus contributing to reduced effect of height (Eller et al. 2013). We show that for *C. microchaete* the pre-dawn leaf water potential increased with height, contrary to expectations (Figure 5.8). This may be due to taller trees being able to recharge water better than short trees, for example due to deeper roots or better fog interception (Christina et al. 2011; Dawson and Goldsmith 2018). This may also explain why small tree leaf water potentials are similar to tall trees in this species, if taller trees are able to access water deeper in the soil relative to short trees (Stahl et al. 2013).

We find that the P50 values for the two higher height classes of *P. laevis* were high relative to *A. ruizii*. This may explain the differences in isohydry between the two species. This is because the P50 value of *A. ruizii* is -4.4 to -5.3MPa and maintains a minimum leaf water potential of no less than -3MPa, whilst the P50 values for *P. laevis* were -2.3 to -4.5MPa and it maintained a minimum leaf water potential higher than -1MPa. These differences between minimum water potential and P50, known as the hydraulic safety margin (HSM), are not as narrow as might be expected based on a global study by Choat et al. (2012) in which 70% of the species reported maintain a HSM <1MPa (Choat et al. 2012). It should be noted that our dry season leaf water potential results may be less negative than the normal minimum leaf water potential due to later than normal heavy rains (the wet period we measure in is normally the month with the least precipitation (Araujo-Murakami et al. 2014)). We also show that the slope of the vulnerability curve at the point of 50% air discharge tends to be lower in smaller trees for *A. ruizii* and *P. laevis*, indicating that reductions in water potential induce less embolism relative to taller trees (Figure 5.9, Table 5.2). We do not find any relationship between sample height and P50 for *A. ruizii* or *C. microchaete*, but also there is no general trend (Figure 5.9, Table 5.2). However, since leaf water potential decreases markedly with

height for *A. ruizii* the HSM likely decreases with height, i.e. embolism blockage of xylem vessels becomes more likely with height. In *P. laevis* we find no change in leaf water potential with height but instead do find that P50 increases with tree height, thus indicating in this species too there is a reduction in the HSM with height (though this is not statistically robust due to a paucity of data with 1 vulnerability curve per height class). We expected to find evidence that P50 values should be higher (more vulnerable to embolism) with sample height. This is because previous studies report that wider vessels are inherently more vulnerable to embolism, and that apical vessels increase in diameter with tree height (Echeverria et al. 2019; Knipfer et al. 2015; Olson et al. 2014; Olson et al. 2018; Scoffoni et al. 2017; Sperry et al. 2006; Wheeler et al. 2005). However, as we show that apical vessels do not increase in width with sample height (Figure 5.6), the expectation of increasing P50 values with height no longer holds. Thus, based on similar xylem diameter at the apex with height, we would expect no change in the embolism vulnerability with height.

5.4.3 Alignment of traits with life-history strategy

We measured a series of ecophysiological properties and functional traits for three tropical forest species. Previous studies have measured similar properties in young trees for these three species in a nearby forest (Table 5.4) and classified these species on the shade-tolerance spectrum (Markesteijn and Poorter 2009; Markesteijn et al. 2011; Poorter 2008; Poorter and Bongers 2006). Specifically Markesteijn and Poorter (2009) describe the biomass growth rates of seedling growing in full sun for the three species we study and the crown exposures of juvenile trees in nature to reflect their shade-tolerance. They found biomass growth in seedlings and the crown exposures of juveniles in nature was highly correlated. The traits they measure show how *P. laevis* and *C. microchaete* consistently differ and thus align with their

classification at either end of the slower growing shade-tolerant to fast growing shade-intolerant axis of life-history strategies. Markesteijn and Poorter (2009) show that *A. ruizii* however shares high seedling growth and shade-tolerance and thus shares different functional traits with both *C. microchaete* and *P. laevis*.

C. microchaete was classed as a fast growing pioneer, with young trees primarily found to be growing in high light environments, whilst *A. ruizii* and *P. laevis* were classified as shade-tolerant, surviving at lower light levels (Markesteijn and Poorter 2009). Greater shade-tolerance in tropical forest trees is often associated with a more conservative, slower growth strategy, whilst less shade-tolerant, light demanding species need to grow quickly to maximally exploit brief temporary increases in light levels due to canopy gaps (Blundell and Peart 2001; Brienen et al. 2010; Hunter et al. 2015). The need for high growth rates in light demanding species suggests that any trade-off between productivity and hydraulic safety will select in favour of traits resulting in increases in maximum growth capacity (de Souza et al. 2016; Fan et al. 2017; Huc et al. 1994; Markesteijn et al. 2011; Poorter et al. 2010; Sterck et al. 2011; Wright et al. 2010).

We show for the suite of functional traits and ecophysiological properties included in this study that *C. microchaete* tends to have traits associated with high growth. At the leaf level low LMA provides a greater area for light interception per unit carbon investment in leaf structure whilst having relatively high maximum theoretical conductance per leaf area for high gas exchange rates. Lower $\delta^{13}\text{C}$ values indicate greater stomatal conductance relative to carbon assimilation and thus may have relatively high productivity if stomatal conductance is high (Figure 5.4). This is suggested by *C. microchaete* being shown to have relatively high

stomatal conductance, high assimilation rate and high nitrogen per leaf mass as per Table 5.4. We also show that stomatal conductance is likely to be high since it permits its leaf water potential to become low throughout the day (Figure 5.7). Further, we show *C. microchaete* has wider xylem vessels that should provide greater conductivity (Figure 5.5), and thus gas exchange if water flow is not limited by stomatal closure. *C. microchaete* also shows lower construction costs of wood (low wood density) and leaf structures (high SLA/ low LMA and low leaf longevity as per Table 5.4 and associated references). This likely permits the fast growth of *C. microchaete* to exploit canopy gaps (Table 5.4).

Almost all traits in Table 5.4 of *P. laevis* indicate this species has an opposite strategy to *C. microchaete*, and is a slow growing, shade-tolerant tree. This is evident from its high LMA, narrow vessels, high midday water potentials, high wood density and leaf longevity, low stomatal conductance and nitrogen per mass and carbon assimilation rate (Table 5.4). Slow growth implies a longer period of time over which many potentially dangerous events may occur, e.g. droughts, and windstorms. Thus, when growing slowly, greater survival is needed to reach a reproductive stage, typically once trees reach the canopy (Ouedraogo et al. 2018; Wright et al. 2005). Thus, we expect traits associated with mechanical and hydraulic safety, namely; higher wood density with smaller xylem vessels, high leaf mass per area and maintenance of high leaf water potentials and relatively large hydraulic safety margins. However these traits confer lower productivity as they trade-off with traits associated with photosynthesis, and higher growth or maintenance costs for example smaller vessels conduct less water and thus limit gas exchange, whilst being associated greater wood density requires more carbon resources to grow (Houter and Pons 2012; Martinez-Cabrera et al. 2011; Reich et al. 1997; Wright et al. 2004). *A. ruizii* meanwhile has many traits intermediate between *C. microchaete* and *P. laevis*. This suggests a relatively intermediate strategy of growth and

achieving the canopy is employed with this species. Such a diversity in functional traits likely permit high species diversity within tropical forests (Bu et al. 2014; Marks and Lechowicz 2006). Such functional diversity may help buffer tropical forests against global climate change (Anderegg 2015).

Table 5.4 20 species traits from this study (upper rows) and based on the literature (lower rows). The lower traits are derived from measurements of seedling traits. Abbreviations: LMA = leaf mass per area, P50 = the water potential at which 50% of xylem conductance is lost, wd = wood density, SLA – specific leaf area (1/LMA), N_{area} = leaf Nitrogen content per leaf area, N_{mass} = leaf nitrogen content per leaf mass, A_{area} = CO₂ assimilation rate per leaf area, R_{area} = respiration rate per leaf area, gs = stomatal conductance, WUE_i = intrinsic water use efficiency.

	LMA	max. leaf area	stomatal length	stomatal density	gmax	δ ¹³ C	xylem vessel area	xylem vessel density	midday water potential	P50
A. ruizii	mid	mid	high	low	low	high	low	mid	low	low
<i>P. laevis</i>	high	high	low	high	high	high	low	high	high	high
C. microchaete	low	low	low	high	mid	low	high	low	low	-
source	present study	present study	present study	present study	present study	present study	present study	present study	present study	present study
	wd	leaf longevity	SLA	N _{area}	N _{mass}	A _{area}	R _{area}	gs	WUE _i	growth rate
A. ruizii	high	mid	mid	high	mid	mid	mid	mid	high	high
<i>P. laevis</i>	mid	high	low	low	low	low	low	low	low	low
C. microchaete	low	low	high	mid	high	high	high	high	mid	high
source	Poorter 2008	Poorter and Bongers 2006	(Poorter and Bongers 2006)	Poorter and Bongers 2006	Markesteyn and Poorter 2009					

5.4.4 A trade-off between safety and productivity?

Growing tall pushes trees from a hydraulically safe but unproductive environment under the canopy, where light is limited, to an environment with high light availability and high productivity. However evaporative demands higher up in the canopy increase due to higher temperature and lower humidity which increases potential risks of hydraulic and thermal stress (McDowell and Allen 2015; Tymen et al. 2017). There was an expectation that trade-offs between productivity and hydraulic safety likely drive different strategies enabling different species to grow tall (Markesteyn et al. 2011; Sterck and Schieving 2011).

We show several common adaptations with height amongst the three species we assessed in this study. Particularly at the leaf level we show that LMA increases, and maximum leaf size decreases with height through the canopy. This may be a consequence of decreasing water potentials with height (as we show for *A. ruizii*) or could be an adaptation to maximise photosynthesis rates per leaf area, whilst providing better thermal and wind stress tolerance. We also show that theoretical maximum stomatal conductance on a leaf area basis increases with height. This suggests that as trees grow taller and as light availability increases, leaves become smaller but are likely able to maintain productivity. This is because mesophyll tissue likely becomes denser with chlorophyll as LMA increases (Coble and Cavaleri 2017), and the per area gas exchange capacity increases due to increasing concentration of stomata. This is further suggested by the strong positive relationship between LMA and maximum theoretical stomatal conductance in two of the species (Figure 5.10).

This increased per leaf area productivity with height may however put these species at more risk of embolism formation in the more hydraulically stressful conditions of the upper canopy. Our data suggest that in at least two of the species (*A. ruizii* and *P. laevis*) the HSM decreases

with height (Table 5.2, Figure 5.8), thus exposing the taller trees to increasing embolism risk, though the minimum water potentials we measured suggested they were well within tolerance limits. So, we do not provide strong evidence of any trade-offs between hydraulic safety and productivity.

However, we find that hydraulic behaviour and the variation in ecophysiological traits align with the life-history strategies of the three species we study, i.e. a fast growth strategy associated with high productivity in *C. microchaete* relative to a slow growth strategy associated with hydraulically safe functional traits in *P. laevis*, whilst *A. ruizii* shares aspects of both *P. laevis* and *C. microchaete*. We also show differences between species across the height gradient (differences in mean trait values). This suggests alignment of traits and life-history strategy throughout ontogeny, not only in the juvenile phase, as studied previously (Markesteijn and Poorter 2009; Poorter and Bongers 2006).

5.4.5 Conclusions

We show clear trends in species functional traits with height through the canopy at the leaf level as they become smaller and more compact with greater theoretical stomatal conductance per leaf area. Changes in height and light increase the intrinsic water use efficiency of the tree as they grow taller, whilst xylem vessels taper to mitigate resistance increases with greater path length. We expected strong decreases in leaf water potential with tree height but found this only for one species. We show different growth and hydraulic strategies amongst species, with shade-tolerant, slow-growing *P. laevis* showing greater hydraulic safety, whilst the fast-growing *C. microchaete* shows greater vertical changes in intrinsic water use efficiency and lower leaf water potentials. This suggests that fast-slow growth strategy trade-offs are aligned with the hydraulic trade-offs.

Chapter 6 Conclusions and synthesis

6.1 Research conclusions

This thesis focused on the ecology of tree height in neotropical forests. Broadly this thesis aimed to better understand how neotropical forest height is limited at the level of taxon and to describe some of the ecophysiological aspects and implications of growing tall. Climate models predict rising temperatures and changes in water availability in neotropical forests. A better understanding of variation in tree height over large scales and ecophysiological responses of trees to tree height together should enable prediction of future changes to forest height, and thus to a large extent biomass.

The first two research Chapters of this thesis focus on the roles of water availability and wood anatomy in controlling maximum tree height. The results of this research add weight to previous research findings, showing that trees are limited in height by water availability and that possible mechanisms underpinning this (within species at least) lie in simple, predictable but functionally very important relationships between tree height and the organisation of xylem anatomy. We further show in Chapter 5, how tree height and canopy position affect a wider variety of ecophysiological properties and functional traits in the context of trees growing through the tropical forest canopy.

In this section I will detail the main findings of each chapter. I will then discuss how they contribute to a better understanding of controls of tree height in neotropical forests and how future research may further improve our understanding of this topic.

6.1.1 Chapter 3 Mean annual precipitation consistently predicts neotropical maximum tree height, both at the community and individual taxa level

In Chapter 3 we show the relationship between water availability and maximum tree height for forest communities across the neotropics. We show that maximum height decreases with decrease in water availability indicators, e.g. mean annual precipitation (MAP), sand%, and precipitation minus potential evapotranspiration (P-PET), show strong decreases in parallel with maximum height at the whole community level. Maximum tree height for the whole community peaks at 2750mm of MAP. Additionally, maximum height decreases at higher water availability. We find that maximum tree height at the family level exhibits similar relationships with water availability to that observed for forest community, with peaks at ~2500mm of MAP. Thus, changes in maximum height of the forest community with water availability appears to be driven by within-family changes in maximum height. A few tall families appear to drive this, whilst families with shorter maximum height that likely make up the rest of the forest canopy shift maximum height with MAP in a similar way. So, at least at the family level there appears not to be a strong change in community maximum height composition, with changes in precipitation driving changes in maximum tree height. Rather a continuation of families which make up the tallest trees along a large precipitation gradient. This research has strong implications for forest biomass and diversity, should precipitation patterns shift, either wetter or drier, with climate change. Specifically, we show possible changes in the maximum height for shifts in MAP (Figure 6.1). If MAP decreases by 500mm the maximum height of the community at 2500mm currently decreases from 41m to 39m. A decrease in MAP from 2000mm to 1500mm results in a decrease in the maximum height of the forest community by 5m, and decreasing MAP by another 500mm decreases maximum

height by an additional 10m. At high MAP increasing MAP by 500mm from 3000mm reduces maximum height by 4m. Thus we can say that forests below ~2000mm of MAP will likely reduce in height if MAP decreases, and forests above ~3000mm will decrease in height if MAP increases.

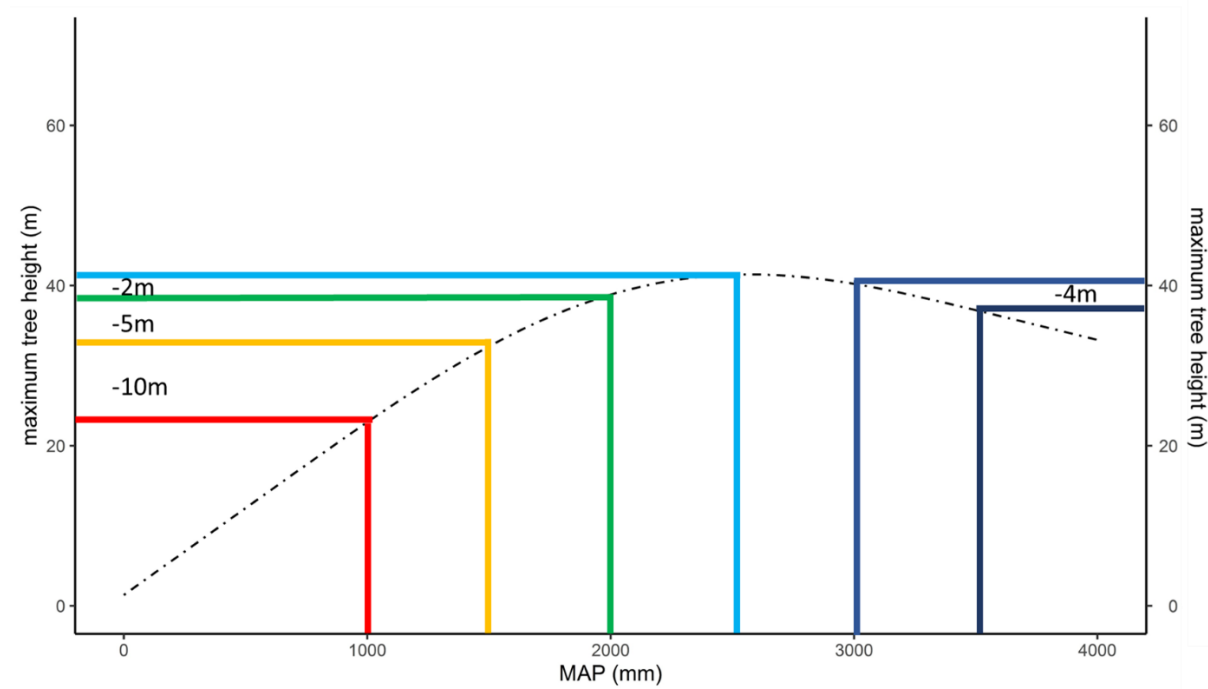


Figure 6.1 Predictions of changes in the maximum height of the forest community studied in Chapter 3 (the stippled line) with changes in mean annual precipitation (MAP). This shows the possible effects of changes in precipitation regimes using 500mm MAP increments. Changes are shown from the peak of the curve (both increasing MAP, light blue to dark blue, and decreasing MAP, blue to red), changes in maximum height are presented in the plot. Please note the 500mm MAP increments are not expected values of change based on any climate models, but rather an exaggerated example.

6.1.2 Chapter 4 A large water availability gradient does not affect the xylem vessel tapering of *Cedrela odorata*.

We find that the xylem network of *Cedrela odorata* and *Cedrela salvadorensis* that we study show clear alignment with tapering theory. Basal vessel diameter increases at the rate required to minimise resistance increases with path length as trees grow taller. We show

strong similarities in the vessel tapering of *Cedrela odorata* trees throughout a strong gradient in water availability. This suggests a lack of plasticity in this trait. Specifically, for a given height the vessel diameter at the base of the tree is fixed, regardless of the water availability. However, we show that as maximum height decreases with decreasing water availability then trees at drier sites have smaller vessels relative to trees at wetter sites at their respective maximum heights. Narrower vessels are thought to convey embolism resistance and may partly explain why trees only grow to shorter heights in drier conditions.

6.1.3 Chapter 5 ecophysiological and functional traits change with tree height, and differences between species likely reflect life-history strategy.

We investigated how a suite of functional traits and ecophysiological properties changes with tree height and canopy position (i.e. light) in a neotropical forest. We show strong changes in certain traits with height in highly similar manner for all three species. Specifically, we find increases in LMA and $\delta^{13}\text{C}$ (indicative of intrinsic water use efficiency) with increases in tree height and decreases in maximum leaf area. We furthermore find that vessels taper with tree height in all three species at the expected tapering rate. Other traits did not change with height or changed in a dissimilar manner between species. Previous studies have shown that apical vessels increase in diameter with tree height, however we did not find this, suggesting assumptions made by the West, Brown, Enquist model (West et al. 1999) of similar vessel diameter at the apex of the tree regardless of tree height apply for these species. We also show a lack of expected change in water potential with height, with only one clear instance of decreasing water potential with height. We suggest mechanisms such as condensation and absorption of water from leaf surfaces, and deep roots accessing wetter layers of the soil may explain the lack of distinct decreases in leaf water potential that we strongly expected based on the literature. Using this suite of traits and dynamic variables we show that traits covary

for these species with given differences in shade-tolerance according to expectations from the literature (Markesteijn and Poorter 2009; Poorter and Bongers 2006). Specifically, shade-intolerance implies low LMA, wide vessels and negative water potential. Whereas shade-tolerance suggests a more hydraulically safe (higher water potential and narrower vessels) but slower growth strategy (higher wood density and higher LMA). We also note a species with an intermediate suite of characteristics likely implying a continuum of strategies that tropical forest trees can adopt in order to reach the canopy and thus may help to explain the diversity of tropical forest canopy trees.

6.2 Synthesis and research implications

6.2.1 Evidence for the hydraulic limitation of maximum tree height in neotropical trees.

The main aims of the research chapters of this thesis were to evaluate how neotropical maximum tree height is limited (expecting a strong role for water availability) and describe anatomical and ecophysiological variability with tree height and discuss how these may influence maximum height attainment in the neotropics. The concept for this approach was based upon the hypothesis of hydraulic limitation of tree height (Ryan and Yoder 1997). This hypothesis requires that as trees grow taller they experience greater hydraulic stress, which has been demonstrated previously in several notably tall temperate species (Ambrose et al. 2016, Mullin et al. 2009, Chin and Sillett 2016, Nonami and Boyer 1990, Chin and Sillett 2017, Koch et al. 2004, Woodruff, Bond and Meinzer 2004). Despite this many mechanisms are available to trees to avoid the problems of height described by Ryan and Yoder (1997). Specifically, hydraulic resistance increases with path length and are reduced by increasing vessel width with tree height as is well known and demonstrated here (chapter 4, 5). Furthermore, trees have developed many mechanisms to avoid low water potentials and thus embolism

risk, as we explain for the deciduous *Cedrela odorata* in chapter 4 and the highly isohydric *Pseudolmedia laevis* in chapter 5. Regardless of avoidance mechanisms, there is likely a trade-off between avoidance of hydraulic failure and maintenance of productivity as we demonstrate and discuss in chapter 5. Thus, we can expect the hydraulic limitation of tree height to occur both directly, and indirectly via trade-offs, but likely not in the same form as the original hydraulic limitation hypotheses posed (Ryan, Phillips and Bond 2006).

We show in Chapter 3 a novel method to examine neotropical forest maximum height and its controls and limitation. This is novel firstly because we use a large dataset of in-situ measured tree height data, whereas previous studies have focused on remote sensing based height measurements to reveal large-scale patterns (Klein, Randin and Korner 2015, Tao et al. 2016, Gorgens et al. 2020). This research is also novel because we focus on the analysis of individual taxon relationships, as no previous studies, as far as the authors are aware, have shown how maximum height changes with precipitation in individual tropical forest taxa. We expected to find similar relationships between water availability and forest maximum height as previous studies had found at the forest community level (Klein et al. 2015, Tao et al. 2016, Gorgens et al. 2020). Some previous studies have shown similar results for individual taxa in less biodiverse temperate and boreal ecosystems and at relatively small scale (Mao et al. 2019, Givnish et al. 2014). In these regions different factors influence tree growth, e.g. the influence of freezing temperatures which tend not be limiting in the tropics (Mao et al. 2019, Loehle 1998, Shi, Korner and Hoch 2008). We show that higher order taxon (family) level tree height-MAP relationships are highly similar to those observed at the forest community level, showing a strong increase in maximum tree height with precipitation up to a peak maximum tree height for precipitation levels of ~2500mm per year. Above this peak we also observe a decline in maximum tree height with increasing MAP. This result is similar to those presented

by previous studies, analysing both tropical forests and other biomes (Klein et al. 2015, Tao et al. 2016, Gorgens et al. 2020). Additionally, we observed a relatively consistent decline in maximum forest community height and taxon specific height at very wet locations (above ~2700mm). This observation of a consistent decline in forest height at very wet locations has been seldom observed (Tao et al. 2016, Gorgens et al. 2020) and less often considered when attempting to understand potential drivers of forest biomass change, specifically related to the limitation of tree height at lower water availabilities (Feldpausch et al. 2012, Feldpausch et al. 2011). Our results suggest that, as is well understood, drier climates negatively affect forest stature and biomass in lowland tropical forests, but so can a forest that will get wetter. This information likely represents evidence of the effects of the hydraulic limitation of maximum tree height at the drier end of the range, both of the forest community and individual taxa. Leading hypotheses of future climate change across the Amazon basin suggest wetter regions will get wetter whilst drier regions will get drier (Gloor et al. 2013, Espinoza et al. 2019, Shiogama et al. 2011). If this is the case, then it is possible that both drier and wetter regions of the Amazon basin are facing a more fraught future than perhaps previously expected (see Figure 6.1). The mechanisms behind the relationships between maximum tree height and precipitation we show for the neotropical forest community and specific taxa in chapter 3, and for the genus *Cedrela* in chapter 4 are not well understood, and it is possible a variety of mechanisms cause these relationships.

6.2.2 Drivers and mechanisms of observed tree height- precipitation relationships.

The apparent increased risk of drought associated mortality of larger trees in the literature may suggest a mortality based mechanism for the patterns of tree height that we show in chapters 3 and 4 here, i.e. declining maximum height at lower MAP (Bennett et al. 2015,

McDowell and Allen 2015, McDowell et al. 2018, Rowland et al. 2015). The physiological drivers behind these patterns however are not well understood, though hydraulic failure via embolism formation has been suggested as a possible mechanism in drought mortality in Amazonian trees (McDowell et al. 2018, Rowland et al. 2015).

For the first time we show that xylem anatomy, specifically how basal xylem vessels widen with tree height, is consistent within a single tropical tree species across a broad water availability gradient. If vessels are the same size within trees of a species of a given height, regardless of the climate (Fajardo et al. 2020), it means basal vessel width can be inferred by measuring any tree's height alone, once a species specific vessel diameter height relationship has been estimated. Considering this and the strong relationship between MAP and maximum tree height that we show across neotropical families in chapter 3, we can suggest the consistency of xylem vessel scaling as a possible medium for the mechanism of height limitation across water availability gradients. Namely that the mechanism of height limitation, either mortality of larger trees or growth reduction at greater height, may be mediated by the relation between height and xylem anatomy (McDowell and Allen 2015). This may occur because the width of xylem vessels is important for a number of tree characteristics and life-history traits (Scoffoni et al. 2017, Olson et al. 2018, Sperry, Hacke and Pittermann 2006, Knipfer et al. 2015, Wheeler et al. 2005, Poorter et al. 2010), as we highlight in Chapter 5, where the largest vessels are found in the shade-intolerant pioneer species with other fast growth traits, relative to the narrower vessels of the slower growing and more shade-tolerant tree species we studied. It is likely that wider xylem vessels are associated with higher mortality (Olson et al. 2018), possibly driving trade-offs between fast growth versus slow growth life-history strategies of tropical trees (Aleixo et al. 2019, Esquivel-Muelbert et al. 2020), specifically via embolism resistance (McDowell and Allen 2015, Fajardo, McIntire and

Olson 2019, Poorter et al. 2010). This is because large vessels that enable faster growth tend to be more susceptible to embolism formation at a given water potential (Scoffoni et al. 2017, Olson et al. 2018, Sperry et al. 2006, Knipfer et al. 2015, Wheeler et al. 2005). Our research in chapter 4 shows that within a species, trees of the same height growing at a dry site relative to a wet site might be expected to experience higher embolism rates due to lower water potentials and similar xylem vessel width (and thus embolism resistance). A similar result was also found in temperate species by Fajardo et al. (2020), and similar conclusions drawn.

Here it is important to note we were not able to test the association between vessel diameter and embolism resistance (i.e. p50) in chapters 4 or 5, nor other sub-lumen properties that may be more functionally linked to embolism resistance, e.g. inter-vessel pits. Whilst in the literature there is building evidence of xylem lumen diameter having a relationship with embolism formation and/or spread (Levionnois et al. 2021, Lobo et al. 2018, Olson et al. 2018, Prendin et al. 2018, Scoffoni et al. 2017, Sperry et al. 2006), this is still controversial (Gleason et al. 2016, Liu et al. 2020). Furthermore, the high diversity of tropical tree species means there is a relatively high degree of uncertainty regarding the assumed universality of tapering of xylem vessel diameter and even more uncertainty regarding associations of wider vessels with lower embolism resistance of larger vessels. This is especially true since the literature is based largely on studies conducted on a very limited pool of temperate species. This is demonstrated where we report a similar apical vessel diameter with tree height for three little studied tropical species in chapter 5, contrary to the universal tapering of apical vessel diameter proposed by Olson et al. (2014).

Regardless of uncertainty it is likely that there exists some link between xylem vessel width and embolism risk, and that vessels do taper to a degree similar to that predicted by West et

al. (1999). Thus, the maximum height of trees at dry sites relative to wet sites may be reduced due to mortality caused by embolism, or the consequences of avoiding low water potentials (e.g. reduced productivity via deciduousness as we discuss in chapter 4). This poses a possible mechanism for the relationships between maximum height and precipitation observed in chapter 3 and chapter 4, and to some extent this may help to explain the overall relationship between forest community maximum height and precipitation observed in chapter 3 and in the literature (Klein et al. 2015, Tao et al. 2016, Gorgens et al. 2020).

6.2.3 The role of trait and biological diversity in determining maximum height attainment

Our research in Chapter 5 reveals how, for little studied tropical trees, different species using different life-history strategies change in their anatomical and ecophysiological properties as they grow taller. We show some similar relationships between functional traits and tree height among these highly unrelated species. This may in-part explain why the relationships of taxa across gradients of MAP are highly consistent between higher order taxa, as we show in Chapter 3. Specifically, assuming tree height affects ecophysiological traits that are important to the limitation of height of unrelated species in a similar way at a single site (e.g. LMA, leaf water potential, and intrinsic water use efficiency) then we might expect the ability of unrelated trees to grow tall to be similarly affected at different points along water availability gradients.

Recent research shows that divergent taxa convergently evolve toward similar ecophysiological traits depending upon the water availability in which they are growing, and conversely species within a taxon diverge in their ecophysiological traits when growing in highly different water availability environments (Fontes et al. 2020). This suggests that at a particular point along a water availability gradient unrelated species will attempt to solve the

problem of height similarly, and that within a higher order taxon species are specifically adapted to that environment which may imply lower maximum height (Fajardo et al. 2019). Furthermore, evidence shows that particular traits affect the responses of Amazonian trees to precipitation extremes, i.e. trees with better drought tolerance traits and slower growth tend to survive drought better, whilst faster growing trees with less drought tolerance grow better and have faster growth in wet years (Barros et al. 2019, Powell et al. 2018, Aleixo et al. 2019, Esquivel-Muelbert et al. 2020). This suggests that, in drier regions, slower growth and drought tolerance are likely solutions to growing tall. Therefore, what might be expected is that both within and between higher order taxa is a turnover in traits. Considering that life-history and ecophysiological traits strongly reflect distributions along the water availability gradient of the Amazon (Esquivel-Muelbert et al. 2017, Oliveira et al. 2019), and species tend to be non-plastic in their hydraulic and drought tolerance traits (Bittencourt et al. 2020), we may expect a turnover in species along a gradient to be driven by such traits, which are in turn reflected in the height attained by the trees as we show in chapter 4 for xylem anatomy specifically.

This idea however is relatively speculative and there is little evidence to suggest any specific mechanism for the similarity of relationships between maximum tree height and MAP of higher order taxa. It could be further hypothesised that based on our research in chapter 5 and previous studies, that a wide variety of strategies may underly the maximum height relationships we show in chapter 3, both within and between taxa at any given point. This may be especially true for transitional areas and regions with less constant climate, such as extremes of high and low precipitation (Powell et al. 2018, Poorter et al. 2010). This may also promote species diversity since individual species tend to show little plasticity in drought tolerance traits (Bittencourt et al. 2020).

6.3 Future research

The decrease in forest maximum height at high water availability has been little discussed in the literature, but more recently has been shown by airborne and spaceborne LiDAR measurements (Gorgens et al. 2020; Tao et al. 2016). It is uncertain as to why such a decrease should exist. We discussed possible explanations, but specific research into the mechanisms behind this trend would be useful to be able to predict future forest responses to increasing water availability. This would require more tree height data in very wet lowland tropical forest including taxon specific height data paired with long-term measurements of ecophysiological properties pertaining to productivity and photosynthesis to investigate possible light limitation of tree growth (Guan et al. 2015). Remote sensing studies using fluorescence measurements can help to study a possible light limitation on growth, as shown in a very recent study, by showing increased photosynthetic activity in drier conditions (Green et al. 2020). However, in-situ measurements at a large geographic scale (similar to the extent of Chapter 3) that pair species specific properties including sap flow measurements and CO₂ assimilation and climate variability should help to understand how forest growth, stature and ultimately biomass is limited in very wet tropical forests.

Furthermore, we suggest more in-situ height data with taxon specific information would greatly benefit this study and strengthen the statistical rigour of our findings and could enable application of this same research to different tropical forests globally. Such research might enable better understanding of the differences between continents. At present tropical tree height data from very dry forest to very wet forest was not available from Asia, nor from Africa for our current study (Chapter 3). Considering that the tropical forests of Southeast Asia are

generally much wetter and taller than those of the neotropics (Shenkin et al. 2019) we could suggest that the relationships between MAP and maximum tree height observed there might differ and provide insights into the mechanism by which water availability limits maximum tree height.

We show that relationships between maximum tree height and water availability are similar across taxa to that of the forest community, however this can be further investigated. Recent, as yet unpublished, work has been undertaken to characterise the hydraulic properties of neotropical trees. This together with large scale databases should enable grouping of forest species into functional groups that may better indicate future changes to forest stature and diversity, e.g. transitioning from wet forest functional types to dry forest functional types as forest become drier (Esquivel-Muelbert et al. 2019). Long term monitoring of the ecophysiological properties of the tallest trees across a range of water availabilities might better enable us to understand the mode of height limitation with water availability, e.g. by continuous, long term ecophysiological property measurements such as sap-flow sensors, and stem psychrometers, as well as regular monitoring of other properties. This could capture tree responses to natural events at a broader scale than can be captured at experimental sites (da Costa et al. 2010).

We show for a single tropical species that vessel diameter scaling with tree height doesn't change with water availability across a large gradient. This may be an important component to explaining why trees cannot grow tall in dry locations. Considering the rate of basal vessel diameter increase is similar to that of the study in Olson et al. (2014), we expect that the vessels in the apex similarly increase at the rate in that same study (lower than basal vessel diameter increases with tree height). However, to confirm this would require additional

evidence from the apex of trees across the same sites. Similar research could also be done on other tropical species with ranges that span across large water availability gradients (Esquivel-Muelbert et al. 2017a). This research should also study other xylem anatomy properties, including pit structure, as it is thought to be a main control of embolism resistance of xylem vessels (Medeiros et al. 2019; Pittermann et al. 2010). This future research could be paired with a suite of other measurements as we made in Chapter 5, and specifically test more rigorously in diverse species the relationships between embolism vulnerability and xylem vessel diameter. This could test the mechanism of height limitation across water availability gradients. Specifically, it must be demonstrated that a particular trait or ecophysiological property changes with height (in a direction that indicates greater hydraulic stress). Then it must be demonstrated that the trait in question is similar at the maximum height across a gradient of water availability, thus it is likely to be important for the limitation of height (Figure 6.2).

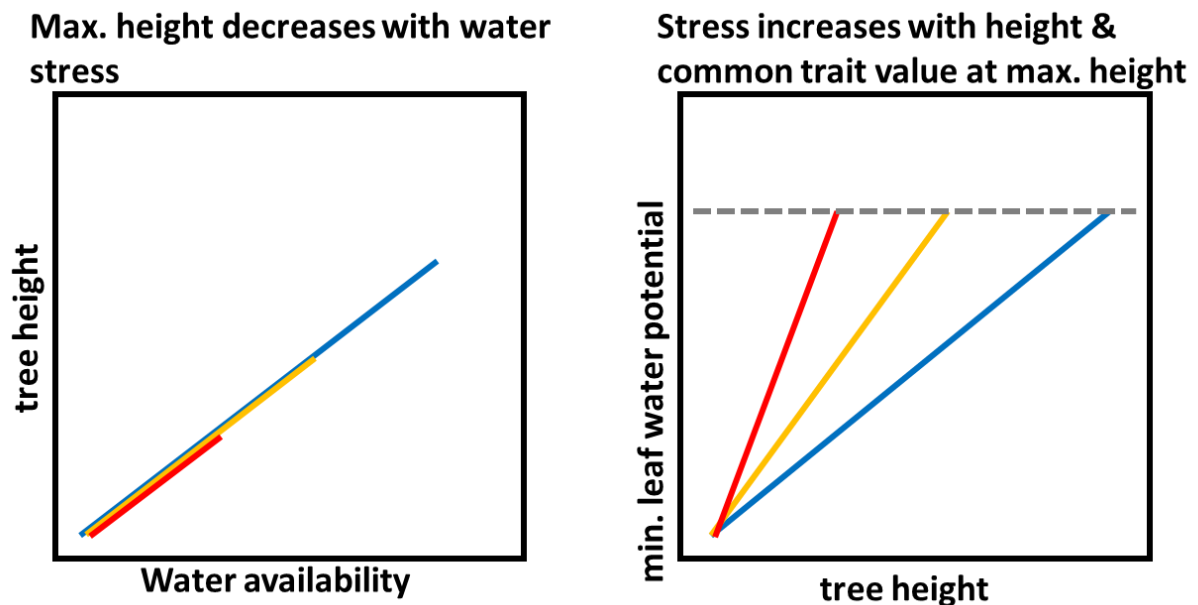


Figure 6.2 Plots demonstrating how to test ecophysiological traits and properties for their role in maximum height limitation, following the study of Givnish et al. (2014). The first plot demonstrates that there is a limitation of tree height across a water availability gradient, i.e. maximum tree height

increases from dry to wet sites. The second plot shows for a trait (in this example minimum leaf water potential) that for a trait to be limiting to height it must become more stressful with tree height (in this example becomes more negative), and should approach a common value at the maximum height of each site across the water availability gradient (grey stippled line). In this example it is possible to envisage that leaf water potential decreases with tree height, and that at a certain level of stress trees begin to either stop growing (e.g. due to increased stomatal closure at a certain limit), or begin to die (e.g. due to increased embolism blockage of xylem). Thus, the height of trees across the gradient may be demonstrated to be limited by this trait.

References

- Adams, H.D., M.J.B. Zeppel, W.R.L. Anderegg, H. Hartmann, S.M. Landhausser, D.T. Tissue, T.E. Huxman, P.J. Hudson, T.E. Franz, C.D. Allen, L.D.L. Anderegg, G.A. Barron-Gafford, D.J. Beerling, D.D. Breshears, T.J. Brodrigg, H. Bugmann, R.C. Cobb, A.D. Collins, L.T. Dickman, H.L. Duan, B.E. Ewers, L. Galiano, D.A. Galvez, N. Garcia-Forner, M.L. Gaylord, M.J. Germino, A. Gessler, U.G. Hacke, R. Hakamada, A. Hector, M.W. Jenkins, J.M. Kane, T.E. Kolb, D.J. Law, J.D. Lewis, J.M. Limousin, D.M. Love, A.K. Macalady, J. Martinez-Vilalta, M. Mencuccini, P.J. Mitchell, J.D. Muss, M.J. O'Brien, A.P. O'Grady, R.E. Pangle, E.A. Pinkard, F.I. Piper, J.A. Plaut, W.T. Pockman, J. Quirk, K. Reinhardt, F. Ripullone, M.G. Ryan, A. Sala, S. Sevanto, J.S. Sperry, R. Vargas, M. Vennetier, D.A. Way, C.G. Xu, E.A. Yezpez and N.G. McDowell. 2017. A multi-species synthesis of physiological mechanisms in drought-induced tree mortality. *Nature Ecology & Evolution*. 1:1285-1291.
- Adeney, J.M., N.L. Christensen, A. Vicentini and M. Cohn-Haft. 2016. White-sand Ecosystems in Amazonia. *Biotropica*. 48:7-23.
- Ahlstrom, A., J.G. Canadell, G. Schurgers, M.C. Wu, J.A. Berry, K.Y. Guan and R.B. Jackson. 2017. Hydrologic resilience and Amazon productivity. *Nature Communications*. 8
- Aleixo, I., D. Norris, L. Hemerik, A. Barbosa, E. Prata, F. Costa and L. Poorter. 2019. Amazonian rainforest tree mortality driven by climate and functional traits. *Nature Climate Change*. 9:384-+.

- Allen, C.D., A.K. Macalady, H. Chenchouni, D. Bachelet, N. McDowell, M. Vennetier, T. Kitzberger, A. Rigling, D.D. Breshears, E.H. Hogg, P. Gonzalez, R. Fensham, Z. Zhang, J. Castro, N. Demidova, J.H. Lim, G. Allard, S.W. Running, A. Semerci and N. Cobb. 2010. A global overview of drought and heat-induced tree mortality reveals emerging climate change risks for forests. *Forest Ecology and Management*. 259:660-684.
- Alvarez-Davila, E., L. Cayuela, S. Gonzalez-Caro, A.M. Aldana, P.R. Stevenson, O. Phillips, A. Cogollo, M.C. Penuela, P. von Hildebrand, E. Jimenez, O. Melo, A.C. Londono-Vega, I. Mendoza, O. Velasquez, F. Fernandez, M. Serna, C. Velazquez-Rua, D. Benitez and J.A.M. Rey-Benayas. 2017. Forest biomass density across large climate gradients in northern South America is related to water availability but not with temperature. *Plos One*. 12
- Ambrose, A.R., W.L. Baxter, C.S. Wong, S.S.O. Burgess, C.B. Williams, R.R. Naesborg, G.W. Koch and T.E. Dawson. 2016. Hydraulic constraints modify optimal photosynthetic profiles in giant sequoia trees. *Oecologia*. 182:713-730.
- Ambrose, A.R., S.C. Sillett, G.W. Koch, R. Van Pelt, M.E. Antoine and T.E. Dawson. 2010. Effects of height on treetop transpiration and stomatal conductance in coast redwood (*Sequoia sempervirens*). *Tree Physiology*. 30:1260-1272.
- Anderegg, W.R.L. 2015. Spatial and temporal variation in plant hydraulic traits and their relevance for climate change impacts on vegetation. *New Phytologist*. 205:1008-1014.
- Anderegg, W.R.L., L.D.L. Anderegg, K.L. Kerr and A.T. Trugman. 2019. Widespread drought-induced tree mortality at dry range edges indicates that climate stress exceeds species' compensating mechanisms. *Global Change Biology*. 25:3793-3802.
- Anderegg, W.R.L., J.A. Berry, D.D. Smith, J.S. Sperry, L.D.L. Anderegg and C.B. Field. 2012. The roles of hydraulic and carbon stress in a widespread climate-induced forest die-off. *Proceedings of the National Academy of Sciences of the United States of America*. 109:233-237.
- Anderegg, W.R.L., A.G. Konings, A.T. Trugman, K.L. Yu, D.R. Bowling, R. Gabbitas, D.S. Karp, S. Pacala, J.S. Sperry, B.N. Sulman and N. Zenes. 2018. Hydraulic diversity of forests regulates ecosystem resilience during drought. *Nature*. 561:538-+.
- Anfodillo, T., V. Carraro, M. Carrer, C. Fior and S. Rossi. 2006. Convergent tapering of xylem conduits in different woody species. *New Phytologist*. 169:279-290.
- Anfodillo, T., A. Deslauriers, R. Menardi, L. Tedoldi, G. Petit and S. Rossi. 2012. Widening of xylem conduits in a conifer tree depends on the longer time of cell expansion downwards along the stem. *Journal of Experimental Botany*. 63:837-845.
- Angeles, G., B. Bond, J.S. Boyer, T. Brodribb, J.R. Brooks, M.J. Burns, J. Cavender-Bares, M. Clearwater, H. Cochard, J. Comstock, S.D. Davis, J.C. Domec, L. Donovan, F. Ewers, B. Gartner, U. Hacke, T. Hinckley, N.M. Holbrook, H.G. Jones, K. Kavanagh, B. Law, J. Lopez-Portillo, C. Lovisolo, T. Martin, J. Martinez-Vilalta, S. Mayr, F.C. Meinzer, P. Melcher, M. Mencuccini, S. Mulkey, A. Nardini, H.S. Neufeld, J. Passioura, W.T. Pockman, R.B. Pratt, S. Rambal, H. Richter, L. Sack, S. Salleo, A. Schubert, P. Schulte, J.P. Sparks, J. Sperry, R. Teskey and M. Tyree. 2004. The Cohesion-Tension theory. *New Phytologist*. 163:451-452.
- Anten, N.P.R., E.J. von Wettberg, M. Pawlowski and H. Huber. 2009. Interactive Effects of Spectral Shading and Mechanical Stress on the Expression and Costs of Shade Avoidance. *American Naturalist*. 173:241-255.
- Antonelli, A. and I. Sanmartin. 2011. Why are there so many plant species in the Neotropics? *Taxon*. 60:403-414.
- Antonelli, A., A. Zizka, D. Silvestro, R. Scharn, B. Cascales-Minana and C.D. Bacon. 2015. An engine for global plant diversity: highest evolutionary turnover and emigration in the American tropics. *Frontiers in Genetics*. 6
- Aparecido, L.M.T., G.R. Miller, A.T. Cahill and G.W. Moore. 2016. Comparison of tree transpiration under wet and dry canopy conditions in a Costa Rican premontane tropical forest. *Hydrological Processes*. 30:5000-5011.

- Aranda, I., M. Pardos, J. Puertolas, M.D. Jimenez and J.A. Pardos. 2007. Water-use efficiency in cork oak (*Quercus suber*) is modified by the interaction of water and light availabilities. *Tree Physiology*. 27:671-677.
- Araujo-Murakami, A., C.E. Doughty, D.B. Metcalfe, J.E. Silva-Espejo, L. Arroyo, J.P. Heredia, M. Flores, R. Sibling, L.M. Mendizabal, E. Pardo-Toledo, M. Vega, L. Moreno, V.D. Rojas-Landivar, K. Halladay, C.A.J. Girardin, T.J. Killeen and Y. Malhi. 2014. The productivity, allocation and cycling of carbon in forests at the dry margin of the Amazon forest in Bolivia. *Plant Ecology & Diversity*. 7:55-69.
- Aubry-Kientz, M., V. Rossi, F. Wagner and B. Herault. 2015. Identifying climatic drivers of tropical forest dynamics. *Biogeosciences*. 12:5583-5596.
- Baird, A.S., L.D. Anderegg, M.E. Lacey, J. HilleRisLambers and E. Volkenburgh. 2017. Comparative leaf growth strategies in response to low-water and low-light availability: variation in leaf physiology underlies variation in leaf mass per area in *Populus tremuloides*. *Tree Physiology*. 37:1140-1150.
- Baker, J.C.A., G.M. Santos, M. Gloor and R.J.W. Brienen. 2017. Does *Cedrela* always form annual rings? Testing ring periodicity across South America using radiocarbon dating. *Trees-Structure and Function*. 31:1999-2009.
- Baker, J.C.A. and D.V. Spracklen. 2019. Climate Benefits of Intact Amazon Forests and the Biophysical Consequences of Disturbance. *Frontiers in Forests and Global Change*. 2
- Balch, J.K., P.M. Brando, D.C. Nepstad, M.T. Coe, D. Silverio, T.J. Massad, E.A. Davidson, P. Lefebvre, C. Oliveira-Santos, W. Rocha, R.T.S. Cury, A. Parsons and K.S. Carvalho. 2015. The Susceptibility of Southeastern Amazon Forests to Fire: Insights from a Large-Scale Burn Experiment. *Bioscience*. 65:893-905.
- Baldocchi, D.D., K.B. Wilson and L.H. Gu. 2002. How the environment, canopy structure and canopy physiological functioning influence carbon, water and energy fluxes of a temperate broad-leaved deciduous forest-an assessment with the biophysical model CANOAK. *Tree Physiology*. 22:1065-1077.
- Banin, L., T.R. Feldpausch, O.L. Phillips, T.R. Baker, J. Lloyd, K. Affum-Baffoe, E. Arets, N.J. Berry, M. Bradford, R.J.W. Brienen, S. Davies, M. Drescher, N. Higuchi, D.W. Hilbert, A. Hladik, Y. Iida, K. Abu Salim, A.R. Kassim, D.A. King, G. Lopez-Gonzalez, D. Metcalfe, R. Nilus, K.S.H. Peh, J.M. Reitsma, B. Sonke, H. Taedoumg, S. Tan, L. White, H. Woll and S.L. Lewis. 2012. What controls tropical forest architecture? Testing environmental, structural and floristic drivers. *Global Ecology and Biogeography*. 21:1179-1190.
- Banin, L., S.L. Lewis, G. Lopez-Gonzalez, T.R. Baker, C.A. Quesada, K.J. Chao, D. Burslem, R. Nilus, K. Abu Salim, H.C. Keeling, S. Tan, S.J. Davies, A.M. Mendoza, R. Vasquez, J. Lloyd, D.A. Neill, N. Pitman and O.L. Phillips. 2014. Tropical forest wood production: a cross-continental comparison. *Journal of Ecology*. 102:1025-1037.
- Barros, F.D., P.R.L. Bittencourt, M. Brum, N. Restrepo-Coupe, L. Pereira, G.S. Teodoro, S.R. Saleska, L.S. Borma, B.O. Christoffersen, D. Penha, L.F. Alves, A.J.N. Lima, V.M.C. Carneiro, P. Gentine, J.E. Lee, L. Aragao, V. Ivanov, L.S.M. Leal, A.C. Araujo and R.S. Oliveira. 2019. Hydraulic traits explain differential responses of Amazonian forests to the 2015 El Niño-induced drought. *New Phytologist*. 223:1253-1266.
- Bartlett, M.K., T. Klein, S. Jansen, B. Choat and L. Sack. 2016. The correlations and sequence of plant stomatal, hydraulic, and wilting responses to drought. *Proceedings of the National Academy of Sciences of the United States of America*. 113:13098-13103.
- Barton, K. 2019. MuMIn: Multi-Model Inference. R package version 1.43.15. <https://CRAN.R-project.org/package=MuMIn>.
- Bates, D.M., Martin, B. Bolker and S. Walker. 2015. Fitting Linear Mixed-Effects Models Using lme4. *Journal of Statistical Software*, pp 1-48.
- Bennett, A.C., N.G. McDowell, C.D. Allen and K.J. Anderson-Teixeira. 2015. Larger trees suffer most during drought in forests worldwide. *Nature Plants*. 1

- Bernal, R., B. Martinez and M.J. Sanin. 2018. The world's tallest palms. *Palms*. 62
- Bertolino, L.T., R.S. Caine and J.E. Gray. 2019. Impact of Stomatal Density and Morphology on Water-Use Efficiency in a Changing World. *Frontiers in Plant Science*. 10
- Bittencourt, P.R.L., R.S. Oliveira, A.C.L. da Costa, A.L. Giles, I. Coughlin, P.B. Costa, D.C. Bartholomew, L.V. Ferreira, S.S. Vasconcelos, F.V. Barros, J.A.S. Junior, A.A.R. Oliveira, M. Mencuccini, P. Meir and L. Rowland. 2020. Amazonia trees have limited capacity to acclimate plant hydraulic properties in response to long-term drought. *Global Change Biology*. 26:3569-3584.
- Blundell, A.G. and D.R. Peart. 2001. Growth strategies of a shade-tolerant tropical tree: the interactive effects of canopy gaps and simulated herbivory. *Journal of Ecology*. 89:608-615.
- Brenes-Arguedas, T., A.B. Roddy, P.D. Coley and T.A. Kursar. 2011. Do differences in understory light contribute to species distributions along a tropical rainfall gradient? *Oecologia*. 166:443-456.
- Brienen, R.J.W., L. Caldwell, L. Duchesne, S. Voelker, J. Barichivich, M. Baliva, G. Ceccantini, A. Di Filippo, S. Helama, G.M. Locosselli, L. Lopez, G. Piovesan, J. Schöngart, R. Villalba and E. Gloor. 2020. Forest carbon sink neutralized by pervasive growth-lifespan trade-offs. *Nature Communications*. 11:4241.
- Brienen, R.J.W., E. Gloor, S. Clerici, R. Newton, L. Arppe, A. Boom, S. Bottrell, M. Callaghan, T. Heaton, S. Helama, G. Helle, M.J. Leng, K. Mielikainen, M. Oinonen and M. Timonen. 2017. Tree height strongly affects estimates of water-use efficiency responses to climate and CO₂ using isotopes. *Nature Communications*. 8
- Brienen, R.J.W., P. Hietz, W. Wanek and M. Gloor. 2013. Oxygen isotopes in tree rings record variation in precipitation delta O-18 and amount effects in the south of Mexico. *Journal of Geophysical Research-Biogeosciences*. 118:1604-1615.
- Brienen, R.J.W., O.L. Phillips, T.R. Feldpausch, E. Gloor, T.R. Baker, J. Lloyd, G. Lopez-Gonzalez, A. Monteagudo-Mendoza, Y. Malhi, S.L. Lewis, R.V. Martinez, M. Alexiades, E.A. Davila, P. Alvarez-Loayza, A. Andrade, L. Aragao, A. Araujo-Murakami, E. Arets, L. Arroyo, G.A. Aymard, O.S. Banki, C. Baraloto, J. Barroso, D. Bonal, R.G.A. Boot, J.L.C. Camargo, C.V. Castilho, V. Chama, K.J. Chao, J. Chave, J.A. Comiskey, F.C. Valverde, L. da Costa, E.A. de Oliveira, A. Di Fiore, T.L. Erwin, S. Fauset, M. Forsthofer, D.R. Galbraith, E.S. Grahame, N. Groot, B. Herault, N. Higuchi, E.N.H. Coronado, H. Keeling, T.J. Killeen, W.F. Laurance, S. Laurance, J. Licona, W.E. Magnussen, B.S. Marimon, B.H. Marimon, C. Mendoza, D.A. Neill, E.M. Nogueira, P. Nunez, N.C.P. Camacho, A. Parada, G. Pardo-Molina, J. Peacock, M. Pena-Claros, G.C. Pickavance, N.C.A. Pitman, L. Poorter, A. Prieto, C.A. Quesada, F. Ramirez, H. Ramirez-Angulo, Z. Restrepo, A. Roopsind, A. Rudas, R.P. Salomao, M. Schwarz, N. Silva, J.E. Silva-Espejo, M. Silveira, J. Stropp, J. Talbot, H. ter Steege, J. Teran-Aguilar, J. Terborgh, R. Thomas-Caesar, M. Toledo, M. Torello-Raventos, R.K. Umetsu, G.M.F. Van der Heijden, P. Van der Hout, I.C.G. Vieira, S.A. Vieira, E. Vilanova, V.A. Vos and R.J. Zagt. 2015. Long-term decline of the Amazon carbon sink. *Nature*. 519:344-+.
- Brienen, R.J.W., P.A. Zuidema and M. Martinez-Ramos. 2010. Attaining the canopy in dry and moist tropical forests: strong differences in tree growth trajectories reflect variation in growing conditions. *Oecologia*. 163:485-496.
- Brodersen, C.R., A.J. McElrone, B. Choat, E.F. Lee, K.A. Shackel and M.A. Matthews. 2013. In Vivo Visualizations of Drought-Induced Embolism Spread in *Vitis vinifera*. *Plant Physiology*. 161:1820-1829.
- Brodribb, T.J. and H. Cochard. 2009. Hydraulic Failure Defines the Recovery and Point of Death in Water-Stressed Conifers. *Plant Physiology*. 149:575-584.
- Brodribb, T.J. and S.A.M. McAdam. 2013. Abscisic Acid Mediates a Divergence in the Drought Response of Two Conifers. *Plant Physiology*. 162:1370-1377.
- Brum, M., J.G. Lopez, H. Asbjornsen, J. Licata, T. Pypker, G. Sanchez and R.S. Oiveira. 2018. ENSO effects on the transpiration of eastern Amazon trees. *Philosophical Transactions of the Royal Society B-Biological Sciences*. 373

- Brum, M., M.A. Vadeboncoeur, V. Ivanov, H. Asbjornsen, S. Saleska, L.F. Alves, D. Penha, J.D. Dias, L. Aragao, F. Barros, P. Bittencourt, L. Pereira and R.S. Oliveira. 2019. Hydrological niche segregation defines forest structure and drought tolerance strategies in a seasonal Amazon forest. *Journal of Ecology*. 107:318-333.
- Brunner, I., C. Herzog, M.A. Dawes, M. Arend and C. Sperisen. 2015. How tree roots respond to drought. *Frontiers in Plant Science*. 6
- Bu, W.S., R.G. Zang and Y. Ding. 2014. Functional diversity increases with species diversity along successional gradient in a secondary tropical lowland rainforest. *Tropical Ecology*. 55:393-401.
- Bugmann, H. and C. Bigler. 2011. Will the CO₂ fertilization effect in forests be offset by reduced tree longevity? *Oecologia*. 165:533-544.
- Burgess, S.S.O. and T.E. Dawson. 2007. Predicting the limits to tree height using statistical regressions of leaf traits. *New Phytologist*. 174:626-636.
- Byng, J.W., M.W. Chase, M.J.M. Christenhusz, M.F. Fay, W.S. Judd, D.J. Mabberley, A.N. Sennikov, D.E. Soltis, P.S. Soltis, P.F. Stevens, B. Briggs, S. Brockington, A. Chautems, J.C. Clark, J. Conran, E. Haston, M. Moller, M. Moore, R. Olmstead, M. Perret, L. Skog, J. Smith, D. Tank, M. Vorontsova, A. Weber and G. Angiosperm Phylogeny. 2016. An update of the Angiosperm Phylogeny Group classification for the orders and families of flowering plants: APG IV. *Botanical Journal of the Linnean Society*. 181:1-20.
- Cavaleri, M.A., S.F. Oberbauer, D.B. Clark, D.A. Clark and M.G. Ryan. 2010. Height is more important than light in determining leaf morphology in a tropical forest. *Ecology*. 91:1730-1739.
- Chen, A.P., S.S. Peng and S.L. Fei. 2019a. Mapping global forest biomass and its changes over the first decade of the 21st century. *Science China-Earth Sciences*. 62:585-594.
- Chen, Z.C., S.R. Liu, H.B. Lu and X.C. Wan. 2019b. Interaction of stomatal behaviour and vulnerability to xylem cavitation determines the drought response of three temperate tree species. *Aob Plants*. 11
- Chin, A.R.O. and S.C. Sillett. 2016. Phenotypic plasticity of leaves enhances water-stress tolerance and promotes hydraulic conductivity in a tall conifer. *American Journal of Botany*. 103:796-807.
- Chin, A.R.O. and S.C. Sillett. 2017. Leaf acclimation to light availability supports rapid growth in tall *Picea sitchensis* trees. *Tree Physiology*. 37:1352-1366.
- Choat, B., E. Badel, R. Burtlett, S. Delzon, H. Cochard and S. Jansen. 2016. Noninvasive Measurement of Vulnerability to Drought-Induced Embolism by X-Ray Microtomography. *Plant Physiology*. 170:273-282.
- Choat, B., C.R. Brodersen and A.J. McElrone. 2015. Synchrotron X-ray microtomography of xylem embolism in *Sequoia sempervirens* saplings during cycles of drought and recovery. *New Phytologist*. 205:1095-1105.
- Choat, B., S. Jansen, T.J. Brodribb, H. Cochard, S. Delzon, R. Bhaskar, S.J. Bucci, T.S. Feild, S.M. Gleason, U.G. Hacke, A.L. Jacobsen, F. Lens, H. Maherali, J. Martinez-Vilalta, S. Mayr, M. Mencuccini, P.J. Mitchell, A. Nardini, J. Pittermann, R.B. Pratt, J.S. Sperry, M. Westoby, I.J. Wright and A.E. Zanne. 2012. Global convergence in the vulnerability of forests to drought. *Nature*. 491:752-+.
- Christensen-Dalsgaard, K.K., M. Fournier, A.R. Ennos and A.S. Barfod. 2007. Changes in vessel anatomy in response to mechanical loading in six species of tropical trees. *New Phytologist*. 176:610-622.
- Christina, M., J.P. Laclau, J.L.M. Goncalves, C. Jourdan, Y. Nouvellon and J.P. Bouillet. 2011. Almost symmetrical vertical growth rates above and below ground in one of the world's most productive forests. *Ecosphere*. 2
- Christman, M.A., J.S. Sperry and F.R. Adler. 2009. Testing the 'rare pit' hypothesis for xylem cavitation resistance in three species of *Acer*. *New Phytologist*. 182:664-674.
- Christoffersen, B.O., M. Gloor, S. Fauset, N.M. Fyllas, D.R. Galbraith, T.R. Baker, B. Kruijt, L. Rowland, R.A. Fisher, O.J. Binks, S. Sevanto, C.G. Xu, S. Jansen, B. Choat, M. Mencuccini, N.G. McDowell

- and P. Meir. 2016. Linking hydraulic traits to tropical forest function in a size-structured and trait-driven model (TFS v.1-Hydro). *Geoscientific Model Development*. 9:4227-4255.
- Cintron, B. 1990. *Cedrela odorata*. Agriculture Handbook. Washington DC, USA: USDA.
- Clark, D.A. and D.B. Clark. 1992. Life-history diversity of canopy and emergent trees in a neotropical rain-forest. *Ecological Monographs*. 62:315-344.
- Coble, A.P. and M.A. Cavaleri. 2017. Vertical leaf mass per area gradient of mature sugar maple reflects both height-driven increases in vascular tissue and light-driven increases in palisade layer thickness. *Tree Physiology*. 37:1337-1351.
- Corona-Nunez, R.O., J. Campo and M. Williams. 2018. Aboveground carbon storage in tropical dry forest plots in Oaxaca, Mexico. *Forest Ecology and Management*. 409:202-214.
- Coste, S., J.C. Roggy, G. Sonnier and E. Dreyer. 2010. Similar irradiance-elicited plasticity of leaf traits in saplings of 12 tropical rainforest tree species with highly different leaf mass to area ratio. *Functional Plant Biology*. 37:342-355.
- Coutand, C. and B. Moullia. 2000. Biomechanical study of the effect of a controlled bending on tomato stem elongation: local strain sensing and spatial integration of the signal. *Journal of Experimental Botany*. 51:1825-1842.
- Cramer, M.D. 2012. Unravelling the limits to tree height: a major role for water and nutrient trade-offs. *Oecologia*. 169:61-72.
- D'Almeida, C., C.J. Vorosmarty, G.C. Hurtt, J.A. Marengo, S.L. Dingman and B.D. Keim. 2007. The effects of deforestation on the hydrological cycle in Amazonia: a review on scale and resolution. *International Journal of Climatology*. 27:633-647.
- da Costa, A.C.L., D. Galbraith, S. Almeida, B.T.T. Portela, M. da Costa, J.D. Silva, A.P. Braga, P.H.L. de Goncalves, A.A.R. de Oliveira, R. Fisher, O.L. Phillips, D.B. Metcalfe, P. Levy and P. Meir. 2010. Effect of 7 yr of experimental drought on vegetation dynamics and biomass storage of an eastern Amazonian rainforest. *New Phytologist*. 187:579-591.
- Dawson, T.E. and G.R. Goldsmith. 2018. The value of wet leaves. *New Phytologist*. 219:1156-1169.
- Dawson, T.E. and J.S. Pate. 1996. Seasonal water uptake and movement in root systems of Australian phraeatophytic plants of dimorphic root morphology: A stable isotope investigation. *Oecologia*. 107:13-20.
- de Souza, F.C., K.G. Dexter, O.L. Phillips, R.J.W. Brienen, J. Chave, D.R. Galbraith, G.L. Gonzalez, A.M. Mendoza, R.T. Pennington, L. Poorter, M. Alexiades, E. Alvarez-Davila, A. Andrade, L. Aragao, A. Araujo-Murakami, E. Arets, G.A. Aymard, C. Baraloto, J.G. Barroso, D. Bonal, R.G.A. Boot, J.L.C. Camargo, J.A. Comiskey, F.C. Valverde, P.B. de Camargo, A. Di Fiore, F. Elias, T.L. Erwin, T.R. Feldpausch, L. Ferreira, N.M. Fyllas, E. Gloor, B. Herault, R. Herrera, N. Higuchi, E.N.H. Coronado, T.J. Killeen, W.F. Laurance, S. Laurance, J. Lloyd, T.E. Lovejoy, Y. Malhi, L. Maracahipes, B.S. Marimon, B.H. Marimon, C. Mendoza, P. Morandi, D.A. Neill, P.N. Vargas, E.A. Oliveira, E. Lenza, W.A. Palacios, M.C. Penuela-Mora, J.J. Pipoly, N.C.A. Pitman, A. Prieto, C.A. Quesada, H. Ramirez-Angulo, A. Rudas, K. Ruokolainen, R.P. Salomao, M. Silveira, J. Stropp, H. ter Steege, R. Thomas-Caesar, P. van der Hout, G.M.F. van der Heijden, P.J. van der Meer, R.V. Vasquez, S.A. Vieira, E. Vilanova, V.A. Vos, O. Wang, K.R. Young, R.J. Zagt and T.R. Baker. 2016. Evolutionary heritage influences Amazon tree ecology. *Proceedings of the Royal Society B-Biological Sciences*. 283
- Dexter, K.G., R.T. Pennington, A.T. Oliveira, M.L. Bueno, P.L.S. de Miranda and D.M. Neves. 2018. Inserting Tropical Dry Forests Into the Discussion on Biome Transitions in the Tropics. *Frontiers in Ecology and Evolution*. 6
- Dixon, H.H. and J. Joly. 1895. On the Ascent of Sap. *Philosophical Transactions of the Royal Society of London*. B. 186:563-576.
- Domec, J.C. 2011. Let's not forget the critical role of surface tension in xylem water relations. *Tree Physiology*. 31:359-360.
- Drake, P.L., R.H. Froend and P.J. Franks. 2013. Smaller, faster stomata: scaling of stomatal size, rate of response, and stomatal conductance. *Journal of Experimental Botany*. 64:495-505.

- Duan, C., R. Karnik, M.C. Lu and A. Majumdar. 2012. Evaporation-induced cavitation in nanofluidic channels. *Proceedings of the National Academy of Sciences of the United States of America*. 109:3688-3693.
- Duffy, P.B., P. Brando, G.P. Asner and C.B. Field. 2015. Projections of future meteorological drought and wet periods in the Amazon. *Proceedings of the National Academy of Sciences of the United States of America*. 112:13172-13177.
- Echeverria, A., T. Anfodillo, D. Soriano, J.A. Rosell and M.E. Olson. 2019. Constant theoretical conductance via changes in vessel diameter and number with height growth in *Moringa oleifera*. *Journal of Experimental Botany*. 70:5765-5772.
- Eller, C.B., F.D. Barros, P.R.L. Bittencourt, L. Rowland, M. Mencuccini and R.S. Oliveira. 2018. Xylem hydraulic safety and construction costs determine tropical tree growth. *Plant Cell and Environment*. 41:548-562.
- Eller, C.B., A.L. Lima and R.S. Oliveira. 2013. Foliar uptake of fog water and transport belowground alleviates drought effects in the cloud forest tree species, *Drimys brasiliensis* (Winteraceae). *New Phytologist*. 199:151-162.
- Eltahir, E.A.B. and R.L. Bras. 1994. PRECIPITATION RECYCLING IN THE AMAZON BASIN. *Quarterly Journal of the Royal Meteorological Society*. 120:861-880.
- Engelbrecht, B.M.J., L.S. Comita, R. Condit, T.A. Kursar, M.T. Tyree, B.L. Turner and S.P. Hubbell. 2007. Drought sensitivity shapes species distribution patterns in tropical forests. *Nature*. 447:80-U2.
- England, J.R. and P.M. Attiwill. 2006. Changes in leaf morphology and anatomy with tree age and height in the broadleaved evergreen species, *Eucalyptus regnans* F. Muell. *Trees-Structure and Function*. 20:79-90.
- Enquist, B.J. 2002. Universal scaling in tree and vascular plant allometry: Toward a general quantitative theory linking plant form and function from cells to ecosystems. *Tree Physiology*. 22:1045-1064.
- Enquist, B.J. 2003. Cope's Rule and the evolution of long-distance transport in vascular plants: allometric scaling, biomass partitioning and optimization. *Plant Cell and Environment*. 26:151-161.
- Espinoza, J.C., J. Ronchail, J.A. Marengo and H. Segura. 2019. Contrasting North-South changes in Amazon wet-day and dry-day frequency and related atmospheric features (1981-2017). *Climate Dynamics*. 52:5413-5430.
- Esquivel-Muelbert, A., T.R. Baker, K.G. Dexter, S.L. Lewis, R.J.W. Brienen, T.R. Feldpausch, J. Lloyd, A. Monteagudo-Mendoza, L. Arroyo, E. Alvarez-Davila, N. Higuchi, B.S. Marimon, B.H. Marimon-Junior, M. Silveira, E. Vilanova, E. Gloor, Y. Malhi, J. Chave, J. Barlow, D. Bonal, N. Davila Cardozo, T. Erwin, S. Fauset, B. Herault, S. Laurance, L. Poorter, L. Qie, C. Stahl, M.J.P. Sullivan, H. ter Steege, V.A. Vos, P.A. Zuidema, E. Almeida, E. Almeida de Oliveira, A. Andrade, S.A. Vieira, L. Aragao, A. Araujo-Murakami, E. Arets, G.A. Aymard C, C. Baraloto, P.B. Camargo, J.G. Barroso, F. Bongers, R. Boot, J.L. Camargo, W. Castro, V. Chama Moscoso, J. Comiskey, F. Cornejo Valverde, A.C. Lola da Costa, J. del Aguila Pasquel, A. Di Fiore, L. Fernanda Duque, F. Elias, J. Engel, G. Flores Llampazo, D. Galbraith, R. Herrera Fernandez, E. Honorio Coronado, W. Hubau, E. Jimenez-Rojas, A.J.N. Lima, R.K. Umetsu, W. Laurance, G. Lopez-Gonzalez, T. Lovejoy, O. Aurelio Melo Cruz, P.S. Morandi, D. Neill, P. Nunez Vargas, N.C. Pallqui Camacho, A. Parada Gutierrez, G. Pardo, J. Peacock, M. Pena-Claros, M.C. Penuela-Mora, P. Petronelli, G.C. Pickavance, N. Pitman, A. Prieto, C. Quesada, H. Ramirez-Angulo, M. Rejou-Mechain, Z. Restrepo Correa, A. Roopsind, A. Rudas, R. Salomao, N. Silva, J. Silva Espejo, J. Singh, J. Stropp, J. Terborgh, R. Thomas, M. Toledo, A. Torres-Lezama, L. Valenzuela Gamarra, P.J. van de Meer, G. van der Heijden, P. van der Hout, et al. 2019. Compositional response of Amazon forests to climate change. *Global Change Biology*. 25:39-56.
- Esquivel-Muelbert, A., T.R. Baker, K.G. Dexter, S.L. Lewis, H. ter Steege, G. Lopez-Gonzalez, A.M. Mendoza, R. Brienen, T.R. Feldpausch, N. Pitman, A. Alonso, G. van der Heijden, M. Pena-Claros, M. Ahuite, M. Alexiades, E.A. Davila, A.A. Murakami, L. Arroyo, M. Aulestia, H. Balslev,

- J. Barroso, R. Boot, A. Cano, V.C. Moscoso, J.A. Comiskey, F. Cornejo, F. Dallmeier, D.C. Daly, N. Davila, J.F. Duivenvoorden, A.J.D. Montoya, T. Erwin, A. Di Fiore, T. Fredericksen, A. Fuentes, R. Garcia-Villacorta, T. Gonzales, J.E.G. Andino, E.N.H. Coronado, I. Huamantupa-Chuquimaco, T.J. Killeen, Y. Malhi, C. Mendoza, H. Mogollon, P.M. Jorgensen, J.C. Montero, B. Mostacedo, W. Nauray, D. Neill, P.N. Vargas, S. Palacios, W.P. Cuenca, N.C.P. Camacho, J. Peacock, J.F. Phillips, G. Pickavance, C.A. Quesada, H. Ramirez-Angulo, Z. Restrepo, C.R. Rodriguez, M.R. Paredes, R. Sierra, M. Silveira, P. Stevenson, J. Stropp, J. Terborgh, M. Tirado, M. Toledo, A. Torres-Lezama, M.N. Umana, L.E. Urrego, R.V. Martinez, L.V. Gamarra, C.I.A. Vela, E.V. Torre, V. Vos, P. von Hildebrand, C. Vriesendorp, O. Wang, K.R. Young, C.E. Zartman and O.L. Phillips. 2017a. Seasonal drought limits tree species across the Neotropics. *Ecography*. 40:618-629.
- Esquivel-Muelbert, A., D. Galbraith, K.G. Dexter, T.R. Baker, S.L. Lewis, P. Meir, L. Rowland, A.C.L. da Costa, D. Nepstad and O.L. Phillips. 2017b. Biogeographic distributions of neotropical trees reflect their directly measured drought tolerances. *Scientific Reports*. 7
- Ewers, F.W. and M.H. Zimmermann. 1984. THE HYDRAULIC ARCHITECTURE OF EASTERN HEMLOCK (TSUGA-CANADENSIS). *Canadian Journal of Botany-Revue Canadienne De Botanique*. 62:940-946.
- Fajardo, A., C. Martinez-Perez, M.A. Cervantes-Alcayde and M.E. Olson. 2020. Stem length, not climate, controls vessel diameter in two trees species across a sharp precipitation gradient. *New Phytologist*
- Fajardo, A., E.J.B. McIntire and M.E. Olson. 2019. When Short Stature Is an Asset in Trees. *Trends in Ecology & Evolution*. 34:193-199.
- Falster, D.S. and M. Westoby. 2003. Plant height and evolutionary games. *Trends in Ecology & Evolution*. 18:337-343.
- Fan, Z.X., F. Sterck, S.B. Zhang, P.L. Fu and G.Y. Hao. 2017. Tradeoff between Stem Hydraulic Efficiency and Mechanical Strength Affects Leaf-Stem Allometry in 28 Ficus Tree Species. *Frontiers in Plant Science*. 8
- Farquhar, G.D., K.T. Hubick, A.G. Condon and R.A. Richards. 1989. Carbon Isotope Fractionation and Plant Water-Use Efficiency. *In Stable Isotopes in Ecological Research* Eds. P.W. Rundel, J.R. Ehleringer and K.A. Nagy. Springer New York, New York, NY, pp 21-40.
- Farquhar, G.D., M.H. O'Leary and J.A. Berry. 1982. On the Relationship between Carbon Isotope Discrimination and the Inter-Cellular Carbon-Dioxide Concentration in Leaves. *Australian Journal of Plant Physiology*. 9:121-137.
- Fasullo, J.T., B.L. Otto-Bliesner and S. Stevenson. 2018. ENSO's Changing Influence on Temperature, Precipitation, and Wildfire in a Warming Climate. *Geophysical Research Letters*. 45:9216-9225.
- Fauset, S., M.O. Johnson, M. Gloor, T.R. Baker, A. Monteagudo, R.J.W. Brienen, T.R. Feldpausch, G. Lopez-Gonzalez, Y. Malhi, H. ter Steege, N.C.A. Pitman, C. Baraloto, J. Engel, P. Petronelli, A. Andrade, J. Camargo, S.G.W. Laurance, W.F. Laurance, J. Chave, E. Allie, P.N. Vargas, J.W. Terborgh, K. Ruokolainen, M. Silveira, G.A. Aymard, L. Arroyo, D. Bonal, H. Ramirez-Angulo, A. Araujo-Murakami, D. Neill, B. Herault, A. Dourdain, A. Torres-Lezama, B.S. Marimon, R.P. Salomao, J.A. Comiskey, M. Rejou-Mechain, M. Toledo, J.C. Licona, A. Alarcon, A. Prieto, A. Rudas, P.J. van der Meer, T.J. Killeen, B.H. Marimon, L. Poorter, R.G.A. Boot, B. Stergios, E.V. Torre, F.R.C. Costa, C. Levis, J. Schietti, P. Souza, N. Groot, E. Arets, V.C. Moscoso, W. Castro, E.N.H. Coronado, M. Pena-Claros, C. Stahl, J. Barroso, J. Talbot, I.C.G. Vieira, G. van der Heijden, R. Thomas, V.A. Vos, E.C. Almeida, E.A. Davila, L. Aragao, T.L. Erwin, P.S. Morandi, E.A. de Oliveira, M.B.X. Valadao, R.J. Zagt, P. van der Hout, P.A. Loayza, J.J. Pipoly, O. Wang, M. Alexiades, C.E. Ceron, I. Huamantupa-Chuquimaco, A. Di Fiore, J. Peacock, N.C.P. Camacho, R.K. Umetsu, P.B. de Camargo, R.J. Burnham, R. Herrera, C.A. Quesada, J. Stropp, S.A. Vieira, M. Steininger, C.R. Rodriiguez, Z. Restrepo, A.E. Muelbert, S.L. Lewis, G.C. Pickavance and O.L.

- Phillips. 2015. Hyperdominance in Amazonian forest carbon cycling. *Nature Communications*. 6
- Feldpausch, T.R., J. Lloyd, S.L. Lewis, R.J.W. Brienen, M. Gloor, A.M. Mendoza, G. Lopez-Gonzalez, L. Banin, K. Abu Salim, K. Affum-Baffoe, M. Alexiades, S. Almeida, I. Amaral, A. Andrade, L. Aragao, A.A. Murakami, E. Arets, L. Arroyo, G.A. Aymard, T.R. Baker, O.S. Banki, N.J. Berry, N. Cardozo, J. Chave, J.A. Comiskey, E. Alvarez, A. de Oliveira, A. Di Fiore, G. Djagbletey, T.F. Domingues, T.L. Erwin, P.M. Fearnside, M.B. Franca, M.A. Freitas, N. Higuchi, E. Honorio, Y. Iida, E. Jimenez, A.R. Kassim, T.J. Killeen, W.F. Laurance, J.C. Lovett, Y. Malhi, B.S. Marimon, B.H. Marimon, E. Lenza, A.R. Marshall, C. Mendoza, D.J. Metcalfe, E.T.A. Mitchard, D.A. Neill, B.W. Nelson, R. Nilus, E.M. Nogueira, A. Parada, K.S.H. Peh, A.P. Cruz, M.C. Penuela, N.C.A. Pitman, A. Prieto, C.A. Quesada, F. Ramirez, H. Ramirez-Angulo, J.M. Reitsma, A. Rudas, G. Saiz, R.P. Salomao, M. Schwarz, N. Silva, J.E. Silva-Espejo, M. Silveira, B. Sonke, J. Stropp, H.E. Taedoumg, S. Tan, H. ter Steege, J. Terborgh, M. Torello-Raventos, G.M.F. van der Heijden, R. Vasquez, E. Vilanova, V.A. Vos, L. White, S. Willcock, H. Woell and O.L. Phillips. 2012. Tree height integrated into pantropical forest biomass estimates. *Biogeosciences*. 9:3381-3403.
- Ferry, B., F. Morneau, J.D. Bontemps, L. Blanc and V. Freycon. 2010. Higher treefall rates on slopes and waterlogged soils result in lower stand biomass and productivity in a tropical rain forest. *Journal of Ecology*. 98:106-116.
- Fichot, R., F. Laurans, R. Monclus, A. Moreau, G. Pilate and F. Brignolas. 2009. Xylem anatomy correlates with gas exchange, water-use efficiency and growth performance under contrasting water regimes: evidence from *Populus deltoides*/*Populus nigra* hybrids. *Tree Physiology*. 29:1537-1549.
- Fick, S.E. and R.J. Hijmans. 2017. WorldClim 2: new 1-km spatial resolution climate surfaces for global land areas. *International Journal of Climatology*. 37:4302-4315.
- Finch, K.N., F.A. Jones and R.C. Cronn. 2019. Genomic resources for the Neotropical tree genus *Cedrela* (Meliaceae) and its relatives. *Bmc Genomics*. 20
- Fisher, J.B., Y. Malhi, I.C. Torres, D.B. Metcalfe, M.J. van de Weg, P. Meir, J.E. Silva-Espejo and W.H. Huasco. 2013. Nutrient limitation in rainforests and cloud forests along a 3,000-m elevation gradient in the Peruvian Andes. *Oecologia*. 172:889-902.
- Fisher, R.A., M. Williams, R.L. Do Vale, A.L. Da Costa and P. Meir. 2006. Evidence from Amazonian forests is consistent with isohydric control of leaf water potential. *Plant Cell and Environment*. 29:151-165.
- Flexas, J. and H. Medrano. 2002. Drought-inhibition of photosynthesis in C-3 plants: Stomatal and non-stomatal limitations revisited. *Annals of Botany*. 89:183-189.
- Flexas, J., M. Ribas-Carbo, A. Diaz-Espejo, J. Galmes and H. Medrano. 2008. Mesophyll conductance to CO₂: current knowledge and future prospects. *Plant Cell and Environment*. 31:602-621.
- Fortin, M., R. Van Couwenberghe, V. Perez and C. Piedallu. 2018. Evidence of climate effects on the height-diameter relationships of tree species. *Annals of Forest Science*. 76
- Franks, P.J. and D.J. Beerling. 2009a. CO₂-forced evolution of plant gas exchange capacity and water-use efficiency over the Phanerozoic. *Geobiology*. 7:227-236.
- Franks, P.J. and D.J. Beerling. 2009b. Maximum leaf conductance driven by CO₂ effects on stomatal size and density over geologic time. *Proceedings of the National Academy of Sciences of the United States of America*. 106:10343-10347.
- Fujii, K., M. Shibata, K. Kitajima, T. Ichie, K. Kitayama and B.L. Turner. 2018. Plant-soil interactions maintain biodiversity and functions of tropical forest ecosystems. *Ecological Research*. 33:149-160.
- Garcia-Cervigon, A.I., J.M. Olano, G. von Arx and A. Fajardo. 2018. Xylem adjusts to maintain efficiency across a steep precipitation gradient in two coexisting generalist species. *Annals of Botany*. 122:461-472.
- Gardner, W.R. 1965. Dynamic aspects of soil-water availability to plants. *Annual Review of Plant Physiology*. 16:323-&

- Gartner, H. and D. Nievergelt. 2010. The core-microtome: A new tool for surface preparation on cores and time series analysis of varying cell parameters. *Dendrochronologia*. 28:85-92.
- GBIF. 2019a. *Ampelocera ruizii* Klotzsch in GBIF Secretariat GBIF Backbone Taxonomy.
- GBIF. 2019b. *Centrolobium microchaete* (Mart. ex Benth.) H.C.Lima in GBIF Secretariat. GBIF Backbone Taxonomy.
- GBIF. 2019c. *Pseudolmedia laevis* J.F.Macbr. in GBIF Secretariat. In GBIF Backbone Taxonomy Checklist dataset.
- Gerrienne, P., P.G. Gensel, C. Strullu-Derrien, H. Lardeux, P. Steemans and C. Prestianni. 2011. A Simple Type of Wood in Two Early Devonian Plants. *Science*. 333:837-837.
- Ghazoul, J. and D. Sheil. 2010a. In *Tropical rain forest ecology, diversity, and conservation*. Oxford University Press, New York, USA, pp 129-177.
- Ghazoul, J. and D. Sheil. 2010b. In *Tropical rain forest ecology, diversity, and conservation*. Oxford University Press, New York, USA, pp 9-32.
- Givnish, T.J., S.C. Wong, H. Stuart-Williams, M. Holloway-Phillips and G.D. Farquhar. 2014. Determinants of maximum tree height in Eucalyptus species along a rainfall gradient in Victoria, Australia. *Ecology*. 95:2991-3007.
- Gleason, S.M., D.W. Butler, K. Zieminska, P. Waryszak and M. Westoby. 2012. Stem xylem conductivity is key to plant water balance across Australian angiosperm species. *Functional Ecology*. 26:343-352.
- Gleason, S.M., M. Westoby, S. Jansen, B. Choat, U.G. Hacked, R.B. Pratt, R. Bhaskar, T.J. Brodribb, S.J. Bucci, K.F. Cao, H. Cochard, S. Delzon, J.C. Domec, Z.X. Fan, T.S. Feild, A.L. Jacobsen, D.M. Johnson, F. Lens, H. Maherali, J. Martinez-Vilalta, S. Mayr, K.A. McCulloh, M. Mencuccini, P.J. Mitchell, H. Morris, A. Nardini, J. Pittermann, L. Plavcova, S.G. Schreiber, J.S. Sperry, I.J. Wright and A.E. Zanne. 2016. Weak tradeoff between xylem safety and xylem-specific hydraulic efficiency across the world's woody plant species. *New Phytologist*. 209:123-136.
- Gloor, E., C. Wilson, M.P. Chipperfield, F. Chevallier, W. Buermann, H. Boesch, R. Parker, P. Somkuti, L.V. Gatti, C. Correia, L.G. Domingues, W. Peters, J. Miller, M.N. Deeter and M.J.P. Sullivan. 2018. Tropical land carbon cycle responses to 2015/16 El Niño as recorded by atmospheric greenhouse gas and remote sensing data. *Philosophical Transactions of the Royal Society B-Biological Sciences*. 373:12.
- Gloor, M., J. Barichivich, G. Ziv, R. Brienen, J. Schongart, P. Peylin, B.B.L. Cintra, T. Feldpausch, O. Phillips and J. Baker. 2015. Recent Amazon climate as background for possible ongoing and future changes of Amazon humid forests. *Global Biogeochemical Cycles*. 29:1384-1399.
- Gloor, M., R.J.W. Brienen, D. Galbraith, T.R. Feldpausch, J. Schongart, J.L. Guyot, J.C. Espinoza, J. Lloyd and O.L. Phillips. 2013. Intensification of the Amazon hydrological cycle over the last two decades. *Geophysical Research Letters*. 40:1729-1733.
- Gorgens, E., M.H. Nunes, T. Jackson, D. Coomes, M. Keller, C.R. Reis, R. Valbuena, J. Rosette, D.R.A. de Almeida, B. Gimenez, R. Cantinho, A.Z. Motta, M. Assis, F.R. de Souza Pereira, G. Spanner, N. Higuchi and J.P. Ometto. 2020. Resource availability and disturbance shape maximum tree height across the Amazon. *bioRxiv:2020.05.15.097683*.
- Gorgens, E.B., A.Z. Motta, M. Assis, M.H. Nunes, T. Jackson, D. Coomes, J. Rosette, L. Aragao and J.P. Ometto. 2019. The giant trees of the Amazon basin. *Frontiers in Ecology and the Environment*. 17:373-374.
- Gould, K.A., T.S. Fredericksen, F. Morales, D. Kennard, F.E. Putz, B. Mostacedo and M. Toledo. 2002. Post-fire tree regeneration in lowland Bolivia: implications for fire management. *Forest Ecology and Management*. 165:225-234.
- Gower, S.T., R.E. McMurtrie and D. Murty. 1996. Aboveground net primary production decline with stand age: Potential causes. *Trends in Ecology & Evolution*. 11:378-382.
- Graham, E.A., S.S. Mulkey, K. Kitajima, N.G. Phillips and S.J. Wright. 2003. Cloud cover limits net CO₂ uptake and growth of a rainforest tree during tropical rainy seasons. *Proceedings of the National Academy of Sciences of the United States of America*. 100:572-576.

- Green, J.K., J. Berry, P. Ciais, Y. Zhang and P. Gentile. 2020. Amazon rainforest photosynthesis increases in response to atmospheric dryness. *Science Advances*. 6
- Guan, K.Y., M. Pan, H.B. Li, A. Wolf, J. Wu, D. Medvigy, K.K. Caylor, J. Sheffield, E.F. Wood, Y. Malhi, M.L. Liang, J.S. Kimball, S.R. Saleska, J. Berry, J. Joiner and A.I. Lyapustin. 2015. Photosynthetic seasonality of global tropical forests constrained by hydroclimate. *Nature Geoscience*. 8:284-289.
- Guerrieri, R., S. Belmecheri, S.V. Ollinger, H. Asbjornsen, K. Jennings, J.F. Xiao, B.D. Stocker, M. Martin, D.Y. Hollinger, R. Bracho-Garrillo, K. Clark, S. Dore, T. Kolb, J.W. Munger, K. Novick and A.D. Richardson. 2019. Disentangling the role of photosynthesis and stomatal conductance on rising forest water-use efficiency. *Proceedings of the National Academy of Sciences of the United States of America*. 116:16909-16914.
- Guo, Q., X.L. Chi, Z.Q. Xie and Z.Y. Tang. 2017. Asymmetric competition for light varies across functional groups. *Journal of Plant Ecology*. 10:74-80.
- Gutierrez-Vazquez, B.N., E.H. Cornejo-Oviedo, M.H. Gutierrez-Vazquez and M. Gomez-Cardenas. 2012. VARIATION AND PREDICTION OF BASIC WOOD DENSITY IN *Cedrela odorata* L. *Revista Fitotecnica Mexicana*. 35:87-90.
- Hacke, U. and J.J. Sauter. 1995. Vulnerability of xylem to embolism in relation to leaf water potential and stomatal conductance in *Fagus-sylvatica f purpurea* and *Populus-balsamifera*. *Journal of Experimental Botany*. 46:1177-1183.
- Hacke, U.G., J.S. Sperry, J.K. Wheeler and L. Castro. 2006. Scaling of angiosperm xylem structure with safety and efficiency. *Tree Physiology*. 26:689-701.
- Hacke, U.G., R. Spicer, S.G. Schreiber and L. Plavcova. 2017. An ecophysiological and developmental perspective on variation in vessel diameter. *Plant Cell and Environment*. 40:831-845.
- Haggi, C., C.M. Chiessi, U. Merkel, S. Multiza, M. Prange, M. Schulz and E. Schefuss. 2017. Response of the Amazon rainforest to late Pleistocene climate variability. *Earth and Planetary Science Letters*. 479:50-59.
- Hammond, W.M., K.L. Yu, L.A. Wilson, R.E. Will, W.R.L. Anderegg and H.D. Adams. 2019. Dead or dying? Quantifying the point of no return from hydraulic failure in drought-induced tree mortality. *New Phytologist*. 223:1834-1843.
- Hanba, Y.T., S.I. Miyazawa and I. Terashima. 1999. The influence of leaf thickness on the CO₂ transfer conductance and leaf stable carbon isotope ratio for some evergreen tree species in Japanese warm-temperate forests. *Functional Ecology*. 13:632-639.
- He, P.C., I.J. Wright, S.D. Zhu, Y. Onoda, H. Liu, R.H. Li, X.R. Liu, L. Hua, O.O. Oyanoghafo and Q. Ye. 2019. Leaf mechanical strength and photosynthetic capacity vary independently across 57 subtropical forest species with contrasting light requirements. *New Phytologist*. 223:607-618.
- Hengl, T., J.M. de Jesus, R.A. MacMillan, N.H. Batjes and G.B.M. Heuvelink. 2014. SoilGrids1km - Global Soil Information Based on Automated Mapping (vol 9, e105992, 2014). *Plos One*. 9
- Henry, C., G.P. John, R.H. Pan, M.K. Bartlett, L.R. Fletcher, C. Scoffoni and L. Sack. 2019. A stomatal safety-efficiency trade-off constrains responses to leaf dehydration. *Nature Communications*. 10
- Herault, B. and C. Piponiot. 2018. Key drivers of ecosystem recovery after disturbance in a neotropical forest. *Forest Ecosystems*. 5
- Hietz, P., S. Rosner, U. Hietz-Seifert and S.J. Wright. 2017. Wood traits related to size and life history of trees in a Panamanian rainforest. *New Phytologist*. 213:170-180.
- Hodnett, M.G. and J. Tomasella. 2002. Marked differences between van Genuchten soil water-retention parameters for temperate and tropical soils: a new water-retention pedo-transfer functions developed for tropical soils. *Geoderma*. 108:155-180.
- Hoerber, S., C. Leuschner, L. Kohler, D. Arias-Aguilar and B. Schuldt. 2014. The importance of hydraulic conductivity and wood density to growth performance in eight tree species from a tropical semi-dry climate. *Forest Ecology and Management*. 330:126-136.

- Hogg, E.H. and P.A. Hurdle. 1997. Sap flow in trembling aspen: implications for stomatal responses to vapor pressure deficit. *Tree Physiology*. 17:501-509.
- Holtta, T. and E. Nikinmaa. 2013. Modelling the Effect of Xylem and Phloem Transport on Leaf Gas Exchange. *Ix International Workshop on Sap Flow*. 991:351-358.
- Houter, N.C. and T.L. Pons. 2012. Ontogenetic changes in leaf traits of tropical rainforest trees differing in juvenile light requirement. *Oecologia*. 169:33-45.
- Huc, R., A. Ferhi and J.M. Guehl. 1994. Pioneer and late-stage tropical rain-forest tree species (French-Guiana) growing under common conditions differ in leaf gas-exchange regulation, carbon-isotope discrimination and leaf water potential. *Oecologia*. 99:297-305.
- Hunter, M.O., M. Keller, D. Morton, B. Cook, M. Lefsky, M. Ducey, S. Saleska, R.C. de Oliveira and J. Schiatti. 2015. Structural Dynamics of Tropical Moist Forest Gaps. *Plos One*. 10
- Huzulak, J. and F. Matejka. 1982. A SIMPLE-MODEL OF THE LEAF DAILY WATER POTENTIAL DYNAMICS OF SOME FOREST TREE SPECIES. *Biologia Plantarum*. 24:109-116.
- Ibanez, T., G. Keppel, C. Menkes, T.W. Gillespie, M. Lengaigne, M. Mangeas, G. Rivas-Torres and P. Birnbaum. 2019. Globally consistent impact of tropical cyclones on the structure of tropical and subtropical forests. *Journal of Ecology*. 107:279-292.
- Iida, Y., L. Poorter, F. Sterck, A.R. Kassim, M.D. Potts, T. Kubo and T.S. Kohyama. 2014. Linking size-dependent growth and mortality with architectural traits across 145 co-occurring tropical tree species. *Ecology*. 95:353-363.
- Jacobsen, A.L., J. Valdovinos-Ayala, F.D. Rodriguez-Zaccaro, M.A. Hill-Crim, M.I. Percolla and M.D. Venturas. 2018. Intra-organismal variation in the structure of plant vascular transport tissues in poplar trees. *Trees-Structure and Function*. 32:1335-1346.
- Jaouen, G., M. Fournier and T. Almeras. 2010. Thigmomorphogenesis versus light in biomechanical growth strategies of saplings of two tropical rain forest tree species. *Annals of Forest Science*. 67
- Jeje, A.A. and M.H. Zimmermann. 1979. RESISTANCE TO WATER-FLOW IN XYLEM VESSELS. *Journal of Experimental Botany*. 30:817-827.
- Jimenez, E.M., M.C. Penuela-Mora, F. Moreno and C.A. Sierra. 2020. Spatial and temporal variation of forest net primary productivity components on contrasting soils in northwestern Amazon. *Ecosphere*. 11
- Jimenez, J.C., J. Barichivich, C. Mattar, K. Takahashi, A. Santamaria-Artigas, J.A. Sobrino and Y. Malhi. 2018. Spatio-temporal patterns of thermal anomalies and drought over tropical forests driven by recent extreme climatic anomalies. *Philosophical Transactions of the Royal Society B-Biological Sciences*. 373
- Jimenez-Munoz, J.C., C. Mattar, J. Barichivich, A. Santamaria-Artigas, K. Takahashi, Y. Malhi, J.A. Sobrino and G. van der Schrier. 2016. Record-breaking warming and extreme drought in the Amazon rainforest during the course of El Nino 2015-2016. *Scientific Reports*. 6:7.
- Joetzier, E., H. Douville, C. Delire and P. Ciais. 2013. Present-day and future Amazonian precipitation in global climate models: CMIP5 versus CMIP3. *Climate Dynamics*. 41:2921-2936.
- Johnson, D., P. Eckart, N. Alsamadisi, H. Noble and C. Martin. 2018a. Polar auxin transport is implicated in vessel differentiation and spatial patterning during secondary growth in *Populus* (vol 105, pg 186, 2018). *American Journal of Botany*. 105:1609-1609.
- Johnson, D.J., J. Needham, C.G. Xu, E.C. Massoud, S.J. Davies, K.J. Anderson-Teixeira, S. Bunyavejchewin, J.Q. Chambers, C.H. Chang-Yang, J.M. Chiang, G.B. Chuyong, R. Condit, S. Cordell, C. Fletcher, C.P. Giardina, T.W. Giambelluca, N. Gunatilleke, S. Gunatilleke, C.F. Hsieh, S. Hubbell, F. Inman-Narahari, A.R. Kassim, M. Katabuchi, D. Kenfack, C.M. Litton, S. Lum, M. Mohamad, M. Nasardin, P.S. Ong, R. Ostertag, L. Sack, N.G. Swenson, I.F. Sun, S. Tan, D.W. Thomas, J. Thompson, M.N. Umana, M. Uriarte, R. Valencia, S. Yap, J. Zimmerman, N.G. McDowell and S.M. McMahon. 2018b. Climate sensitive size-dependent survival in tropical trees. *Nature Ecology & Evolution*. 2:1436-1442.

- Jones, H.G. 1998. Stomatal control of photosynthesis and transpiration. *Journal of Experimental Botany*. 49:387-398.
- Kaack, L., C.M. Altaner, C. Carmesin, A. Diaz, M. Holler, C. Kranz, G. Neusser, M. Odstrcil, H.J. Schenk, V. Schmidt, M. Weber, Z. Ya and S. Jansen. 2019. Function and three-dimensional structure of intervessel pit membranes in angiosperms: a review. *Iawa Journal*. 40:673-702.
- Kafuti, C., N. Bourland, T. De Mil, S. Meeus, M. Rousseau, B. Toirambe, P.C. Bolaluembe, L. Ndjele and H. Beeckman. 2020. Foliar and Wood Traits Covary along a Vertical Gradient within the Crown of Long-Lived Light-Demanding Species of the Congo Basin Semi-Deciduous Forest. *Forests*. 11
- Kahn, F., K. Mejia and A. Decastro. 1988. SPECIES RICHNESS AND DENSITY OF PALMS IN TERRA-FIRME FORESTS OF AMAZONIA. *Biotropica*. 20:266-269.
- Kang, J., J.U. Hwang, M. Lee, Y.Y. Kim, S.M. Assmann, E. Martinoia and Y. Lee. 2010. PDR-type ABC transporter mediates cellular uptake of the phytohormone abscisic acid. *Proceedings of the National Academy of Sciences of the United States of America*. 107:2355-2360.
- Kassambara, A. 2019. rstatix: Pipe-Friendly Framework for Basic Statistical Tests.
- Keeling, H.C. and O.L. Phillips. 2007. A calibration method for the crown illumination index for assessing forest light environments. *Forest Ecology and Management*. 242:431-437.
- Kempes, C.P., G.B. West, K. Crowell and M. Girvan. 2011. Predicting Maximum Tree Heights and Other Traits from Allometric Scaling and Resource Limitations. *Plos One*. 6
- Kenrick, P. and P.R. Crane. 1997. The origin and early evolution of plants on land. *Nature*. 389:33-39.
- Kenzo, T., T. Ichie, Y. Watanabe, R. Yoneda, I. Ninomiya and T. Koike. 2006. Changes in photosynthesis and leaf characteristics with tree height in five dipterocarp species in a tropical rain forest. *Tree Physiology*. 26:865-873.
- Killeen, T.J., E. Chavez, M. Pena-Claros, M. Toledo, L. Arroyo, J. Caballero, L. Correa, R. Guillen, R. Quevedo, M. Saldias, L. Soria, Y. Uslar, I. Vargas and M. Steininger. 2006. The Chiquitano dry forest, the transition between humid and dry forest in Eastern Lowland Bolivia. *Neotropical Savannas and Seasonally Dry Forests: Plant Diversity, Biogeography, and Conservation*:213-233.
- Klein, T. 2014. The variability of stomatal sensitivity to leaf water potential across tree species indicates a continuum between isohydric and anisohydric behaviours. *Functional Ecology*. 28:1313-1320.
- Klein, T., C. Randin and C. Korner. 2015. Water availability predicts forest canopy height at the globalscale. *Ecology Letters*. 18:1311-1320.
- Knipfer, T., C.R. Brodersen, A. Zedan, D.A. Kluepfel and A.J. McElrone. 2015. Patterns of drought-induced embolism formation and spread in living walnut saplings visualized using X-ray microtomography. *Tree Physiology*. 35:744-755.
- Koch, G.W., S.C. Sillett, G.M. Jennings and S.D. Davis. 2004. The limits to tree height. *Nature*. 428:851-854.
- Kohyama, T. 1993. Size-structured tree populations in gap-dynamic forest - the forest architecture hypothesis for the stable coexistence of species. *Journal of Ecology*. 81:131-143.
- Kohyama, T., E. Suzuki, T. Partomihardjo, T. Yamada and T. Kubo. 2003. Tree species differentiation in growth, recruitment and allometry in relation to maximum height in a Bornean mixed dipterocarp forest. *Journal of Ecology*. 91:797-806.
- Korver, R.A., I.T. Koevoets and C. Testerink. 2018. Out of Shape During Stress: A Key Role for Auxin. *Trends in Plant Science*. 23:783-793.
- Kupers, S.J., C. Wirth, B.M.J. Engelbrecht, A. Hernandez, R. Condit, S.J. Wright and N. Ruger. 2019. Performance of tropical forest seedlings under shade and drought: an interspecific trade-off in demographic responses. *Scientific Reports*. 9
- Kuppers, M., H. Timm, F. Orth, J. Stegeman, R. Stober, H. Schneider, K. Paliwal, K. Karunaichamy and R. Ortiz. 1996. Effects of light environment and successional status on lightfleck use by understory trees of temperate and tropical forests. *Tree Physiology*. 16:69-80.

- Kusumi, K., S. Hirotsuka, T. Kumamaru and K. Iba. 2012. Increased leaf photosynthesis caused by elevated stomatal conductance in a rice mutant deficient in SLAC1, a guard cell anion channel protein. *Journal of Experimental Botany*. 63:5635-5644.
- Körner, C. 1998. A re-assessment of high elevation treeline positions and their explanation. *Oecologia*. 115:445-459.
- Lamb, A.F.A. 1968. *Cedrela odorata*. Commonwealth Forestry Institute, University of Oxford.
- Lancashire, J.R. and A.R. Ennos. 2002. Modelling the hydrodynamic resistance of bordered pits. *Journal of Experimental Botany*. 53:1485-1493.
- Lautrup, B. 2005. *In Physics of continuous matter: exotic and everyday phenomena in the macroscopic world* Ed. 1. Institute of Physics, pp 69 - 94.
- Lautrup, B. 2011. *Physics of Continuous Matter: Exotic and Everyday Phenomena in the Macroscopic World*. CRC Press, pp 69-94.
- Lawlor, D.W. and G. Cornic. 2002. Photosynthetic carbon assimilation and associated metabolism in relation to water deficits in higher plants. *Plant Cell and Environment*. 25:275-294.
- Lawson, T. and M.R. Blatt. 2014. Stomatal Size, Speed, and Responsiveness Impact on Photosynthesis and Water Use Efficiency. *Plant Physiology*. 164:1556-1570.
- Lazzarin, M., A. Crivellaro, C.B. Williams, T.E. Dawson, G. Mozzi and T. Anfodillo. 2016a. Tracheid and pit anatomy vary in tandem in a tall *Sequoiadendron giganteum* tree. *Iawa Journal*. 37:172-185.
- Lazzarin, M., A. Crivellaro, C.B. Williams, T.E. Dawson, G. Mozzi and T. Anfodillo. 2016b. Tracheid and pit anatomy vary in tandem in a tall *Sequoiadendron giganteum* tree. *Iawa Journal*. 37:172-185.
- Lechthaler, S., T.L. Turnbull, Y. Gelmini, F. Pirotti, T. Anfodillo, M.A. Adams and G. Petit. 2019. A standardization method to disentangle environmental information from axial trends of xylem anatomical traits. *Tree Physiology*. 39:495-502.
- Lee, M., H. Lim and J. Lee. 2017. Fabrication of Artificial Leaf to Develop Fluid Pump Driven by Surface Tension and Evaporation. *Scientific Reports*. 7
- Lehnebach, R., H. Morel, J. Bossu, G. Le Moguedec, N. Amusant, J. Beauchene and E. Nicolini. 2017. Heartwood/sapwood profile and the tradeoff between trunk and crown increment in a natural forest: the case study of a tropical tree (*Dicorynia guianensis* Amsh., Fabaceae). *Trees-Structure and Function*. 31:199-214.
- Lemoine, D., A. Granier and H. Cochard. 1999. Mechanism of freeze-induced embolism in *Fagus sylvatica* L. *Trees-Structure and Function*. 13:206-210.
- Lens, F., J.L. Luteyn, E. Smets and S. Jansen. 2004. Ecological trends in the wood anatomy of Vaccinioideae (Ericaceae s.l.). *Flora*. 199:309-319.
- Lens, F., R.A. Vos, G. Charrier, T. van der Niet, V. Merckx, P. Baas, J.A. Gutierrez, B. Jacobs, L.C. Doria, E. Smets, S. Delzon and S.B. Janssens. 2016. Scalariform-to-simple transition in vessel perforation plates triggered by differences in climate during the evolution of Adoxaceae. *Annals of Botany*. 118:1043-1056.
- Lenth, R. 2018. emmeans: Estimated Marginal Means, aka Least-Squares Means. R package version 1.3.0. <https://CRAN.R-project.org/package=emmeans>.
- Levionnois, S., S. Jansen, R.T. Wandji, J. Beauchene, C. Ziegler, S. Coste, C. Stahl, S. Delzon, L. Authier and P. Heuret. Linking drought-induced xylem embolism resistance to wood anatomical traits in Neotropical trees. *New Phytologist*
- Levionnois, S., S. Jansen, R.T. Wandji, J. Beauchêne, C. Ziegler, S. Coste, C. Stahl, S. Delzon, L. Authier and P. Heuret. 2021. Linking drought-induced xylem embolism resistance to wood anatomical traits in Neotropical trees. *New Phytologist*. 229:1453-1466.
- Levitt, J. 1956. THE PHYSICAL NATURE OF TRANSPIRATIONAL PULL. *Plant Physiology*. 31:248-251.
- Li, Y., D.S. Tian, H. Yang and S.L. Niu. 2018. Size-dependent nutrient limitation of tree growth from subtropical to cold temperate forests. *Functional Ecology*. 32:95-105.

- Liu, H., S.M. Gleason, G.Y. Hao, L. Hua, P.C. He, G. Goldstein and Q. Ye. 2019. Hydraulic traits are coordinated with maximum plant height at the global scale. *Science Advances*. 5
- Liu, H., Q. Ye, S.M. Gleason, P.C. He and D.Y. Yin. 2020. Weak tradeoff between xylem hydraulic efficiency and safety: climatic seasonality matters. *New Phytologist*
- Liu, Y.Y., J. Song, M. Wang, N. Li, C.Y. Niu and G.Y. Hao. 2015. Coordination of xylem hydraulics and stomatal regulation in keeping the integrity of xylem water transport in shoots of two compound-leaved tree species. *Tree Physiology*. 35:1333-1342.
- Liu, Y.Y., A.Y. Wang, Y.N. An, P.Y. Lian, D.D. Wu, J.J. Zhu, F.C. Meinzer and G.Y. Hao. 2018. Hydraulics play an important role in causing low growth rate and dieback of aging *Pinus sylvestris* var. *mongolica* trees in plantations of Northeast China. *Plant Cell and Environment*. 41:1500-1511.
- Lloyd, J. and G.D. Farquhar. 2008. Effects of rising temperatures and CO₂ on the physiology of tropical forest trees. *Philosophical Transactions of the Royal Society B-Biological Sciences*. 363:1811-1817.
- Lobo, A., J.M. Torres-Ruiz, R. Burlett, C. Lemaire, C. Parise, C. Francioni, L. Truffaut, I. Tomaskova, J.K. Hansen, E.D. Kjaer, A. Kremer and S. Delzon. 2018. Assessing inter- and intraspecific variability of xylem vulnerability to embolism in oaks. *Forest Ecology and Management*. 424:53-61.
- Locosselli, G.M., R.J.W. Brienen, M.d.S. Leite, M. Gloor, S. Krotenthaler, A.A.d. Oliveira, J. Barichivich, D. Anhof, G. Ceccantini, J. Schöngart and M. Buckeridge. 2020. Global tree-ring analysis reveals rapid decrease in tropical tree longevity with temperature. *Proceedings of the National Academy of Sciences*. 117:33358.
- Locosselli, G.M., M.S. Buckeridge, M.Z. Moreira and G. Ceccantini. 2013. A multi-proxy dendroecological analysis of two tropical species (*Hymenaea* spp., Leguminosae) growing in a vegetation mosaic. *Trees-Structure and Function*. 27:25-36.
- Lopez-Gonzalez, G., S. Lewis, M. Burkitt and O. Phillips. 2011. ForestPlots.net: a web application and research tool to manage and analyse tropical forest plot data. *Journal of Vegetation Science* 22:610–613.
- Lopez-Gonzalez, G.L., S., M. Burkitt and O. Phillips. 2009. ForestPlots.net Database Ed. www.forestplots.net.
- Losso, A., T. Anfodillo, A. Ganthaler, W. Kofler, Y. Markl, A. Nardini, W. Oberhuber, G. Purin and S. Mayr. 2018. Robustness of xylem properties in conifers: analyses of tracheid and pit dimensions along elevational transects. *Tree Physiology*. 38:212-222.
- Lovelock, C.E., M. Jebb and C.B. Osmond. 1994. Photoinhibition and recovery in tropical plant-species - response to disturbance. *Oecologia*. 97:297-307.
- Malizia, A., C. Blundo, J. Carilla, O.O. Acosta, F. Cuesta, A. Duque, N. Aguirre, Z. Aguirre, M. Ataroff, S. Baez, M. Calderon-Loor, L. Cayola, L. Cayuela, S. Ceballos, H. Cedillo, W.F. Rios, K.J. Feeley, A.F. Fuentes, L.E.G. Alvarez, R. Grau, J. Homeier, O. Jadan, L.D. Llambi, M.I.L. Rivera, M.J. Macia, Y. Malhi, L. Malizia, M. Peralvo, E. Pinto, S. Tello, M. Silman and K.R. Young. 2020. Elevation and latitude drives structure and tree species composition in Andean forests: Results from a large-scale plot network. *Plos One*. 15
- Manzoni, S., G. Vico, S. Thompson, F. Beyer and M. Weih. 2015. Contrasting leaf phenological strategies optimize carbon gain under droughts of different duration. *Advances in Water Resources*. 84:37-51.
- Mao, L.F., C.W. Bator, J.J. Stadt, B. White, P. Tompalski, N.C. Coops and S.E. Nielsen. 2019. Environmental landscape determinants of maximum forest canopy height of boreal forests. *Journal of Plant Ecology*. 12:96-102.
- Marengo, J.A. and J.C. Espinoza. 2016. Extreme seasonal droughts and floods in Amazonia: causes, trends and impacts. *International Journal of Climatology*. 36:1033-1050.
- Marengo, J.A., C.A. Souza, K. Thonicke, C. Burton, K. Halladay, R.A. Betts, L.M. Alves and W.R. Soares. 2018. Changes in Climate and Land Use Over the Amazon Region: Current and Future Variability and Trends. *Frontiers in Earth Science*. 6

- Markesteijn, L. and L. Poorter. 2009. Seedling root morphology and biomass allocation of 62 tropical tree species in relation to drought- and shade-tolerance. *Journal of Ecology*. 97:311-325.
- Markesteijn, L., L. Poorter, F. Bongers, H. Paz and L. Sack. 2011. Hydraulics and life history of tropical dry forest tree species: coordination of species' drought and shade tolerance. *New Phytologist*. 191:480-495.
- Marks, C.O. and M.J. Lechowicz. 2006. Alternative designs and the evolution of functional diversity. *American Naturalist*. 167:55-66.
- Martin-StPaul, N., S. Delzon and H. Cochard. 2017. Plant resistance to drought depends on timely stomatal closure. *Ecology Letters*. 20:1437-1447.
- Martinez-Cabrera, H.I., H.J. Schenk, S.R.S. Cevallos-Ferriz and C.S. Jones. 2011. Integration of vessel traits, wood density, and height in angiosperm shrubs and trees. *American Journal of Botany*. 98:915-922.
- Martinez-Vilalta, J., R. Poyatos, D. Aguade, J. Retana and M. Mencuccini. 2014. A new look at water transport regulation in plants. *New Phytologist*. 204:105-115.
- Mayer, H. 1987. Wind-induced tree sways. *Trees-Structure and Function*. 1:195-206.
- McDowell, N., C.D. Allen, K. Anderson-Teixeira, P. Brando, R. Brienen, J. Chambers, B. Christoffersen, S. Davies, C. Doughty, A. Duque, F. Espirito-Santo, R. Fisher, C.G. Fontes, D. Galbraith, D. Goodsman, C. Grossiord, H. Hartmann, J. Holm, D.J. Johnson, A. Kassim, M. Keller, C. Koven, L. Kueppers, T. Kumagai, Y. Malhi, S.M. McMahon, M. Mencuccini, P. Meir, P. Moorcroft, H.C. Muller-Landau, O.L. Phillips, T. Powell, C.A. Sierra, J. Sperry, J. Warren, C.G. Xu and X.T. Xu. 2018. Drivers and mechanisms of tree mortality in moist tropical forests. *New Phytologist*. 219:851-869.
- McDowell, N., H. Barnard, B.J. Bond, T. Hinckley, R.M. Hubbard, H. Ishii, B. Kostner, F. Magnani, J.D. Marshall, F.C. Meinzer, N. Phillips, M.G. Ryan and D. Whitehead. 2002. The relationship between tree height and leaf area: sapwood area ratio. *Oecologia*. 132:12-20.
- McDowell, N., W.T. Pockman, C.D. Allen, D.D. Breshears, N. Cobb, T. Kolb, J. Plaut, J. Sperry, A. West, D.G. Williams and E.A. Yezzer. 2008. Mechanisms of plant survival and mortality during drought: why do some plants survive while others succumb to drought? *New Phytologist*. 178:719-739.
- McDowell, N.G. and C.D. Allen. 2015. Darcy's law predicts widespread forest mortality under climate warming. *Nature Climate Change*. 5:669-672.
- McDowell, N.G., B.J. Bond, L.T. Dickman, M.G. Ryan and D. Whitehead. 2011. Relationships Between Tree Height and Carbon Isotope Discrimination. *In Size- and Age-Related Changes in Tree Structure and Function* Eds. F. Meinzer, B. Lachenbruch and T. Dawson. Springer, Dordrecht.
- McElwain, J.C., C. Yiotis and T. Lawson. 2016. Using modern plant trait relationships between observed and theoretical maximum stomatal conductance and vein density to examine patterns of plant macroevolution. *New Phytologist*. 209:94-103.
- McNevin, D.B., M.R. Badger, S.M. Whitney, S. von Caemmerer, G.G.B. Tcherkez and G.D. Farquhar. 2007. Differences in carbon isotope discrimination of three variants of d-ribulose-1,5-bisphosphate carboxylase/oxygenase reflect differences in their catalytic mechanisms. *Journal of Biological Chemistry*. 282:36068-36076.
- Medeiros, J.S., F. Lens, H. Maherali and S. Jansen. 2019. Vestured pits and scalariform perforation plate morphology modify the relationships between angiosperm vessel diameter, climate and maximum plant height. *New Phytologist*. 221:1802-1813.
- Meinzer, F.C., D.M. Johnson, B. Lachenbruch, K.A. McCulloh and D.R. Woodruff. 2009. Xylem hydraulic safety margins in woody plants: coordination of stomatal control of xylem tension with hydraulic capacitance. *Functional Ecology*. 23:922-930.
- Mencuccini, M. 2003. The ecological significance of long-distance water transport: short-term regulation, long-term acclimation and the hydraulic costs of stature across plant life forms. *Plant Cell and Environment*. 26:163-182.

- Mencuccini, M., J. Martinez-Vilalta, D. Vanderklein, H.A. Hamid, E. Korakaki, S. Lee and B. Michiels. 2005. Size-mediated ageing reduces vigour in trees. *Ecology Letters*. 8:1183-1190.
- Mencuccini, M., F. Minunno, Y. Salmon, J. Martinez-Vilalta and T. Holtta. 2015. Coordination of physiological traits involved in drought-induced mortality of woody plants. *New Phytologist*. 208:396-409.
- Meyer-Berthaud, B., S.E. Scheckler and J. Wendt. 1999. Archaeopteris is the earliest known modern tree. *Nature*. 398:700-701.
- Moles, A.T., D.I. Warton, L. Warman, N.G. Swenson, S.W. Laffan, A.E. Zanne, A. Pitman, F.A. Hemmings and M.R. Leishman. 2009. Global patterns in plant height. *Journal of Ecology*. 97:923-932.
- Moon, K., T.J. Duff and K.G. Tolhurst. 2019. Sub-canopy forest winds: understanding wind profiles for fire behaviour simulation. *Fire Safety Journal*. 105:320-329.
- Moore, N., E. Arima, R. Walker and R.R. da Silva. 2007. Uncertainty and the changing hydroclimatology of the Amazon. *Geophysical Research Letters*. 34
- Mori, S., K. Yamaji, A. Ishida, S.G. Prokushkin, O.V. Masyagina, A. Hagihara, A. Hoque, R. Suwa, A. Osawa, T. Nishizono, T. Ueda, M. Kinjo, T. Miyagi, T. Kajimoto, T. Koike, Y. Matsuura, T. Toma, O.A. Zyryanova, A.P. Abaimov, Y. Awaya, M.G. Araki, T. Kawasaki, Y. Chiba and M. Umari. 2010. Mixed-power scaling of whole-plant respiration from seedlings to giant trees. *Proceedings of the National Academy of Sciences of the United States of America*. 107:1447-1451.
- Muellner, A.N., T.D. Pennington and M.W. Chase. 2009. Molecular phylogenetics of Neotropical Cedreleae (mahogany family, Meliaceae) based on nuclear and plastid DNA sequences reveal multiple origins of "Cedrela odorata". *Molecular Phylogenetics and Evolution*. 52:461-469.
- Muellner, A.N., T.D. Pennington, A.V. Koecke and S.S. Renner. 2010. Biogeography of Cedrela (Meliaceae, Sapindales) in Central and South America. *American Journal of Botany*. 97:511-518.
- Mullin, L.P., S.C. Sillett, G.W. Koch, K.P. Tu and M.E. Antoine. 2009. Physiological consequences of height-related morphological variation in *Sequoia sempervirens* foliage. *Tree Physiology*. 29:999-1010.
- Myers, B.J., R.H. Robichaux, G.L. Unwin and I.E. Craig. 1987. Leaf water relations and anatomy of a tropical rainforest tree species vary with crown position. *Oecologia*. 74:81-85.
- Nagashima, H. and K. Hikosaka. 2011. Plants in a crowded stand regulate their height growth so as to maintain similar heights to neighbours even when they have potential advantages in height growth. *Annals of Botany*. 108:207-214.
- Nakagawa, S. and H. Schielzeth. 2013. A general and simple method for obtaining R² from generalized linear mixed-effects models. *Methods in Ecology and Evolution*. 4:133-142.
- Nepstad, D.C., I.M. Tohver, D. Ray, P. Moutinho and G. Cardinot. 2007. Mortality of large trees and lianas following experimental drought in an amazon forest. *Ecology*. 88:2259-2269.
- Niinemets, U. 1999. Components of leaf dry mass per area - thickness and density - alter leaf photosynthetic capacity in reverse directions in woody plants. *New Phytologist*. 144:35-47.
- Niinemets, U. 2007. Photosynthesis and resource distribution through plant canopies. *Plant Cell and Environment*. 30:1052-1071.
- Niklas, K.J. 1999. A mechanical perspective on foliage leaf form and function. *New Phytologist*. 143:19-31.
- Niklas, K.J. 2007. Maximum plant height and the biophysical factors that limit it. *Tree Physiology*. 27:433-440.
- Nonami, H. and J.S. Boyer. 1990. Wall extensibility and cell hydraulic conductivity decrease in enlarging stem tissues at low water potentials. *Plant Physiology*. 93:1610-1619.
- O'Brien, J.J., S.F. Oberbauer and D.B. Clark. 2004. Whole tree xylem sap flow responses to multiple environmental variables in a wet tropical forest. *Plant Cell and Environment*. 27:551-567.
- Oldham, A.R., S.C. Sillett, A.M.F. Tomescu and G.W. Koch. 2010. The hydrostatic gradient, not light availability, drives height-related variation in *Sequoia sempervirens* (Cupressaceae) leaf anatomy. *American Journal of Botany*. 97:1087-1097.

- Oleary, M.H. 1988. Carbon isotopes in photosynthesis. *Bioscience*. 38:328-336.
- Oliveira, R.S., F.R.C. Costa, E. van Baalen, A. de Jonge, P.R. Bittencourt, Y. Almanza, F.D. Barros, E.C. Cordoba, M.V. Fagundes, S. Garcia, Z.T. Guimaraes, M. Hertel, J. Schietti, J. Rodrigues-Souza and L. Poorter. 2019. Embolism resistance drives the distribution of Amazonian rainforest tree species along hydro-topographic gradients. *New Phytologist*. 221:1457-1465.
- Olson, M.E., T. Anfodillo, J.A. Rosell, G. Petit, A. Crivellaro, S. Isnard, C. León-Gómez, L.O. Alvarado-Cárdenas and M. Castorena. 2014. Universal hydraulics of the flowering plants: vessel diameter scales with stem length across angiosperm lineages, habits and climates. *Ecology Letters*. 17:988-997.
- Olson, M.E., D. Soriano, J.A. Rosell, T. Anfodillo, M.J. Donoghue, E.J. Edwards, C. Leon-Gomez, T. Dawson, J.J.C. Martinez, M. Castorena, A. Echeverria, C.I. Espinosa, A. Fajardo, A. Gazol, S. Isnard, R.S. Lima, C.R. Marcati and R. Mendez-Alonzo. 2018. Plant height and hydraulic vulnerability to drought and cold. *Proceedings of the National Academy of Sciences of the United States of America*. 115:7551-7556.
- Ouedraogo, D.Y., J.L. Doucet, K. Dainou, F. Baya, A.B. Biwole, N. Bourland, F. Feteke, J.F. Gillet, Y.L. Kouadio and A. Fayolle. 2018. The size at reproduction of canopy tree species in central Africa. *Biotropica*. 50:465-476.
- Penuelas, J., J.G. Canadell and R. Ogaya. 2011. Increased water-use efficiency during the 20th century did not translate into enhanced tree growth. *Global Ecology and Biogeography*. 20:597-608.
- Pereira, L., P.R.L. Bittencourt, R.S. Oliveira, M.B.M. Junior, F.V. Barros, R.V. Ribeiro and P. Mazzafera. 2016. Plant pneumatics: stem air flow is related to embolism - new perspectives on methods in plant hydraulics. *New Phytologist*. 211:357-370.
- Perez-Garcia, E.A., J.A. Meave, J.L. Villasenor, J.A. Gallardo-Cruz and E.E. Lebrija-Trejos. 2010. Vegetation Heterogeneity and Life-Strategy Diversity in the Flora of the Heterogeneous Landscape of Nizanda, Oaxaca, Mexico. *Folia Geobotanica*. 45:143-161.
- Perperoglou, A., W. Sauerbrei, M. Abrahamowicz, M. Schmid and T.S. Initiative. 2019. A review of spline function procedures in R. *Bmc Medical Research Methodology*. 19:16.
- Peterson, T.C. and R.S. Vose. 1997. Global Historical Climatology Network - Monthly (GHCN-M), Version 3. GHCN-M (all) precipitation. . NOAA National Centers for Environmental Information.
- Petit, G., S. Pfautsch, T. Anfodillo and M.A. Adams. 2010. The challenge of tree height in *Eucalyptus regnans*: when xylem tapering overcomes hydraulic resistance. *New Phytologist*. 187:1146-1153.
- Pfautsch, S., M. Harbusch, A. Wesolowski, R. Smith, C. Macfarlane, M.G. Tjoelker, P.B. Reich and M.A. Adams. 2016. Climate determines vascular traits in the ecologically diverse genus *Eucalyptus*. *Ecology Letters*. 19:240-248.
- Pinto, O. and Ieee. 2013. Lightning and climate: a review. 2013 International Symposium on Lightning Protection (Xii Sipda):402-404.
- Pires, H.R.A., A.C. Franco, M.T.F. Piedade, V.V. Scudeller, B. Kruijt and C.S. Ferreira. 2018. Flood tolerance in two tree species that inhabit both the Amazonian floodplain and the dry Cerrado savanna of Brazil. *Aob Plants*. 10
- Pittermann, J. 2010. The evolution of water transport in plants: an integrated approach. *Geobiology*. 8:112-139.
- Pittermann, J., B. Choat, S. Jansen, S.A. Stuart, L. Lynn and T.E. Dawson. 2010. The Relationships between Xylem Safety and Hydraulic Efficiency in the Cupressaceae: The Evolution of Pit Membrane Form and Function. *Plant Physiology*. 153:1919-1931.
- Ponomarenko, A., O. Vincent, A. Pietriga, H. Cochard, E. Badel and P. Marmottant. 2014. Ultrasonic emissions reveal individual cavitation bubbles in water-stressed wood. *Journal of the Royal Society Interface*. 11

- Poorter, H., U. Niinemets, N. Ntagkas, A. Siebenkas, M. Maenpaa, S. Matsubara and T. Pons. 2019. A meta-analysis of plant responses to light intensity for 70 traits ranging from molecules to whole plant performance. *New Phytologist*. 223:1073-1105.
- Poorter, H., U. Niinemets, L. Poorter, I.J. Wright and R. Villar. 2009. Causes and consequences of variation in leaf mass per area (LMA): a meta-analysis. *New Phytologist*. 182:565-588.
- Poorter, L. 2008. The relationships of wood-, gas- and water fractions of tree stems to performance and life history variation in tropical trees. *Annals of botany*. 102:367-375.
- Poorter, L. 2009. Leaf traits show different relationships with shade tolerance in moist versus dry tropical forests. *New Phytologist*. 181:890-900.
- Poorter, L. and F. Bongers. 2006. Leaf traits are good predictors of plant performance across 53 rain forest species. *Ecology*. 87:1733-1743.
- Poorter, L., L. Bongers and F. Bongers. 2006. Architecture of 54 moist-forest tree species: Traits, trade-offs, and functional groups. *Ecology*. 87:1289-1301.
- Poorter, L., I. McDonald, A. Alarcon, E. Fichtler, J.C. Licona, M. Pena-Claros, F. Sterck, Z. Villegas and U. Sass-Klaassen. 2010. The importance of wood traits and hydraulic conductance for the performance and life history strategies of 42 rainforest tree species. *New Phytologist*. 185:481-492.
- Posada, J.M. and E.A.G. Schuur. 2011. Relationships among precipitation regime, nutrient availability, and carbon turnover in tropical rain forests. *Oecologia*. 165:783-795.
- Powell, T.L., C.D. Koven, D.J. Johnson, B. Faybishenko, R.A. Fisher, R.G. Knox, N.G. McDowell, R. Condit, S.P. Hubbell, S.J. Wright, J.Q. Chambers and L.M. Kueppers. 2018. Variation in hydroclimate sustains tropical forest biomass and promotes functional diversity. *New Phytologist*. 219:932-946.
- Prendin, A.L., S. Mayr, B. Beikircher, G. von Arx and G. Petit. 2018. Xylem anatomical adjustments prioritize hydraulic efficiency over safety as Norway spruce trees grow taller. *Tree Physiology*. 38:1088-1097.
- Pumijumng, N. and W.K. Park. 1999. Vessel chronologies from teak in northern Thailand and their climatic signal. *Iawa Journal*. 20:285-294.
- Putz, F.E., G.G. Parker and R.M. Archibald. 1984. Mechanical abrasion and intercrown spacing. *American Midland Naturalist*. 112:24-28.
- Qi, Y.L., W. Wei, C.G. Chen and L.D. Chen. 2019. Plant root-shoot biomass allocation over diverse biomes: A global synthesis. *Global Ecology and Conservation*. 18
- Quesada, C.A., J. Lloyd, M. Schwarz, S. Patino, T.R. Baker, C. Czimczik, N.M. Fyllas, L. Martinelli, G.B. Nardoto, J. Schmerler, A.J.B. Santos, M.G. Hodnett, R. Herrera, F.J. Luizao, A. Arneith, G. Lloyd, N. Dezzio, I. Hilke, I. Kuhlmann, M. Raessler, W.A. Brand, H. Geilmann, J.O. Moraes, F.P. Carvalho, R.N. Araujo, J.E. Chaves, O.F. Cruz, T.P. Pimentel and R. Paiva. 2010. Variations in chemical and physical properties of Amazon forest soils in relation to their genesis. *Biogeosciences*. 7:1515-1541.
- Quesada, C.A., O.L. Phillips, M. Schwarz, C.I. Czimczik, T.R. Baker, S. Patino, N.M. Fyllas, M.G. Hodnett, R. Herrera, S. Almeida, E.A. Davila, A. Arneith, L. Arroyo, K.J. Chao, N. Dezzio, T. Erwin, A. di Fiore, N. Higuchi, E.H. Coronado, E.M. Jimenez, T. Killeen, A.T. Lezama, G. Lloyd, G. Lopez-Gonzalez, F.J. Luizao, Y. Malhi, A. Monteagudo, D.A. Neill, P.N. Vargas, R. Paiva, J. Peacock, M.C. Penuela, A.P. Cruz, N. Pitman, N. Priante, A. Prieto, H. Ramirez, A. Rudas, R. Salomao, A.J.B. Santos, J. Schmerler, N. Silva, M. Silveira, R. Vasquez, I. Vieira, J. Terborgh and J. Lloyd. 2012. Basin-wide variations in Amazon forest structure and function are mediated by both soils and climate. *Biogeosciences*. 9:2203-2246.
- R Core Team. 2018. R: A language and environment for statistical computing. R Foundation for Statistical Computing, Vienna, Austria.
- Reich, P.B., M.B. Walters and D.S. Ellsworth. 1997. From tropics to tundra: Global convergence in plant functioning. *Proceedings of the National Academy of Sciences of the United States of America*. 94:13730-13734.

- Resende, A.F., M.T.F. Piedade, Y.O. Feitosa, V.H.F. Andrade, S.E. Trumbore, F.M. Durgante, M.O. Macedo and J. Schongart. 2020. Flood-pulse disturbances as a threat for long-living Amazonian trees. *New Phytologist*. 227:1790-1803.
- Rijkers, T., T.L. Pons and F. Bongers. 2000. The effect of tree height and light availability on photosynthetic leaf traits of four neotropical species differing in shade tolerance. *Functional Ecology*. 14:77-86.
- Roberts, J., O.M.R. Cabral and L.F. Deaguiar. 1990. Stomatal and boundary-layer conductances in an Amazonian terra-firme rain-forest. *Journal of Applied Ecology*. 27:336-353.
- Rodriguez-Calcerrada, J., R.L. Salomon, G.G. Gordaliza, J.C. Miranda, E. Miranda, E.G. de la Riva and L. Gil. 2019. Respiratory costs of producing and maintaining stem biomass in eight co-occurring tree species. *Tree Physiology*. 39:1838-1854.
- Rosell, J.A., M.E. Olson and T. Anfodillo. 2017. Scaling of Xylem Vessel Diameter with Plant Size: Causes, Predictions, and Outstanding Questions. *Current Forestry Reports*. 3:46-59.
- Rowland, L., A.C.L. da Costa, D.R. Galbraith, R.S. Oliveira, O.J. Binks, A.A.R. Oliveira, A.M. Pullen, C.E. Doughty, D.B. Metcalfe, S.S. Vasconcelos, L.V. Ferreira, Y. Malhi, J. Grace, M. Mencuccini and P. Meir. 2015. Death from drought in tropical forests is triggered by hydraulics not carbon starvation. *Nature*. 528:119-+.
- Rozendaal, D.M.A., R.J.W. Brienen, C.C. Soliz-Gamboa and P.A. Zuidema. 2010. Tropical tree rings reveal preferential survival of fast-growing juveniles and increased juvenile growth rates over time. *New Phytologist*. 185:759-769.
- Ruger, N., R. Condit, D.H. Dent, S.J. DeWalt, S.P. Hubbell, J.W. Lichstein, O.R. Lopez, C. Wirth and C.E. Farrior. 2020. Demographic trade-offs predict tropical forest dynamics. *Science*. 368:165-+.
- Ryan, M.G., N. Phillips and B.J. Bond. 2006. The hydraulic limitation hypothesis revisited. *Plant Cell and Environment*. 29:367-381.
- Ryan, M.G. and B.J. Yoder. 1997. Hydraulic limits to tree height and tree growth. *Bioscience*. 47:235-242.
- Sack, L. and N.M. Holbrook. 2006. LEAF HYDRAULICS. *Annual Review of Plant Biology*. 57:361-381.
- Santiago, L.S. 2015. Nutrient limitation of eco-physiological processes in tropical trees. *Trees-Structure and Function*. 29:1291-1300.
- Sastry, A., A. Guha and D. Barua. 2018. Leaf thermotolerance in dry tropical forest tree species: relationships with leaf traits and effects of drought. *Aob Plants*. 10
- Satyamurty, P., A.A. de Castro, J. Tota, L.E.D. Gulate and A.O. Manzi. 2010. Rainfall trends in the Brazilian Amazon Basin in the past eight decades. *Theoretical and Applied Climatology*. 99:139-148.
- Savage, V.M., L.P. Bentley, B.J. Enquist, J.S. Sperry, D.D. Smith, P.B. Reich and E.I. von Allmen. 2010. Hydraulic trade-offs and space filling enable better predictions of vascular structure and function in plants. *Proceedings of the National Academy of Sciences of the United States of America*. 107:22722-22727.
- Savage, V.M., E.J. Deeds and W. Fontana. 2008. Sizing Up Allometric Scaling Theory. *Plos Computational Biology*. 4
- Sawada, Y., R. Suwa, K. Jindo, T. Endo, K. Oki, H. Sawada, E. Arai, Y.E. Shimabukuro, C.H.S. Celes, M.A.A. Campos, F.G. Higuchi, A.J.N. Lima, N. Higuchi, T. Kajimoto and M. Ishizuka. 2015. A new 500-m resolution map of canopy height for Amazon forest using spaceborne LiDAR and cloud-free MODIS imagery. *International Journal of Applied Earth Observation and Geoinformation*. 43:92-101.
- Scheffer, M., C. Xu, S. Hantson, M. Holmgren, S.O. Los and E.H. van Nes. 2018. A global climate niche for giant trees. *Global Change Biology*. 24:2875-2883.
- Schenk, H.J., S. Espino, C.M. Goedhart, M. Nordenstahl, H.I.M. Cabrera and C.S. Jones. 2008. Hydraulic integration and shrub growth form linked across continental aridity gradients. *Proceedings of the National Academy of Sciences of the United States of America*. 105:11248-11253.

- Schenk, H.J., S. Espino, A. Visser and B.K. Esser. 2016. Dissolved atmospheric gas in xylem sap measured with membrane inlet mass spectrometry. *Plant Cell and Environment*. 39:944-950.
- Scholander, P.F., H.T. Hammel, E.D. Bradstreet and E.A. Hemmingsen. 1965. SAP PRESSURE IN VASCULAR PLANTS - NEGATIVE HYDROSTATIC PRESSURE CAN BE MEASURED IN PLANTS. *Science*. 148:339-+.
- Scholz, A., M. Klepsch, Z. Karimi and S. Jansen. 2013. How to quantify conduits in wood? *Frontiers in Plant Science*. 4
- Schuster, S., J.U. Kreft, A. Schroeter and T. Pfeiffer. 2008. Use of Game-Theoretical Methods in Biochemistry and Biophysics. *Journal of Biological Physics*. 34:1-17.
- Schwendenmann, L., E. Pendall, R. Sanchez-Bragado, N. Kunert and D. Holscher. 2015. Tree water uptake in a tropical plantation varying in tree diversity: interspecific differences, seasonal shifts and complementarity. *Ecohydrology*. 8:1-12.
- Scoffoni, C., C. Albuquerque, C.R. Brodersen, S.V. Townes, G.P. John, H. Cochard, T.N. Buckley, A.J. McElrone and L. Sack. 2017. Leaf vein xylem conduit diameter influences susceptibility to embolism and hydraulic decline. *New Phytologist*. 213:1076-1092.
- Scoffoni, C., C. Vuong, S. Diep, H. Cochard and L. Sack. 2014. Leaf Shrinkage with Dehydration: Coordination with Hydraulic Vulnerability and Drought Tolerance. *Plant Physiology*. 164:1772-1788.
- Seiler, C., R.W.A. Hutjes, B. Kruijt, J. Quispe, S. Anez, V.K. Arora, J.R. Melton, T. Hickler and P. Kabat. 2014. Modeling forest dynamics along climate gradients in Bolivia. *Journal of Geophysical Research-Biogeosciences*. 119:758-775.
- Sheil, D., C.S. Eastaugh, M. Vlam, P.A. Zuidema, P. Groenendijk, P. van der Sleen, A. Jay and J. Vanclay. 2017. Does biomass growth increase in the largest trees? Flaws, fallacies and alternative analyses. *Functional Ecology*. 31:568-581.
- Shenkin, A., B. Bolker, M. Pena-Claros, J.C. Licona, N. Ascarrunz and F.E. Putz. 2018. Interactive effects of tree size, crown exposure and logging on drought-induced mortality. *Philosophical Transactions of the Royal Society B-Biological Sciences*. 373
- Shenkin, A., C.J. Chandler, D.S. Boyd, T. Jackson, M. Disney, N. Majalap, R. Nilus, G. Foody, J. bin Jami, G. Reynolds, P. Wilkes, M.E.J. Cutler, G.M.F. van der Heijden, D. Burslem, D.A. Coomes, L.P. Bentley and Y. Malhi. 2019. The World's Tallest Tropical Tree in Three Dimensions. *Frontiers in Forests and Global Change*. 2
- Shi, W.W., R.M. Dalrymple, C.J. McKenny, D.S. Morrow, Z.T. Rashed, D.A. Surinach and J.B. Boreyko. 2020. Passive water ascent in a tall, scalable synthetic tree. *Scientific Reports*. 10
- Shinozaki, K., K. Yoda, K. Hozumi and T. Kira. 1964. a quantitative analysis of plant form-the pipe model theory : ii. further evidence of the theory and its application in forest ecology. *Japanese Journal of Ecology*. 14:133-139.
- Shiogama, H., S. Emori, N. Hanasaki, M. Abe, Y. Masutomi, K. Takahashi and T. Nozawa. 2011. Observational constraints indicate risk of drying in the Amazon basin. *Nature Communications*. 2
- Sillett, S.C., R. Van Pelt, G.W. Koch, A.R. Ambrose, A.L. Carroll, M.E. Antoine and B.M. Mifsud. 2010. Increasing wood production through old age in tall trees. *Forest Ecology and Management*. 259:976-994.
- Simard, M., N. Pinto, J.B. Fisher and A. Baccini. 2011. Mapping forest canopy height globally with spaceborne lidar. *Journal of Geophysical Research-Biogeosciences*. 116
- Solargis. Direct Normal Irradiance *obtained from* the Global Solar Atlas 2.0, a free, web-based application is developed and operated by the company Solargis s.r.o. on behalf of the World Bank Group, utilizing Solargis data, with funding provided by the Energy Sector Management Assistance Program (ESMAP). For additional information: <https://globalsolaratlas.info>.
- Soong, J.L., I.A. Janssens, O. Grau, O. Margalef, C. Stahl, L. Van Langenhove, I. Urbina, J. Chave, A. Dourdain, B. Ferry, V. Freycon, B. Herault, J. Sardans, J. Penuelas and E. Verbruggen. 2020a.

- Soil properties explain tree growth and mortality, but not biomass, across phosphorus-depleted tropical forests. *Scientific Reports*. 10:13.
- Soong, J.L., I.A. Janssens, O. Grau, O. Margalef, C. Stahl, L. Van Langenhove, I. Urbina, J. Chave, A. Dourdain, B. Ferry, V. Freycon, B. Herault, J. Sardans, J. Peñuelas and E. Verbruggen. 2020b. Soil properties explain tree growth and mortality, but not biomass, across phosphorus-depleted tropical forests. *Scientific Reports*. 10:2302.
- Sousa, T.R., J. Schiatti, F.C. de Souza, A. Esquivel-Muelbert, I.O. Ribeiro, T. Emilio, P. Pequeno, O. Phillips and F.R.C. Costa. 2020. Palms and trees resist extreme drought in Amazon forests with shallow water tables. *Journal of Ecology*
- Spawn, S.A., C.C. Sullivan, T.J. Lark and H.K. Gibbs. 2020. Harmonized global maps of above and belowground biomass carbon density in the year 2010. *Scientific Data*. 7
- Sperry, J.S. 1986. Relationship of xylem embolism to xylem pressure potential, stomatal closure, and shoot morphology in the palm *Rhapis excelsa*. *Plant Physiology*. 80:110-116.
- Sperry, J.S., U.G. Hacke and J. Pittermann. 2006. Size and function in conifer tracheids and angiosperm vessels. *American Journal of Botany*. 93:1490-1500.
- Sperry, J.S. and D.M. Love. 2015. What plant hydraulics can tell us about responses to climate-change droughts. *New Phytologist*. 207:14-27.
- Sperry, J.S. and M.T. Tyree. 1988. Mechanism of water stress-induced xylem embolism. *Plant Physiology*. 88:581-587.
- Stahl, C., B. Herault, V. Rossi, B. Burban, C. Brechet and D. Bonal. 2013. Depth of soil water uptake by tropical rainforest trees during dry periods: does tree dimension matter? *Oecologia*. 173:1191-1201.
- Stein, W.E., F. Mannolini, L.V. Hernick, E. Landing and C.M. Berry. 2007. Giant cladoxlopid trees resolve the enigma of the Earth's earliest forest stumps at Gilboa. *Nature*. 446:904-907.
- Stephenson, N.L., A.J. Das, N.J. Ampersee, B.M. Bulaon and J.L. Yee. 2019. Which trees die during drought? The key role of insect host-tree selection. *Journal of Ecology*. 107:2383-2401.
- Stephenson, N.L., A.J. Das, R. Condit, S.E. Russo, P.J. Baker, N.G. Beckman, D.A. Coomes, E.R. Lines, W.K. Morris, N. Ruger, E. Alvarez, C. Blundo, S. Bunyavejchewin, G. Chuyong, S.J. Davies, A. Duque, C.N. Ewango, O. Flores, J.F. Franklin, H.R. Grau, Z. Hao, M.E. Harmon, S.P. Hubbell, D. Kenfack, Y. Lin, J.R. Makana, A. Malizia, L.R. Malizia, R.J. Pabst, N. Pongpattananurak, S.H. Su, I.F. Sun, S. Tan, D. Thomas, P.J. van Mantgem, X. Wang, S.K. Wisser and M.A. Zavala. 2014. Rate of tree carbon accumulation increases continuously with tree size. *Nature*. 507:90-+.
- Sterck, F., L. Markesteijn, F. Schieving and L. Poorter. 2011. Functional traits determine trade-offs and niches in a tropical forest community. *Proceedings of the National Academy of Sciences of the United States of America*. 108:20627-20632.
- Sterck, F. and F. Schieving. 2011. Modelling functional trait acclimation for trees of different height in a forest light gradient: emergent patterns driven by carbon gain maximization. *Tree Physiology*. 31:1024-1037.
- Stovall, A.E.L., H. Shugart and X. Yang. 2019. Tree height explains mortality risk during an intense drought. *Nature Communications*. 10
- Stroock, A.D., V.V. Pagay, M.A. Zwieniecki and N.M. Holbrook. 2014. The Physicochemical Hydrodynamics of Vascular Plants. *Annual Review of Fluid Mechanics*, Vol 46. 46:615-642.
- Sullivan, M.J.P., S.L. Lewis, K. Affum-Baffoe, C. Castilho, F. Costa, A.C. Sanchez, C.E.N. Ewango, W. Hubau, B. Marimon, A. Monteagudo-Mendoza, L. Qie, B. Sonke, R.V. Martinez, T.R. Baker, R.J.W. Brienen, T.R. Feldpausch, D. Galbraith, M. Gloor, Y. Malhi, S.I. Aiba, M.N. Alexiades, E.C. Almeida, E.A. de Oliveira, E.A. Davila, P.A. Loayza, A. Andrade, S.A. Vieira, L. Aragao, A. Araujo-Murakami, E. Arets, L. Arroyo, P. Ashton, C.G. Aymard, F.B. Baccaro, L.F. Banin, C. Baraloto, P.B. Camargo, J. Barlow, J. Barroso, J.F. Bastin, S.A. Batterman, H. Beeckman, S.K. Begne, A.C. Bennett, E. Berenguer, N. Berry, L. Blanc, P. Boeckx, J. Bogaert, D. Bonal, F. Bongers, M. Bradford, F.Q. Brearley, T. Brncic, F. Brown, B. Burban, J.L. Camargo, W. Castro, C. Ceron, S.C. Ribeiro, V.C. Moscoso, J. Chave, E. Chezeaux, C.J. Clark, F.C. de Souza, M. Collins, J.A. Comiskey,

- F.C. Valverde, M.C. Medina, L. da Costa, M. Dancak, G.C. Dargie, S. Davies, N.D. Cardozo, T. de Haulleville, M.B. de Medeiros, J.D. Pasquel, G. Derroire, A. Di Fiore, J.L. Doucet, A. Dourdain, V. Droissart, L.F. Duque, R. Ekoungoulou, F. Elias, T. Erwin, A. Esquivel-Muelbert, S. Fauset, J. Ferreira, G.F. Llampazo, E. Foli, A. Ford, M. Gilpin, J.S. Hall, K.C. Hamer, A.C. Hamilton, D.J. Harris, T.B. Hart, R. Hedl, B. Herault, et al. 2020. Long-term thermal sensitivity of Earth's tropical forests. *Science*. 368:869-+.
- Suzuki, M., K. Umeki, O. Orman, M. Shibata, H. Tanaka, S. Iida, T. Nakashizuka and T. Masaki. 2019. When and why do trees begin to decrease their resource allocation to apical growth? The importance of the reproductive onset. *Oecologia*. 191:39-49.
- Swann, A.L.S., F.M. Hoffman, C.D. Koven and J.T. Randerson. 2016. Plant responses to increasing CO2 reduce estimates of climate impacts on drought severity. *Proceedings of the National Academy of Sciences of the United States of America*. 113:10019-10024.
- Taneda, H. and M. Tateno. 2007. Effects of transverse movement of water in xylem on patterns of water transport within current-year shoots of kudzu vine, *Pueraria lobata*. *Functional Ecology*. 21:226-234.
- Tang, H. and R. Dubayah. 2017. Light-driven growth in Amazon evergreen forests explained by seasonal variations of vertical canopy structure. *Proceedings of the National Academy of Sciences of the United States of America*. 114:2640-2644.
- Tao, S.L., Q.H. Guo, C. Li, Z.H. Wang and J.Y. Fang. 2016. Global patterns and determinants of forest canopy height. *Ecology*. 97:3265-3270.
- Tardieu, F. and T. Simonneau. 1998. Variability among species of stomatal control under fluctuating soil water status and evaporative demand: modelling isohydric and anisohydric behaviours. *Journal of Experimental Botany*. 49:419-432.
- Tng, D.Y.P., G.J. Williamson, G.J. Jordan and D.M.J.S. Bowman. 2012. Giant eucalypts – globally unique fire-adapted rain-forest trees? *New Phytologist*. 196:1001-1014.
- Trenberth, K.E. 1999. Atmospheric moisture recycling: Role of advection and local evaporation. *Journal of Climate*. 12:1368-1381.
- Tu, C.Y. 2019. The scaling relationship of leaf area and total mass of sample plots across world trees. *Journal of Forestry Research*. 30:2137-2142.
- Turner, B.L., T. Brenes-Arguedas and R. Condit. 2018. Pervasive phosphorus limitation of tree species but not communities in tropical forests. *Nature*. 555:367-+.
- Tymen, B., G. Vincent, E.A. Courtois, J. Heurtebize, J. Dauzat, I. Marechaux and J. Chave. 2017. Quantifying micro-environmental variation in tropical rainforest understory at landscape scale by combining airborne LiDAR scanning and a sensor network. *Annals of Forest Science*. 74
- Tyree, M.T. and F.W. Ewers. 1991. The hydraulic architecture of trees and other woody-plants. *New Phytologist*. 119:345-360.
- Tyree, M.T. and J.S. Sperry. 1989a. Vulnerability of xylem to cavitation and embolism. *Annual Review of Plant Physiology and Plant Molecular Biology*. 40:19-38.
- Tyree, M.T. and J.S. Sperry. 1989b. Vulnerability of xylem to cavitation and embolism. *Annual Review of Plant Physiology and Plant Molecular Biology*. 40:19-38.
- Valencia, R., R. Condit, R.B. Foster, K. Romoleroux, G. Villa, J.-C. Svenning, E. Magård, M. Bass, E. Losos, C. and H. Balslev. 2004. Yasuní Forest Dynamics Plot, Ecuador. *In Tropical forest diversity and dynamism: findings from a large-scale plot network* Eds. E.C. Losos and E.C.J. Leigh. The University of Chicago Press, Chicago, pp 609–620.
- van der Sande, M.T., L. Poorter, S.A. Schnitzer, B.M.J. Engelbrecht and L. Markesteijn. 2019. The hydraulic efficiency-safety trade-off differs between lianas and trees. *Ecology*. 100
- van der Sleen, P., P. Groenendijk, M. Vlam, N.P.R. Anten, A. Boom, F. Bongers, T.L. Pons, G. Terburg and P.A. Zuidema. 2015. No growth stimulation of tropical trees by 150 years of CO2 fertilization but water-use efficiency increased. *Nature Geoscience*. 8:24-28.

- Van Wittenberghe, S., S. Adriaenssens, J. Staelens, K. Verheyen and R. Samson. 2012. Variability of stomatal conductance, leaf anatomy, and seasonal leaf wettability of young and adult European beech leaves along a vertical canopy gradient. *Trees-Structure and Function*. 26:1427-1438.
- Venturas, M.D., J.S. Sperry and U.G. Hacke. 2017. Plant xylem hydraulics: What we understand, current research, and future challenges. *Journal of Integrative Plant Biology*. 59:356-389.
- Vico, G., D. Dralle, X. Feng, S. Thompson and S. Manzoni. 2017. How competitive is drought deciduousness in tropical forests? A combined eco-hydrological and eco-evolutionary approach. *Environmental Research Letters*. 12
- Vilagrosa, A.a.C.E.a.P.-P.J.J.a.B.T.a.C.H.a.P.E. 2012. Plant Responses to Drought Stress:63-109.
- Vilanova, E., H. Ramirez-Angulo, A. Torres-Lezama, G. Aymard, L. Gamez, C. Duran, L. Hernandez, R. Herrera, G. van der Heijden, O.L. Phillips and G.J. Ettl. 2018. Environmental drivers of forest structure and stem turnover across Venezuelan tropical forests. *Plos One*. 13
- Villagra, M., P.I. Campanello, S.J. Bucci and G. Goldstein. 2013a. Functional relationships between leaf hydraulics and leaf economic traits in response to nutrient addition in subtropical tree species. *Tree Physiology*. 33:1308-1318.
- Villagra, M., P.I. Campanello, L. Montti and G. Goldstein. 2013b. Removal of nutrient limitations in forest gaps enhances growth rate and resistance to cavitation in subtropical canopy tree species differing in shade tolerance. *Tree Physiology*. 33:285-296.
- Villar, J.C.E., J. Ronchail, J.L. Guyot, G. Cochonneau, F. Naziano, W. Lavado, E. De Oliveira, R. Pombosa and P. Vauchel. 2009. Spatio-temporal rainfall variability in the Amazon basin countries (Brazil, Peru, Bolivia, Colombia, and Ecuador). *International Journal of Climatology*. 29:1574-1594.
- Wagner, F.H., B. Hérault, D. Bonal, C. Stahl, L.O. Anderson, T.R. Baker, G.S. Becker, H. Beeckman, D.B. Souza, P.C. Botosso, D. Bowman, A. Brauning, B. Brede, F.I. Brown, J.J. Camarero, P.B. Camargo, F.C.G. Cardoso, F.A. Carvalho, W. Castro, R.K. Chagas, J. Chave, E.N. Chidumayo, D.A. Clark, F.R.C. Costa, C. Couralet, P.H.D. Mauricio, H. Dalitz, V.R. de Castro, J.E.D. Milani, E.C. de Oliveira, L.D.S. Arruda, J.L. Devineau, D.M. Drew, O. Dunisch, G. Durigan, E. Elifuraha, M. Fedele, L.F. Fedele, A. Figueiredo, C.A.G. Finger, A.C. Franco, J.L. Freitas, F. Galvao, A. Gebrekirstos, R. Gliniars, P. Graca, A.D. Griffiths, J. Grogan, K. Guan, J. Homeier, M.R. Kanieski, L.K. Kho, J. Koenig, S.V. Kohler, J. Krepkowski, J.P. Lemos, D. Lieberman, M.E. Lieberman, C.S. Lisi, T.L. Santos, J.L.L. Ayala, E.E. Maeda, Y. Malhi, V.R.B. Maria, M.C.M. Marques, R. Marques, H.M. Chamba, L. Mbwambo, K.L.L. Melgaco, H.A. Mendivelso, B.P. Murphy, J.J. O'Brien, S.F. Oberbauer, N. Okada, R. Pelissier, L.D. Prior, F.A. Roig, M. Ross, D.R. Rossatto, V. Rossi, L. Rowland, E. Rutishauser, H. Santana, M. Schulze, D. Selhorst, W.R. Silva, M. Silveira, S. Spann, M.D. Swaine, J.J. Toledo, M.M. Toledo, M. Toledo, T. Toma, M. Tomazello, J.I.V. Hernandez, J. Verbesselt, S.A. Vieira, G. Vincent, C.V. de Castilho, F. Volland, et al. 2016. Climate seasonality limits leaf carbon assimilation and wood productivity in tropical forests. *Biogeosciences*. 13:2537-2562.
- Wagner, F.H., B. Hérault, V. Rossi, T. Hilker, E.E. Maeda, A. Sanchez, A.I. Lyapustin, L.S. Galvao, Y.J. Wang and L. Aragao. 2017. Climate drivers of the Amazon forest greening. *Plos One*. 12
- Wallace, J.S., J.A. Clark and M. McGowan. 1983. WATER RELATIONS OF WINTER-WHEAT .3. COMPONENTS OF LEAF WATER POTENTIAL AND THE SOIL PLANT WATER POTENTIAL GRADIENT. *Journal of Agricultural Science*. 100:581-589.
- Walsh, K.J.E., S.J. Camargo, T.R. Knutson, J. Kossin, T.C. Lee, H. Murakami and C. Patricola. 2019. Tropical cyclones and climate change. *Tropical Cyclone Research and Review*. 8:240-250.
- Warwick, N.W.M., L. Hailey, K.L. Clarke and P.E. Gasson. 2017. Climate trends in the wood anatomy of *Acacia sensu stricto* (Leguminosae: Mimosoideae). *Annals of Botany*. 119:1249-1266.
- West, G.B., J.H. Brown and B.J. Enquist. 1997. A general model for the origin of allometric scaling laws in biology. *Science*. 276:122-126.
- West, G.B., J.H. Brown and B.J. Enquist. 1999. A general model for the structure and allometry of plant vascular systems. *Nature*. 400:664-667.

- West, P.W. 2020. Do increasing respiratory costs explain the decline with age of forest growth rate? *Journal of Forestry Research*. 31:693-712.
- Wheeler, J.K., J.S. Sperry, U.G. Hacke and N. Hoang. 2005. Inter-vessel pitting and cavitation in woody Rosaceae and other vesselless plants: a basis for a safety versus efficiency trade-off in xylem transport. *Plant Cell and Environment*. 28:800-812.
- White, D.A. and C.S. Hood. 2004. Vegetation patterns and environmental gradients in tropical dry forests of the northern Yucatan Peninsula. *Journal of Vegetation Science*. 15:151-160.
- Wieloch, T., G. Helle, I. Heinrich, M. Voigt and P. Schyma. 2011. A novel device for batch-wise isolation of alpha-cellulose from small-amount wholewood samples. *Dendrochronologia*. 29:115-117.
- Winckler, J., Q. Lejeune, C.H. Reick and J. Pongratz. 2019. Nonlocal Effects Dominate the Global Mean Surface Temperature Response to the Biogeophysical Effects of Deforestation. *Geophysical Research Letters*. 46:745-755.
- Wittich, B., V. Horna, J. Homeier and C. Leuschner. 2012. Altitudinal Change in the Photosynthetic Capacity of Tropical Trees: A Case Study from Ecuador and a Pan-tropical Literature Analysis. *Ecosystems*. 15:958-973.
- Wolfe, B.T. 2017. Retention of stored water enables tropical tree saplings to survive extreme drought conditions. *Tree Physiology*. 37:469-480.
- Wong, S.C., I.R. Cowan and G.D. Farquhar. 1979. Stomatal conductance correlates with photosynthetic capacity. *Nature*. 282:424-426.
- Woodruff, D.R., B.J. Bond and F.C. Meinzer. 2004. Does turgor limit growth in tall trees? *Plant Cell and Environment*. 27:229-236.
- Woodruff, D.R. and F.C. Meinzer. 2011. Size-Dependent Changes in Biophysical Control of Tree Growth: The Role of Turgor. *In* Size- and Age-Related Changes in Tree Structure and Function. Ed. L.B. Meinzer F., Dawson T. Springer, Dordrecht.
- Woodruff, D.R., F.C. Meinzer, B. Lachenbruch and D.M. Johnson. 2009. Coordination of leaf structure and gas exchange along a height gradient in a tall conifer. *Tree Physiology*. 29:261-272.
- Worbes, M. 1999. Annual growth rings, rainfall-dependent growth and long-term growth patterns of tropical trees from the Caparo Forest Reserve in Venezuela. *Journal of Ecology*. 87:391-403.
- Wright, I.J., P.B. Reich, M. Westoby, D.D. Ackerly, Z. Baruch, F. Bongers, J. Cavender-Bares, T. Chapin, J.H.C. Cornelissen, M. Diemer, J. Flexas, E. Garnier, P.K. Groom, J. Gulias, K. Hikosaka, B.B. Lamont, T. Lee, W. Lee, C. Lusk, J.J. Midgley, M.L. Navas, U. Niinemets, J. Oleksyn, N. Osada, H. Poorter, P. Poot, L. Prior, V.I. Pyankov, C. Roumet, S.C. Thomas, M.G. Tjoelker, E.J. Veneklaas and R. Villar. 2004. The worldwide leaf economics spectrum. *Nature*. 428:821-827.
- Wright, S.J. 2019. Plant responses to nutrient addition experiments conducted in tropical forests. *Ecological Monographs*. 89
- Wright, S.J., M.A. Jaramillo, J. Pávan, R. Condit, S.P. Hubbell and R.B. Foster. 2005. Reproductive size thresholds in tropical trees: variation among individuals, species and forests. *Journal of Tropical Ecology*. 21:307-315.
- Wright, S.J., K. Kitajima, N.J.B. Kraft, P.B. Reich, I.J. Wright, D.E. Bunker, R. Condit, J.W. Dalling, S.J. Davies, S. Diaz, B.M.J. Engelbrecht, K.E. Harms, S.P. Hubbell, C.O. Marks, M.C. Ruiz-Jaen, C.M. Salvador and A.E. Zanne. 2010. Functional traits and the growth-mortality trade-off in tropical trees. *Ecology*. 91:3664-3674.
- Xu, S.S., Y. Li and G.X. Wang. 2014. Scaling Relationships between Leaf Mass and Total Plant Mass across Chinese Forests. *Plos One*. 9
- Yang, Y., S.S. Saatchi, L. Xu, Y.F. Yu, S. Choi, N. Phillips, R. Kennedy, M. Keller, Y. Knyazikhin and R.B. Myneni. 2018a. Post-drought decline of the Amazon carbon sink. *Nature Communications*. 9
- Yang, Y., S.S. Saatchi, L. Xu, Y.F. Yu, S. Choi, N. Phillips, R. Kennedy, M. Keller, Y. Knyazikhin and R.B. Myneni. 2018b. Post-drought decline of the Amazon carbon sink. *Nature Communications*. 9:9.

- Yanoviak, S.P., E.M. Gora, P.M. Bitzer, J.C. Burchfield, H.C. Muller-Landau, M. Detto, S. Paton and S.P. Hubbell. 2020. Lightning is a major cause of large tree mortality in a lowland neotropical forest. *New Phytologist*. 225:1936-1944.
- Yeh, S.W., W.J. Cai, S.K. Min, M.J. McPhaden, D. Dommenges, B. Dewitte, M. Collins, K. Ashok, S.I. An, B.Y. Yim and J.S. Kug. 2018. ENSO Atmospheric Teleconnections and Their Response to Greenhouse Gas Forcing. *Reviews of Geophysics*. 56:185-206.
- Yi, K., D. Dragoni, R.P. Phillips, D.T. Roman and K.A. Novick. 2017. Dynamics of stem water uptake among isohydric and anisohydric species experiencing a severe drought. *Tree Physiology*. 37:1379-1392.
- Yi, K., J.T. Maxwell, M.K. Wenzel, D.T. Roman, P.E. Sauer, R.P. Phillips and K.A. Novick. 2019. Linking variation in intrinsic water-use efficiency to isohydricity: a comparison at multiple spatiotemporal scales. *New Phytologist*. 221:195-208.
- Zuur, A., E. Ieno, N. Walker, A. Saveliev and G. Smith. 2009. *In Mixed effects models and extensions in ecology with R*. Springer, New York, USA, pp 35-69.
- Zweifel, R., L. Zimmermann, F. Zeugin and D.M. Newbery. 2006. Intra-annual radial growth and water relations of trees: implications towards a growth mechanism. *Journal of Experimental Botany*. 57:1445-1459.

Appendix for Chapter 3

SI Table 3.1. Species mean maximum height with position of mean maximum height along a mean annual precipitation (MAP) gradient.

Species	mean MAP	st.err MAP	mean top percentile height	st.err top percentile height
<i>Aparisthmium cordatum</i>	2042.4	213.0641	17.3	1.565248
<i>Apuleia leiocarpa</i>	2280.8	345.2538	49.015	3.392229
<i>Aspidosperma excelsum</i>	2381.8	249.4939	54.366	3.809171
<i>Astrocaryum gynacanthum</i>	1953.4	186.7734	9.48	3.519517
<i>Brosimum guianense</i>	2136.4	618.0132	33.3846	3.171268
<i>Brosimum lactescens</i>	2109.4	405.791	44.696	3.242385
<i>Brosimum rubescens</i>	2586.2	269.716	36.504	4.970139
<i>Brosimum utile</i>	2473.8	486.174	41.28	8.769433
<i>Bursera simaruba</i>	1151.6	264.4301	21.6	2.073644

<i>Celtis schippii</i>	1867	316.1218	33.6882	5.001669
<i>Cheiloclinium cognatum</i>	1732.4	380.9755	20.9876	4.848111
<i>Eschweilera coriacea</i>	2548.8	533.7834	42.313	3.487258
<i>Euterpe precatoria</i>	1853.8	527.5028	31.9932	5.198267
<i>Guarea kunthiana</i>	1781	1026.252	31.6058	3.609912
<i>Helicostylis tomentosa</i>	1479	0	28.8952	0.550711
<i>Hura crepitans</i>	2053.4	535.4977	36	1.414214
<i>Hymenaea courbaril</i>	2227.4	265.6027	44.2	3.156739
<i>Inga alba</i>	2764.4	462.1026	37.71992	9.074628
<i>Inga marginata</i>	1654.4	392.2063	25.1694	1.380243
<i>Iriartea deltoidea</i>	2785.4	192.543	35.5138	6.279488
<i>Iryanthera juruensis</i>	2065.4	366.8158	32.39099	3.538401
<i>Jacaranda copaia</i>	2811.4	396.2837	40.04	1.942421
<i>Leonia glycyarpa</i>	2319.2	241.2099	38.0382	10.97603
<i>Licania heteromorpha</i>	2403	425.1335	37.6522	6.125737
<i>Metrodorea flavida</i>	1635.2	405.078	23.2722	2.827534
<i>Micropholis guyanensis</i>	2619	164.6147	31.772	2.472745
<i>Micropholis venulosa</i>	2606.2	727.0431	29.456	7.46637
<i>Minquartia guianensis</i>	2637.6	602.4349	38.732	6.9331
<i>Oenocarpus bataua</i>	2807.2	12.96919	28.7258	0.570051
<i>Otoba parvifolia</i>	2690.6	292.4838	37.8642	1.73256
<i>Pourouma guianensis</i>	2230.2	640.3801	31.7588	8.784563
<i>Pourouma minor</i>	2211.8	286.7903	45.3448	6.095347
<i>Pouteria caimito</i>	2535.4	211.1215	28.514	3.764064
<i>Pouteria guianensis</i>	2553.2	198.5628	33.5968	6.66354
<i>Protium heptaphyllum</i>	1919.8	26.29068	29.4	3.277194
<i>Pseudolmedia laevigata</i>	2122.6	698.6171	34.9262	1.649187
<i>Pseudolmedia laevis</i>	1958	397.1014	41.8604	3.230105
<i>Pseudolmedia macrophylla</i>	1957.2	396.0034	33.564	8.192593
<i>Simarouba amara</i>	2261.8	375.6231	45.5676	3.095537
<i>Sloanea eichleri</i>	2268.6	772.121	26.88688	2.149146
<i>Socratea exorrhiza</i>	1712.4	167.0832	34.0168	3.109568
<i>Spondias mombin</i>	2341.6	302.7636	37.44404	1.769137
<i>Tapirira guianensis</i>	2666	296.1782	37.494	2.490147
<i>Tetragastris altissima</i>	1950.2	386.6163	37.3166	6.053829
<i>Virola calophylla</i>	1861.6	427.0115	26.8844	1.928553
<i>Virola pavonis</i>	2651.8	721.3458	30.128	1.477048
<i>Virola sebifera</i>	2304.8	622.2401	32.8204	5.745418

SI Table 3.2. List of explanatory variables used to relate to maximum height, showing full name of each variable, unit and source.

Variable code	Variable name	unit	source
ai_eto	potential evapotranspiration	mm day-1	Trabucco, A., and Zomer, R.J. 2018. Global Aridity Index and Potential Evapo-Transpiration (ET0) Climate Database v2. CGIAR Consortium for Spatial Information (CGIAR-CSI). Published online, available from the CGIAR-CSI GeoPortal at https://cgiarcsi.community
bio1	Annual Mean Temperature	°C * 10	Fick, S.E. and R.J. Hijmans, 2017. WorldClim 2: new 1km spatial resolution climate surfaces for global land areas. International Journal of Climatology 37 (12): 4302-4315.
bio2	Mean Diurnal Range (Mean of monthly (max temp - min temp))	°C * 10	Fick, S.E. and R.J. Hijmans, 2017. WorldClim 2: new 1km spatial resolution climate surfaces for global land areas. International Journal of Climatology 37 (12): 4302-4315.
bio3	Isothermality (BIO2/BIO7) (× 100)		Fick, S.E. and R.J. Hijmans, 2017. WorldClim 2: new 1km spatial resolution climate surfaces for global land areas. International Journal of Climatology 37 (12): 4302-4315.
bio4	Temperature Seasonality (standard deviation × 100)		Fick, S.E. and R.J. Hijmans, 2017. WorldClim 2: new 1km spatial resolution climate surfaces for global land areas. International Journal of Climatology 37 (12): 4302-4315.
bio5	Max Temperature of Warmest Month	°C * 10	Fick, S.E. and R.J. Hijmans, 2017. WorldClim 2: new 1km spatial resolution climate surfaces for global land areas. International Journal of Climatology 37 (12): 4302-4315.
bio6	Min Temperature of Coldest Month	°C * 10	Fick, S.E. and R.J. Hijmans, 2017. WorldClim 2: new 1km spatial resolution climate surfaces for global land areas. International Journal of Climatology 37 (12): 4302-4315.
bio7	Temperature Annual Range (BIO5-BIO6)	°C * 10	Fick, S.E. and R.J. Hijmans, 2017. WorldClim 2: new 1km spatial resolution climate surfaces for global land areas. International Journal of Climatology 37 (12): 4302-4315.
bio8	Mean Temperature of Wettest Quarter	°C * 10	Fick, S.E. and R.J. Hijmans, 2017. WorldClim 2: new 1km spatial resolution climate surfaces for global land areas. International Journal of Climatology 37 (12): 4302-4315.
bio9	Mean Temperature of Driest Quarter	°C * 10	Fick, S.E. and R.J. Hijmans, 2017. WorldClim 2: new 1km spatial resolution climate surfaces for global land areas. International Journal of Climatology 37 (12): 4302-4315.
bio10	Mean Temperature of Warmest Quarter	°C * 10	Fick, S.E. and R.J. Hijmans, 2017. WorldClim 2: new 1km spatial resolution climate surfaces for global land areas. International Journal of Climatology 37 (12): 4302-4315.
bio11	Mean Temperature of Coldest Quarter	°C * 10	Fick, S.E. and R.J. Hijmans, 2017. WorldClim 2: new 1km spatial resolution climate surfaces for global land areas. International Journal of Climatology 37 (12): 4302-4315.
bio12	Annual Precipitation	mm	Fick, S.E. and R.J. Hijmans, 2017. WorldClim 2: new 1km spatial resolution climate surfaces for global land areas. International Journal of Climatology 37 (12): 4302-4315.
bio13	Precipitation of Wettest Month	mm	Fick, S.E. and R.J. Hijmans, 2017. WorldClim 2: new 1km spatial resolution climate surfaces for global land areas. International Journal of Climatology 37 (12): 4302-4315.
bio14	Precipitation of Driest Month	mm	Fick, S.E. and R.J. Hijmans, 2017. WorldClim 2: new 1km spatial resolution climate surfaces for global land areas. International Journal of Climatology 37 (12): 4302-4315.
bio15	Precipitation Seasonality		Fick, S.E. and R.J. Hijmans, 2017. WorldClim 2: new 1km spatial resolution climate surfaces for global land areas. International Journal of Climatology 37 (12): 4302-4315.

	(Coefficient of Variation)		
bio16	Precipitation of Wettest Quarter	mm	Fick, S.E. and R.J. Hijmans, 2017. WorldClim 2: new 1km spatial resolution climate surfaces for global land areas. International Journal of Climatology 37 (12): 4302-4315.
bio17	Precipitation of Driest Quarter	mm	Fick, S.E. and R.J. Hijmans, 2017. WorldClim 2: new 1km spatial resolution climate surfaces for global land areas. International Journal of Climatology 37 (12): 4302-4315.
bio18	Precipitation of Warmest Quarter	mm	Fick, S.E. and R.J. Hijmans, 2017. WorldClim 2: new 1km spatial resolution climate surfaces for global land areas. International Journal of Climatology 37 (12): 4302-4315.
bio19	Precipitation of Coldest Quarter	mm	Fick, S.E. and R.J. Hijmans, 2017. WorldClim 2: new 1km spatial resolution climate surfaces for global land areas. International Journal of Climatology 37 (12): 4302-4315.
bulk_density	bulk density	cg/cm3	https://soilgrids.org/#/?layer=ORCDRC_M_sl2_250m&vector=0
Clay%	percentage of clay	%	https://soilgrids.org/#/?layer=ORCDRC_M_sl2_250m&vector=1
Sand%	percentage of sand	%	https://soilgrids.org/#/?layer=ORCDRC_M_sl2_250m&vector=2
Silt%	percentage of silt	%	https://soilgrids.org/#/?layer=ORCDRC_M_sl2_250m&vector=3
CWD	Climatic water deficit	mm yr-1	Chave et al. (2014) <i>Improved allometric models to estimate the above-ground biomass of tropical trees</i> , Global Change Biology, 20 (10), 3177-3190
DIR	mean annual direct normal irradiation (DNI) 1999-2018	kWh/m2,	https://globalsolaratlas.info/map?c=11.609193,8.4375,3
dry_season_length	dry season length	months <100mm	CRU-TS 4.03 (Harris et al., 2014) downscaled with WorldClim 2.1 (Fick and Hijmans, 2017).

SI Table 3.3. Multivariate GAM results relating environmental variables to the maximum height (mean of upper 6 percentiles) per forest plot. Two climate variables and one soil variable were selected. The GAM was produced using penalised cubic regression splines on the three independent variables, where the number of knots was restricted to 4. Variables were selected based upon explanatory power of the model and independence from one another.

R ²	deviance explained	n	edf	Ref.df	F	p-value	climvar
----------------	--------------------	---	-----	--------	---	---------	---------

0.352189	0.375146	104	1.011958	3	2.68476	0.001751	max temp of warmest month
			2.188202	3	14.04211	3.05E-09	MAP
			0.45	3	0.310654	0.131117	% sand

SI Table 3.4 Table of GAM results per taxon (left columns), presented are the adjusted R squared for each taxon, the significance of the smooth term of the models, and the estimated degrees of freedom, k=5 for all taxa. The right hand columns show the maximum height per 200mm MAP bin (mean of the tallest 5 percentiles per 200mm MAP bin with standard error) per taxon and at what value of MAP these occur, with standard error of the mean of these occurrences in MAP.

taxon	R ²	edf	df	p-value	MAP at max H (s.e.)	max H (s.e.)
Anacardiaceae	0.55	2.06	3.06	0.009	2520 (460.4)	36.8 (1.8)
Annonaceae	0.41	2.03	3.03	0.028	2640 (477.5)	37.2 (4.4)
Apocynaceae	0.57	2.48	3.48	0.01	2480 (414.7)	42.9 (3.8)
Arecaceae	0.39	1.38	2.38	0.028	2600 (632.5)	28.1 (1.3)
Bignoniaceae	0.61	1.97	2.97	0.002	2640 (477.5)	40.7 (3.2)

Burseraceae	0.47	2.26	3.26	0.017	2840 (638.7)	30.9 (1.2)
Chrysobalanaceae	0.59	2.43	3.43	0.01	2760 (517.7)	36.6 (2.4)
Elaeocarpaceae	0.28	2.05	3.05	0.11	2280 (672.3)	31.7 (6.7)
Euphorbiaceae	0.59	2.2	3.2	0.002	2400 (547.7)	40.4 (1.7)
Fabaceae	0.65	2.19	3.19	0	2520 (481.7)	47.9 (5.3)
Lauraceae	0.54	2.67	3.67	0.015	2520 (481.7)	47.8 (8.3)
Lecythidaceae	0.17	1.79	2.79	0.192	2240 (622.9)	45.7 (9.8)
Malvaceae	0.7	2.17	3.17	0	2680 (414.7)	41 (5.7)
Melastomataceae	0.12	1.72	2.72	0.309	2120 (460.4)	27.2 (5.2)
Meliaceae	0.45	2.26	3.26	0.021	2080 (807.5)	37.1 (3.3)
Moraceae	0.73	2.36	3.36	0	2600 (447.2)	40.7 (2.9)
Myristicaceae	0.28	1.86	2.86	0.101	2480 (540.4)	37.9 (1.3)
Nyctaginaceae	0.51	1.04	2.04	0.006	2480 (414.7)	26.1 (2.4)
Rubiaceae	0.4	2.63	3.63	0.058	2600 (316.2)	33.8 (5.9)
Salicaceae	0.12	1.67	2.67	0.291	1960 (517.7)	31.2 (10.5)
Sapindaceae	0.22	2.65	3.65	0.219	2080 (672.3)	34.9 (7.8)
Sapotaceae	0.25	1.5	2.5	0.071	2760 (638.7)	40.9 (8.1)
Urticaceae	0.28	1.7	2.7	0.079	2320 (540.4)	38.2 (3.2)
Violaceae	0.54	2.4	3.4	0.03	2280 (481.7)	26.5 (4)
Aspidosperma	0.66	2.45	3.45	0.004	2480 (414.7)	47.6 (4.7)
Brosimum	0.64	2.38	3.38	0.003	2600 (447.2)	40.3 (5.6)
Euterpe	0.37	2.73	3.73	0.184	2000 (583.1)	26.2 (3.4)

Guarea	0.41	2.77	3.77	0.055	2280 (843.8)	34.5 (1.9)
Inga	0.45	1.37	2.37	0.011	2640 (477.5)	38.6 (6.5)
Jacaranda	0.63	2.01	3.01	0.004	2640 (477.5)	38.4 (2.6)
Licania	0.4	2.15	3.15	0.076	2400 (447.2)	33.4 (4.2)
Neea	0.35	0.9	1.9	0.025	2440 (477.5)	25.5 (3.8)
Ocotea	0.47	2.69	3.69	0.042	2480 (460.4)	39.5 (5)
Oenocarpus	0.61	2.01	3.01	0.048	2320 (609.9)	24.9 (2.5)
Protium	0.48	1.41	2.41	0.005	2920 (593.3)	29.5 (2.8)
Sloanea	0.29	1.96	2.96	0.12	2280 (672.3)	31.7 (6.7)
Socratea	0.22	0.74	1.74	0.115	2000 (583.1)	28.1 (4.3)
Tachigali	0.19	1.47	2.47	0.151	2240 (517.7)	38.5 (5)
Virola	0.17	1.73	2.73	0.191	2280 (609.9)	34.8 (2.3)
Apuleia leiocarpa	0.93	2.85	3.85	0.034	1840 (384.7)	42.7 (6.9)
Brosimum guianense	0.5	2.75	3.75	0.14	2000 (583.1)	30.3 (5.1)
Brosimum rubescens	0.74	1.42	2.42	0.033	2320 (460.4)	32.8 (6.6)
Euterpe precatória	0.26	1.79	2.79	0.262	2000 (583.1)	26.4 (3.5)
Inga alba	0.15	0.63	1.63	0.147	2640 (841.4)	33 (11.1)
Iriarteia deltoidea	0.66	1.97	2.97	0.102	2800 (316.2)	29.6 (3)
Jacaranda copaia	0.39	1.72	2.72	0.055	2640 (477.5)	38.4 (2.6)

Licania heteromorpha	0.1	0.41	1.41	0.246	2400 (447.2)	34.1 (5.5)
Metrodorea flavida	0.97	2.81	3.81	0.576	1900 (416.3)	20 (2.7)
Oenocarpus bataua	0.36	1.65	2.65	0.257	2480 (540.4)	25.2 (2.4)
Protium heptaphyllum	0.18	1.67	2.67	0.329	2040 (517.7)	23.8 (6.1)
Socratea exorrhiza	0.26	0.76	1.76	0.096	2000 (583.1)	28.4 (4.7)
Tapirira guianensis	0.61	1.22	2.22	0.003	2440 (622.9)	34.7 (3.8)

SI Table 3.5. Plot properties for plots used in analyses, mean annual temperature and mean annual precipitation are from WorldClim, all other information is from forestplots.net. Please note to keep the table concise we only state the first PI if multiple PIs were listed on a single plot (a full list of data collectors is present at the front of this thesis). Height measurement method is shown, 1= estimated by eye, 2= manually by trigonometry (clinometer), 3= manually by trigonometry (clinometer) carefully trained, 4= laser or ultrasonic distance to tree, electronic tilt sensor for angle, 5= laser hypsometer from directly below crown, “last return” filter function,6= directly (e.g. climbing, cutting, adjacent tower). Some plots were without height measurement method flags and thus are blank.

Plot Code	Country	Biogeographical Region Name	Latitude	Longitude	Altitude	Forest Moisture	Forest Edaphic Type	Forest Status	Projected Planar Area	Mean Annual Temperature (°C)	Mean Annual Precipitation (mm)	Height measurement method	Number of Height Measured Trees	Plot PI
YAN-02	PERU	Western Amazon	-3.43	-72.84	109	Moist	Terra Firma	Old-growth	1	26.3	2786	3	61	Timothy Baker
YAN-01	PERU	Western Amazon	-3.43	-72.84	132	Moist	Terra Firma	Old-growth	1	26.3	2786	3	103	Timothy Baker
VCR-02	BRAZIL	Southern Amazon	-14.83	-52.17	297	Moist	Terra Firma	Old-growth	1.2	25.1	1506	4	1296	Ben Hur
VCR-01	BRAZIL	Southern Amazon	-14.83	-52.16	303	Moist	Terra Firma	Old-growth	0.64	25.3	1506	4	538	Marimon Junior Ben Hur
VAV-01	BRAZIL	Eastern Amazon	-1.18	-46.68	61	Moist	Terra Firma	Old-growth	0.25	26.1	2323		279	Marimon Junior Jos Barlow
TUC-01	BOLIVIA	Southern Amazon	-18.52	-60.81	310	Dry	Terra Firma	Old-growth	1	24.6	815	4	123	Ted Feldpausch
TPT-01	PERU	Western Amazon	-6.74	-76.3	472	Dry	Terra Firma	Old-growth	0.5	25.4	1273		25	Jose Luis Marcelo Peña
TAN-04	BRAZIL	Southern Amazon	-12.92	-52.37	389	Moist	Terra Firma	Old-growth	1	25.2	1666	4	553	Ben Hur
TAN-03	BRAZIL	Southern Amazon	-12.83	-52.35	356	Moist	Terra Firma	Old-growth	1	25.3	1705	4	669	Marimon Junior Ben Hur
TAN-02	BRAZIL	Southern Amazon	-13.08	-52.38	382	Moist	Terra Firma	Old-growth	1	25.1	1622	4	570	Ben Hur
TAM-09	PERU	Western Amazon	-12.83	-69.28	199	Moist	Terra Firma	Old-growth	1	25.4	2391	3	51	Marimon Junior Timothy Baker

TAM-08	PERU	Western Amazon	-12.83	-69.27	220	Moist	Terra Firma	Old-growth	1	25.4	2391	3	88	Timothy Baker
TAM-07	PERU	Western Amazon	-12.83	-69.26	225	Moist	Terra Firma	Old-growth	1	25.4	2391	3	233	Timothy Baker
TAM-05	PERU	Western Amazon	-12.83	-69.27	220	Moist	Terra Firma	Old-growth	1	25.4	2391	3	220	Timothy Baker
TAM-04	PERU	Western Amazon	-12.84	-69.28	210	Moist	Terra Firma	Old-growth	0.42	25.3	2523	3	116	Timothy Baker
TAM-02	PERU	Western Amazon	-12.83	-69.29	210	Moist	Terra Firma	Old-growth	1	25.4	2391	3	361	Timothy Baker
TAM-01	PERU	Western Amazon	-12.84	-69.29	205	Moist	Terra Firma	Old-growth	1	25.3	2523	3	101	Timothy Baker
SUC-05	PERU	Western Amazon	-3.26	-72.89	118	Moist	Terra Firma	Old-growth	1	26.3	2813	3	63	Timothy Baker
SUC-04	PERU	Western Amazon	-3.25	-72.89	107	Moist	Terra Firma	Old-growth	1	26.3	2813	3	56	Timothy Baker
SUC-02	PERU	Western Amazon	-3.25	-72.9	98	Moist	Terra Firma	Old-growth	1	26.3	2813	3	75	Timothy Baker
SUC-01	PERU	Western Amazon	-3.25	-72.91	107	Moist	Terra Firma	Old-growth	1	26.3	2813	3	85	Timothy Baker
SSA-01	COLOMBIA	Northern South America	8.39	-77.13	139	Wet	Terra Firma	Old-growth	0.6	25.7	2165		210	Luisa Fernanda Duque
SMT-02	BRAZIL	Southern Amazon	-12.82	-51.77	332	Dry	Terra Firma	Old-growth	1	25.9	1613	4	461	Ben Hur
SIP-01	BRAZIL	Southern Amazon	-11.41	-55.32	385	Moist	Terra Firma	Old-growth	1	25	1871	5	580	Marimon Junior Ben Hur
SCT-06	BOLIVIA	Western Amazon	-17.09	-64.77	248	Moist	Terra Firma	Old-growth	1	25.1	3084	4	37	Marimon Junior Roel Brienen
SCT-01	BOLIVIA	Western Amazon	-17.09	-64.77	248	Moist	Terra Firma	Old-growth	1	25.1	3084	4	37	Roel Brienen
SCR-05	VENEZUELA	Central Amazon	1.93	-67.04	105	Moist	Terra Firma	Old-growth	1	26.2	3436	6	27	Timothy Baker
SCR-04	VENEZUELA	Central Amazon	1.93	-67.04	105	Moist	White sand	Old-growth	1	26.2	3436	6	22	Oliver Phillips
SAT-01	BRAZIL	Southern Amazon	-9.84	-50.46	243	Moist	Terra Firma	Mixed: Old-growth and Burned	1	26.9	1840	4	550	Ben Hur
SAA-02	BRAZIL	Southern Amazon	-9.64	-50.45	207	Moist	Terra Firma	Old-growth	1	26.6	1765	4	593	Marimon Junior Ben Hur
SAA-01	BRAZIL	Southern Amazon	-9.79	-50.43	177	Moist	Terra Firma	Old-growth	1	26.8	1809	4	532	Marimon Junior Ben Hur
RST-01	BRAZIL	Western Amazon	-9.04	-72.27	279	Moist	Terra Firma	Old-growth	1	25.6	1803	6	17	Marimon Junior Timothy Baker
RIO-02	VENEZUELA	Eastern Amazon	8.11	-61.69	318	Moist	Terra Firma	Old-growth	0.25	25.4	1307	1	11	Julio Serrano
RIO-01	VENEZUELA	Guyana	8.11	-61.69	312	Moist	Terra Firma	Old-growth	0.25	25.4	1307	1	11	Julio Serrano

RFH-01	BRAZIL	Western Amazon	-9.75	-67.67	176	Moist	Terra Firma	Old-growth	1	25.8	1952	2	38	Oliver Phillips
RET-09	BOLIVIA	Southern Amazon	-	-65.72	160	Moist	Terra Firma	Old-growth	1	26.5	1668	4	330	Rene Boot
RET-08	BOLIVIA	Southern Amazon	-	-65.72	160	Moist	Terra Firma	Old-growth	1	26.5	1668	4	329	Rene Boot
RET-06	BOLIVIA	Southern Amazon	-	-65.72	160	Moist	Terra Firma	Old-growth	1	26.5	1668	4	345	Rene Boot
RET-05	BOLIVIA	Southern Amazon	-	-65.72	160	Moist	Terra Firma	Old-growth	1	26.5	1668	4	360	Rene Boot
RCS-06	PERU	Western Amazon	-9.62	-74.93	267	Moist	Terra Firma	Old-growth	1	26	1900	3	56	Luis Valenzuela Gamarra
RCS-05	PERU	Western Amazon	-9.62	-74.93	251	Moist	Terra Firma	Old-growth	1	26	1900	3	50	Luis Valenzuela Gamarra
RBU-01	BRAZIL	Atlantic Forest	-	-42.02	60	Moist	Terra Firma	Old-growth	0.2	22.4	1182		425	Fabrcio Alvim Carvalho
PUC-01	GUYANA	NULL	6.21	-59.72	371	Moist	Terra Firma	Old-growth	1	25.9	2335	4 6	552	Michelle Kalamandeen
PTN-01	COLOMBIA	Northern South America	6.12	-74.67	230	Moist	Terra Firma	Old-growth	1	26.3	2437	1	521	Wilmar Lopez Oviedo
PRA-01	COLOMBIA	Northern South America	8.57	-77.3	193	Wet	Terra Firma	Old-growth	0.36	26	2119		159	Luisa Fernanda Duque
POR-02	BRAZIL	Western Amazon	-10.8	-68.77	268	Moist	Terra Firma	Old-growth	1	25.2	1720	6	86	Timothy Baker
POR-01	BRAZIL	Western Amazon	-	-68.77	268	Moist	Terra Firma	Old-growth	1	25.2	1720	6	108	Timothy Baker
POQ-02	PERU	Western Amazon	-12.9	-71.37	525	Wet	Terra Firma	Old-growth	1	23.7	3011	1	630	Isau Huamantupa-Chuquimaco Abel
PNY-07	PERU	Western Amazon	-	-75.26	414	Wet	Terra Firma	Old-growth	1	21.7	2343	3	40	Monteagudo Abel
PNY-06	PERU	Western Amazon	-	-75.25	462	Wet	Terra Firma	Old-growth	1	21.7	2343	3	41	Monteagudo Abel
PNY-05	PERU	Western Amazon	-	-75.25	448	Wet	Terra Firma	Old-growth	1.002	21.7	2343	3	39	Monteagudo Abel
PNY-04	PERU	Western Amazon	-	-75.25	414	Moist	Terra Firma	Old-growth	1	21.7	2343	3	41	Monteagudo Abel
PND-02	BOLIVIA	NULL	-	-67.36	208	Moist	Terra Firma	Old-growth	1	26	1731	1	511	William Milliken
PIB-12	GUYANA	Guyana	5.03	-58.6	94	Moist	Terra Firma	Old-growth	1	26.3	2712	5	403	Roel Brienen
PIB-06	GUYANA	Guyana	5.01	-58.62	81	Moist	Terra Firma	Old-growth	1	26.3	2712	5	594	Roel Brienen
PIB-05	GUYANA	Guyana	5.02	-58.62	93	Moist	Terra Firma	Old-growth	1	26.3	2712	5	479	Roel Brienen

PAK-01	PERU	Western Amazon	-11.94	-71.28	345	Moist	Terra Firma	Old-growth	1	25	2554	3	59	Timothy Baker
OTT-03	BOLIVIA	Southern Amazon	-16.42	-61.19	451	Dry	Terra Firma	Mixed: Old-growth and Burned	1	23.2	1141	4	76	Ted Feldpausch
OTT-01	BOLIVIA	Southern Amazon	-16.39	-61.21	442	Dry	Terra Firma	Old-growth	1	23.2	1141	4	130	Ted Feldpausch
NXV-09	BRAZIL	Southern Amazon	-14.69	-52.35	324	Dry	Terra Firma	Old-growth	0.5	24.7	1530	4	1928	Ben Hur
NXV-07	BRAZIL	Southern Amazon	-14.72	-52.36	322	Moist	Terra Firma	Old-growth	0.47	24.7	1530	4	413	Marimon Junior
NXV-06	BRAZIL	Southern Amazon	-14.72	-52.36	346	Moist	Terra Firma	Old-growth	0.47	24.7	1530	4	491	Ben Hur
NOU-08	FRENCH GUIANA	Guyana	4.08	-52.68	110	Moist	Terra Firma	Old-growth	1	25.2	3280	5	5	Marimon Junior
NOU-07	FRENCH GUIANA	Guyana	4.08	-52.68	110	Moist	Terra Firma	Old-growth	1	25.2	3280	5	5	Jerôme Chave
NOU-06	FRENCH GUIANA	Guyana	4.09	-52.68	110	Moist	Terra Firma	Old-growth	1	25.2	3280	5	5	Jerôme Chave
NOU-05	FRENCH GUIANA	Guyana	4.09	-52.68	110	Moist	Terra Firma	Old-growth	1	25.2	3280	5	4	Jerôme Chave
NOU-03	FRENCH GUIANA	Guyana	4.09	-52.68	110	Moist	Terra Firma	Old-growth	1	25.2	3280	5	7	Jerôme Chave
NOU-01	FRENCH GUIANA	Guyana	4.09	-52.67	110	Moist	Terra Firma	Old-growth	1	25.2	3280	5	5	Jerôme Chave
MTH-01	BRAZIL	Western Amazon	-8.88	-72.79	246	Moist	Terra Firma	Old-growth	1	25.8	1655	5	18	Oliver Phillips
MTG-08	BOLIVIA	Southern Amazon	-19.27	-63.85	1090	Dry	Terra Firma	Old-growth	0.25	21.8	1044	1 4	9	Jeanneth Villalobos Cayo
MTG-07	BOLIVIA	Southern Amazon	-19.27	-63.84	1109	Dry	Terra Firma	Old-growth	0.25	21.8	1044	1 4	10	Jeanneth Villalobos Cayo
MTG-06	BOLIVIA	Southern Amazon	-19.27	-63.84	1119	Dry	Terra Firma	Old-growth	0.25	21.8	1044	1 4	9	Jeanneth Villalobos Cayo
MTG-05	BOLIVIA	Southern Amazon	-19.27	-63.84	1126	Dry	Terra Firma	Old-growth	0.25	21.8	1044	1 4	10	Jeanneth Villalobos Cayo
MNU-06	PERU	Western Amazon	-11.89	-71.4	345	Moist	Rarely flooded	Old-growth	2.25	25.1	2477	3 5	62	Timothy Baker
MNU-04	PERU	Western Amazon	-11.9	-71.4	358	Moist	Terra Firma	Old-growth	2	25.1	2477	3 5	61	Timothy Baker
MNU-03	PERU	Western Amazon	-11.9	-71.4	312	Moist	Terra Firma	Old-growth	2	25.1	2477	3 5	56	Timothy Baker
MNU-01	PERU	Western Amazon	-11.89	-71.41	312	Moist	Rarely flooded	Old-growth	2.25	25.1	2477	3 5	60	Timothy Baker
MIN-01	BRAZIL	Western Amazon	-8.57	-72.9	226	Moist	Terra Firma	Old-growth	1	25.7	1861	5	41	Oliver Phillips
MHC-02	GUYANA	Guyana	5.31	-58.98	132	Moist	Terra Firma	Old-growth	1	26.5	2859		413	Michelle Kalamandeen

MHC-01	GUYANA	Guyana	5.32	-59.14	325	Moist	Terra Firma	Old-growth	1	26	3021		704	Michelle Kalamandeen
LOR-02	COLOMBIA	Western Amazon	-3.06	-69.99	93	Moist	Terra Firma	Old-growth	0.52	25.7	2790	6	6	Sandra Patiño
LOR-01	COLOMBIA	Western Amazon	-3.06	-69.99	94	Moist	Terra Firma	Old-growth	1	25.7	2790	6	8	Sandra Patiño
LFB-02	BOLIVIA	Southern Amazon	-	-60.83	227	Moist	Terra Firma	Old-growth	1	22.5	1479	1 2	344	Alejandro Araujo Murakami
LFB-01	BOLIVIA	Southern Amazon	-	-60.83	245	Moist	Terra Firma	Old-growth	1	22.5	1479	1 2	349	Alejandro Araujo Murakami
LAS-01	PERU	Western Amazon	-	-70.11	280	Moist	Terra Firma	Old-growth	2	24.9	3253	2	80	Oliver Phillips
KAL-01	COLOMBIA	Northern South America	11.24	-74.14	206	Dry	Terra Firma	Old-growth	1	25.6	1507	1 5	305	Luisa Fernanda Duque
JFR-09	BRAZIL	Southern Amazon	-	-58.51	242	Moist	Terra Firma	Old-growth	0.975	24.8	1891		77	Ted Feldpausch
JFR-08	BRAZIL	Southern Amazon	-	-58.5	248	Moist	Terra Firma	Old-growth	1	24.9	1939		110	Ted Feldpausch
JFR-07	BRAZIL	Southern Amazon	-	-58.5	240	Moist	Terra Firma	Old-growth	1.025	24.9	1939		96	Ted Feldpausch
JFR-06	BRAZIL	Southern Amazon	-	-58.49	249	Moist	Terra Firma	Old-growth	1	24.9	1939		94	Ted Feldpausch
JFR-05	BRAZIL	Southern Amazon	-	-58.48	278	Moist	Terra Firma	Old-growth	1	24.9	1939		122	Ted Feldpausch
JFR-04	BRAZIL	Southern Amazon	-	-58.48	277	Moist	Terra Firma	Old-growth	1	24.9	1939		126	Ted Feldpausch
JFR-03	BRAZIL	Southern Amazon	-	-58.52	245	Moist	Terra Firma	Old-growth	1.025	24.8	1891		67	Ted Feldpausch
JFR-02	BRAZIL	Southern Amazon	-	-58.49	262	Moist	Terra Firma	Old-growth	0.525	24.8	1867		42	Ted Feldpausch
JFR-01	BRAZIL	Southern Amazon	-	-58.47	273	Moist	Terra Firma	Old-growth	0.93	24.9	1939		67	Ted Feldpausch
JEN-13	PERU	Western Amazon	-4.92	-73.54	145	Moist	Rarely flooded	Old-growth	1	26.8	2642	3	34	Timothy Baker
JEN-12	PERU	Western Amazon	-4.9	-73.63	122	Moist	White sand	Old-growth	1	26.8	2642	3	141	Timothy Baker
JEN-11	PERU	Western Amazon	-4.88	-73.63	151	Moist	Terra Firma	Old-growth	1	26.8	2642	3	122	Timothy Baker
JBS-01	BOLIVIA	NULL	-	-63.06	440	Dry	Terra Firma	Old-growth	1	24.3	1110	1 2	428	Alejandro Araujo Murakami
JBP-04	COLOMBIA	El Choco	6.27	-77.38	54	Wet	Terra Firma	Old-growth	0.96	25.5	5296		71	Luisa Fernanda Duque
JBP-01	COLOMBIA	El Choco	6.26	-77.38	100	Wet	Terra Firma	Mixed: Old-growth and Logged	6	25.5	5296		537	Luisa Fernanda Duque
JBI-01	BRAZIL	Eastern Amazon	-5.78	-48.92	167	Moist	Terra Firma	Old-growth	0.25	26.5	1817		238	Jos Barlow

JAS-04	ECUADOR	Western Amazon	-1.07	-77.61	430	Moist	Terra Firma	Old-growth	1	23.8	3645	3 6	15	Timothy Baker
JAS-03	ECUADOR	Western Amazon	-1.08	-77.61	384	Moist	Terra Firma	Old-growth	1	23.8	3645	3 6	55	Timothy Baker
JAS-02	ECUADOR	Western Amazon	-1.07	-77.62	452	Moist	Terra Firma	Old-growth	1	23.8	3645	3 6	52	Timothy Baker
IWO-12	GUYANA	Guyana	4.73	-58.72	61	Moist	Terra Firma	Old-growth	1	26.7	2405	5	418	Roel Brienen
IWO-03	GUYANA	Guyana	4.53	-58.78	100	Moist	Terra Firma	Old-growth	1	26.8	2248	5	561	Roel Brienen
IPM-99	BRAZIL	Central Amazon	-5.94	-62.52	70	Moist	Terra Firma	Old-growth	1	26.3	2542	4	89	Flávia Costa
IPM-98	BRAZIL	Central Amazon	-5.95	-62.51	69	Moist	Terra Firma	Old-growth	1	26.3	2542	4	133	Flávia Costa
IPM-88	BRAZIL	Central Amazon	-5.64	-62.18	70	Moist	Terra Firma	Old-growth	1	26.4	2574	4	109	Flávia Costa
IPM-87	BRAZIL	Central Amazon	-5.63	-62.19	65	Moist	Terra Firma	Old-growth	1	26.4	2574	4	65	Flávia Costa
IPM-86	BRAZIL	Central Amazon	-5.63	-62.19	69	Moist	Terra Firma	Old-growth	1	26.4	2574	4	107	Flávia Costa
IPM-80	BRAZIL	Central Amazon	-5.25	-61.96	63	Moist	Terra Firma	Old-growth	1	26.5	2589	4	94	Flávia Costa
IPM-79	BRAZIL	Central Amazon	-5.25	-61.96	62	Moist	Terra Firma	Old-growth	1	26.5	2589	4	92	Flávia Costa
IPM-64	BRAZIL	Central Amazon	-5	-61.54	59	Moist	Terra Firma	Old-growth	1	26.5	2615	4	81	Flávia Costa
IPM-63	BRAZIL	Central Amazon	-5	-61.55	58	Moist	Terra Firma	Old-growth	1	26.5	2615	4	61	Fernanda Coelho
IPM-62	BRAZIL	Central Amazon	-4.99	-61.56	57	Moist	Terra Firma	Old-growth	1	26.6	2617	4	110	Fernanda Coelho
IPM-55	BRAZIL	Central Amazon	-4.6	-61.26	51	Moist	Terra Firma	Old-growth	1	26.7	2591	4	144	Fernanda Coelho
IPM-46	BRAZIL	Central Amazon	-4.4	-60.92	46	Moist	Terra Firma	Old-growth	1	26.9	2410	4	114	Flávia Costa
IPM-43	BRAZIL	Central Amazon	-4.38	-60.94	48	Moist	Terra Firma	Old-growth	1	26.9	2410	4	96	Flávia Costa
IPM-42	BRAZIL	Central Amazon	-4.38	-60.95	45	Moist	Terra Firma	Old-growth	1	26.9	2410	4	57	Flávia Costa
IPM-40	BRAZIL	Central Amazon	-4.15	-60.73	30	Moist	Terra Firma	Old-growth	1	27	2256	4	90	Flávia Costa
IPM-39	BRAZIL	Central Amazon	-4.14	-60.73	40	Moist	Terra Firma	Old-growth	1	27	2256	4	62	Flávia Costa
IPM-37	BRAZIL	Central Amazon	-4.16	-60.72	37	Moist	Terra Firma	Old-growth	1	27	2256	4	105	Flávia Costa
IPM-28	BRAZIL	Central Amazon	-3.67	-60.3	44	Moist	Terra Firma	Old-growth	1	27.2	2158	4	134	Fernanda Coelho

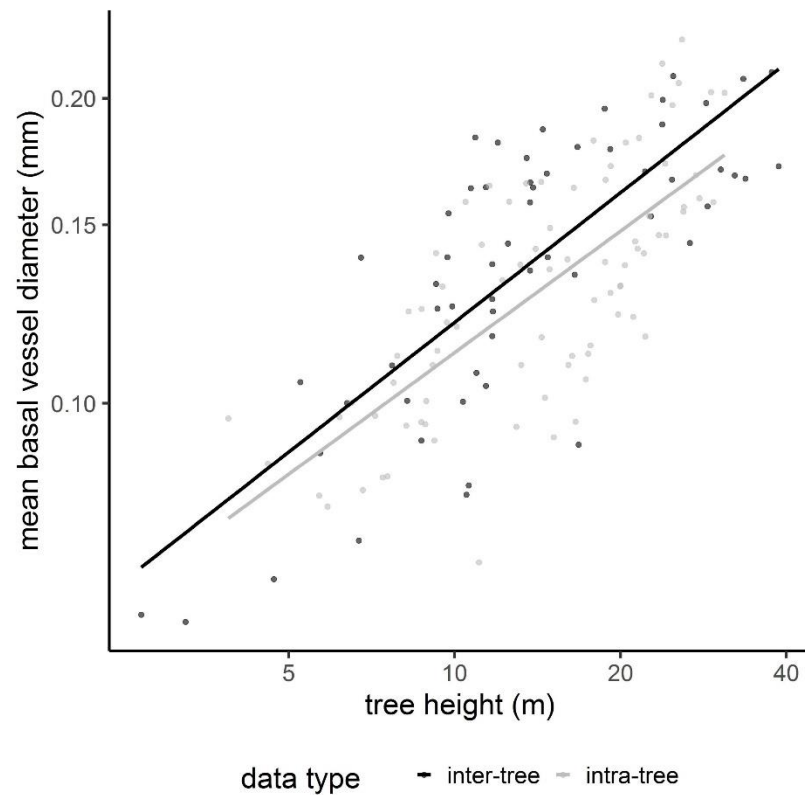
IPM-27	BRAZIL	Central Amazon	-4.99	-61.56	50	Moist	Terra Firma	Old-growth	1	26.6	2617	4	109	Flávia Costa
IPM-26	BRAZIL	Central Amazon	-4.98	-61.57	61	Moist	Terra Firma	Old-growth	1	26.6	2617	4	128	Fernanda Coelho
IPM-25	BRAZIL	Central Amazon	-3.67	-60.31	44	Moist	Terra Firma	Old-growth	1	27.2	2158	4	42	Flávia Costa
IPM-22	BRAZIL	Central Amazon	-3.68	-60.32	44	Moist	Terra Firma	Old-growth	1	27.2	2158	4	132	Fernanda Coelho
IPM-20	BRAZIL	Central Amazon	-3.69	-60.33	50	Moist	Terra Firma	Old-growth	1	27.2	2158	4	134	Fernanda Coelho
IMA-02	VENEZUELA	Guyana	7.45	-61.17	190	Moist	Terra Firma	Old-growth	1	26.1	1447		20	Gerardo A. Aymard C.
IMA-01	VENEZUELA	Guyana	7.44	-61.17	190	Moist	Terra Firma	Old-growth	1	26.1	1447		20	Gerardo A. Aymard C.
HCC-24	BOLIVIA	Southern Amazon	-14.57	-60.75	735	Moist	Terra Firma	Old-growth	1	22.5	1479	1 2	374	Alejandro Araujo Murakami
HCC-22	BOLIVIA	Southern Amazon	-14.53	-60.73	747	Moist	Terra Firma	Old-growth	1	22.5	1479	1 2	401	Alejandro Araujo Murakami
HCC-21	BOLIVIA	Southern Amazon	-14.53	-60.74	729	Moist	Terra Firma	Old-growth	1	22.5	1479	1 2	510	Alejandro Araujo Murakami
GEN-03	PERU	Western Amazon	-11.1	-75.34	900	Dry	Terra Firma	Old-growth	0.6	18.3	1438		319	Carlos Reynel Rodriguez
GDA-01	BRAZIL	Eastern Amazon	-5.63	-49.13	123	Moist	Terra Firma	Old-growth	0.25	26.7	1901		249	Jos Barlow
GAU-07	BRAZIL	Southern Amazon	-13.1	-53.35	357	Moist	Terra Firma	Old-growth	1	24.7	1807		556	Ben Hur Marimon Junior
GAU-06	BRAZIL	Southern Amazon	-13.31	-53.41	390	Moist	Terra Firma	Old-growth	1	24.5	1754	4	483	Edmar Almeida de Oliveira
GAU-04	BRAZIL	Southern Amazon	-13.1	-53.35	390	Moist	Terra Firma	Old-growth	1	24.7	1807	4	412	Edmar Almeida de Oliveira
GAU-02	BRAZIL	Southern Amazon	-13.43	-53.31	440	Moist	Terra Firma	Old-growth	1	24.2	1698		549	Ben Hur Marimon Junior
FRP-01	BRAZIL	Southern Amazon	-11.48	-51.52	258	Moist	Terra Firma	Old-growth	1	26.9	1636		567	Ben Hur Marimon Junior
FRE-01	BRAZIL	Eastern Amazon	-1.53	-46.63	50	Moist	Terra Firma	Old-growth	0.25	26.3	2217		316	Jos Barlow
FMH-03	GUYANA	Guyana	5.18	-58.7	115	Moist	White sand	Old-growth	1	26.4	2822	5	610	Roel Brien
FMH-02	GUYANA	Guyana	5.17	-58.69	122	Moist	Terra Firma	Old-growth	1	26.4	2822	5	356	Roel Brien
FMH-01	GUYANA	Guyana	5.17	-58.69	98	Moist	Terra Firma	Old-growth	1	26.4	2822	5	415	Roel Brien
FLO-02	BRAZIL	Southern Amazon	-12.75	-51.88	366	Moist	Terra Firma	Old-growth	1	25.6	1627	4	589	Ben Hur Marimon Junior
FLO-01	BRAZIL	Southern Amazon	-12.81	-51.85	377	Moist	Terra Firma	Old-growth	1	25.6	1627	4	607	Ben Hur Marimon Junior

FEC-01	BRAZIL	Western Amazon	-10.07	-67.62	204	Moist	Terra Firma	Old-growth	1	26	1915	2	34	Oliver Phillips
ELD-04	VENEZUELA	Guyana	6.09	-61.35	366	Moist	Terra Firma	Old-growth	0.25	25.4	2522	6	10	Julio Serrano
ELD-03	VENEZUELA	Guyana	6.09	-61.4	404	Moist	Terra Firma	Old-growth	0.25	25.4	2522	6	12	Julio Serrano
ELD-02	VENEZUELA	Guyana	6.11	-61.41	244	Moist	Terra Firma	Old-growth	0.25	25.4	2522	6	5	Jean-Pierre Veillon
ELD-01	VENEZUELA	Guyana	6.11	-61.41	220	Moist	Terra Firma	Old-growth	0.25	25.4	2522	6	10	Jean-Pierre Veillon
ECE-01	COLOMBIA	Northern South America	10.68	-75.27	50	Dry	Terra Firma	Old-growth	1	27.7	962	1	440	Luisa Fernanda Duque
EBB-09	BOLIVIA	Western Amazon	-14.73	-66.32	220	Moist	Terra Firma	Old-growth	1	25.2	1828		562	Rachel Graham
EBB-05	BOLIVIA	Western Amazon	-14.76	-66.34	210	Moist	Terra Firma	Old-growth	1	25.2	1800		461	Rachel Graham
DOI-02	BRAZIL	Western Amazon	-10.55	-68.31	203	Moist	Terra Firma	Old-growth	1	26	1902	2	76	Timothy Baker
DOI-01	BRAZIL	Western Amazon	-10.57	-68.32	203	Moist	Terra Firma	Old-growth	1	26	1902	2	97	Timothy Baker
DNA-01	BRAZIL	Eastern Amazon	-5.66	-49.17	141	Moist	Terra Firma	Old-growth	0.26	26.7	1962		215	Jos Barlow
CVP-01	BRAZIL	Atlantic Forest	-21.41	-41.08	30	Dry	Terra Firma	Old-growth	0.2	23.1	992	1	386	Karla Pedra de Abreu
CRP-02	BOLIVIA	Southern Amazon	-14.54	-61.5	350	Dry	Terra Firma	Old-growth	1	24.1	1383	1 2	418	Alejandro Araujo Murakami
CNA-64	BRAZIL	Western Amazon	-8.12	-63.45	77	Moist	Terra Firma	Old-growth	0.998	26.2	2198		425	Ricardo Andrade
CNA-41	BRAZIL	Western Amazon	-8.1	-63.48	83	Moist	Terra Firma	Old-growth	0.977	26.2	2198		459	Ricardo Andrade
CNA-34	BRAZIL	Western Amazon	-8.09	-63.45	72	Moist	Terra Firma	Old-growth	0.967	26.2	2198		451	Ricardo Andrade
CNA-22	BRAZIL	Western Amazon	-8.08	-63.47	87	Moist	Terra Firma	Old-growth	0.9989	26.2	2198		549	Ricardo Andrade
CLA-04	VENEZUELA	Northern South America	10.01	-65.32	283	Dry	Terra Firma	Old-growth	0.252	26.7	620	1	7	Julio Serrano
CAX-02	BRAZIL	Eastern Amazon	-1.74	-51.46	15	Moist	Terra Firma	Old-growth	1	26.8	2206	6	17	Samuel Almeida
CAX-01	BRAZIL	Eastern Amazon	-1.74	-51.46	15	Moist	Terra Firma	Old-growth	1	26.8	2206	6	20	Samuel Almeida
CAU-03	COLOMBIA	Northern South America	8.65	-77.35	30	Dry	Terra Firma	Old-growth	0.24	25.1	2048		170	Luisa Fernanda Duque
CAU-01	COLOMBIA	Northern South America	8.63	-77.37	181	Wet	Terra Firma	Old-growth	0.36	25.1	2048		184	Luisa Fernanda Duque
CAJ-03	BRAZIL	Eastern Amazon	-6.07	-50.25	670	Moist	Terra Firma	Old-growth	0.25	23.9	1904		210	Jos Barlow

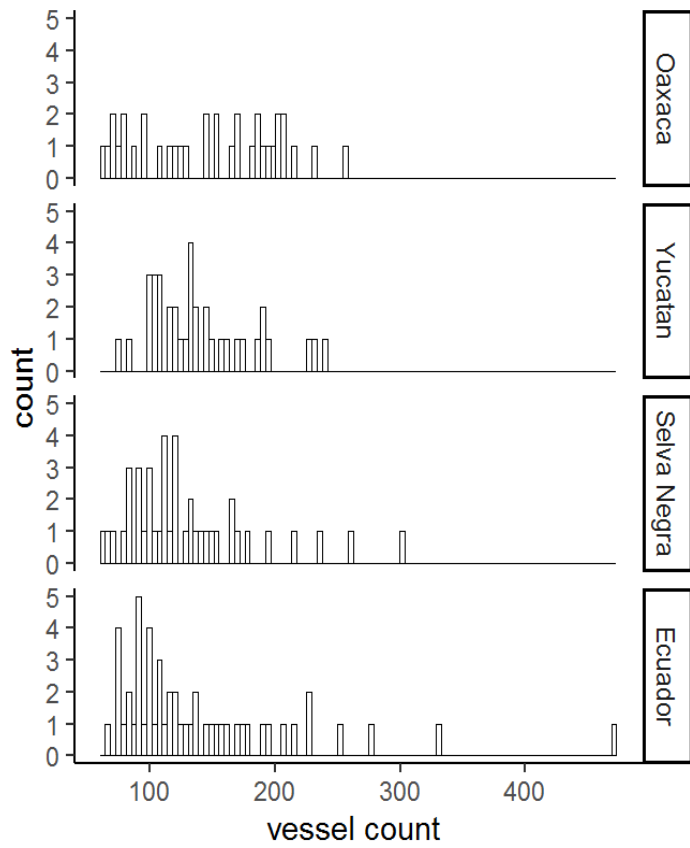
CAJ-02	BRAZIL	Eastern Amazon	-6.04	-50.09	694	Moist	Terra Firma	Old-growth	0.25	24.7	1876		210	Jos Barlow
CAJ-01	BRAZIL	Eastern Amazon	-6.07	-50.03	650	Moist	Terra Firma	Old-growth	0.25	24.7	1876		186	Jos Barlow
BOG-02	ECUADOR	Western Amazon	-0.7	-76.47	284	Moist	Terra Firma	Old-growth	1	25	3133	4 6	31	Timothy Baker
BOG-01	ECUADOR	Western Amazon	-0.7	-76.48	257	Moist	Terra Firma	Old-growth	1	25	3133	3 6	63	Timothy Baker
BNT-04	BRAZIL	Central Amazon	-2.63	-60.15	73	Moist	Terra Firma	Old-growth	1	27	2244	3	45	Niro Higuchi
BES-01	COLOMBIA	Northern South America	10.53	-73.29	550	Dry	Terra Firma	Old-growth	0.8	25.4	1365	1	324	Luisa Fernanda Duque
BAR-01	PERU	Western Amazon	-11.9	-71.42	345	Moist	Terra Firma	Old-growth	1	25.1	2477	3	142	Timothy Baker
BAC-06	VENEZUELA	Northern South America	7.47	-71.02	140	Moist	Terra Firma	Old-growth	0.25	26.7	1832	5	4	Emilio Vilanova Torre
BAC-05	VENEZUELA	Northern South America	7.47	-71.02	142	Moist	Terra Firma	Old-growth	0.25	26.7	1832	5	3	Emilio Vilanova Torre
BAC-04	VENEZUELA	Northern South America	7.46	-71.01	138	Moist	Terra Firma	Old-growth	0.25	26.7	1832	5	4	Emilio Vilanova Torre
BAC-03	VENEZUELA	Northern South America	7.46	-71.01	144	Moist	Terra Firma	Old-growth	0.25	26.7	1832	5	5	Emilio Vilanova Torre
BAC-02	VENEZUELA	Northern South America	7.46	-71.01	143	Moist	Terra Firma	Old-growth	0.25	26.7	1832	5	7	Emilio Vilanova Torre
BAC-01	VENEZUELA	Northern South America	7.46	-71.01	141	Moist	Terra Firma	Old-growth	0.25	26.7	1832	5	1	Emilio Vilanova Torre
AMA-03	COLOMBIA	El Choco	5.61	-77.49	71	Wet	Terra Firma	Old-growth	4	25.4	6126		1918	Luisa Fernanda Duque
AMA-02	COLOMBIA	El Choco	5.58	-77.5	65	Wet	Terra Firma	Old-growth	1	25.4	6126	1	463	Luisa Fernanda Duque
ALP-50	PERU	Western Amazon	-3.95	-73.41	145	Moist	White sand	Old-growth	1	26.4	2784	3	59	Timothy Baker
ALP-40	PERU	Western Amazon	-3.94	-73.44	146	Moist	White sand	Old-growth	1	26.4	2784	3	77	Timothy Baker
ALP-30	PERU	Western Amazon	-3.95	-73.43	130	Moist	White sand	Old-growth	1	26.4	2784	3 6	100	Timothy Baker
ALP-20	PERU	Western Amazon	-3.96	-73.43	114	Moist	Terra Firma	Old-growth	0.1	26.4	2784		286	Oliver Phillips
ALP-19	PERU	Western Amazon	-3.96	-73.44	114	Moist	Terra Firma	Old-growth	0.1	26.4	2784		331	Oliver Phillips
ALP-18	PERU	Western Amazon	-3.95	-73.43	130	Moist	White sand	Old-growth	0.1	26.4	2784		328	Oliver Phillips
ALP-17	PERU	Western Amazon	-3.94	-73.43	114	Moist	Terra Firma	Old-growth	0.1	26.4	2784		306	Oliver Phillips
ALP-16	PERU	Western Amazon	-3.94	-73.42	125	Moist	Terra Firma	Old-growth	0.1	26.4	2784		281	Oliver Phillips

ALP-02	PERU	Western Amazon	-3.95	-73.44	125	Moist	Terra Firma	Old-growth	1	26.4	2784	3 6	136	Timothy Baker
ALP-01	PERU	Western Amazon	-3.95	-73.43	114	Moist	Brown sand	Old-growth	1	26.4	2784	3	136	Timothy Baker
ALM-01	PERU	Western Amazon	-11.8	-71.47	400	Moist	Terra Firma	Old-growth	2	25	2395	3 5	61	Timothy Baker
ALF-02	BRAZIL	Southern Amazon	-9.58	-55.92	277	Moist	Terra Firma	Old-growth	1	25.4	2356	4	567	Edmar Almeida de Oliveira
ALF-01	BRAZIL	Southern Amazon	-9.6	-55.94	269	Moist	Terra Firma	Old-growth	1	25.4	2356	4	533	Edmar Almeida de Oliveira
ALE-01	BRAZIL	Eastern Amazon	-1.14	-46.73	35	Moist	Terra Firma	Old-growth	0.25	26.1	2354	1	266	Jos Barlow
AGP-02	COLOMBIA	Western Amazon	-3.72	-70.3	120	Moist	Terra Firma	Old-growth	1	25.8	2795	6	18	Adriana Prieto
AGP-01	COLOMBIA	Western Amazon	-3.72	-70.31	120	Moist	Terra Firma	Old-growth	1	25.8	2795	6	17	Adriana Prieto

Appendix for Chapter 4



SI Figure 4.1. Comparison of two sampling methods, not including very small trees that are largely intra-tree data type. Both data types have similar slopes given by the LMM interaction term between sample type and height being non-significant (Sum Sq= 0.007, F=0.19 ,p=0.66). intercepts do not differ significantly as tested by Tukey multiple comparisons test (difference = 0.0338 mm, s.e. = 0.104, df = 137, t = 0.324, p=0.745). Note, the residuals of the intra-tree data is slightly non-normal as tested using a Shapiro-Wilk Normality Test (p=0.0199).



SI Figure 4.2. Histograms of the number of vessels (x-axis) measured in each sample (y axis values are the number of samples with x number of vessels) per site.

SI Table 4.1 Linear mixed effects model results for the relationship between tree height and vessel density. This model excluded Oaxaca, indicating that without Oaxaca the wetter three sites have similar slopes.

model	var ~ site * height	df	Sum Sq	F	p-value
	height	31. 746	1	625.704	0
log mean vessel density v log tree height	site	0.1 29	2	1.272	0.285
	site:height	0.2 29	2	2.253	0.111

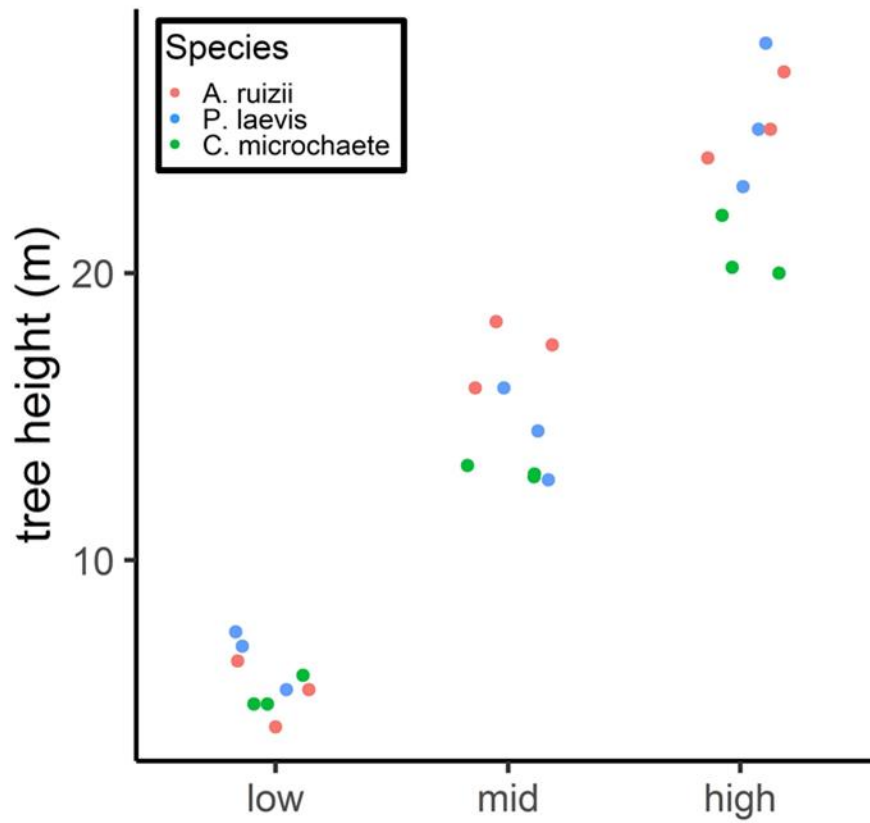
SI Table 4.2. Intercept comparisons between sites for the linear mixed effects model for vessel diameter and vessel density, presented as the ratio between sites in the value of the back-transformed value of intercept. For vessel density Oaxaca was excluded since the slope differed significantly from the other three sites.

model	site contrast	ratio	SE	df	t.ratio	p.value
log mean basal vessel diameter v log tree height	Oaxaca/Yucatan	0.687	0.129	148	-1.992	0.196
	Oaxaca/Selva Negra	1.212	0.236	139.2	0.988	0.757
	Oaxaca/Yasuni	0.889	0.172	138.6	-0.608	0.929
log mean basal vessel density v log tree height	Yucatan/Selva Negra	1.763	0.299	122.2	3.347	0.006
	Yucatan/Yasuni	1.293	0.211	131.4	1.575	0.397
	Selva Negra/Yasuni	0.733	0.127	110.2	-1.788	0.285
log mean basal vessel density v log tree height	Yucatan/Selva Negra	0.745	0.204	121.9	-1.074	0.706
	Yucatan/Yasuni	1.164	0.309	121.7	0.573	0.94
	Selva Negra/Yasuni	1.563	0.43	105.7	1.623	0.37

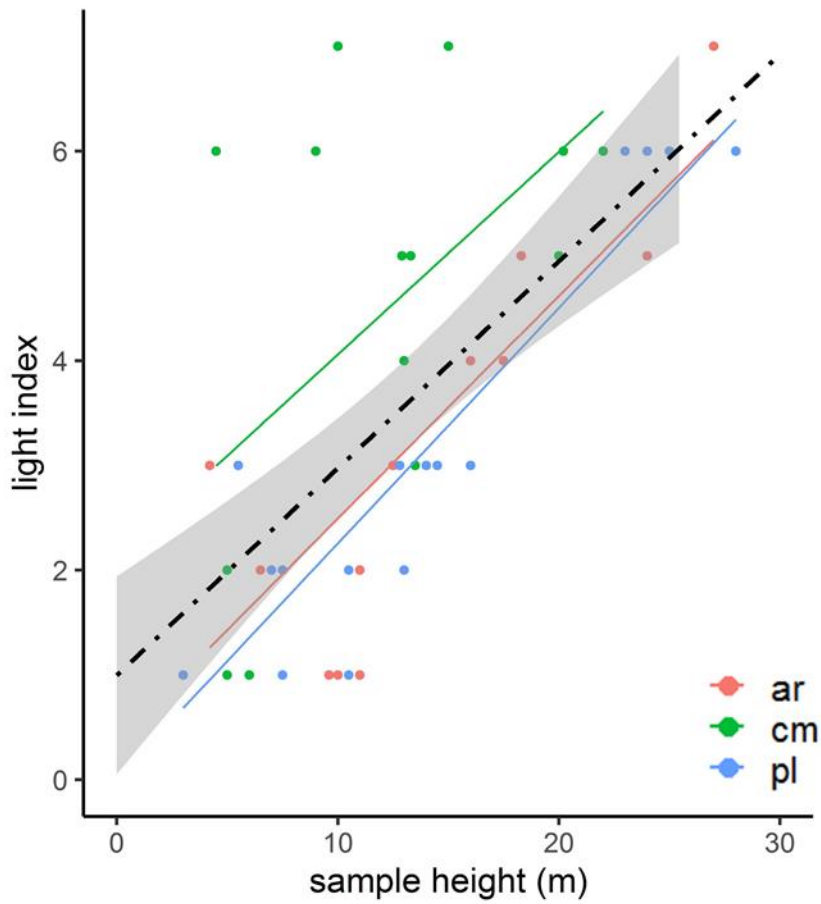
SI Table 4.3. The mean height (and standard deviation) for the 2.5-7.5m tree height bin is used for Figure 4.5 in text.

Site	2.5-7.5m
Yasuni	3.14 (0.46)
Oaxaca	5.43 (1.48)
Selva	4.60 (1.65)
Negra	
Yucatan	4.96 (2.07)

Appendix for Chapter 5



SI Figure 5.1 Trees sampled per species per height class showing the height of trees per species. Three individual trees were sampled per height class per species.



SI Figure 5.2 Relationship between height and light index representing canopy openness. Species are ar = *Ampelocera ruizii*, cm= *Centrolobium microchaete*, pl=*Pseudolmedia laevis*.

SI Table 5.4 Species specific relationship fit values between functional traits, as per Figure 5.10.

relationship	species	R ²	n	res. se	F	p-value
log vessel density v log mean vessel diameter	ar	0.6	2	0.465	46.34	<0.000
		6	4	3		
	cm	0.8	2	0.264	116.0	<0.000
		4	2	1		
	pl	0.8	2	0.467	111.9	<0.000
		2	4	8		
mean guard cell length v stomatal density	ar	0.2	1	0.001	4	0.0668
		4	3	3		
	cm	0.8	1	0.000	64.42	<0.000
		3	3	5		
	pl	0.6	1	0.000	23.13	<0.000
		1	5	6		
$\delta^{13}\text{C}$ v LMA	ar	0.6	1	0.661	23.24	<0.000
		4	3	5		
	cm	0.8	1	0.925	64.39	0
		3	3	7		
	pl	0.5	1	0.866	24.66	<0.000
		9	7	4		
LMA v gmax	ar	0.4	1	1.034	12.01	0.0042
		8	3	2		
	cm	0.6	1	1.986	24.3	<0.000
		5	3	4		
	pl	0.1	1	3.296	2.69	0.1217
		5	5	4		

SI Table 5.5 Coefficient values for between traits relationships per species , as per Figure 5.10.

relationship	species	term	estimate	standard error	t-value	p-value
log vessel density v log mean vessel diamter	ar	intercept	-0.92237	0.73	-1.26	0.2206
	ar	slope	-1.254011	0.18	-6.81	<0.0001
	cm	intercept	-1.646955	0.50	-3.31	0.0032
	cm	slope	-1.508865	0.14	-10.77	<0.0001
	pl	intercept	-2.745642	0.64	-4.27	<0.0001
	pl	slope	-1.747185	0.17	-10.58	<0.0001
mean guard cell length v stomatal density	ar	intercept	0.027243	0.003	9.94	<0.0001
	ar	slope	-0.000012	0.000006	-2	0.0668
	cm	intercept	0.021461	0.00056	38.62	<0.0001
	cm	slope	-0.000005	0.000001	-8.03	<0.0001
	pl	intercept	0.020403	0.00085	23.98	<0.0001
	pl	slope	-0.000004	0.000001	-4.81	<0.0001
$\delta^{13}\text{C}$ v LMA	ar	intercept	-33.459617 59992.4948	1.29	-25.96	<0.0001
	ar	slope	6	12444.05	4.82	<0.0001
	cm	intercept	-37.729104 90067.0148	0.95	-39.62	<0.0001
	cm	slope	9	11224.33	8.02	<0.0001
	pl	intercept	-32.817446 32816.9811	0.81	-40.29	<0.0001
	pl	slope	9	6609.04	4.97	<0.0001
LMA v gmax	ar	intercept	5.313703 67416.8368	2.02	2.64	0.5499
	ar	slope	3	19455.23	3.47	0.0042
	cm	intercept	8.188685 118739.735	2.04	4.01	0.4353
	cm	slope	9	24085.47	4.93	<0.0001
	pl	intercept	18.023034 44106.4730	3.40	5.3	0.4111
	pl	slope	5	26886.23	1.64	0.1217

